Gravity Anomalies: Unsurveyed Areas (1966)

Pages
161

Size
6 x 9

ISBN
0309339510

Hyman Orlin, Editor; National Research Council

Geophysical Monograph Series

American Geophysical Union

Geophysical Monograph Series
American Geophysical Union
WALDO E. SMITH, *Managing Editor*

1. **Antarctica in the International Geophysical Year**
   A. P. Crary, L. M. Gould, E. O. Hulburt, Hugh Odishaw, and Waldo E. Smith, Eds.

2. **Geophysics and the IGY**
   Hugh Odishaw and Stanley Ruttenberg, Eds.

3. **Atmospheric Chemistry of Chlorine and Sulfur Compounds**
   James P. Lodge, Jr., Ed.

4. **Contemporary Geodesy**
   Charles A. Whitten and Kenneth H. Drummond, Eds.

5. **Physics of Precipitation**
   Helmut Weickmann, Ed.

6. **The Crust of the Pacific Basin**
   Gordon A. Macdonald and Hisashi Kuno, Eds.

7. **Antarctic Research**
   H. Wexler, M. J. Rubin, and J. E. Caskey, Jr., Eds.

8. **Terrestrial Heat Flow**
   William H. K. Lee, Ed.

9. **Gravity Anomalies: Unsurveyed Areas**
   Hyman Orlin, Ed.

Gravity Anomalies: Unsurveyed Areas

SYMPOSIUM ON EXTENSION OF THE GRAVITY ANOMALIES
TO UNSURVEYED AREAS. COLUMBUS, OHIO, 1964

Geophysical Monograph Series

Number 9

GRAVITY ANOMALIES: UNSURVEYED AREAS

Hyman Orlin, *Editor*

Papers presented at the symposium
'Extension of Gravity Anomalies to Unsurveyed Areas,'
at Ohio State University, Columbus, November 18–20, 1964

Published with the aid of a grant from the Charles F. Kettering Foundation

PUBLISHER

AMERICAN GEOPHYSICAL UNION

of the

NATIONAL ACADEMY OF SCIENCES—NATIONAL RESEARCH COUNCIL

Publication No. 1357

1966

Geophysical Monograph Series Number 9

GRAVITY ANOMALIES: UNSURVEYED AREAS

HYMAN ORLIN, *Editor*

Suite 506, 1145 Nineteenth Street, N.W.
Washington, D. C. 20036

Library of Congress Catalog No. 66-60038

List Price, $7.00

Printed by
William Byrd Press, Inc.
Richmond, Virginia

Dedicated to

Weikko A. Heiskanen

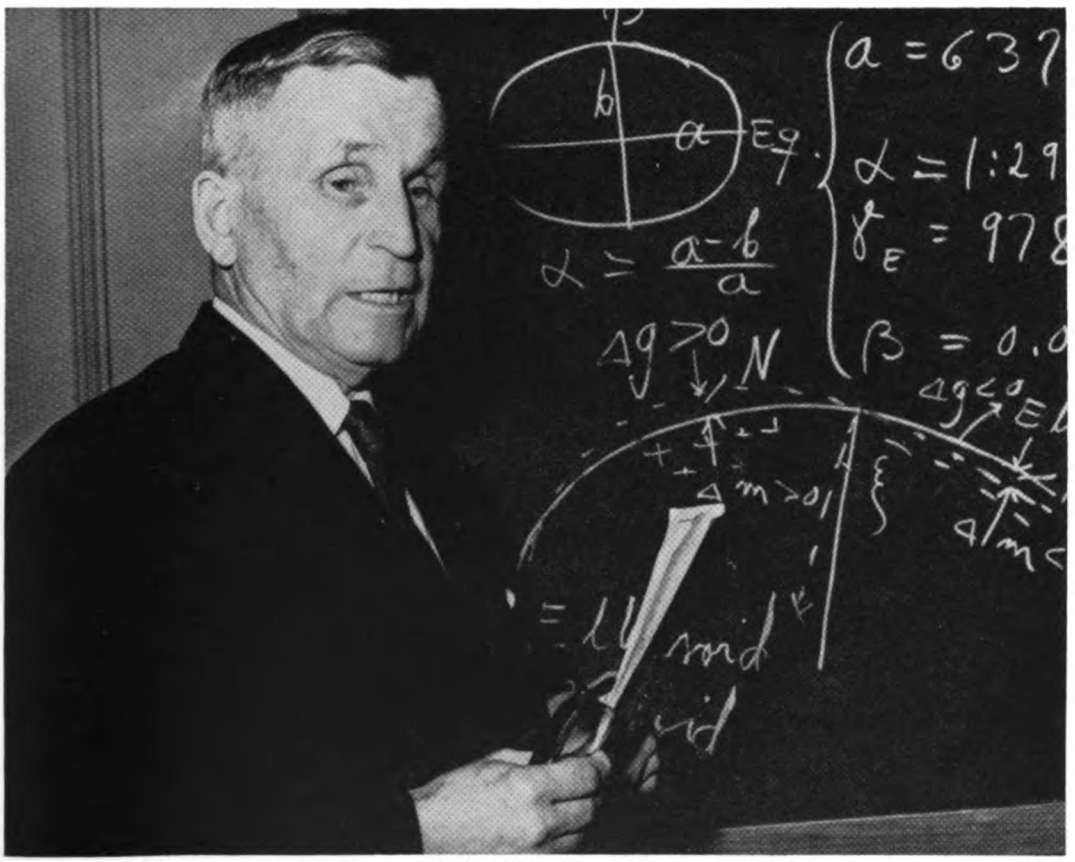

Professor Heiskanen lectures (1956) at the Rensselaer Institute of Technology.

Curriculum Vitae of Weikko A. Heiskanen

Personal Data

Weikko Aleksanteri Heiskanen, born 1895 in Finland. B.A. 1917, M.A. 1919, Ph.D. 1924, all from State University, Helsinki. State Geodesist, 1921–1928. Professor of Geodesy at Finland's Institute of Technology, 1928–1949; Chairman of the Surveying Department, 1935–1949; Director of the Finnish Geodetic Institute, 1949–1961 (from 1951 mostly in absentia); Director of the International Isostatic Institute of the International Association of Geodesy since its founding in 1936 (now in absentia); Professor of Geodesy, Ohio State University, since 1951; Scientific Director of the Institute of Geodesy, Photogrammetry, and Cartography of Ohio State University, 1951–1953, Director since 1953; Establisher (1950) and Supervisor of the Worldwide Gravity Project of Ohio State University since 1952.

Offices Held

President, Finnish Astronomical Society 1932–1948; President, Finnish Geographic Society, 1942; President, Society of Finnish Surveyors, 1948; President, Finnish Society of Christian Culture, 1948–1951; General Reporter on Isostasy of the IAG since 1930; President of Section 5, 'Physical Geodesy' of the IAG, 1957–1963; Vice President, International Union of Geodesy and Geophysics, 1957–1960; Supervisor of Solar Eclipse Project, February 1953–March 1955; Member of Working Group on Tracking and Computation of the USNC-IGY Technical Panel on the Earth Satellite Program, 1955–1958.

Memberships

Finland's Parliament, 1933–1936; Finnish Academy of Science, 1928; Foreign Member, Norwegian Academy of Science, 1947; German Academy of Science, 1950; Accademia Nazionale dei Lincei, 1950; *Instituto Lombardo Accademia di Szienze e Letter,* 1950; Geological Society of London, 1958; Fellow, American Academy of Arts and Sciences, 1959; Fellow, American Geophysical Union, 1962; Pontifical Academy of Science, Vatican, 1964.

Honorary Memberships

Dutch Geographical Society, 1938; Association for the Advancement of Finnish Culture, 1949; Finnish Astronomical Society, 1949; Ohio Epsilon Chapter, Phi Beta Kappa Society, 1956; Finnish Society of Christian Culture, 1957; Society of Finnish Surveyors, 1962; Geographical Society of Finland, 1963.

Honors and Awards

The Grand Prix of the Government of Finland for the period 1948-1951; Grand Award of Antti Wihuri Foundation, 1953; William Bowie Medal of the American Geophysical Union, 1956; Honorary doctor's degree, Bonn University, Germany, 1956; Honorary doctor's degree, Finland's Institute of Technology, 1958; Honorary doctor's degree, Uppsala University, Sweden, 1960; Commander of White Star, Estonia, 1938; Commander of St. Stephan, Hungary, 1941; Commander of White Rose, Finland, 1948; Commander of first class, Order of Lion, Finland, 1957.

Research Fields

Formerly, astronomy, isostasy, inner structure of the Earth, size and shape of the Earth, triangulation, city surveying.

Presently, physical geodesy, dimensions of the Earth and of the sphero- and geopotential surface above it, gravity anomaly field on the Earth and at any elevations above it, geometric and gravimetric constants of the Earth.

Professor Heiskanen has published about 150 scientific papers, mostly on isostasy, dimensions of the Earth, physical geodesy and astronomy; ten textbooks on astronomy and geodesy; and about 15 geodetic articles in different encyclopedias.

He has contributed the 'root of the mountains' isostatic system, called the Airy-Heiskanen system, to gravimetric geodesy and geophysics.

He derived the gravity formula, which the International Union of Geodesy and Geophysics accepted in 1930 (with a correction of 0.6 $\sin^2 \varphi$ mgal to the second-order term and 1.1 $\sin^2 2\varphi$ mgal to the third-order term) as the International Gravity Formula and which is still in use.

The International Association of Geodesy established the Isostatic Institute in 1936 in Helsinki. Professor Heiskanen has been Director since 1936; since 1950 mostly by 'remote control.'

He founded physical geodesy in a modern sense in 1932 in Finland.

In 1950 he brought physical geodesy on a worldwide scale to America (Columbus, Ohio).

Principal Publications

Über den Einfluss der Gezeiten auf die säkuläre Acceleration des Mondes, *Ann. Acad. Sci. Fennicae, Ser. A., XVIII*(2), 84 pp. and 2 maps, Helsinki, 1921.

Untersuchungen über die Schwerkraft und Isostasie

dissertation), *Veröff d. Finn. Geodetic Inst. 4,* 93 pp. and 1 map, Helsinki, 1924. (Translated into English by V. Pelts, Survey of India, 1928.)

Die Erddimensionen nach den Europäischen Gradmessungen, *Veröff d. Finn. Geodetic Inst. 6,* 26 pp., Helsinki, 1926.

Ist die Erde ein dreiachsiges Ellipsoid, *Gerlands Beitr. Geophys., B, XLX, 4,* 356–377, 1928.

Tables isostatiques après l'hypothèse d'Airy, *Bull. Geodesy, 30,* 87–153, 1931. (Also translated into English.)

Investigations on the gravity formula, *Publ. 1, Isostatic Inst. IAG,* 22 pp., Helsinki, 1938.

New isostatic tables for the reduction of gravity, *Publ. 2, Isostatic Inst. IAG,* 42 pp., Helsinki, 1938.

On the figure and structures of the Earth, *Publ. 8, Isostatic Inst. IAG,* 47 pp., Helsinki, 1941.

On the determination of the geoid, *Veröff d. Finn. Geodetic Inst. 36,* 10 pp., Helsinki, 1949.

On the world geodetic system, *Veröff d. Finn. Geodetic Inst. 39,* 25 pp., Helsinki, 1951; *Publ. 25, Isostatic Inst. IAG,* Helsinki, 1951; *Publ. 1, Inst. Geodesy Photogrammetry, Cartography,* Columbus, Ohio; *Intern. Hydrographic Rev.,* 25 pp., 1953.

The geodetic significance of the worldwide gravity studies, MCRL, Columbus, Ohio, *Tech. Paper 124,* November 1950.

On the isostatic structure of the Earth's crust, *Publ. 24, Isostatic Inst. IAG,* 60 pp., Helsinki, 1950.

Columbus geoid, *Trans. Am. Geophys. Union, 38*(6), 842–848, 1957.

The Earth and Its Gravity Field, McGraw-Hill, New York, 1958 (with Professor F. A. Vening Meinesz).

Physical Geodesy (with Helmut Moritz), about 450 pp., submitted for publication.

Activity of the Columbus Geodetic Group in physical geodesy since 1960, *Publ. 41, Isostatic Inst. IAG,* 26 pp., Helsinki, 1964.

Present problems of physical geodesy, *Publ. 49, Isostatic Inst. IAG,* 36 pp., Helsinki, 1965.

Contents

Opening Address

Chairman: W. A. Heiskanen

As chairman, I take great pleasure in opening this symposium on behalf of the Department of Geodetic Science and the Institute of Geodesy, Photogrammetry, and Cartography of Ohio State University and in welcoming the representative of the Ohio State University, Robert Oetjen, the Associate Dean of the Arts and Science College of OSU; Irene Fisher, the representative of the International Association of Geodesy and secretary of the section of physical geodesy of the IAG; and Walter D. Lambert, the representative of the American Geophysical Union, former president of the IAG, and Honorary Doctor of OSU.

Telegrams and congratulatory letters have been received from the following presidents or former officers of the IAG who, for various reasons, are not able to participate: Guy Bomford, President of the IAG; J. D. Boulanger, Vice President of the IAG; J. de Graaff-Hunter, former President of the IAG; H. Arnold Karo, Director of the U. S. Coast and Geodetic Survey; and Erik Tengström, Director of the Institute of Geodesy of Uppsala University and President of the section of physical geodesy of the IAG.

Particularly, I welcome representatives of the American Air Force, which since 1952 has continuously supported research of the IGPC of OSU. Without this support we would have neither the Columbus Geodetic Center nor this symposium. It is a great pleasure for me to see and welcome many former and present students of the Department of Geodetic Science. Finally, I welcome all other participants, many of whom are my personal friends.

Some explanation of the subject of our symposium, 'Extension of the Gravity Anomalies to Unsurveyed Areas,' is necessary. This problem is one part of physical geodesy or of the gravimetric method, which is in principle simple, in practice difficult and fascinating, and in results the most powerful part of geodesy. The method is simple because it needs only one tool: the gravity anomaly Δg. The principle is that the unknown disturbing masses Δm, of and under the Earth's crust, will cause the gravity anomalies Δg, the undulations N of the geoid, and the deflections of the vertical ξ and η. The gravity anomalies Δg can be observed, and the other quantities can be computed from them.

If the gravity anomalies are known around the world, all problems of physical geodesy can be solved.

However, we know that there are huge gaps in the gravity anomaly field, particularly in the oceans. The key problem of physical geodesy is therefore *how to fill these anomaly gaps.* There are three methods: (1) we can make additional measurements; (2) we can extrapolate from the existing gravity anomalies, obtaining mean gravity anomalies for the unsurveyed areas by *statistical methods;* or (3) we can extrapolate by *geophysical methods.* The first is,

of course, the best. But until the gravity anomaly gaps are filled by additional measurements, we must employ the other methods, because only in this way will research in physical geodesy avoid coming to a standstill.

The symposium is divided into four sessions. Session 1, 'Report on the Existing Gravity Material,' tells *where* we are now and *how* we can best improve the measurement *methods* and increase the accuracy of the *results*. Two sessions have been reserved for the extrapolation of the gravity anomaly field to the unsurveyed areas: Session 2, 'Extension of the Gravity Net to the Unsurveyed Areas of the Earth—*Statistical Methods*'; and Session 3, *'Geophysical Methods.'* Session 4, 'External Gravity Field of the Earth,' discusses the correlation between the gravity anomalies and equipotential surfaces at the Earth's surface above it.

This symposium is not the first that the IGPC of OSU has arranged. Previously, there have been four symposia: (1) Geophysics and Geodesy,' November 11–12, 1952; (2) 'New Era of Geodesy,' November 12–13, 1954; (3) 'Size and Shape of the Earth,' November 13–15, 1956; and (4) 'Geodesy in the Space Age,' February 6–8, 1961. These four symposia were arranged and the speakers selected by Heiskanen. Today we open the fifth symposium, November 18–20, 1964.

The graduate school of OSU and the National Science Foundation have kindly supported these symposia. The proceedings of the symposia have been published in different series. The subject of all these symposia has been very broad. Since this symposium is sponsored by the IAG and the American Geophysical Union, it is on a broader international basis than the former symposia. We also look forward to the proceedings of this symposium being published by the AGU in its *Geophysical Monograph Series*.

Existing Surface Gravity Material

Reporter: U. A. Uotila[1]

About four years ago a report was presented on the same topic in another symposium at Ohio State University [*Uotila,* 1961]. The title of that paper was very similar to this one; however, we are not speaking about existing gravity surveys but about the data we have discovered in our search for observed gravity material.

In the preceding symposium we predicted rapid increases in gravity survey activities around the world. Sea gravimeters were believed to be operational, and reports about airborne gravimeters were very promising. It was known that governments were planning to give more support for determination of the gravity field of the Earth. The past years have shown that sea gravimeters are not as reliable as we believed; and airborne gravimeters have not been sufficiently flight tested. We believe that the most significant reason for the slow-down of gravity survey programs has been the over-advertising of other methods for obtaining gravity information. We can only hope that this kind of over-selling will not occur too frequently at the expense of the other methods. Different methods should not compete but should complement each other. Researchers well know that combinations of data from different methods give the best results.

It is encouraging to see that surface and near-surface gravity observation programs are getting more attention and more support today than they have been getting since the first symposium. There will be papers presented later in the program which assure us that instrumentation is getting better and reduction methods are getting more accurate and convenient.

This report is based on the information which exists in some form in the files of the Department of Geodetic Science. The additional information received just before or during the symposium has been partly incorporated into this report. We must omit the very detailed location information of gravity surveys because the material is so extensive.

From Figure 1 we can see today's locations of gravity measurements, excluding polar areas. If each 1°-by-1° block with at least one observation is taken as an area having gravity observation coverage, we can state that there has been

[1] Department of Geodetic Science, Ohio State University, Columbus.

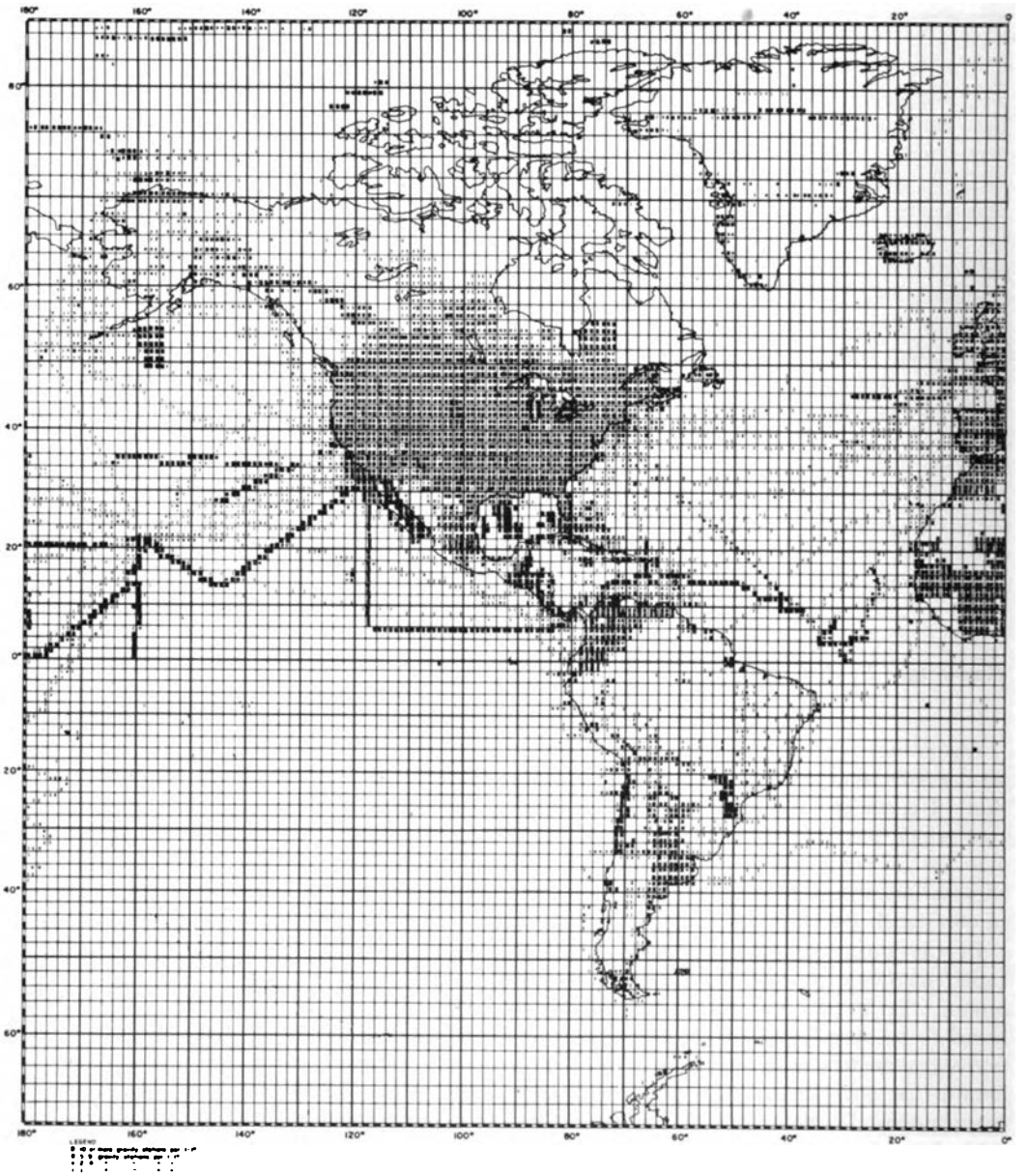

Fig. 1. Location of gravity measurements. Solid block indicates 10 or more gravity stations per 1° by 1°; heavy asterisk, 5–9 gravity stations per 1° by 1°; plus sign, 2–4 gravity stations per 1° by 1°; and vertical bar, 1 gravity station per 1° by 1°.

a 13% increase in the area coverage in the northern hemisphere since the last symposium. The corresponding number for the southern hemisphere represents a 19% increase. For the whole world the increase is 14%. According to these numbers, the total coverage for the entire Earth is now about 35%. There still exist very large gaps in the gravity surveys; the largest gap is still in the southern Pacific Ocean. These very large unsurveyed areas have very dangerous effects in our computational results because, as we well know, the gravity anomalies are correlated with each other; therefore, the large unsurveyed areas might have a serious system-

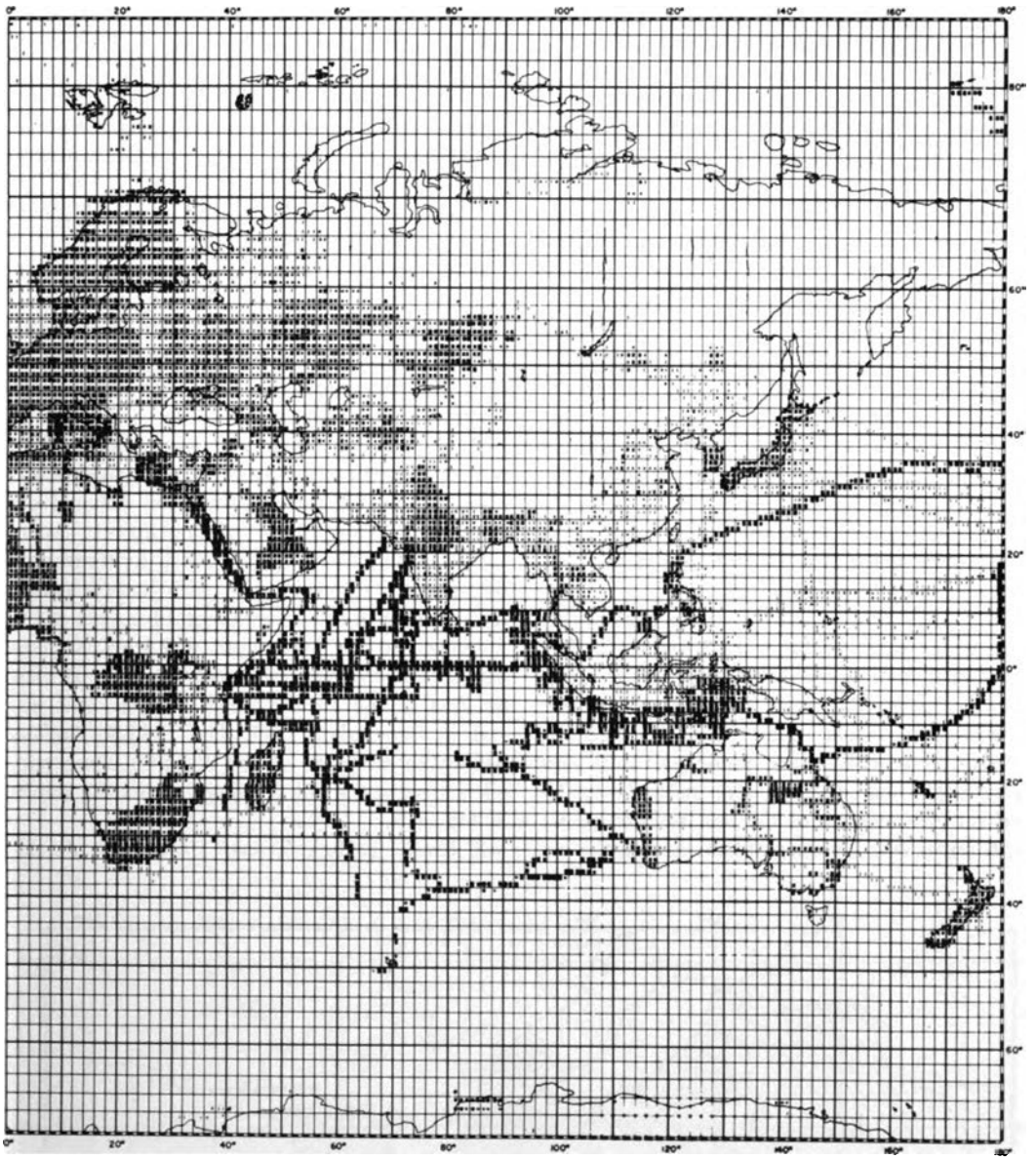

Fig. 1 (continued)

atic effect. It is of utmost importance that close coordination be established between scientists planning and doing gravity surveys to achieve the maximum benefit from these surveys. Several suggestions have been made earlier for this kind of cooperation at the international level. We must continue to emphasize that all gravity surveying organizations should know what the others are doing or planning to do in the near future.

The extent of published material is demonstrated by the listing of 858 publications which will be available at a later date and which will include about 150,000 stations for which gravity information is given. However, some stations are repeated in several publications. The small number of gravity stations from this published material may be surprising. Each of us knows that there exists several times this amount of gravity information in the world. For example,

there is a vast amount of gravity information in the files of oil companies. Some of that material has been released to certain organizations; some has not been released. Several surveying organizations have done very extensive gravity surveys, but they have not published their results. Publishing such results has become very difficult because of the considerable expense involved and the limited market for this kind of publication. It has therefore become a general practice that large gravity surveys are not published, except possibly in map form. The tabulations or IBM cards are made available to those who have requested them. In this connection, it should be emphasized that the Department of Geodetic Science is very much interested in receiving all published and unpublished material in order to incorporate it into a worldwide gravity library. We hope to publish mean gravity anomaly maps at a later date and to make them available to all scientists.

Until that time, however, there are several steps which must be taken between the collection and reduction and the production of mean anomaly maps. We must evaluate all gravity surveys and adjust them into the uniform Potsdam system. We must remove all duplicate information and develop the methods to be used for computation of the best representative mean anomalies. To accomplish these tasks we must have much more information about gravity surveys [*Uotila*, 1959] than just observed gravity values with the coordinates.

We are happy to see that in modern publications most of the scientists are giving the necessary information to accomplish what we have proposed.

We have received the following additional information for the report:

1. C. Morelli, Osservatorio Geofisico, Trieste, Italy, gave us information in map form about their activities (see Figure 2). The map shows the gravity survey coverage through 1964 in the Mediterranean area. It also shows the planned gravity survey for 1965.

2. G. J. Bruins, Technische Hogeschool, Delft, informed us that they are participating in the so-called Navado project with the Askania sea gravimeter. The purpose of the project, undertaken by the English and Dutch hydrographic departments in cooperation with some scientific institutes, is to collect oceanographic data of the Atlantic Ocean. The project will start November 26, 1964, when the recording ship H.M.S. *Snellius* of the Dutch Navy will sail, and will end in September 1965. The H.M.S. *Snellius* will make crossings of the Atlantic along parallels that are about 3 degrees apart, as shown in Figure 3.

3. Chuji Tsuboi, Tokyo University, Japan,

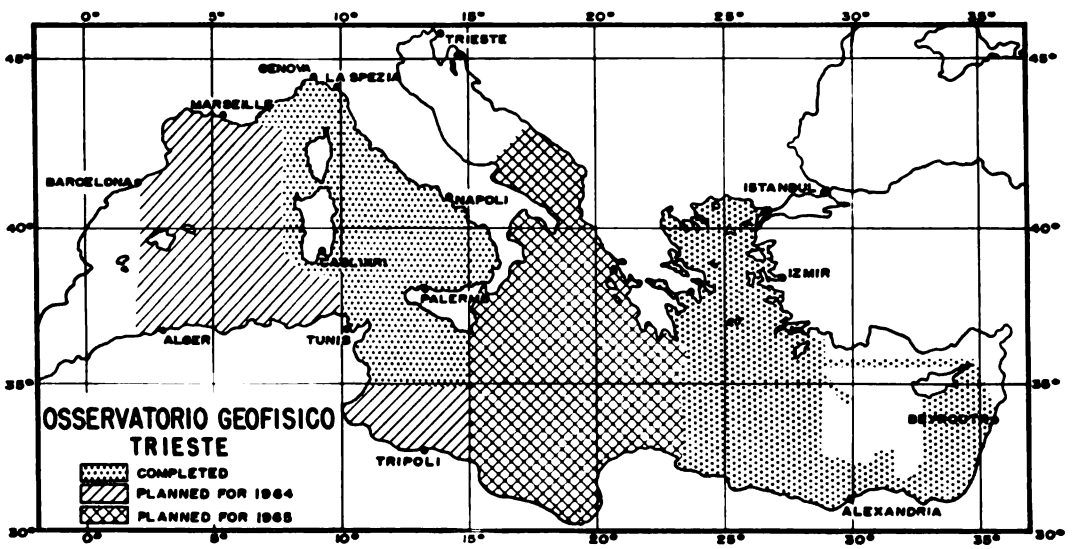

Fig. 2. Gravity survey coverage through 1964 in the Mediterranean area and planned surveys through 1965.

sent us a map showing courses along which they have surveyed gravity by their seaborne gravimeter. The dotted lines in our Figure 4 show these courses.

4. B. C. Browne, Department of Geodesy and Geophysics, University of Cambridge, sent us the following summary of shipborne gravity measurements made by their department with Askania Gss2 gravimeter 11.

Nov. 1961 to May 1962	H.M.S. *Owen*. International Indian Ocean Expedition. General reconnaissance of the Arabian Sea area. Results published by Hydrographic Dept., British Navy, *Admiralty Marine Science Publication 4* (1963).
Sept. 1962 to June 1963	H.M.S. *Owen*. International Indian Ocean Expedition. More detailed investigation of some special areas of the Arabian Sea. Results to be published shortly as above (in press).
Sept. 1963 to June 1964	H.M.S. *Vidal*. Operation Navado east-west profiles across the Atlantic Ocean at 10°, 13°, 16°, and 19° and east-west profiles to and from the Azores at 37° and 40°N. Results are now being reduced.

5. Peter Dehlinger, Department of Oceanography, Oregon State University, sent us a map indicating the sea gravity profiles which they obtained in 1963–1964. These profile lines are given in Figure 5 as dotted lines. In addition, Dehlinger informed us that they have run some sea gravity lines in the Hawaiian area, especially north of Hawaii, and off the coast of Washington.

6. J. C. Harrison, Hughes Research Laboratories, informed us that their laboratories have made local gravity surveys to evaluate instruments. He has personally been working with the data observed during earlier extensive evaluations. He has computed mean anomalies and prepared a program for the computation, plotting, and contouring of Bouguer anomalies for any chosen density assumptions and regional averaging.

Following are short summaries of the information delivered from the floor and submitted to the reporter.

1. A. C. Hamilton presented a report on 'The State of Gravity Mapping in Canada, Novem-

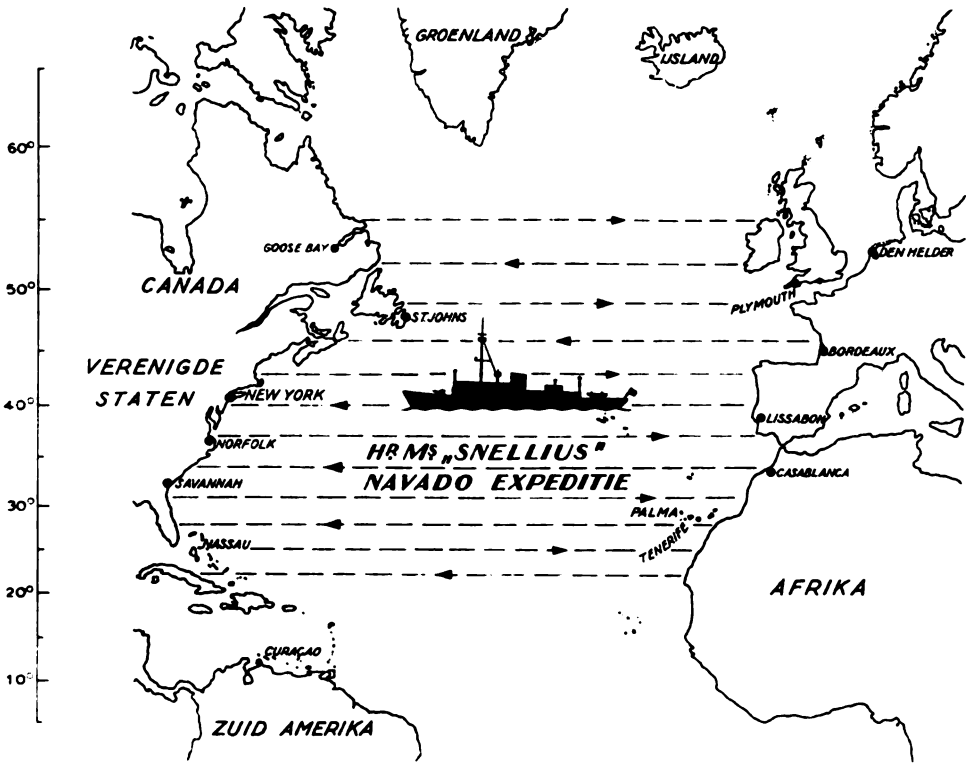

Fig. 3. Planned surveys of the H. M. S. *Snellius*, November 26, 1964, through September 1965.

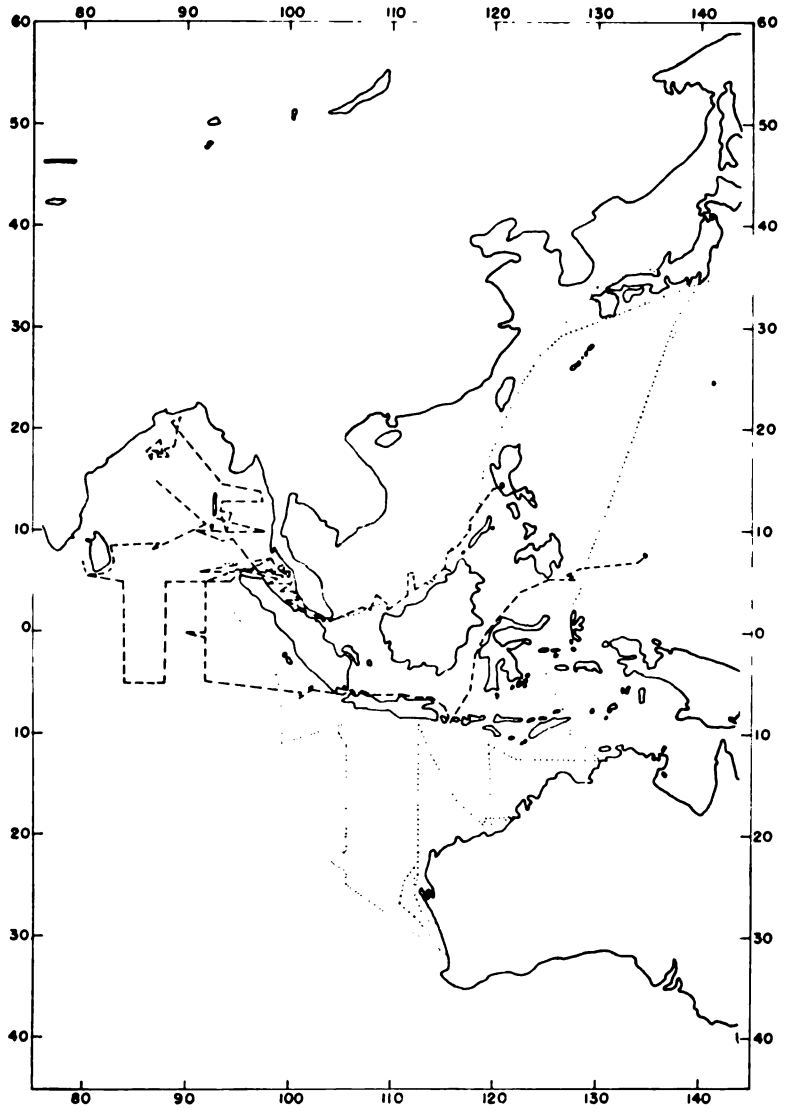

Fig. 4. Gravity surveys in Asiatic waters. Dotted lines indicate Japanese measurements; dashed lines indicate U. S. Coast and Geodetic Survey measurements.

ber 1964' by M. J. S. Innes, Chief, Gravity Division, Dominion Observatory, Ottawa, Canada. The report is printed separately in this volume.

2. Hyman Orlin, U. S. Coast and Geodetic Survey, showed charts covering the data which they have collected through 1963. Tracks of the ships are shown in Figures 4 and 5 by dotted and solid lines. He stated that their gravity surveys are performed as part of the general oceanographic program. Their only possibility for determining the accuracy of data has been either to compare the results where track lines cross or to operate over a region where the gravity values are well defined. As for future plans, Orlin mentioned that they hope to continue operating in the Pacific between the Aleutians and the Hawaiian Islands. In addition, an area 500 miles wide between 35° and 39° latitudes will be developed along the east and west coasts of the United States. A survey of the Atlantic ridge and operations

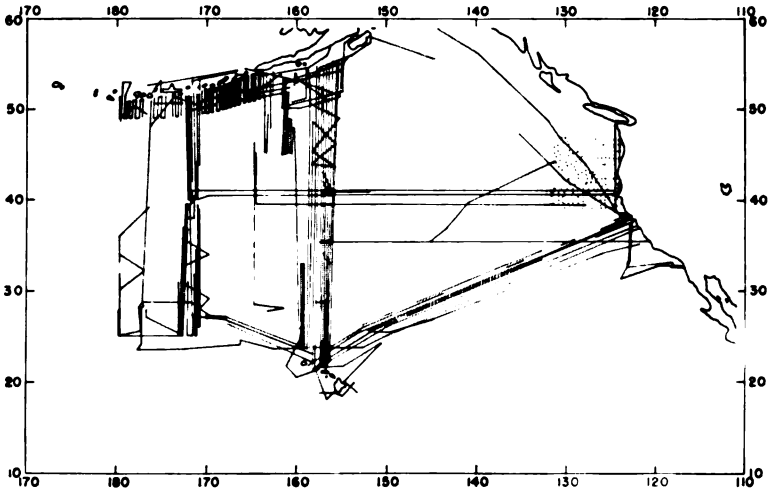

Fig. 5. Sea gravity profiles, 1963–1964. The dotted lines, which are the profile lines, indicate Oregon State University measurements. Solid lines indicate U. S. Coast and Geodetic Survey measurements.

in the South Atlantic are contemplated and will depend upon the availability of adequate navigational control. Figure 6 shows the U. S. Coast and Geodetic Survey gravity network in the U. S. A. as of January 31, 1964. Orlin said that land surveys will continue, with emphasis to be placed upon the first-order traverses and some area coverage when possible. Special surveys, such as the survey in the vicinity of Prince William Sound, will be conducted as the need arises.

3. George P. Woollard, Director, Hawaii Institute of Geophysics, University of Hawaii, related their recent work and their plans for the following types of work:

Land regional surveys:	Antarctica, Spain, Wyoming, Solomon Islands, Hawaiian Islands, Tahiti.
Planned or in progress:	Mexico.
Marine regional surveys:	Arctic Basin, Hawaiian area.
Planned or in progress:	Solomon Islands area.
Land Control Surveys (for evaluating oil company data):	New Guinea, India.
Planned or in progress:	Mexico, India, Pakistan, North Africa, Spain.
Standardization Lines (Pendulum and Gravimeter):	European-African Line, Hammerfest-Cape Town, North American Line, Point Barrow-La Paz.
Planned:	Pacific Line, Sapporo-Melbourne.

4. A. L. McCahan, Gravity Branch, U. S. Naval Oceanographic Office, delivered the following report on gravity surveys by the U. S. Naval Oceanographic Office.

a. Office surveys. Commencing with the tests of the then new LaCoste and Romberg sea gravity meter in April 1955, the U. S. Naval Oceanographic Office has pursued a program of ocean gravity measurements. The first test runs were made along the west coast of the U. S. and between Hawaii and the west coast. Since then, observations were made in the vicinity of Clipperton Island, on several broadly spaced lines southwest of Hawaii, and as a continuous profile around the world aboard the U.S.S. *Triton* during her circumnavigation of the submerged world in 1960. This office is at present cooperating with the University of Hawaii in a survey around the Solomon Islands.

In addition, observations have been made with underwater gravity meters near Puerto Rico, Rhode Island Sound, the Chesapeake Bay, and in the approaches to San Francisco harbor, the last-mentioned in cooperation with the U. S. Coast and Geodetic Survey. These areas are used for tests and evaluation of shipboard gravity instruments.

b. Land surveys. Gravity observations are being made regularly in conjunction with worldwide airborne magnetic surveys. Base stations are being established in many countries toward

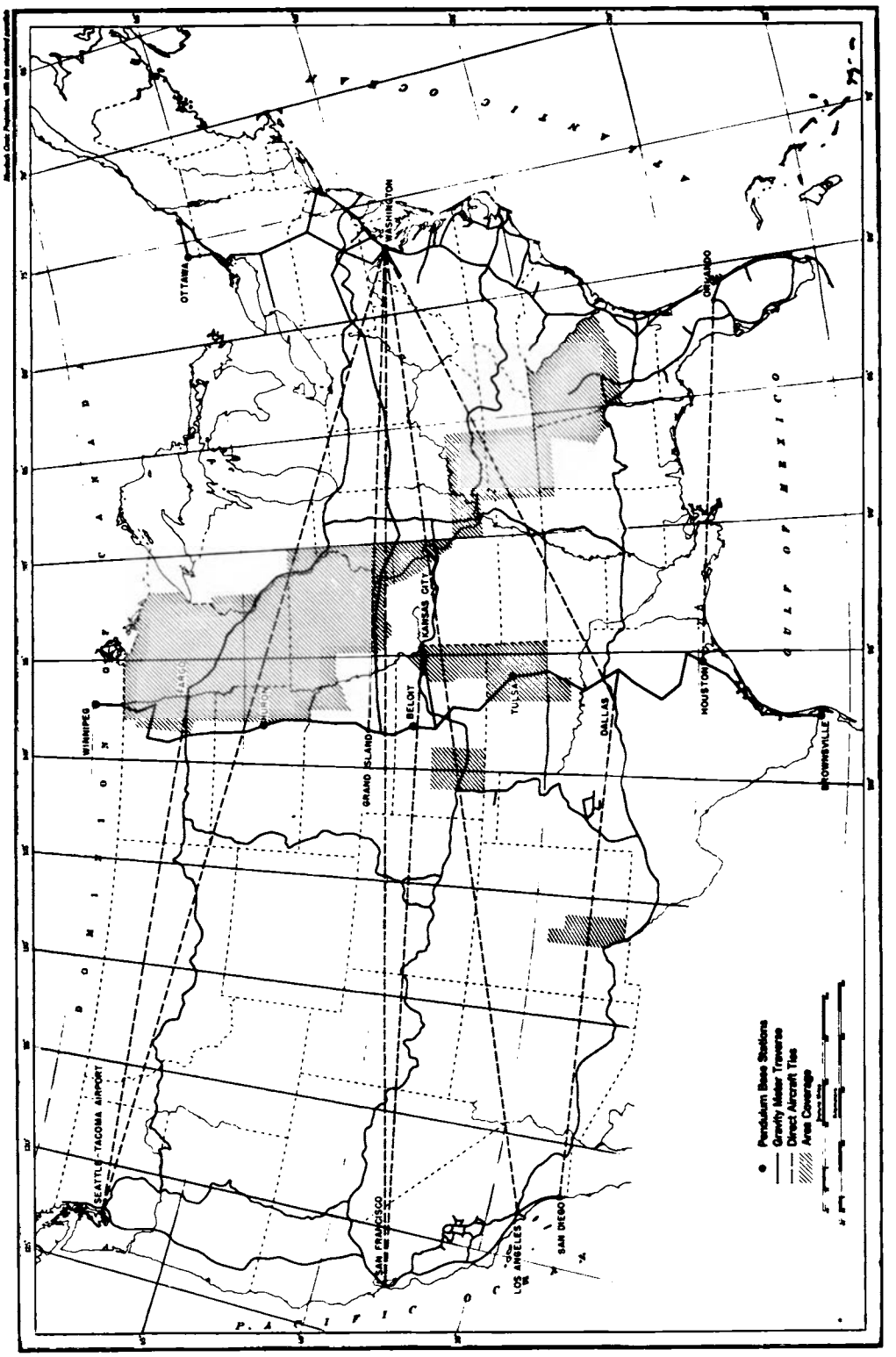

Fig. 6. U. S. Coast and Geodetic Survey gravity network in the U.S.A. (as of January 31, 1964).

development of a world network. Observations have also been made along the European and North American calibration lines, in Bermuda, and in parts of Hawaii, Guam, and New Guinea.

5. David Anthony, Data Reduction Division, 1381st Geodetic Survey Squadron, Orlando Air Force Base, sent the following report of their activities which was given from the floor by Charles Whalen. 1381st gravity surveys carried out in the past year with approximate number of stations include

1. 2600 stations in the area 44°–49°N, 106°–115°W.
2. 460 stations in the area 45°–49°N, 98°–101°W.
3. 65 stations on Mahe Island, Indian Ocean.
4. 40 base stations in Ethiopia (in progress).
5. 25 stations in Florida, from Key West to Jacksonville.
6. 150 stations in west central Missouri.
7. 200 stations in southeast Wyoming.
8. +100 stations of the American calibration line from Point Barrow to Ushuaia, Argentina.
9. 200 plus stations of the Euro-African calibration line from Hammerfest to Cape Town.

In addition, P. A. Mohr, of the Ethiopian Geophysical Observatory, has an Ethiopian network of approximately 1000 stations referred to an arbitrary observatory base station. In exchange for these data we will tie his observatory base station to the Euro-African line and determine a scale factor for his Sharp gravimeter.

6. Michele Caputo, University of California at Los Angeles, gave the report of their activities in gravity surveying. His report is published separately in this volume.

7. B. D. Loncarevic, Bedford Institute of Oceanography, Dartmouth, Canada, gave a report of their activities. As we well know, their institute has been very active concerning gravity surveys on the ocean. The summary of his contribution has not yet been received.

8. Manik Talwani, Lamont Geological Observatory of Columbia University, Palisades, New York, gave an excellent report of the activities of his group. His report is published separately in this volume.

We have seen from the preceding presentations that there is a large percentage of the Earth's surface to be covered by gravity observations. The momentum in the flow of support for conducting surface gravity measurements seems to be slowing because of the appearance of artificial satellites. We hope that it has become clear that detailed gravity information on the Earth's surface can be obtained only through surface measurements or near-surface measurements. Therefore, we urge very strongly that all Earth scientists powerfully support their fellow scientists in their efforts to obtain additional gravity measurements in unsurveyed areas, especially in the areas where very large gaps exist, and to develop better instrumentation for future gravity surveys. We hope that in the next symposium we can present a much more positive report of the gravity coverage on the surface of the Earth.

References

Uotila, U. A., Existing gravity material, paper presented at the symposium 'Geodesy in the Space Age,' Ohio State University, Columbus, Ohio, February 6–8, 1961, *Inst. Geodesy Photogrammetry Cartography Publ. 15,* 1961.

Uotila, U. A., Investigations on the gravity field and shape of the Earth, *Inst. Geodesy Photogrammetry Cartography Rept. 6,* 1959.

The Status of the World Gravity Standardization and First-Order Net

BELA SZABO

Air Force Cambridge Research Laboratories
L. G. Hanscom Field, Bedford, Massachusetts

Abstract. The progress of the work for the establishment of a uniform world gravity system, initiated at the Fourth Assembly of the International Gravity Commission (Paris, September 1962) is described and illustrated on graphics. The measurements performed under this program since 1963 consist of observations by selected pendulums and groups of gravimeters along three primary calibration lines (Euro-African, American, and West Pacific) and of transverse pendulum and gravimeter connections between these lines. The completed observations are described and a tentative schedule is indicated for the additionally planned observations. Finally, the status of several portable absolute experiments that would contribute to the program for establishment of a new international absolute reference system is described.

INTRODUCTION

In accordance with the agreements reached during the Fourth Assembly of the International Gravity Commission in September 1962, selected pendulum apparatus and groups of gravimeters have been used to perform the measurements required for the accomplishment of a world gravity system. A uniform worldwide gravity system can be accomplished by the solution of three closely interrelated problems: (*a*) the world calibration standard, (*b*) the first-order world gravity net, and (*c*) the international absolute reference or gravity datum.

On the basis of the analysis of existing measurements, and of the availability of instruments, observers, and funds, plans and observation schedules have been prepared to achieve this goal. The measurements have been in progress since 1963 under the central direction of Special Study Group 4.05 of the International Association of Geodesy. The plans for this program are described by *Morelli* [1963] and *Szabo* [1963]. The proposed new observations are shown in Figure 1.

This report presents the observations completed under this program by pendulums and groups of gravimeters; the tentative schedule for the remaining measurements is also indicated. Finally, the status of the portable absolute experiments is discussed.

THE STATUS OF THE PENDULUM OBSERVATIONS

On the basis of the general plan shown in Figure 1, the pendulum observations were started in the spring of 1963. Considering the few instruments available to achieve the required accuracy (± 0.2 mgal) and the high cost of operation, it was agreed that the selected pendulums will be used only for: (1) the establishment of the primary calibration lines for gravimeters, (2) interline (east-west) connections between very distant stations with large gravity intervals, and (3) control of important intersections of the first-order gravity net.

It was also agreed that the pendulum measurements along the calibration lines are to be made in a ladder fashion starting from central station on each line. Identical sites have been occupied, with a few exceptions, by all participating instruments.

The pendulum measurements completed under this program between 1963 and August 1, 1965, are shown in Figure 2. The scheduled additional observations are indicated in Figure 3.

Euro-African Calibration Line (EACL)

This line has been fully completed by two instruments: the Gulf pendulums of the University of Hawaii, U.S.A., under the direction of George P. Woollard; and the pendulums of the Department of Geodesy and Geophysics, Cam-

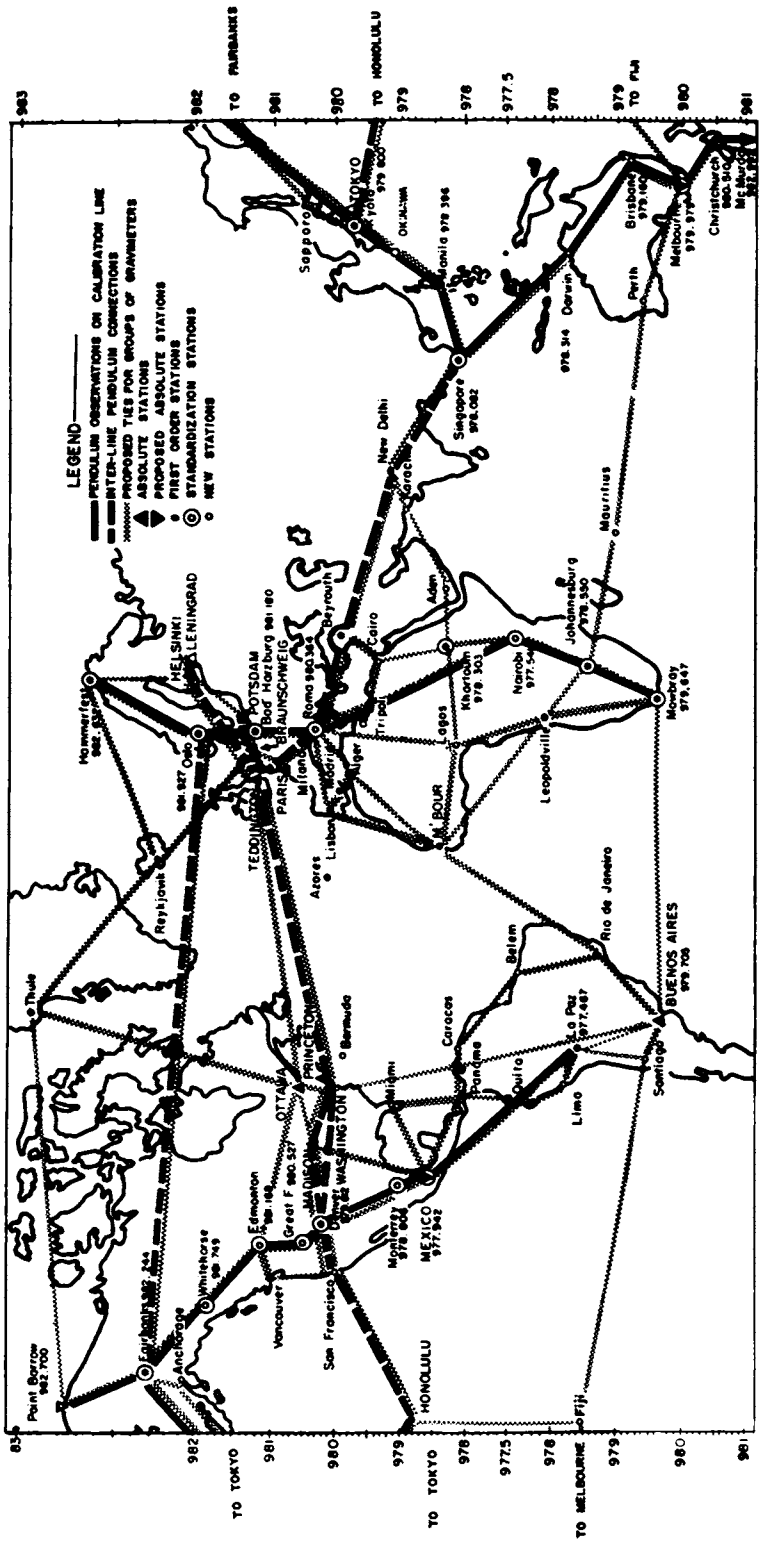

Fig. 1. Proposed new observations for the world calibration standard first-order gravity net and absolute gravity system.

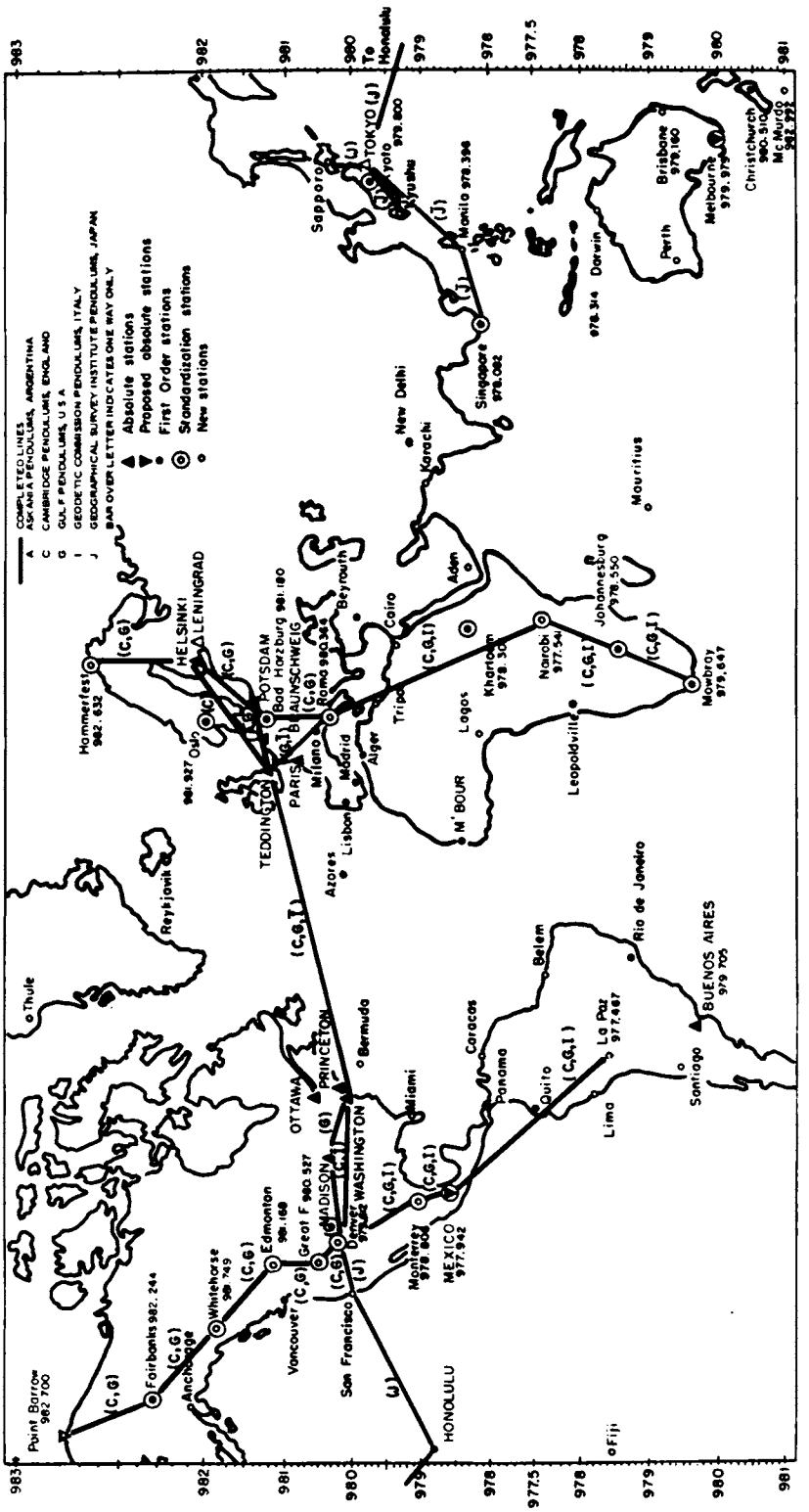

Fig. 2. Completed pendulum observations since 1963 as of August 1, 1965.

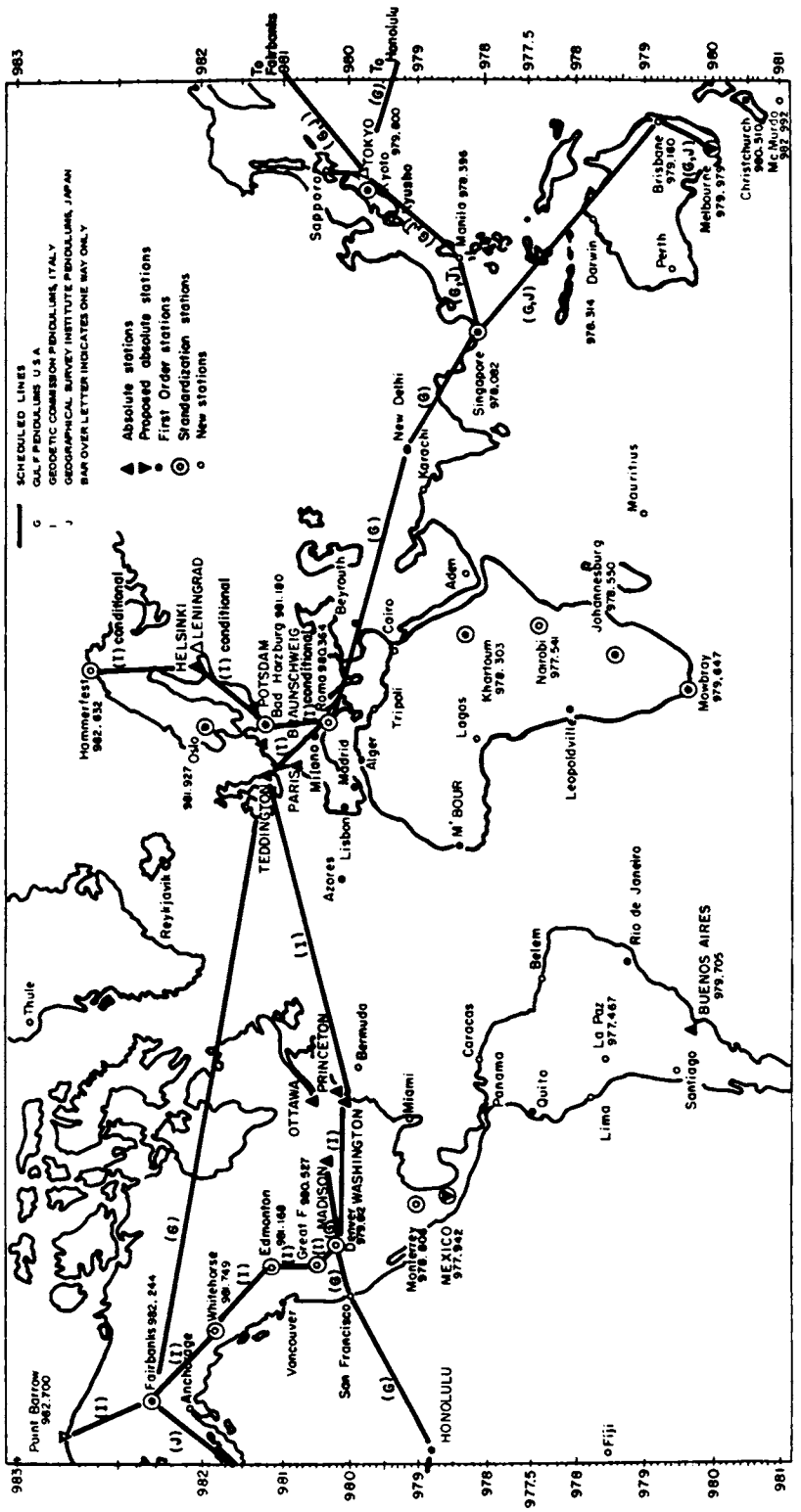

Fig. 3. Scheduled pendulum observations.

bridge, England, under the direction of Benjamin C. Browne. Two apparatus of the Italian Geodetic Commission, Milano, Italy, under the direction of L. Solaini and C. Mazzon observed only the southern part of the line (Rome–Mowbray).

The Gulf 'M' pendulums. The Gulf 'M' pendulums occupied the following sequence of stations during the 1963 measurements: 1, Madison, Wisconsin, as base station; 2, Washington, D. C.; 3, Teddington; 4, Potsdam; 5, Potsdam; 6, Teddington; 7, Rome; 8, Nairobi; 9, Johannesburg; 10, Mowbray; 11, Mowbray; 12, Johannesburg; 13, Nairobi; 14, Rome; 15, Bad Harzburg; 16, Helsinki; 17, Hammerfest; 18, Hammerfest; 19, Helsinki; 20, Bad Harzburg; 21, Rome; 22, Teddington; 23, Potsdam; 24, Teddington; 25, Washington, D. C.; 26, Madison. The observations were made by Richard Longfield and Barry Carlson of the University of Hawaii.

Simultaneously, Jose Mateo of the University of La Plata, Argentina, made observations with an Askania (Invar) four-pendulum apparatus. The sequence of the observations and the sites occupied were identical with those occupied by the Gulf apparatus: 1, Madison; 2, Washington, D. C.; 3, Teddington; 4, Potsdam; 5, Potsdam; 6, Teddington; 7, Rome; 8, Nairobi. Unfortunately, illness necessitated Mateo's return from Nairobi to Argentina before the observations were completed.

The Cambridge pendulum apparatus. This apparatus was used on the EACL in 1963 by two observers; T. Honkasalo of the Finnish Geodetic Institute observed the northern section of the line and J. E. Jackson of Cambridge University, England, swung the pendulums along the southern section. The observations were made between March and September 1963. The sequence of observations and the sites occupied were as follows: Northern section: 1, Teddington; 2, Helsinki; 3, Helsinki; 4, Bad Harzburg; 5, Rome; 6, Rome; 7, Bad Harzburg; 8, Helsinki; 9, Hammerfest; 10, Hammerfest; 11, Helsinki. Southern section: 1, Rome; 2, Nairobi; 3, Johannesburg; 4, Mowbray; 5, Mowbray; 6, Johannesburg; 7, Nairobi; 8, Rome.

The apparatus no. 1 and no. 3 of the Italian Geodetic Commission. This apparatus was operated by C. Mazzon and V. Tomelleri of the Geodetic Institute of the Politecnico of Milan, who observed the southern part of the Euro-African line in November and December 1963. The stations and the sequence of the observations were the following: 1, Milan (base station); 2, Rome; 3, Nairobi; 4, Mowbray; 5, Mowbray; 6, Nairobi; 7, Rome; 8, Milan. Owing to damages to both instruments during transportation, the results of these measurements are doubtful.

American Calibration line (ACL)

The American calibration line (between Point Barrow, Alaska, and La Paz, Bolivia) has been completed during the 1964 season by the Cambridge pendulum apparatus and the Gulf 'M' pendulums. Apparatus no. 2 of the Italian Geodetic Commission started the observations in April 1965, and at the present time the observations are completed on the southern section of the line (Denver–La Paz). The northern sector will be completed by November 1965.

The Cambridge pendulum apparatus. This apparatus was operated by D. I. Gough of the Southwest Center for Advanced Studies, Dallas, Texas, who completed the northern section between June and September 1964 according to the following schedule: 1, Teddington; 2, Washington, D. C.; 3, Denver, Colorado; 4, Great Falls, Montana; 5, Edmonton, Canada; 6, Whitehorse, Canada; 7, Fairbanks, Alaska; 8, Point Barrow, Alaska; and back to Denver. Each station was occupied twice.

The southern section of the ACL was observed by B. C. Browne between September and December 1964, observing at the following stations: 1, Denver, Colorado; 2, Monterrey, Mexico; 3, Mexico City, Mexico; 4, La Paz, Bolivia; and back to Denver, occupying each station twice; thence to Washington, D. C., and Teddington.

The Gulf 'M' pendulums. These pendulums, operated by R. Longfield, completed the ACL during the summer of 1964. The sequence of the observations based on the University of Wisconsin base station (Madison) was as follows: 1, Madison; 2, Denver; 3, Great Falls; 4, Edmonton; 5, Whitehorse; 6, Fairbanks; 7, Point Barrow; 8, Point Barrow; 9, Fairbanks; 10, Whitehorse; 11, Edmonton; 12, Great Falls; 13, Denver; 14, Monterrey; 15, Mexico City;

16, La Paz; 17, La Paz; 18, Mexico City; 19, Monterrey; 20, Denver; 21, Madison.

West Pacific Calibration Line (WPCL)

The pendulums of the Geophysical Survey Institute, Tokyo, Japan (G. S. I. pendulums), and the Gulf 'M' pendulums are scheduled for observations along this line during the 1965 observation season.

The G. S. I. pendulums. These pendulums completed the following measurements:

(*a*) 1, Tokyo; 2, Honolulu; 3, San Francisco; 4, Denver; 5, San Francisco; 6, Honolulu; 7, Tokyo. Thus a horizontal connection between the central stations of the WPCL and ACL was provided.

(*b*) Tokyo–Sapporo–Tokyo.

(*c*) Tokyo–Kyushu–Tokyo.

The observations scheduled for 1965 are: 1, Tokyo; 2, Manila; 3, Singapore; 4, Brisbane; 5, Melburne; 6, Melburne; 7, Brisbane; 8, Singapore; 9, Manila; 10, Tokyo; and Tokyo–Fairbanks–Tokyo.

The Gulf 'M' pendulums. The 1965 program of the Gulf 'M' pendulums, which started on July 15, 1965, and will be completed by December 1965, is as follows:

(*a*) 1, Madison; 2, Denver; 3, San Francisco; 4, Honolulu; 5, Tokyo; 6, Fairbanks; 7, Teddington; 8, Teddington; 9, Fairbanks; 10, Tokyo.

(*b*) Tokyo–Sapporo–Tokyo.

(*c*) Tokyo–Kyushu–Tokyo.

(*d*) 1, Tokyo; 2, Manila; 3, Singapore; 4, Brisbane; 5, Melburne; 6, Melburne; 7, Brisbane; 8, New Delhi; 9, Rome; 10, Rome; 11, New Delhi; 12, Singapore; 13, Manila; 14, Tokyo.

(*e*) 1, Tokyo; 2, Honolulu; 3, San Francisco; 4, Denver; 5, Madison.

These observations will provide the required measurements on the WPCL; in addition, they will connect the three primary calibration lines.

Reduction of the Pendulum Measurements

The pendulum observations carried out under this program in 1963 and 1964 have been reduced by the respective observers and the data examined by the principal investigators. The preliminary results have been discussed during two sessions of Study Group 5. The first meeting was held in Milan in April 1964 and was concerned with the 1963 observations. The measurements made during 1964 were presented and discussed in Turin on April 24–25, 1965.

Although the accuracy of the observations, as obtained from the preliminary reductions, are satisfactory (with few exceptions) the publication of the data has been postponed until the comprehensive study of the material and reduction methods is completed. Since pendulum observations frequently are biased by tares, period creep, and environmental effects, G. P. Woollard proposed that the available accurate gravimeter measurements be used for the detection of these systematic effects. The suggestion has been accepted in principle by the group; however, the investigations regarding the mode and the extent of utilization of gravimeter comparisons and the establishment of a uniform reduction method have not yet been completed. It is anticipated that by the next meeting of Study Group 5 (September 1965 in Paris) the problems will be resolved and the results of the observations can be published. The preliminary results are available in the report on the meeting of Study Group 5 (Turin, April 1965).

THE STATUS OF THE GRAVIMETER OBSERVATIONS

The gravimeter measurements started in 1963 with the participation of the following organizations and instruments:

1. Air Photographic and Charting Service (APCS), LCR g 43, g 44, g 47, g 48.

2. Air Force Cambridge Research Laboratories (AFCRL), LCR G 3, G 8, LCR g 2.

3. University of Hawaii, LCR G 1, G 7, W-607.

4. U. S. Naval Oceanographic Office (NAVOCEANO), LCR G 2, LCR g 5, g 15.

5. Army Map Service (AMS), LCR g 45, g 46.

6. Osservatorio Geofisico Sperimentale (OGS), Trieste, LCR G 3, LCR g 2, LCR G 7.

7. Inter American Geodetic Survey (IAGS), LCR g 56, g 57, g 11.

8. Dominion Observatory, Canada, LCR g 7, g 9.

The observations required for the establishment of a uniform world gravity system have

been divided into four basic categories: (*a*) observations along the calibration lines, (*b*) transversal ties between the calibration lines, (*c*) connections between absolute gravity stations, and (*d*) re-occupation of previous pendulum and first-order stations not observed under *a*, *b*, and *c*.

The gravimeter observations completed between 1963 and August 1, 1965, are schematically illustrated on Figure 4. The additional planned measurements are illustrated on Figure 5.

Euro-African Calibration Line (EACL)

The observations on this calibration line have been completed in 1963 and 1964. Most of the instruments listed in the previous paragraph made measurements at least along a section of the line for the purpose of testing the instruments for linearity, periodic errors, and drift.

The pendulum sites occupied during this program have been connected by a 'minimum drift' run utilizing air transport by the following instruments: LCR G 3, G 7, and g 2; in addition, LCR G 1 performed simultaneous observations along the ECL with the Gulf pendulums, and LCR g 2 has been utilized for the same purpose by the Italian pendulum party along the southern section of the line.

In 1964 APCS re-observed the existing European calibration line and extended it to Cape Town, South Africa, establishing gravimeter stations at about 100-mgal intervals. The previous and new pendulum sites along the line have been re-observed.

Gravimeter Connections in Europe

In connection with the Euro-African gravimeter and pendulum operations, the following gravimeter connections have been made in Europe: (*a*) Bad Harzberg–Potsdam (LCR G 3, G 7, g 2 by Osservatorio Geofisico Sperimentale, Trieste); (*b*) Teddington–Potsdam (LCR G 1, G 7, University of Hawaii); and (*c*) Potsdam–Paris–Teddington (LCR G 1, W-607, G. P. Woollard).

American Calibration Line (ACL)

In 1963 APCS completed the ACL in two trips. In the first trip the present North American calibration line was measured occupying the pendulum sites between Houston and Point Barrow, utilizing seven small LCR gravimeters. In the second trip the line was extended to South America, establishing new stations at about 100-mgal intervals between Mexico City, Mexico, and Ushauaia, Argentina. Eight LCR gravimeters (five identical with the instruments used along the northern section) were used for these measurements.

In 1964 a party composed of AFCRL, OGS, and University of Hawaii performed a 'minimum drift' run between Point Barrow and Panama, utilizing LCR G 1, G 3, G 7, G 8, and g 54 gravimeters transported by a special aircraft.

During 1962 and 1963 Dominion Observatory, Ottawa, performed observations along the ACL, using LCR g 7 and g 9. The data are under recomputation.

West Pacific Calibration Line (WPCL)

APCS connected existing pendulum stations between Fairbanks, Alaska, and Christchurch, New Zealand. Intermediate gravimeter stations have been established at 100-mgal intervals. The observations have been accomplished in 1964. The WPCL and EACL have been connected between Rome and Singapore, occupying Ankara (Turkey), Beirut (Lebanon), Teheran (Iran), Kabul (Afganistan), and New Delhi (India) intermediate stations.

Secondary Calibration Lines

APCS will establish three 'secondary' calibration lines to serve the purpose of instrument calibration in the respective areas and to provide connections for the first-order world gravity net (FOWGN). Figures 4 and 5 show only those portions of the secondary lines that are anticipated to serve the purpose of the FOWGN.

American secondary calibration line. The presently existing line between Key West, Florida, and Maine is extended southward along the eastern coast of South America, joining the ACL at Buenos Aires. The observations include existing pendulum and first-order stations and provide intermediate stations at approximately 100-mgal intervals. The line will be extended to the northern edge of the North American continent.

Euro-African secondary calibration line. This line is partly completed and includes several

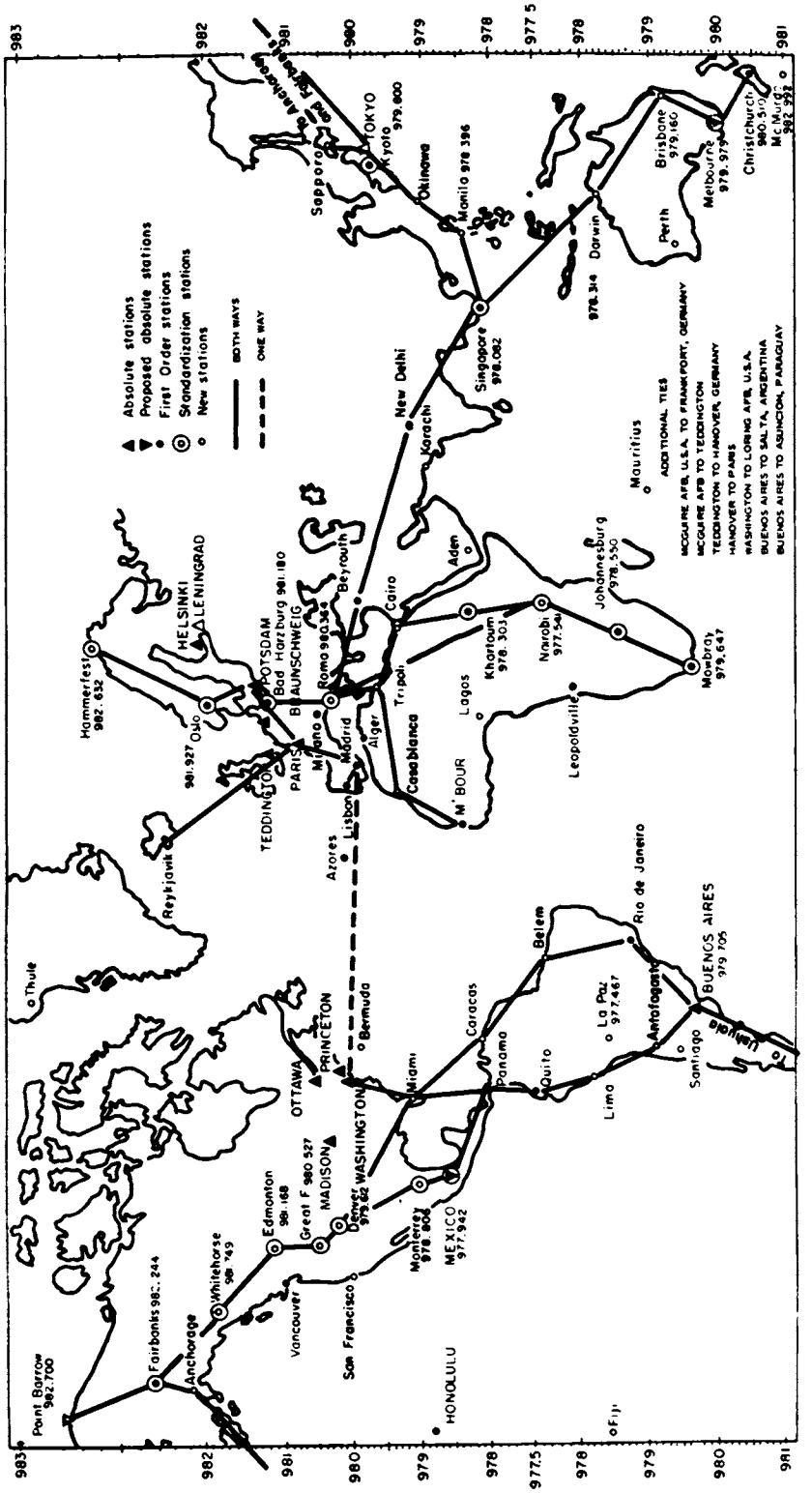

Fig. 4. Completed gravimeter observations since 1963 as of August 1, 1965.

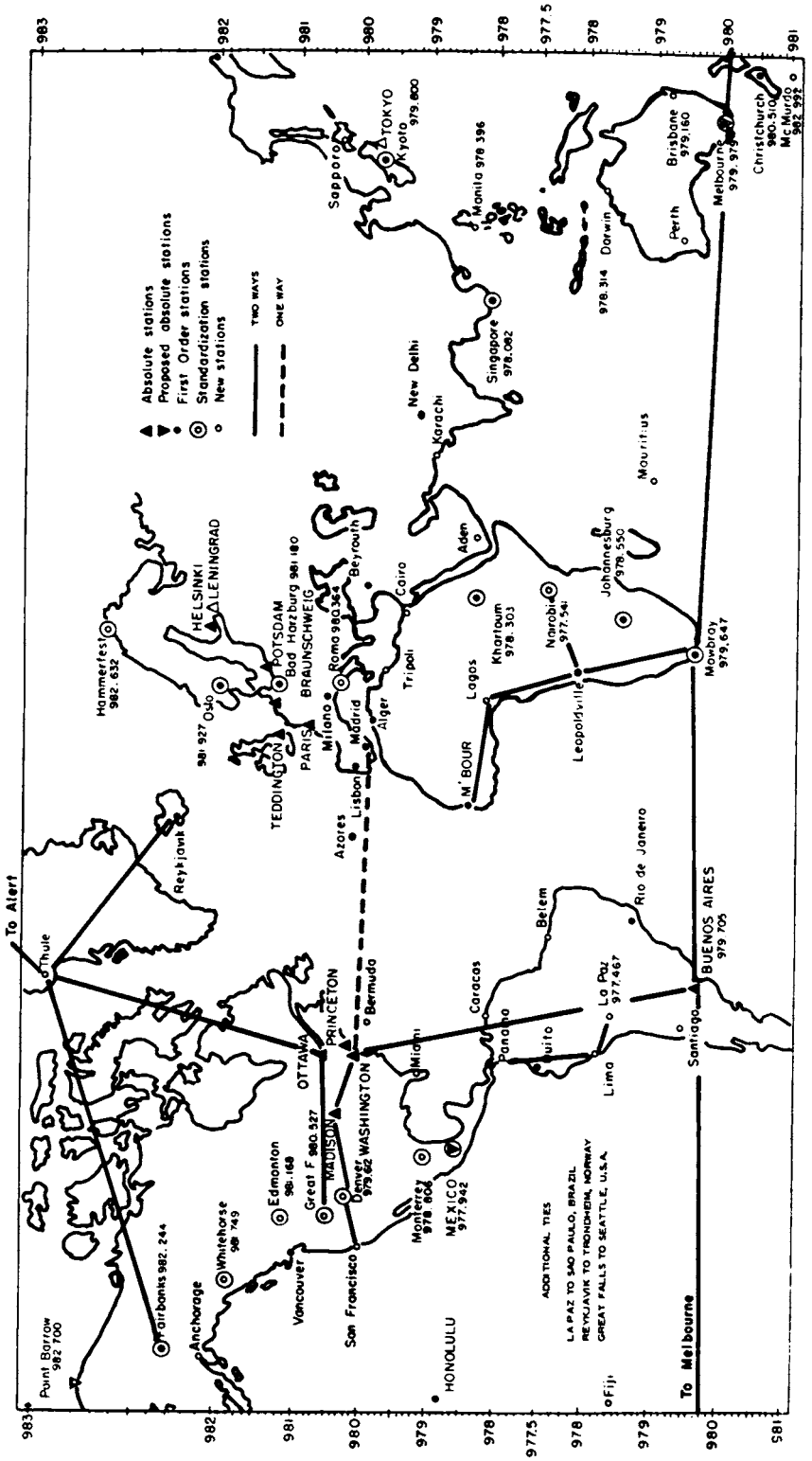

FIG. 5. Planned gravimeter observations.

first-order stations along the west coast of Africa and Europe.

Central Asian calibration line. This line has been established by APCS during the return trip from the WPCL. It is a north-south line between New Delhi and Ceylon, including the stations established by Woollard in 1962.

Data Deduction and Analysis

The large quantity of gravimeter observations collected since 1963 are provisionally reduced by the observers. For some observations, adjusted values are also available. Obviously, these results remain provisional until a unique calibration standard is established. The observation material with few exceptions has been submitted to Study Group 5. The Osservatorio Geofisico Sperimentale, Trieste, analyzes these observations and utilizes the measurement for (*a*) determination of instrument characteristics and accuracies, (*b*) comparison of the measurements and cataloguing the data, (*c*) evaluation of the reduction methods for the purpose of establishing standardized computation procedures, (*d*) comparison of the scale of existing calibration lines, and (*e*) preparation of the existing material for the purpose of the FOWGN.

International Absolute Reference System

Completed Experiments

Since the 1962 Assembly of the International Gravity Commission, one absolute experiment has been reported as successfully completed. This experiment was conducted by Cook at the National Physics Laboratory, Teddington, England. The mean square error of the obtained value is ±0.15 mgal. Although Cook's upward projected ball experiment is transportable, the size, the weight, and the time needed for repetition of the experiment at another site require careful and elaborate preparations. The possibilities and the required arrangements for the repetition of Cook's experiment at a site in the United States or Canada will be discussed during the forthcoming session of the International Gravity Commission.

Experiments in Preparation

For the solution of the absolute gravity reference problem, portable experiments have critical importance. Currently, AFCRL is directly engaged in, or supports, the preparation of such portable absolute experiments. Currently three experiments are in various stages of refinement, construction, or research. It is anticipated that two of these experiments will be completed during 1965 or the first part of 1966, and the instruments could be used for experiments at other absolute sites within the framework of this program.

The AFCRL reversible pendulum apparatus. During the past year efforts have been concentrated on the detection and elimination of systematic effects. The interferometric measurement of the length of the pendulums has been checked by independent methods, and the accuracy obtained by the apparatus is satisfactory. An electrostatic investigation of the pendulums has determined the existence of a charge. The relationship between charge and period has been experimentally established and the effect eliminated by neutralization of the charge. Measurements are being made to determine the indentation of the flat and curvature on the knife edge. It is expected that a complete experiment will be made by December 1965 with better than ±1-mgal accuracy.

A laser-interferometric absolute experiment. This experiment is being constructed at National Bureau of Standards in Boulder, Colorado, under AFCRL support. The fabrication of the actual dropped piece is completed, and the high vacuum section of the apparatus is under construction. The laser, specially constructed by the Spectra Physics Corporation, will be delivered in August 1965. Investigations are conducted to eliminate the effect of ground motion. The delivery of this apparatus is anticipated in early 1966.

A charged particle free-fall experiment. This experiment is in the research stage at Martin Company, Orlando, Florida, under contract to AFCRL. Laboratory experiments are being conducted to determine the parameters of an experimental apparatus. Application of this technique in a complete experiment is not anticipated until the end of 1966.

Conclusions

The present status of the field measurements indicates that the program launched in September 1962 is on schedule. Both the pendulum

and gravimeter measurements will be completed by July 1966 with the possible remaining requirement of a few measurements for verification. The reduction of the observations is somewhat behind schedule, but, after the solution of several initial difficulties, it is expected that this phase of the work will proceed on schedule. The absolute experiments accomplished less than anticipated in 1962; however, during the forthcoming meeting of the International Gravity Commission, additional information will be available regarding the progress of the various fixed-site laboratory experiments. It is anticipated that by the end of 1966 the results of several portable experiments would be available and that they could provide one step toward the refinement of the presently best known absolute reference value. As soon as these portable experiments have eliminated the initial difficulties, additional measurements at the required stations would be possible in a relatively short time.

Many difficulties that have been overcome in the realization of the program could not have been accomplished without the excellent cooperation and support of the U. S. and foreign governments, universities, scientific institutions, and interested scientists.

Appendix. Unpublished Reports

Browne, B. C., Gravity measurements made with the Cambridge pendulums on the southern sector of the American gravity calibration base, 1965.

Gough, D. I., Report for Special Study Group No. 5 on gravity measurements on the first-order world gravity net with the Cambridge pendulum apparatus, carried out by the Southwest Center for Advanced Studies, Dallas, Texas.

Honkasalo, T., Report for Special Study Group No. 5 of the International Association of Geodesy on gravity measurements in the first-order gravity net with Cambridge pendulum apparatus, carried out by the Finnish Geodetic Institute, 1963.

Jackson, J. E., Continuation of the Europe-Africa calibration lines southward from Rome to Cape Town, 1963.

Mateo, Jose, Report on University of La Plata Askania pendulum measurements 1963, United States-Europe-Africa connections.

Mazzon, C., and V. Tomelleri, Temporary report on the pendular and gravimeter expedition in South Africa executed by Instituto di Geodesia, Topografia e Fotogrammetric of the politecnico of Milano, 1963.

Wahlen, C. T., The American calibration line (ACL) phase report no. 1, APCS OPLAN 503, 1964.

Wahlen, C. T., The Euro-African calibration line (EACL) phase report no. 2, APCS OPLAN 503, 1965.

Woollard, G. P., The role of gravimeter observations in the establishment of gravity standardization values, Hawaii Institute of Geophysics.

Woollard, G. P., An evaluation of the Potsdam station, *Hawaii Inst. Geophys. Sci. Rept. 1*, (contract AF19(628)-2849), 1963.

Woollard, G. P., Report on Gulf pendulum measurements, European-African calibration line, 1963.

Woollard, G. P., An analysis of the reliability of gravimeter measurements, *Hawaii Inst. Geophys. Sci. Rept. 3* (contract AF19(628)-2849), 1964.

Woollard, G. P., and R. L. Longfield, Results of the 1964 Gulf pendulum measurements on the American gravity standardization range, April 1965.

References

Morelli, C. The first-order and absolute world gravity nets, *Boll. Geofis. Teorica Appl.*, *5*(19), 1963.

Szabo, B. World calibration standard first-order gravity net and absolute gravity system, *Boll. Geofis. Teorica Appl. 5*(19), 1963.

Gravity Surveys at Sea by the Institute of Geophysics at UCLA

MICHELE CAPUTO[1]

Institute of Geophysics and Planetary Physics
University of California, Los Angeles

For the past five years the Marine Gravity Project of the Institute of Geophysics at the University of California, Los Angeles, has been operating a LaCoste-Romberg surface ship gravity meter on various cruises in the Pacific, Indian, and Atlantic oceans. Approximately 80,000 miles of track have been measured. Widely spaced tracks make up the majority of the mileage (20,000 miles in the Pacific Ocean, 24,000 in the Indian Ocean, 2,000 in the South China Sea, and 4,000 in the Atlantic Ocean), but three areas have been surveyed in detail (52,000 miles with 21,000 stations in the Gulf of California, 8,500 miles with 3,400 stations in the California borderland, and 15,000 miles with 6,000 stations in the Indonesian archipelago). Free-air anomalies have been published in interim reports on the results of the various cruises. Reports have been issued for all these cruises and are available. Research is in progress on the gravity anomalies in the California borderland, in the Gulf of California, and in Indonesia.

The reports on these surveys are listed below; data on ships used during surveys are given in Table 1.

1. Comparisons of Readings of Sea Gravimeter, Bottom Gravimeter, and Geodetic Gravimeter, and Gravity Survey in the Gulf of California, 1959. Interim report by J. C. Harrison and F. N. Spiess, 1961. (R. V. *Horizon*)

32 profiles crossing the Gulf; 2,078 gravity stations at 2-mile intervals in Gulf and near mouth of Gulf. Port connections: San Diego (California) and Mazatlan, La Paz, Guaymas, San Felipe (Mexico).

Free-air and Bouguer anomalies.

Data checked at 27 locations with underwater meter (mean difference, 2.7 mgal; std. dev., ±1.5) and at 9 locations with geodetic meter (mean difference, 1.1 mgal; std. dev., ±2.6 mgal).

2. Gravity Measurements in the Northern Continental Borderland Area off Southern California, 1958–1959. Interim report by J. C. Harrison, 1961. (U.S.S. *Butternut,* 809 stations; R. V. *Horizon,* 168 stations).

Area lies between 32° and 34°N and 117° and 120°W; 977 gravity values at 2-mile intervals relatively evenly spaced east of 119°W; few measurements SW of 119°W, 33°N. Port Connections: Long Beach (California).

Free-air and Bouguer anomalies.

41 crossings (mean difference, 4.9 mgal). (See Table 2 of *Caputo et al.* [1963].)

3. Gravity Measurements in the Southern Continental Borderland West of Baja California, 1959. Interim report by J. C. Harrison. (R.V. *Horizon,* 1169 stations; R.V. *Smith,* 232 stations; R.V. *Baird,* 208 stations).

Area lies between 28° and 32°30′N and 114°30′ and 119°30′W; 1609 gravity values at 2-mile intervals, about two-thirds of them north of 30°30′N. Port connections: San Diego (California).

Free-air anomalies.

32 crossings (mean difference, 5.3 mgal). (See Table 2 of *Caputo el al.* [1963].)

4. Gravity Measurements on the Cruise of the U.S.S. *Gear,* 1961. Interim report by C. E. Corbato and M. D. Helfer.

Additional measurements in northern borderland area 32°30′, 34°30′N, 121°30′, 118°W but with two extensions beyond the continental slope; 495 measurements at 2-mile intervals. Port connections: San Pedro (California).

Free-air and Bouguer anomalies.

32 crossings, including crossings of previous

[1] Now at Department of Geophysics, University of British Columbia, Canada.

TABLE 1. Ships Used during Surveys

Name	Length, ft	Displacement, tons	Survey for Which Used
R.V. *Horizon*	143	900	1, 2, 3
U.S.S. *Butternut*	146	805	2
R.V. *Smith*	128	561	3
R.V. *Baird*	143	997	3
U.S.S. *Gear*	207	1897	4
U.S.S. *Rexburg*	181	850	5
R.V. *Argo*	213	2097	6, 8

surveys (mean difference, 5.6 mgal). (See Table 2 of *Caputo et al.* [1963].)

5. Gravity Survey of the Santa Barbara Channel (California) with the U.S.S. *Rexburg*, 1962. Interim report by M. D. Helfer, R. von Huene, and Michele Caputo.

458 gravity measurements: 118 on the way to the Channel from San Diego at 2-mile intervals and 340 in the Santa Barbara Channel. 13 N-S lines, 4 E-W. Port connections: San Diego (California).

Free-air and Bouguer anomalies.

81 crossings including crossings of previous surveys (mean difference, 3.9 mgal). (See Table 2 of *Caputo et al.* [1963].)

6. Gravity Measurements across the Pacific and Indian Oceans (Monsoon Expedition, 1960.) Interim report by M. D. Helfer, Michele Caputo, and J. C. Harrison. (R. V. *Argo*)

37,000 mile cruise with 7,009 gravity measurements in portions at 2-mile intervals across the Pacific Ocean and the Indian Ocean. Port connections: San Diego (California), Honolulu (Hawaii), Cairns and Darwin (Australia), Jakarta (Indonesia), Port Louis (Mauritius), Freemantle and Hobart (Australia), Papeete (Tahiti), San Diego (California).

Free-air anomalies.

13 crossings (mean difference, 6.5 mgal).

7. Gravity observations in the equatorial Pacific November-December 1961. (U.S.S. *Rehoboth*)

Observations made in conjunction with U. S. Navy Hydrographic Office equatorial surveys. Approximately 7,000 miles of measured track. Port connections: Pearl Harbor (Hawaii) and San Francisco (California).

Free-air anomalies.

8. Gravity Measurements over the Pacific, Indian, and Atlantic Oceans during 1962–1963. Interim report by M. Caputo, R. Masada, M. D. Helfer; C. L. Hager, 1964. (R.V. *Argo*)

Port Connections: San Diego (California), Manila (Philippines), Jesselton (Borneo), Singapore, Mombasa (Kenya), Colombo (Ceylon), Cochin (India), Port Louis (Mauritius), Freemantle, Darwin (Australia), Djarkarta (Indonesia), Colombo (Ceylon), Mombasa (Kenya), Cape Town (South Africa), Freetown (Sierra Leone), Balboa (Panama), San Diego (California). About 20,000 stations.

Free-air anomalies.

9. Gravity Measurements in the Indonesian Archipelago, January 1963. Interim report by M. D. Helfer and Michele Caputo, 1964. (R.V. *Argo*)

9,400 miles of measured track from New Guinea to the Nicobar Islands along the Indonesian gravity low, with 3,760 stations. Port Connections: Darwin (Australia), Djarkarta, (Indonesia), and Colombo (Ceylon).

Free-air anomalies.

Accuracy. In a paper published in the *Journal of Geophysical Research* [*Caputo et al.*, 1963] we analyzed the results of 231 track intersections in the California borderland. We showed that 80% of the intersections agreed to 10 mgal or less and that, if intersections with large sounding discrepancies were not included, about 80% would then agree to 7 mgal or less. On the last cruise made in the borderland with the meter in its most advanced state of development and navigation by means of land fixes, over 85% of the intersections agreed to 5 mgal or less. Probably navigation errors on this cruise almost equaled instrument errors, and we are at the point now where it is as important to improve navigation methods as it is to improve the gravity meter. Ocean navigation generally consists of three or less fixes per day; therefore errors of up to 4 mgal in Eotvos correction and up to two from position error (latitude) would not be unusual. A conservative guess at

the accuracy of our data would be that 80% are within 10 mgal of the true values.

Acknowledgment. L. B. Slichter is the Director of the Marine Gravity Project of the Institute of Geophysics and Planetary Physics of UCLA.

References

Caputo, Michele, J. C. Harrison, Roland von Huene, and M. D. Helfer, Accuracy of gravity measurements off the coast of southern California, *J. Geophys. Res.*, *68*(10), 3273–3282, 1963.

The State of Gravity Mapping in Canada, November 1964

M. J. S. INNES

Dominion Observatory, Ottawa, Ontario, Canada

This major objective of the Gravity Division at the Dominion Observatory is to complete the gravity survey of Canada, including inland waters and the continental shelves, as rapidly as possible. A regional mapping program with stations at 8- to 10-mile intervals has been under way since 1958, and in recent years about 8,000 stations have been added each year.

In 1961 the Gravity Map Series was initiated as a publication series of the Dominion Observatory, Department of Mines and Technical Surveys. In this series Bouguer anomaly maps are published at a scale of 1:500,000 using maps of the National Topographic Series as a base. Background planimetric data are in gray, water systems in light blue, with gravity information overprinted in red. Contours are shown at five-milligal intervals. The state of progress in this series is illustrated on the accompanying index map (Figure 1).

Generally, these maps are released in groups accompanied by a report on the quality of the data and a preliminary interpretation in terms of geological structure. The following maps have been published in this series.

Nos. 1–4

General Characteristics of the Gravity Field in West Central Quebec, by J. G. Tanner, 1961.

1. Eastmain
2. La Grande
3. Lac Bienville
4. Great Whale

Nos. 5 & 6

The Gravity Anomaly field in the Ungava Region of Northern Quebec, by J. G. Tanner and R. K. McConnell, 1964.

5. Cape Smith-Povungnituk
6. Wakeham Bay

No. 11

Regional Gravity Survey of the Sverdrup Islands and Vicinity, by L. W. Sobczak, 1963.

Nos. 12–15

Preliminary Results of Gravity Surveys in the Queen Elizabeth Islands, by L. W. Sobczak, J. R. Weber, A. K. Goodacre, and J-L. Bisson, 1963.

12. Sverdrup Islands
13. Devon Island
14. Melville Island
15. Prince Patrick Island

No. 46

Preliminary Result of Underwater Gravity Surveys in the Gulf of St. Lawrence, by A. K. Goodacre, 1964.

46. Gulf of St. Lawrence

In general, data are not released until the maps and reports are published. After publication, copies of the listing of principal facts or copies of the punched cards are available on request. Thirteen map sheets are in press and several others are in an advanced stage of compilation.

Older maps are included in Publications of the Dominion Observatory as follows:

Vol. 16, No. 7

Gravity Measurements in the Maritime Provinces, by G. D. Garland, 1953.

Vol. 19, No. 4

Gravity Measurements in Quebec, South of Latitude 52°N (containing Gravity Anomaly Map on a scale 24 miles to 1 inch), by L. G. D. Thompson and G. D. Garland, 1957.

Vol. 19, No. 5

Investigations of Gravity and Isostasy in the Southern Canadian Cordillera (containing Gravity Anomaly Map on a scale 40 miles to 1 inch), by G. D. Garland and J. G. Tanner, 1957.

Vol. 21, No. 5

Gravity Anomalies in the Gaspé Peninsula, Quebec (containing one Gravity Anomaly Map on a scale of 4 miles to 1 inch), by J. G. Tanner and R. J. Uffen, 1960.

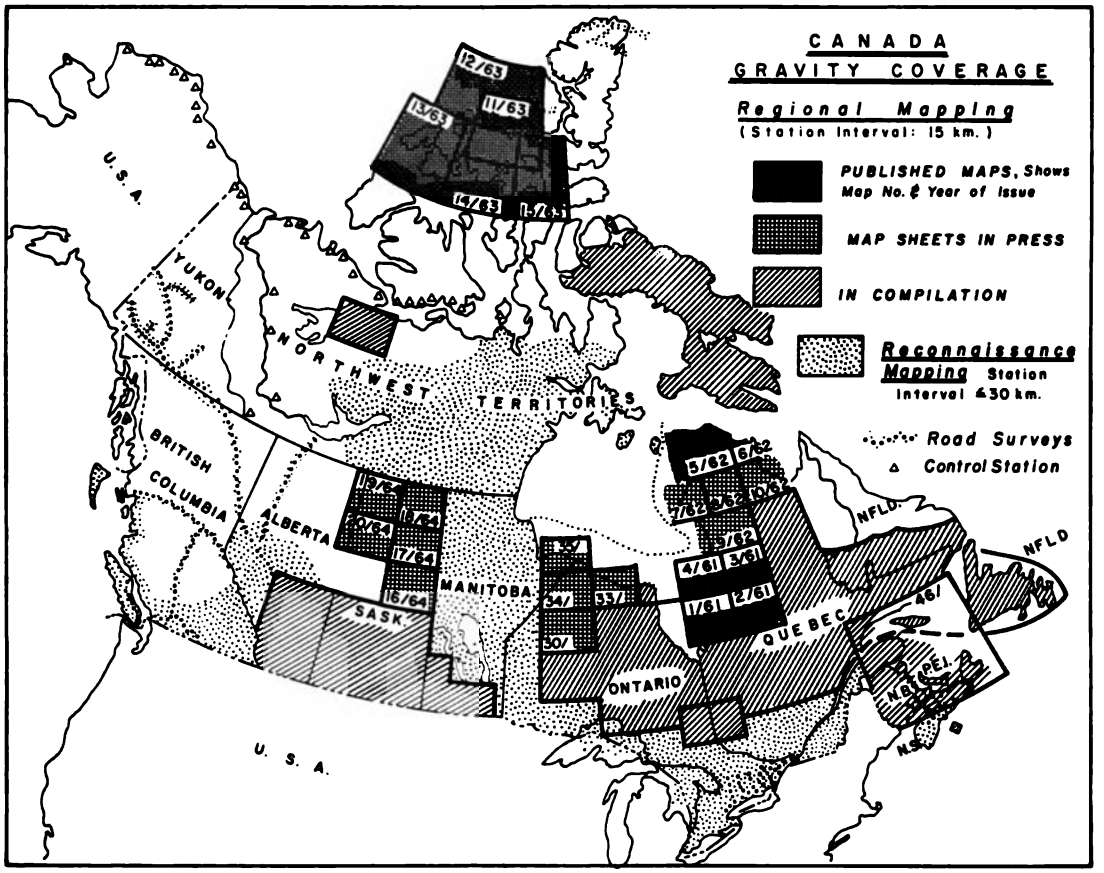

Fig. 1. Index map showing progress of the Gravity Map Series of the Dominion Observatory, Department of Mines and Technical Surveys.

Vol. 21, No. 6

Gravity and Isostasy in Northern Ontario and Manitoba (containing Gravity Anomaly Map on a scale of 20 miles to 1 inch), by M. J. S. Innes, 1960.

Additional older maps are also available:

Gravity Anomaly Map, Province of Alberta (scale of 1 inch to 20 miles), 1952.

Gravity Anomaly Map, Province of Manitoba (scale of 1 inch to 20 miles), 1952.

Gravity Anomaly Map, Province of Saskatchewan (scale of 1 inch to 20 miles), 1952.

Gravity Anomaly Map, Canada (scale of 1 inch to 100 miles), 1957.

A limited number of reconnaissance surveys have been completed in the Northwest Territories in preparation for an updated edition of the gravity map of Canada.

Advances in Aerial Gravity 1963–1964

LLOYD G. D. THOMPSON[1] AND CHARLES S. HAWKINS

Air Force Cambridge Research Laboratories
L. G. Hanscom Field, Bedford, Massachusetts

Abstract. Continuing research at AFCRL (Air Force Cambridge Research Laboratories) during 1963 and 1964 produced a C-130 and a KC-135 aircraft modified and instrumented for aerial gravity measurements, a new stabilized platform for airborne gravity meters, a new configuration of the LaCoste-Romberg gravity meter on the new stabilized platform with new transistorized electronics, a new revision of the Askania-Graf gravity meter on a stabilized platform with new transistorized electronics, a digital magnetic tape recording system for both of the above meters and for the Air Profile Recorder, and a new Worden miniature digital airborne gravity meter.

INTRODUCTION

Since the conclusion of AFCRL aerial gravity flight tests in 1962 [*Thompson,* 1963], significant improvements have been made in the airborne gravity meters and associated equipment. Unfortunately, delays in aircraft modification, fuel leaks on assigned aircraft, and insufficient allocation of time for aircraft support have precluded further flight tests.

AIRCRAFT INSTRUMENTATION

During 1963 a KC-135 aircraft was equipped with a modified Air Profile Recorder to provide absolute altitude of the aircraft to ±10 ft, a 35-mm vertical camera to provide the nadir point of the aircraft continually or on command, a photo-panel to record navigational data from an N-1 compass, an APN-81 Doppler navigation system, and an ASN-7 navigational computer. These systems should provide direction to an accuracy of ±½° and ground speed to ±1 knot. This modification provided for the installation of both the LaCoste-Romberg meter and the Askania-Graf meter in their 1962 configurations on modified ART-25 stabilized platforms [*Thompson,* 1963]. Owing primarily to repeated fuel leaks, actual flight testing was not accomplished before the aircraft was assigned to support a higher priority project.

During 1963–1964 a C-130 aircraft was equipped with a modified Air Profile Recorder, a T-11 vertical mapping camera on a modified ART-25 stable platform, two side-looking T-11 cameras, an MD-1 astro tracker, an APN-144 Doppler radar, an APA-95 navigational computer, a photo-panel to record navigational parameters, and some meteorological instruments. The accuracy of this combined system would be approximately the same as the accuracy outlined for the KC-135 aircraft, with an anticipated reduction in directional error. This modification also provided for the installation of both the LaCoste-Romberg meter and the Askania-Graf meter in their 1962 configurations on modified ART-25 stabilized platforms. After this modification was completed, the remaining time for utilization of the aircraft on the gravity project was insufficient to allow flight testing of the equipment, and the aircraft was released to the other project it supports.

AIRBORNE GRAVITY METERS

The LaCoste-Romberg gravity meter was flown in the early 1962 tests in a gimbal suspension, which is basically a sea-meter configuration. The Askania-Graf gravity meter was flown in the 1962 tests on a modified ART-25 stabilized mount. Modifications to the mount consist of an integrating erection amplifier system to give a more accurate vertical.

During the last of the 1962 tests the LaCoste-

[1] Now at Geo Space Gravity Observatory, Division of Western Equities, Inc., Woburn, Massachusetts.

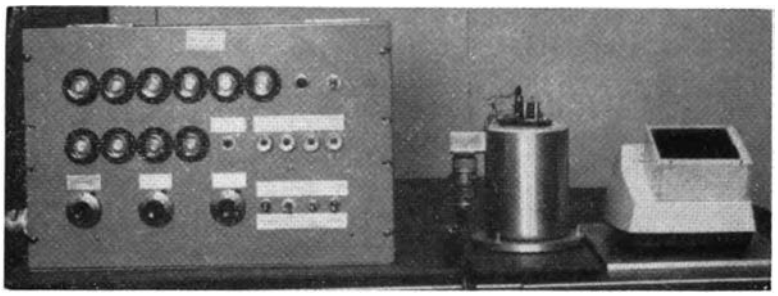

Fig. 1. Worden miniature digital airborne gravity meter.

Romberg meter was flown on a modified ART-25 stabilized mount.

Results of the 1962 tests indicated that the stabilized platform technique was superior to the gimbal suspension configuration [*Thompson*, 1963] for aerial gravity measurements. Therefore, a new stabilized platform was specifically designed for an airborne gravity meter and was developed in 1963–1964 at the Aeroflex Laboratories, where the ART-25 was also manufactured and modified. The new platform, designated ART-57, is a general purpose mount for a research and development program. It is not a high-precision or expensive mount, but it does include a high-quality gyro and an integrating erection amplifier system which should have a capability of 2–5 min arc in verticality under good flight conditions. It has transistorized components and 30° of freedom in the pitch and roll axes.

The LaCoste-Romberg gravity meter has been mounted on the new ART-57 stabilized platform. Since previous tests indicated that the LaCoste-Romberg meter is extremely sensitive to vibrations, special cable isolators were incorporated on this mount in an effort to eliminate or at least to reduce spurious readings resulting from vibrations. A three-component accelerometer system for measuring aircraft accelerations and an electrolytic level bubble system for monitoring the platform verticality have also been incorporated on the mount.

The original electronic equipment provided with the LaCoste-Romberg gravity meter has been a continual source of trouble and a suspected source of error in the measurements. A long warm-up time and frequent, if not daily, ground calibrations were required. The environment on board the aircraft was a contributing factor, because much of the electronic equipment was designed for use on submarines and surface ships where ambient temperatures are relatively constant, whereas on an aircraft there are large temperature changes as well as vibrations. This condition has caused tube failures and shifts in calibration factors. In an effort to solve this problem, the entire electronic package has been transistorized to give more stable operation. This entire system has been completely checked in the laboratory but has not been flight tested.

The Askania-Graf meter has also been modified by providing an outer heater jacket, transistorizing the electronics, and adding a wide chart recorder. These modifications should overcome the temperature problem and also facilitate more accurate and reliable gravity readings. This equipment has also been checked in the laboratory and is ready for flight testing.

The new Worden miniature digital gravity meter shown in Figure 1 is the only meter designed and fabricated as an airborne gravity meter. This prototype instrument has been successfully tested in the laboratory but at present requires a new binary counter and a few minor modifications before actual flight testing.

Previous flight tests demonstrated that the analog systems of recording used by the LaCoste-Romberg meter and the Askania-Graf meter were extremely costly in both time and funds from the standpoint of data reduction. Accordingly, a digital tape recording system has been designed and fabricated to accept the outputs of both meters plus the output of the Air Profile Recorder. In addition, this recording system is

capable of accepting and recording all navigational parameters when an optimum navigation system has been definitely selected. This capability will allow direct input to a computer for rapid data reduction.

References

Thompson, Lloyd G. D., Comparison of LaCoste-Romberg and Askania-Graf airborne gravity meters in gimbal and stabilized mounts (abstract), *Trans. Am. Geophys. Union, 44,* 31, 1963.

Some Recent Developments in Gravity Measurements Aboard Surface Ships[1]

MANIK TALWANI

Lamont Geological Observatory
Columbia University, Palisades, New York

Abstract. Errors experienced by surface ship gravimeters which arise from the ship's horizontal accelerations are discussed. Results from a continuously recording analog computer show that the cross-coupling errors can be appreciable under normal sea conditions. Off-leveling errors for the Anschutz gyrotable aboard R.V. *Robert D. Conrad* are small. It is shown that the off-leveling error in the determination of the Browne correction for a gimbal-suspended gravimeter is identical to the off-leveling error experienced by a gravity meter on a stable platform, provided that the same vertical reference is used and the servo errors are the same. The gyros are more error free as vertical references than are long-period pendulums. A simple slope correction can be applied to the record of the Graf-Askania Gss2 gravity meter to correct for the instrument response; thus 'instantaneous' gravity values can be obtained. An analog computer to compute and record the Eotvos correction continuously has been developed. Data reduction and display procedures are described.

INTRODUCTION

The accuracy of gravity measurements at sea is generally tested by going over a gravity range or by making track intersections. The present paper will, however, be devoted primarily to a different aspect of the problem of accuracy, namely the possible magnitudes of the various errors, their causes, etc. Since the author is most familiar with the Graf-Askania sea gravimeter mounted on a stable platform, this paper will mainly concern itself with the errors of measurement with such a system.

STUDIES OF ERRORS

Cross-coupling error for gravity meter mounted on a stable platform. LaCoste and Harrison [1961] first called attention to the cross-coupling effect. Consider a gravimeter mounted so that the beam lies along the ship's fore and aft direction and moves only in the vertical plane through small angles around the horizontal. Let $\ddot{x}$ be the instantaneous value of the surge acceleration. Let ϕ_1 be the instantaneous value of the periodic part of the beam motion, caused primarily by heave. In this paper the terms heave, surge, and sway will be used, respectively, for the vertical, fore and aft, and athwartship accelerations. The instantaneous cross-coupling acceleration is given by $\ddot{x}\phi_1$. Both $\ddot{x}$ and ϕ_1 can be broken up into their respective Fourier components and, if any of the Fourier terms in $\ddot{x}$ and ϕ_1 with the same period have a phase difference other than 90°, the time average of the product $\ddot{x}\phi_1$ will not be zero and a cross-coupling error will result. The gravity meter does not distinguish this error from gravity. For the cross-coupling error, as for the off-leveling errors discussed later in the paper, we will concern ourselves mainly with the time averages rather than the instantaneous errors, owing to the averaging characteristic of the meter due to its high damping. Assuming for simplicity that $\ddot{x}$ and ϕ_1 are sinusoidal with respective amplitudes $\ddot{x}_{amp}$ and $\phi_{1\,amp}$ and that they have the same period but with phase difference θ, the average cross-coupling error is given by $\frac{1}{2}\,\ddot{x}_{amp}\,\phi_{1\,amp}\cos\theta$.

Some confusion has arisen about the magnitude of the cross-coupling effect, mainly because different authors have used different instrument constants in their calculations. For all practical purposes $\phi_{1\,amp}$ is determined by the magnitude of ship's heave. Assuming the heave acceleration

[1] Lamont Geological Observatory Contribution 875.

to be sinusoidal with amplitude $\ddot{z}_{amp}$ and frequency ω, $\phi_{1\ amp}$ is given by the relation $\phi_{1\ amp} = \ddot{z}_{amp}(E/B\omega)$; E the static sensitivity of Graf-Askania Gss2 meter is 5×10^{-3} rad/gal, B the time constant [*Graf and Schulze*, 1961] is 250 sec. On the other hand, LaCoste and Harrison assume for their calculations a static sensitivity of 10^{-3} rad/gal and a time constant of about 33 sec; hence the actual values of cross coupling with the Gss2 meter are about 1/16 the estimates given by LaCoste and Harrison. The static sensitivity is related to the natural period p of the beam system by the relationship $E = (p^2a/4\pi^2k^2)$, where k equals the radius of gyration, and a the distance from the hinge point to the center of gravity of the beam. For the Gss2 meter $p = 2.4$ sec and $k^2/a \simeq 30$ cm. It is also of some interest to note that, for damping equal to critical, the time constant B would have been equal to p/π. Thus the damping of the Gss2 meter is about 325 times critical. For such a highly damped meter the beam motion ϕ_1 lags very nearly 90° behind $\ddot{z}$. If the horizontal and vertical accelerations have a phase difference of 90°, θ would be nearly equal to zero, bringing about maximum cross coupling. Theoretical considerations predict circular motions for water particles at some depth, thereby giving a phase difference of 90° between the vertical and horizontal accelerations [*LaCoste and Harrison*, 1961; *Fritsch*, 1964].

Until recently, however, it was not clear what the actual values of cross coupling for a surface ship would be. Definitive answers were obtained in a study of the cross-coupling effect by *Wall et al.* [1966]. In this study records of beam motion and horizontal accelerations obtained aboard R.V. *Vema* were digitized, and the instantaneous cross-coupling accelerations were obtained by direct multiplication on a high-speed digital computer. These studies showed that, when *Vema* was headed into the sea and swell, the surge accelerations (forward) did indeed lead the heave accelerations (upward) by nearly 90°, and, when *Vema* had a following sea and swell, the surge accelerations lagged the heave accelerations by nearly 90°. For beam seas there was no consistent phase difference between surge and heave that lasted for more than a few cycles of the ship's motion. Thus for a gravity meter mounted with its beam along the fore and aft direction on a ship such as the *Vema*, cross coupling would not be small unless the seas were very calm or the sea and swell were on the beam. The problem is not solved by mounting the meter with its beam athwartship, since cross coupling is appreciable for beam seas because the sway accelerations also tend to lead or to lag the heave accelerations by 90°.

It was, therefore, decided that an analog computer that would continuously compute and record the cross-coupling error be constructed. Details of the operations of this computer and the results obtained will be published elsewhere [*Talwani et al.*, 1966]. The principle used in the construction of the computer and some of the results are summarized below.

Figure 1 shows a schematic block diagram of the gravity meter and the analog computer. The top part of the figure shows how the periodic beam motion ϕ_1, arising (primarily) out of the heave acceleration, interacts with the surge acceleration to give a cross-coupling acceleration. The heavily damped gravimeter acts as a simple low-pass filter of time constant 250 sec for accelerations with the period of sea motions. In the analog computer the analog of the beam motion is obtained by filtering the electrical signal from a heave-measuring accelerometer through a simple RC filter of time constant 250 sec. A magnetic four-quadrant multiplier multiplies the analog of beam motion with the analog of surge acceleration (obtained from a surge-measuring accelerometer) to get the instantaneous cross-coupling acceleration. Examples of the instantaneous cross-coupling acceleration obtained by the analog computer aboard R.V. *Conrad* are shown in Figure 2 together with traces of the heave and surge acceleration as well as the periodic beam motion. For the ship heading into the swell (Figure 2, *bottom*), we note that the heave acceleration (up) lags the surge acceleration (forward) by about 90°. The beam motion which lags the heave acceleration by 90° (noting that an upward heave is equivalent to a downward beam motion) is, therefore, almost 180° out of phase with the surge acceleration. The product of beam motion and surge acceleration, which is the instantaneous cross-coupling acceleration, is almost always positive (for the installation on the *Robert D. Conrad*, where the beam length is along the fore and aft direction and the center

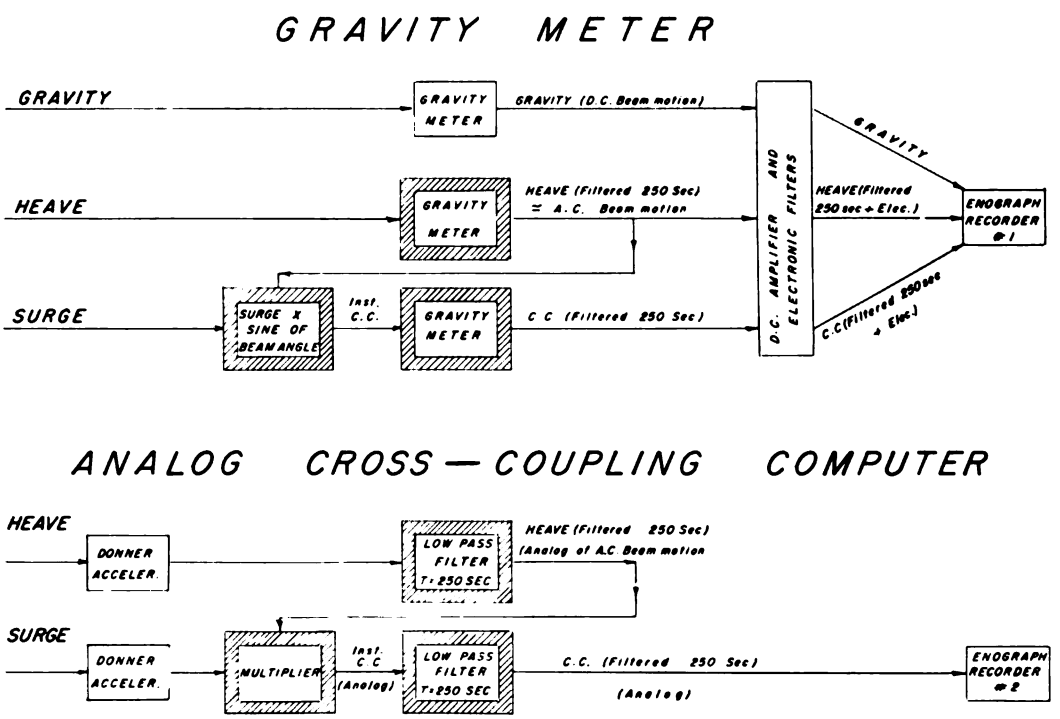

Fig. 1. Schematic block diagrams of the analog cross-coupling computer and the Graf-Askania Gss2 gravity meter. For clarity the gravity meter has been drawn thrice. Actually, of course, there is a single gravimeter with one input channel and one output channel. To obtain pitch off-leveling error the inputs to the multiplier are pitch off-leveling angle and surge acceleration, and to obtain roll off-leveling error the inputs are roll off-leveling angle and sway acceleration. (The beam deflection and the off-leveling angles are very small, so that the sines of the angles can be assumed to be equal to the angles themselves.)

of gravity of the beam is aft of its hinge point). In Figure 2 (*top*), for a following sea, the heave acceleration tends to lead the surge acceleration by 90°; thus the beam motion is generally in phase with the surge acceleration, giving rise to a negative instantaneous cross-coupling acceleration.

Since our interest in the cross-coupling acceleration is in how it affects the gravity records, we filter the instantaneous analog of cross-coupling acceleration through a filter of time constant 250 sec. Then we can compare it with the signal coming out of the gravimeter. We note, however, that the gravimeter signal is filtered once more through a series of electronic filters (Figure 1), whereas in our present system the cross-coupling signal is not. This does not, of course, affect the dc level of the cross coupling. Figures 4, 5, and the top curve in Figure 3 show records of the cross-coupling acceleration filtered through the 250-sec time constant low-pass filter.

It is convenient to think of the cross-coupling acceleration as mainly involving three period ranges. The lowest period range is from about 1 to 10 sec and corresponds to twice the frequency of sea motions that give rise to cross coupling. These periods are prominent in the instantaneous cross-coupling record of Figure 2 but almost disappear after the subsequent low-pass filtering. At the other end of the spectrum are the cross-coupling accelerations with periods ranging from several tens of minutes to dc. These accelerations are indistinguishable from gravity on the gravimeter records. Their amplitudes depend on the sea state and on the angle of approach of sea and swell. In Figures 4 and 5, if a mean line be drawn through the cross-coupling records (ignoring the shortest-period fluctuations), such a mean line would represent

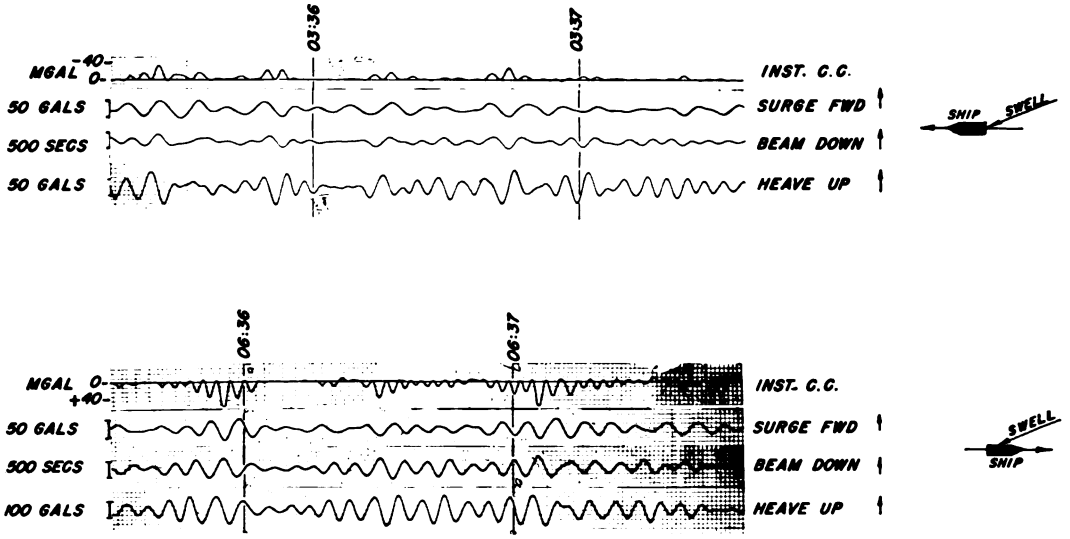

Fig. 2. Instantaneous cross-coupling error for a following sea (*top*) and for the ship heading into the sea (*bottom*). In this first case the surge acceleration forward tends to be in phase with the beam motion down, and in the second case the surge acceleration and beam motion are almost exactly 180° out of phase. For a following sea the instantaneous cross coupling is mostly negative, and when the ship is heading into the sea it is mostly positive. (The beam lies along the fore and aft direction of the ship with the center of gravity of the beam aft of its hinge point.) If the meter is facing the other way, the cross-coupling signs are reversed. The cross coupling records shown in Figures 3, 4, and 5 are obtained from the instantaneous cross-coupling records, such as those shown in this figure, by passing them through a low-pass filter of time constant 250 sec to simulate the response of the meter to the cross-coupling acceleration.

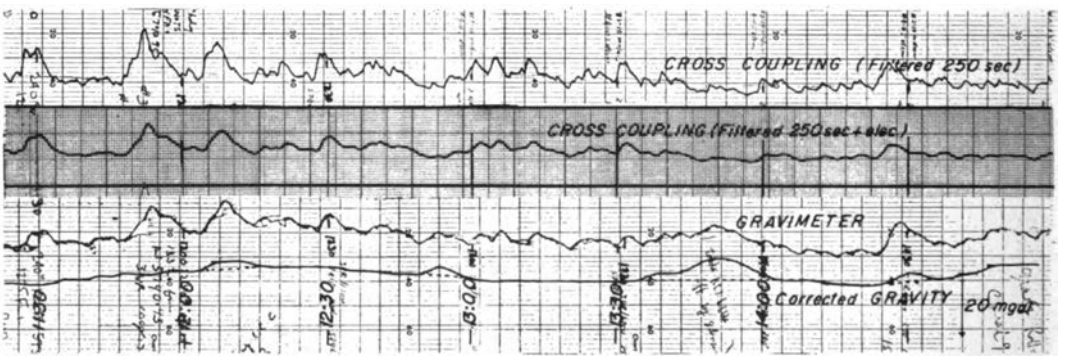

Fig. 3. The top trace is the cross-coupling record for a 3½-hour interval. The zero line is below this trace. The scale is nearly the same for all the traces and is indicated near the bottom of the figure on the right side. The top trace shows a dc level of cross coupling of about −15 mgal, with shorter-period wobbles superimposed. The top trace was digitized, then filtered with a digital computer to the same extent as the gravity record, and plotted (second trace from the top). Note the close correspondence of the filtered cross-coupling trace to the gravity record. Where the records do not correspond, as at 13:45, the cause is a large static off leveling of the stable platform because it was not performing very well in a rough sea. If the filtered cross-coupling trace is subtracted from the gravity trace, the resultant trace is smooth (corrected gravity) except at times where large static off leveling of the table took place.

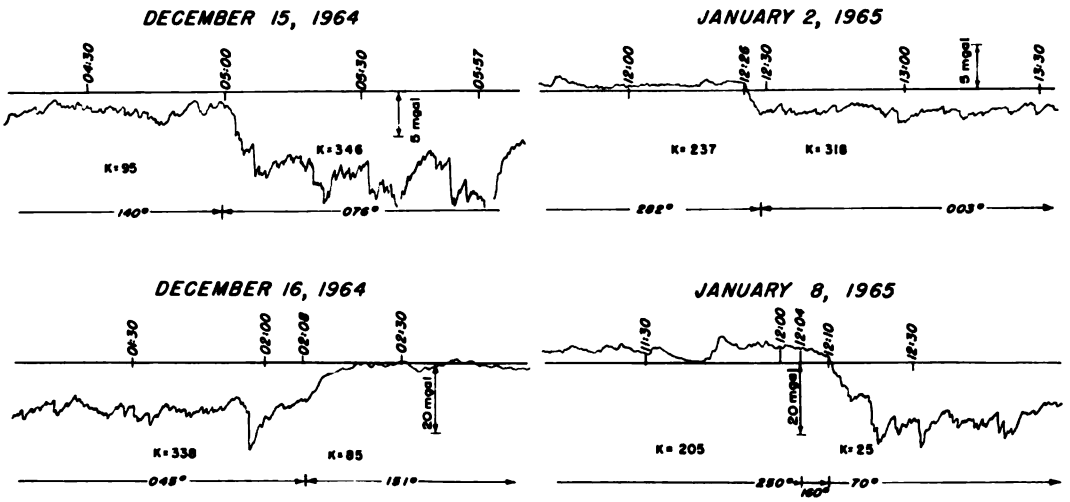

Fig. 4. Examples of cross-coupling records chosen to show the change in magnitude and sign of cross coupling with change in the angle of approach of swell κ (measured in an anticlockwise sense relative to the ship's heading). Ship's heading and value of κ are indicated for each example. Records of December 15 and December 16 show that the cross coupling is small for beam seas and large when the ship heads into the sea. Examples of January 2 and January 8 show an increase of cross coupling when the ship changes course in such a way that the sea and swell approach from forward of beam rather than from aft of beam.

these cross-coupling accelerations of very long periods. Between these two extremes lie the cross-coupling accelerations with periods ranging from a few tens of seconds to perhaps ten or fifteen minutes. In simplest terms their periods can be thought of as arising from the time intervals at which groups of waves arrive at the ship. The cross-coupling accelerations in this period range appear as characteristic wobbles (see Figure 3, top trace, and Figures 4 and 5). Since gravity variations, especially in deep water, have much longer periods, these wobbles would be duplicated in the gravimeter records, if no other errors exist in the same period range. Further, if identical wobbles appear in the gravity records, the results of the cross-coupling computer would be verified in a simple fashion and would ensure that what the computer records does indeed exist as an error in the gravity records.

At present in the analog computer the cross-coupling acceleration is only filtered through a single filter of time constant 250 sec as shown in Figure 1, whereas the cross-coupling acceleration in the gravimeter records is filtered further through a bank of electronic filters with total effective time constant (defined as the delay introduced in recording a linear gravity change) of about 80 sec.

For the purpose of correcting the gravity records we are mainly interested in the very-long-period or dc cross coupling, and this difference is immaterial. For comparing the wobbles, however, this difference is important. Therefore, the cross-coupling record (top trace, Figure 3) was digitized, and digital filtering to

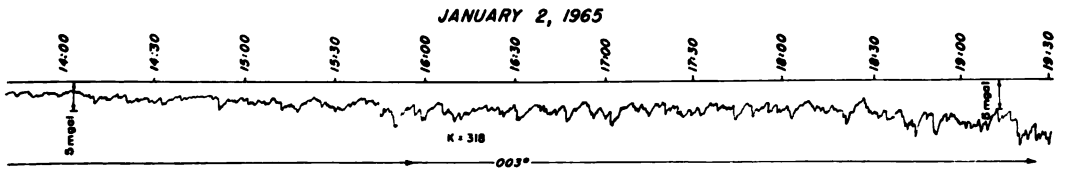

Fig. 5. Increase of cross coupling with increase of sea state. κ is the same throughout the record.

simulate the electronic filtering of the gravity record was applied. The processed signal was plotted as the middle trace in Figure 3. Note the great similarity in character of this trace to the gravity record plotted below, especially in the repetitions of the wobbles at 11:30, around 12:00, and at 12:30. Subtracting this record graphically from the gravimeter record we get the 'corrected gravity' solid trace at the bottom. In this example the cross-coupling correction approaches about 15 mgal. This condition is rather rare (see histogram, Figure 6); wobbles of the amplitude shown in Figures 3 and 4 and the latter part of Figure 5 are also uncommon. (These records with atypically large values of cross coupling were chosen to demonstrate some of the properties of the cross-coupling error.) If there are any remaining dc errors in the corrected gravity trace in Figure 3, they cannot be detected by inspection. However, we find that, even after correcting for cross coupling, there are shorter-period errors remaining in the record. These errors are indicated by the difference between the dotted line (assuming smooth gravity changes) and the solid line. We believe we can attribute these errors to static off leveling of the table. (At 13:45 the table was actually observed to be off level.) In a very rough sea the stable platform was not maintaining level very well. Although the dc (or long-period) cross coupling is appreciable under ordinary sea conditions, large wobbles such as those shown in Figure 3 are relatively uncommon, and the record at this time was chosen to compare with the gravity record even though the stable platform was not performing properly.

Figure 4 shows examples of the variation of cross coupling with change of angle κ of approach of sea and swell. κ is measured in an anticlockwise direction from the ship's heading. The examples of December 15 and 16, 1964, show that cross coupling is small for beam seas and is large while heading into the sea. The examples of January 2 and 8, 1965, show how the cross coupling changes sign as the ship changes course in such a way that the direction of approach of sea and swell changes from the starboard quarter to the starboard bow in one case (January 2) and to the port bow in the other. Note also that the cross coupling is larger heading into the sea than with following seas. This occurrence is apparently due to both the surge and heave accelerations usually being larger while heading into the sea. The fact that ship motions have longer periods with following seas, thus giving rise to larger gravimeter beam motions for the same heave amplitudes, is less important. If the ship does not change course, the cross coupling remains the same unless the sea state or sea and swell directions change. Changes in sea state take place slowly (at least over a few hours). A somewhat rare case of a relatively sudden increase in sea state and consequently large change in the dc cross-coupling error is shown in Figure 5.

Figure 6 (*left*) shows a histogram of the cross-coupling error during about a month's ship time in the Caribbean. The cross-coupling records were read (after smoothing) every half-hour. With the gravimeter as installed aboard *Conrad*, cross coupling is positive when headed into the sea and negative in following seas. Note that the positive errors are somewhat larger than the negative errors, which can be attributed to the fact that, under the same sea conditions, the cross coupling is larger heading into the sea than with a following sea. Figure 6 (*right*) shows accumulative cross-coupling errors that are smaller than a given value of the error in mgal.

We plan to modify the analog computer to filter the cross-coupling acceleration by the same amount as gravity and to subtract the cross-coupling signal in analog fashion from the gravity signal. The resultant record will give gravity values corrected for cross coupling.

Off-leveling errors for gravity meter mounted on a stable platform. The off-leveling errors for a gravity meter mounted on a stable platform have been discussed by *LaCoste and Harrison* [1961]. In the present discussion we shall confine ourselves to the dynamic off-leveling errors, that is, errors caused by the periodic off leveling of the stable platform in the presence of periodic horizontal accelerations. For small periodic pitch and roll off-leveling angles α_1 and β_1, respectively, the instantaneous off-leveling errors are given by $\alpha_1\ddot{x} + \beta_1\ddot{y}$, where $\ddot{x}$ and $\ddot{y}$ are the surge and sway accelerations of the ship. We can break up α_1 and $\ddot{x}$, as well as β_1 and $\ddot{y}$, into their respective Fourier components, and for either product, if the Fourier components of two terms with the same period

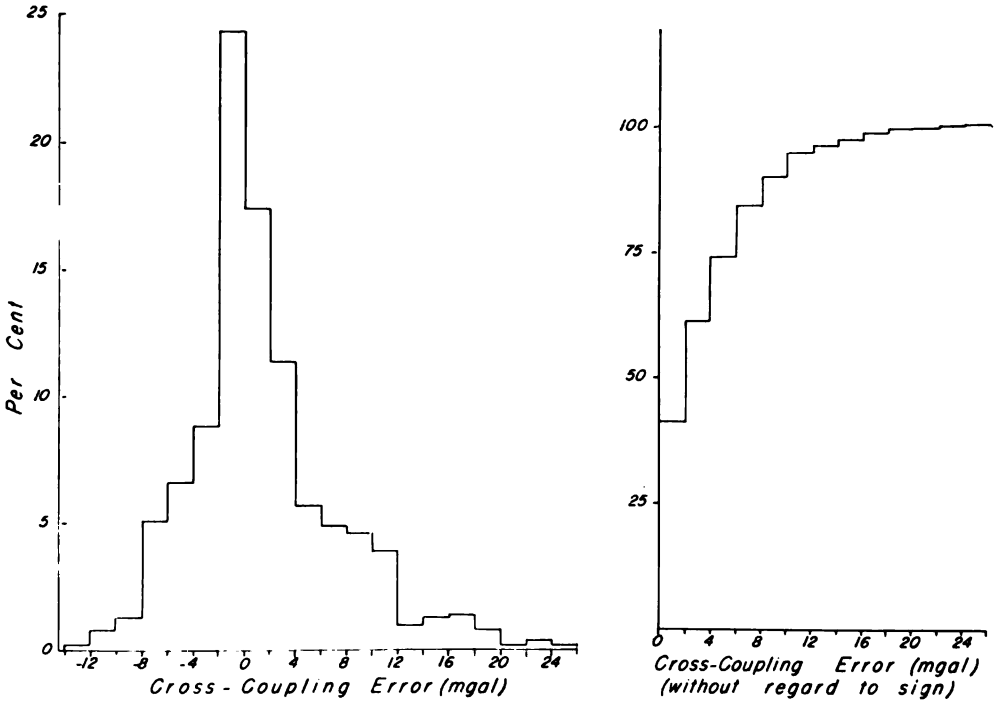

Fig. 6. *Left:* Histogram of cross-coupling error during about a month's ship time in the Caribbean Sea. Positive errors that occur when the ship is heading into the sea are somewhat larger than negative errors with following seas. *Right:* Accumulative percentage of cross-coupling errors smaller than values indicated along the abscissa.

have a phase difference other than 90°, the time average of the product will not be zero, thereby giving rise to off-leveling errors. The surge and sway accelerations are easily measured by means of accelerometers placed on the stable platform (the errors caused by the off leveling of the table in the measurements of the accelerations can be ignored for the present discussion). As for the off-leveling angles α_1 and β_1, in theory direct measurement can be made only with respect to an external vertical reference. However, it is simple to get an adequate measure of α_1 and β_1 from signals that are used in the operation of the stable platform. A stable platform is usually stabilized by a servo system with reference to a vertical reference. The pitch off-leveling angle α_1 can be split up as follows: $\alpha_1 = \alpha_{1\,servo} + \alpha_{1\,ref}$, where $\alpha_{1\,servo}$ arises from the inability of the servo to follow the vertical reference (which may be a gyro or a long-period pendulum) and $\alpha_{1\,ref}$ gives the instantaneous off leveling of the vertical reference itself. Similarly, we can express the roll off-leveling angle β_1 as $\beta_1 = \beta_{1\,servo} + \beta_{1\,ref}$.

Correspondingly, the instantaneous pitch and roll off-leveling errors are given by

$$\ddot{x}\alpha_1 = \ddot{x}\alpha_{1\,servo} + \ddot{x}\alpha_{1\,ref} \qquad (1)$$
$$\ddot{y}\beta_1 = \ddot{y}\beta_{1\,servo} + \ddot{y}\beta_{1\,ref}$$

Let us, for the moment, assume that the errors arising from the second terms in the right-hand side of (1) are negligible. We will later consider the validity of this assumption. The angles $\alpha_{1\,servo}$ and $\beta_{1\,servo}$ are easily obtained in analog form. These angles are between the vertical reference and the stable platform, and analog signals proportional to them are used to drive the servo motors in the stable platform to maintain the horizontal. The same signals can, of course, be separately recorded. A provision has been made for doing so in the Anschutz gyrotable.

By using a four-quadrant multiplier followed by a low-pass filter, as in the cross-coupling computer, we have been able to obtain in-

stantaneous, as well as time-averaged, values of $\ddot{x}\alpha_{1\ servo} + \ddot{y}\beta_{1\ servo}$. In Figure 7 we have called these errors pitch and roll off-leveling errors (ignoring the errors in the vertical reference itself). Continuous recording of these errors was possible, but, since only one multiplier was available for the calculation of these errors, we obtained daily samples of the pitch and roll off-leveling errors. Each pitch off-leveling error sample was for the duration of about 30 minutes and was immediately followed by a 30-minute roll off-leveling error sample. Figure 7 shows a histogram of these errors obtained during *Conrad* cruise 9 (Kingston–Panama leg). We see that both the pitch and roll off-leveling errors are small, that the pitch off-leveling errors are generally negative, but that the roll off-leveling errors are generally positive. The sum of the two off-leveling errors is almost always less than 1 mgal in Figure 7. It is of some interest to inquire into the small values of the roll and pitch off-leveling errors and the consistency of the signs of the errors as noted above. Somewhat larger than typical values for the amplitudes of $\alpha_{1\ servo}$ and $\ddot{x}$ are 1.5′ of arc and 30 gals, respectively. If the two signals were in-phase sinusoids with the above amplitudes, the time average of the pitch off-leveling error would be slightly larger than 6 mgal. The actual observed errors are much smaller. This fact can be ascribed to magnitudes of $\alpha_{1\ servo}$ and $\ddot{x}$ that are smaller than those given above, irregularity of the signals, and differences in phase angles. Yet the consistency in sign points to an 'average phase angle' between $\ddot{x}$ and $\alpha_{1\ servo}$ that lies in the first or fourth quadrants, and an 'average phase angle' between $\ddot{y}$ and $\beta_{1\ servo}$ that lies in the second or third quadrants. From more limited data, the error signs were similar on the *Vema*, though the magnitudes were somewhat larger.

Let us consider next the angular errors $\alpha_{1\ ref}$ and $\beta_{1\ ref}$ in the vertical reference that also contribute to the off-leveling errors. *LaCoste and Harrison* [1961] have shown that these errors are serious if the vertical reference is a long-period pendulum. An undamped long-period pendulum of natural frequency ω_0, free to swing fore and aft, will execute forced oscillations of frequency ω_1, when subjected to hori-

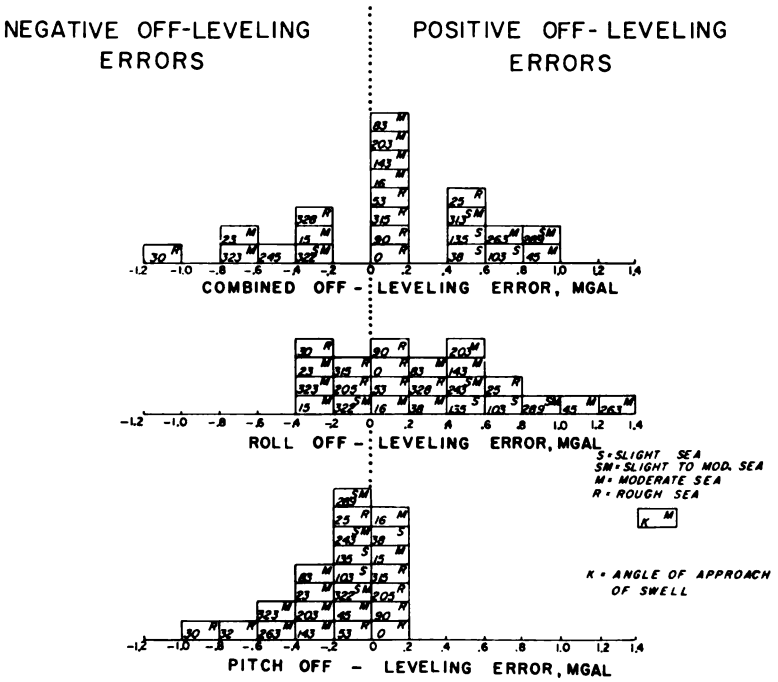

Fig. 7. Histogram made from 23 half-hour samples of pitch and roll off-leveling errors (due to servo off leveling alone) obtained during a one-month period in the Caribbean Sea.

zontal sinusoidal surge accelerations of amplitude $\ddot{x}_{amp}$ and frequency ω_1. Since the movement of this pendulum is the error in the vertical reference, we can term it $\alpha_{1\,ref}$ and the amplitude of $\alpha_{1\,ref}$ (for $\omega_0 \ll \omega_1$) is given by

$$(\omega_0^2/\omega_1^2) \cdot \ddot{x}_{amp}/g \qquad (2)$$

$\alpha_{1\,ref}$ will be very nearly in phase with the impressed horizontal acceleration.

From (1), however, it can be shown that, if $\alpha_{1\,ref}$ and $\ddot{x}$ are in-phase sinusoids, then, for the time-averaged value of the corresponding error to be less than 1 mgal, the amplitude of $\alpha_{1\,ref}$ in minutes of arc must be less than about $7/\ddot{x}_{amp}$, where $\ddot{x}_{amp}$ is measured in gals. For an amplitude of 30 gals for surge, $\alpha_{1\,ref}$ should have an amplitude less than about 15 sec, which is an exacting requirement for a long-period pendulum. Using this value for the amplitude of $\alpha_{1\,ref}$ and 30 gals for $\ddot{x}$, we get from (2) a value of about 1/400 for ω_0^2/ω_1^2. In other words, the natural period for the long-period pendulum should be 20 times that of sea motions. If $\ddot{x}_{amp} = 50$ gals, the amplitude for $\alpha_{1\,ref}$ should be less than about 8 sec of arc and $\omega_0^2/\omega_1^2 = 1/1200$, or the ratio of periods is about 35. Peaks of surge acceleration commonly lie in a period range between 5 and 10 sec, and, even though the amplitudes seldom exceed 30 gals, pendulums with very long periods are required if they are to serve as adequate vertical references. Although LaCoste and Harrison's arguments about the problems involved in using a long-period pendulum as a vertical reference for a stable platform are quite correct, they are simply inapplicable for the stable platforms now being used in gravity work. None of these platforms uses long-period pendulums for vertical references; they use gyros instead.

Horizontal periodic accelerations should have no direct effect on the gyros. However, the gyros do tend to drift over a long period of time, and for this reason, unless they are controlled by another vertical reference (which, to avoid confusion, we will call the primary vertical reference), the stable platform will go off level. This primary vertical reference is usually a damped short-period pendulum and is necessarily affected by horizontal accelerations. We can think of the swinging of this short-period pendulum as an error in the primary vertical reference, and the question arises whether this error is passed on to the gyro. The answer is that it is a relatively simple task to ensure that the short-period motions of the primary vertical reference are not passed on to the gyro. We note that the gyro is made to precess at a rate proportional to a signal that depends on the angle between the vertical reference and the gyro axis. By first passing this signal through a low-pass filter, the effect of the short-period (error) motions of the primary vertical reference can be severely reduced. Additionally, the constant of proportionality that determines the rate at which the gyro is made to precess can be made small. This has one disadvantage: the constant angle between the vertical reference and the gyro needed to balance out the rate of the rotation of the Earth will be large and, consequently, it will be necessary to make manual alterations to change the table level after changes in ship's course.

The phase difference between the gyro errors and the horizontal accelerations is also of interest. A short-period pendulum (primary vertical reference) will be nearly 180° out of phase with the horizontal accelerations if its natural period is smaller than that of the accelerations. If the angular displacement of this pendulum is proportional to the *rate* at which the gyro precesses, the angular error motions of the gyro $\alpha_{1\,ref}$ will tend to lag 90° behind the motions of the pendulum. Thus there will also be a phase difference of 90° between the $\alpha_{1\,ref}$ and $\ddot{x}$, which will be the most favorable case for the minimum off-leveling error. If, on the other hand, the signal from the short-period pendulum is passed through a low-pass filter, phase delays will be introduced and the phase difference between $\alpha_{1\,ref}$ and $\ddot{x}$ will be different from 90°. This disadvantage would, of course, be offset by the reduction of amplitude of $\alpha_{1\,ref}$ due to the filtering.

The point to be made from this discussion is that for a gyro-stabilized platform the off-leveling errors need not be serious for the following reasons:

1. The part of the errors caused by servo response ($\ddot{x}\alpha_{1\,servo}$, $\ddot{y}\beta_{1\,servo}$) is small, at least for the Anschutz gyro table. In any event, it can be monitored and a correction applied if necessary.

2. The vertical reference that controls the gyro is used only for correcting the long-period drift of the gyro. Thus the short-period errors of the primary vertical reference can be filtered out. In addition, the gyro can be made to precess at a very slow rate, so that it is essentially not affected by the horizontal accelerations caused by ship motions. Thus $\alpha_{1\,ref}$ and $\beta_{1\,ref}$ can be made negligible.

It is not difficult to test the magnitude of the error caused by $\alpha_{1\,ref}$ and $\beta_{1\,ref}$ in the laboratory. One method of testing is to subject the stable platform (with the gravity meter mounted on it) to horizontal accelerations. The total off-leveling error (left-hand side of equation 1) can be obtained from gravimeter record. The part of the error caused by servo errors ($\ddot{x}\alpha_{1\,servo}$) can be obtained by measuring the horizontal accelerations and recording $\alpha_{1\,servo}$. Any difference between the error indicated by the gravimeter and the off-leveling error caused by the servos should give the off-leveling error due to errors in the vertical reference ($\ddot{x}\alpha_{1\,ref}$). *Wall et al.* [1966] made such a test on the Gss2 meter mounted on the Anschutz stable platform by subjecting the platform to horizontal accelerations of amplitude 25 gals and period 4 sec. Any errors due to off leveling of the primary vertical reference were less than 1 mgal.

Off-leveling error for gravity meter in a gimbal frame. A meter (such as the LaCoste-Romberg sea gravity meter) suspended in a short-period gimbal frame hangs along the instantaneous vertical (resultant of the horizontal accelerations and g) and measures the component of gravity in this direction. A correction known as the horizontal Browne correction has to be applied. The value of the instantaneous horizontal Browne correction is given by $\frac{1}{2}\Theta^2 g$, where Θ is the angle between the instantaneous and the true vertical. To measure the angle Θ, a vertical reference is necessary. It is of interest to inquire what errors in the determination of the Browne correction would be caused by a slight off leveling of the vertical reference. Assuming for simplicity that the off-leveling errors, as well as the horizontal accelerations, exist only in the fore and aft direction, and letting $\alpha_{1\,ref}$ remain as before the error in the vertical reference, the instantaneous error in the Browne correction from this cause only will be $\frac{1}{2}(\Theta - \alpha_{1\,ref})^2 g - \frac{1}{2}\Theta^2 g$. This result is obtained because, instead of measuring the angle Θ, an erroneous angle $\Theta - \alpha_{1\,ref}$ will be measured. Ignoring the second-order terms in $\alpha_{1\,ref}$, we get an instantaneous off-leveling error in the determination of the Browne correction equal to $\Theta\alpha_{1\,ref} g$. For small Θ, we can set $\Theta = \ddot{x}/g$. Hence, the error equals $\ddot{x}\alpha_{1\,ref}$. This expression is identical to one of the terms in the right-hand side of equation 1 for the pitch off-leveling error. *Thus we see that, whether we use a stable platform or determine the horizontal Browne correction for a gimbal-suspended meter, the error caused by the off-leveling of the vertical reference is the same, provided, of course, that the same vertical reference is used.*

The earlier discussion about the relative merits of long-period pendulums or gyros as vertical references still holds. In particular, we note that the problems inherent in using a long-period pendulum for a control reference are severe.

In addition, as in the use of the stable platform, there is also a servo off-leveling error in the determination of Θ. In the LaCoste-Romberg sea gravity meter, for instance, the vertical reference is a long-period pendulum suspended inside a box. The box is driven by a servo motor to remain parallel to the pendulum [*Caputo et al.*, 1963], and the angle Θ between the box and the gravimeter frame is measured. The inability of the servo to keep up with the pendulum gives rise to an error $\alpha_{1\,servo}$ in the measurement of Θ (assuming for simplicity, as before, that all motions are in the fore and aft direction). This error will in turn give rise to a servo off-leveling error $\ddot{x}\alpha_{1\,servo}$ in the presence of fore and aft horizontal accelerations $\ddot{x}$. This error is again identical to one of the terms in the right-hand side of (1). As in the case of the stable platform, this off-leveling angle can be measured and recorded and, with the help of an analog computer, $\ddot{x}\alpha_{1\,servo}$ easily evaluated. Apparently this evaluation has not been performed. Other errors in the determination of the Browne correction for the LaCoste-Romberg sea gravity meter have been discussed by *Caputo et al.* [1963].

Time averaging of gravity data. It has often been stated or implied in the literature that, since instantaneous vertical accelerations of a ship amount to many thousands of milligals, instantaneous gravity values at sea cannot be

obtained; one must average over a finite time interval, usually of 5–10 minutes. This statement is certainly true if a single *discrete* observation is being made. However, if continuous observations are being made, it is merely a matter of being able to resolve the gravity 'signal' from the 'noise' due to ship motions. Ship motions can be considered to have a period of the order of 10 sec. The gravity signal can be considered to have a minimum period of interest of about 10 minutes (the corresponding distance traveled is 1.6 nautical miles for a ship at 10 knots). The ratio between the two sets of periods is 1 to 60. Even if the 'noise' (principally caused by heave) must be reduced by a factor of 50,000, filters can be easily constructed for this purpose and instantaneous values of gravity obtained. The problem is somewhat analogous to filtering out 60-cps hum from a 1-cps signal and is certainly not insurmountable. Thus, at least in principle, there are no inherent reasons why instantaneous gravity measurement cannot be made aboard a ship.

In the recording of gravity by a Graf-Askania Gss2 meter a somewhat different though related problem occurs. On account of its very high damping the gravity meter behaves like a simple low-pass filter (of the *RC* type). The time constant of this filter is 250 sec. For constant gravity gradients this filter merely introduces a constant time delay of 250 sec [*Graf and Schulze*, 1961]. For sinusoidal gravity signals of periods very much longer than 250 sec, again a constant time delay of 250 sec is introduced without any relative attenuation (as compared with dc signals). But gravity signals of periods of several tens of minutes (which are very much of interest in sea gravity measurements) are distorted as well as delayed by the gravity meter acting as a low-pass filter. A very simple way to restore the original signal is suggested by the equation of motion itself of the gravity meter. Ignoring the inertial term (it does not affect the beam in the period range of interest) and following *Graf and Schulze* [1961], we have

$$B\dot{\phi}_0 + \phi_0 = E\,\Delta g \qquad (3)$$

where ϕ_0 is the actual beam motion due to gravity as distinct from the short-period motion ϕ_1 discussed earlier and Δg is the change of gravity that would correspond to ϕ_0 in the static case, i. e. when $\dot{\phi}_0 = 0$ and B and E are as before the time constant and the static sensitivity, respectively, of the meter. The constant E is, of course, accounted for in the instrument calibration; the error (distortion and attenuation) introduced by the gravity meter acting as a low-pass filter is given by $B\dot{\phi}_0$. The gravity meter recorder records the quantity ϕ_0. $B\dot{\phi}_0$ can be obtained simply by determining the slope of the curve for ϕ_0 at any point on the record and multiplying it by B. $B\dot{\phi}_0$ can then be added to ϕ_0. From (3) we see that the above procedure will yield the *instantaneous* value of gravity.

A simple template can be constructed on transparent paper with lines on it having different slopes, each corresponding to a certain slope correction in mgal. This template can be laid on the gravity record and the correction directly determined at any point on the record. Thus far we have ignored the effect of the additional electronic low-pass filters also used in the Graf-Askania Gss2 system. These additional electronic filters are three filters in cascade (with time constant 16 sec each). Since the filters are not isolated from each other their behavior is somewhat more complicated than that of a simple low-pass filter. It can be shown, however, that they introduce negligible relative attenuation or distortion to the gravity signal and have the sole effect of delaying the signal by about 80 sec. Therefore the original gravity signal can be restored by applying the 'slope' correction as described earlier and then moving the record 80 sec earlier in time. At ship speeds of 10 knots the latter correction will exceed 1 mgal only if the gravity gradients are larger than about 3 mgal/km. On the other hand, at gradients of 20 mgal/km, the 'slope' correction due to the meter will be about 20 mgal and the correction due to the electronic filters is about 6 mgal. Both will have to be determined carefully.

Figure 8 shows an actual recording of a gravity trace by the Graf-Askania Gss2 meter to which the slope correction has been applied by means of the simple template mentioned earlier. (The corrected trace has *not* been shifted 80 sec to allow for the extra delay caused by the electronic filters.) Note in particular that the gravity peak at 09:30 not only is shifted in time as a result of this slope correction but is also made higher. The sudden trace deflection just after 10:00 is caused by a large alteration

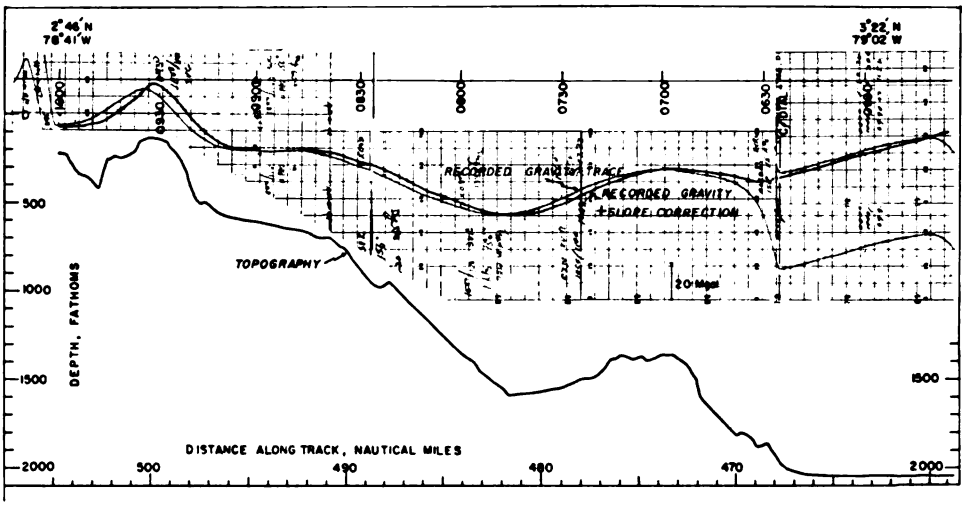

Fig. 8. The gravity trace as recorded by the gravimeter is shown at top together with a trace to which slope correction has been applied graphically. Note that the peak at 09:30 is not only shifted in position but is also increased in height. Just before 06:30 a gravimeter dial change was made. The dial change corresponds to a step in gravity as far as the gravimeter is concerned, and a slope correction can be applied after a period of about 5 minutes after the dial change. The gravity trace before the dial change has been raised by the number of chart divisions that correspond to the dial change to show the continuity of the gravity trace. After the slope correction has been applied the gravity record can be considered instantaneous (not time averaged). (Time runs from right to left.)

in the Eotvos effect due to a course change. On the right side of Figure 8 two traces are shown. The lower trace was the one actually recorded. A gravimeter dial change was made shortly before 06:30, because the observer expected the trace to go off scale. The dial change corresponds to a step in gravity as far as the gravimeter response is concerned. After a period of about 5 minutes the slope correction can be applied as shown to obtain the corrected gravity. The gravity trace before the dial change has been raised by the number of chart divisions that correspond to the dial change in order to show the continuity of the gravity trace. The dotted portion of the corrected trace (between 06:25 and 06:30) is the only gap where gravity data were missed owing to the dial change. Thus an important use of the slope correction is to minimize the interval during which gravity data are lost after a dial change.

The corrected trace of Figure 8 will (after shifting it by 80 sec) correspond to the original gravity signal. The effect of the instrument response has been removed. The gravity measurements are *instantaneous* not *time averaged*.

It is a simple task to obtain the continuous free-air anomaly profile from the gravity trace, since, along any particular course, both the international formula and the Eotvos effect vary slowly and can be represented by a straight line to be subtracted from the gravity trace. Preliminary values of free-air anomalies can be easily obtained on board ship while the gravity data are being recorded.

Schulze [1962] describes a servo system that can be attached to the Gss2 meter. It constantly nulls the beam (as far as gravity changes are concerned) by rotating the gravimeter screw. The position of the screw is then read electrically to obtain the gravity reading. The servo system improves the response of the instrument considerably (a time delay of about 2 minutes as against 250 sec) and also eliminates resetting the gravimeter dial (without the servo system the range of the gravimeter is only 200 mgal at a single setting of the gravimeter dial). However, at Lamont Observatory we have preferred to make the 'slope' correction and to add it to gravity. Recently aboard R. V. *Vema* we have built a 'differentiator' which obtains the slope correction electrically while gravity is being recorded. Our future plans include adding

the electrical 'slope' signal to the gravity signal; thus the correction would be made automatically.

In the LaCoste-Romberg sea gravimeter, gravity values are obtained from the velocity of the beam; that is, only the term $B\dot{\phi}_0$ of equation 3 is used [*Nettleton et al.*, 1962]. In theory this method should yield instantaneous values of gravity, but in practice it appears that the beam record is not smooth and an average velocity has to be determined for a period of 6–12 minutes. The gravity values are then necessarily averaged over this time interval.

Summary of Errors and Some General Remarks

In this section causes for the gravimeter errors discussed earlier are summarized, and some general remarks are made about the problems of measuring or eliminating these errors.

The large values of cross coupling for a gravity meter mounted on a stable platform, predicted by *LaCoste and Harrison* [1961], have been reduced in the Graf-Askania Gss2 meter by reducing beam motion. This reduction was accomplished by using a small static sensitivity as well as a very high damping. The small beam motion also reduces the errors due to the inherent nonlinearity of a non-nulled beam gravimeter (the gravity measured by the gravimeter is not g but the time average $\overline{g \cos \phi_1}$, where ϕ_1 denotes the periodic beam motion). For the Graf-Askania Gss2 meter sinusoidal heave accelerations of amplitude 100 gals and period 6 sec will give rise to a nonlinearity effect of only 1 mgal. On the other hand, in spite of the reduction in beam motion the cross-coupling effect is still not negligible (Figure 6); but with the cross-coupling computer described earlier it can be continuously recorded with an accuracy of better than 1 mgal. The increase in gravimeter damping has a disadvantage in that it attenuates and distorts the gravity signal. But a slope correction can be applied either graphically or electrically to correct for the gravimeter response.

Two other ways of reducing the cross-coupling error suggest themselves. One way is to reduce the static sensitivity of the meter by, say, a factor of 10, which can be done by reducing the natural period p (or, more properly by reducing the quantity $p\sqrt{a/k}$) of the suspension. This result in turn can be effected by either making the gravimeter spring stiffer or by reducing the turning moment of the beam. There are more sensitive transducers available to offset the effect of the reduced sensitivity, but problems arising from gravimeter drift and from gravimeter 'noise' in general will have to be carefully considered. A different way is to employ the force balance method in which the gravimeter beam is constantly nulled and the nulling current yields gravity plus the heave acceleration. Critical requirements in this method will be for a fast servo response, as well as for large dynamic range and linearity in the measuring and filtering systems. The constant nulling of the beam will eliminate the cross-coupling effect as well as any errors due to the $g \cos \phi_1$ term mentioned earlier.

For a gravity meter suspended in a frictionless short-period gimbal frame, the ship accelerations are normal to the beam and no cross-coupling errors arise.

As far as the off-leveling errors are concerned, it has been shown that in the presence of horizontal acceleration a gravity meter mounted on a stable platform is subject to the same errors as are involved in the determination of Browne correction for a gimbal-suspended gravity meter, provided that the same vertical reference is used and the same servo errors are introduced in both cases. For the Anschutz gyrotable mounted on R. V. *Conrad* the off-leveling errors due to servo errors are less than 1 mgal (Figure 7), and we believe that the errors due to the off leveling of the vertical reference (gyro) are similarly small. For a meter suspended in a gimbal frame, the servo errors may give rise to appreciable errors in the determination of the Browne correction, but they can be evaluated by a continuous analog multiplication. Errors arising from off leveling of the vertical reference can be serious where a long-period pendulum is used for a vertical reference. For horizontal acceleration of amplitude 30 gals the natural period of the long-period pendulum used as a vertical reference must be 20 times that of the horizontal acceleration period to reduce errors below 1 mgal. The use of a gyro for a vertical reference would appear to be preferable.

Given the same vertical reference and equivalent servo errors, the only theoretical basis for choice between a gravimeter on a stable plat-

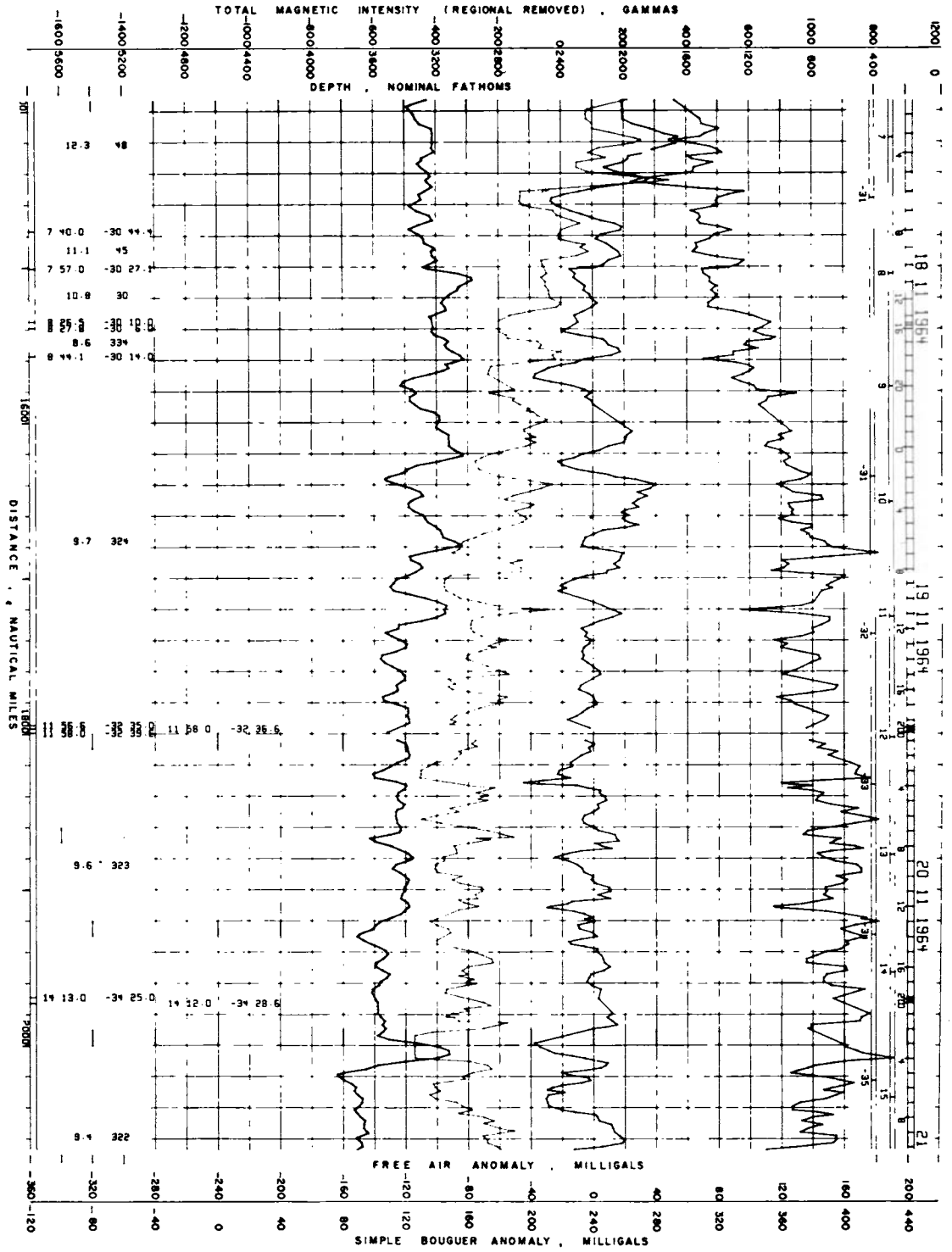

Fig. 9. From top to bottom, the traces represent simple Bouguer anomaly, free-air anomaly, depth and magnetic intensity (regional removed). The traces were plotted automatically by a Calcomp digital plotter on line with an IBM 1620. The input data for the plotting program are the output data of the data reduction programs. The coordinates of points at which the ship changes speed or course are indicated along the bottom of the figure. The speed in knots and the course are also annotated. At the top the day, month, and year, as well as the hours, are indicated. Also shown are the positions at which the track crosses even latitudes or longitudes. All annotations except the scales at either end were made by the plotter.

form and one suspended in a gimbal frame comes from the relative ease with which the cross-coupling and Browne corrections can be made. The cross-coupling errors with the existing gravity meters are smaller than the Browne corrections. What is perhaps even more important is that, since they are not large enough to drive the meter out of its measuring range (200 mgal for the Graf-Askania Gss2 meter), they can be recorded separately or can be added electrically to the gravity signal; both are simple operations. The Browne corrections are large, so that the percentage accuracy in their evaluation (aside from off-leveling errors,

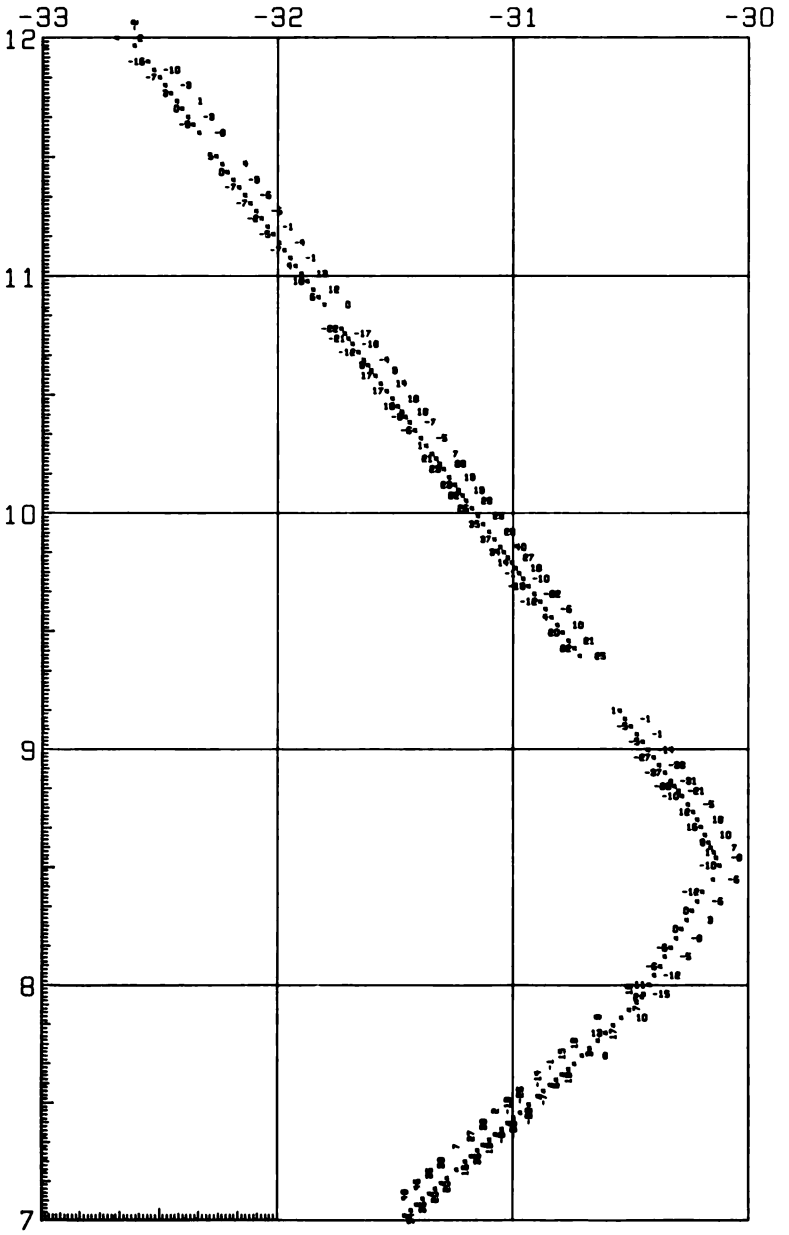

Fig. 10. Free-air gravity values plotted and annotated automatically on a Mercator chart by the Calcomp digital plotter on line with an IBM 1620.

etc.) is more important; also, it appears to be necessary to convert them to a mechanical rotation of the gravimeter screw to continuously compensate the beam motion for the Browne correction. For small horizontal accelerations (less than 15 gals, which give rise to time-averaged Browne corrections less than 60 mgal) encountered in some airplane measurements, it might be profitable to suspend either kind of gravity meter in a gimbal frame and to measure the Browne correction separately by using a gyro for a vertical reference.

Distortion of the gravity signal by a heavily damped gravimeter can be corrected by applying a slope correction. The correction will become difficult to apply when the gravity signal has periods shorter than about 15 minutes because of progressively larger attenuation at shorter periods.

For a gravity meter such as the LaCoste-Romberg, in which the gravity values are proportional to the beam velocity, in principle the measurements can be considered to be instantaneous. In practice, however, since an average beam velocity is determined over a period of 6–12 minutes, this advantage is lost and it is not possible to detect anomalies with periods less than several times the averaging interval. It can be seen that for both meters the difficulty stems from the necessity for correct determination of the beam velocity. The problem would seem to be less acute for the Graf-Askania Gss2 meter, since the velocity term here is a correction rather than the only term that gives the gravity value.

Eotvos Effect

A moving object on the rotating Earth is subjected to a vertical Coriolis acceleration known as the Eotvos effect. The second-order term involving the ship's speed [see *Worzel*, 1959] is not important for oceanographic vessels; thus the Eotvos error in milligals equals $-7.5\ v_E \cos l$, where v_E is the eastward component of the ship's velocity in knots and l is the latitude of the ship.

On Lamont research vessels *Vema* and *Robert D. Conrad* the corrected track is usually obtained by determining the 'current' from the discrepancy between a fix and the dead-reckoning position based on the previous fix. ('Current' is used here, as is customary in navigation, to include all factors introducing geographical error in the dead reckoning, whether their immediate effects are on the vessel or on water.) The 'current' is assumed to be constant between the two fixes. The error in the determination of Eotvos effect from the corrected track depends almost entirely on the error in the longitude of the fixes. Errors in dead reckoning that arise from errors of the ship's electromagnetic (or pitometer) log, leeway of the ship in the wind, etc., are relatively less important, because such errors are largely compensated by a corresponding error in the determination of the 'current,' and consequently the corrected track changes little. If we continuously compute and record an Eotvos correction from the same data used in the dead reckoning computations, we can later add the additional Eotvos correction due to the easterly component of 'current' to obtain the same Eotvos effect as would be obtained from the corrected track. An analog computer has been constructed and is being used aboard *Vema* which takes its inputs from the ship's pitometer log and the ship's gyro and computes continuously the Eotvos correction, which is then recorded. Our current plans envisage the addition of this Eotvos correction directly to the gravity signal. The correction for the 'current' will be added at data reduction time. The advantage of this approach over the use of the corrected track is that changes in ship's speed (through water) and course for relatively short intervals of time are not ignored in the Eotvos calculations. Otherwise the errors will be the same in both methods and will arise mainly from the errors in fixes and the fact that the 'current' may not stay constant between the two fixes.

We are planning a system in which the gravity, Eotvos and cross-coupling signals will all be continuously added. The slope correction of the combined signal will be determined and added to the combined signal, and the sum recorded. During data reduction only the Eotvos effect due to 'current' will have to be added and will be assumed to stay constant or to vary slowly between fixes.

Data Reduction Procedures

The high rate of acquisition of gravity data aboard surface ships has made the problem of

data reduction and display an urgent one. With the present problems of errors in gravity data and the necessity of making subjective judgments as to when the data are good or poor, it is believed that the data should still be recorded in analog rather than digital form. On the other hand, reduction of data on digital computers (after the records have been read) and automatic plotting by digital plotters have proved very useful. A basic function of the data reduction programs written at Lamont Observatory is to convert the chart readings (of gravity, depth, or magnetic field), which are read at irregular intervals with respect to time, into gravity or magnetic anomalies and depths with respect to the distance along track and latitude and longitude.

The output of these data reduction programs is used as input to two kinds of plotting programs. The Calcomp digital plotter is used on line with an IBM 1620 computer to make both kinds of plots. The first kind consists of profiles (with respect to distance) and is illustrated in Figure 9. Notations along the bottom of the figure indicate the latitude and longitude of points on the track at which speed, course, or both were altered. The notations at the top indicate time. The points at which the track crosses even latitudes at longitudes are also indicated. The entire plot including the annotations (but excluding the scales on either side) is made by the plotter. The second kind of plots is shown in Figure 10. Here the gravity values are plotted on a Mercator chart and annotated. Similar programs exist for plotting and annotating topographic and magnetic data on Mercator charts.

The reduced gravity data are available on cards, one value to a card. In addition to depth and station coordinates we feel that it is very necessary to indicate distance along the track on the same card. The distance is required if any profiles are to be plotted. In addition, the Eotvos correction is also indicated for each point. We do not, however, indicate the accuracy of the observations. One of the reasons for not doing so is that the errors due to wrong Eotvos corrections, as well as due to cross coupling, remain constant so long as the ship's heading, as well as the sea state, remains constant. Thus relative errors on a constant course are smaller than the over-all errors, and a statement of error can be misleading.

Acknowledgments. Thanks are due to J. Dorman, D. E. Hayes, J. R. Heirtzler, G. H. Sutton, R. E. Wall, and J. L. Worzel for reviewing the manuscript.

This work was supported by contracts Nonr 266(48) and Nonr 266(79) from the Office of Naval Research.

References

Caputo, M., J. C. Harrison, R. Von Huene, and M. D. Helfer, Accuracy of gravity measurements off the coast of southern California, *J. Geophys. Res., 68,* 3273–3282, 1963.

Fritsch, V. J., Erfahrungsbericht uber Messungen mit dem Askania-Seegravimeter, *Deutsche Hydrograph. Z., 15,* 142–173, 1962.

Graf, A., and R. Schulze, Improvements on the sea gravimeter Gss2, *J. Geophys. Res., 66,* 1813–1821, 1961.

LaCoste, L. J. B., and J. C. Harrison, Some theoretical considerations in the measurement of gravity at sea. *Geophys. J., 5,* 89–103, 1961.

Nettleton, L. L., L. J. B. LaCoste, M. Glicken, Quantitative evaluation of precision of airborne gravity meter, *J. Geophys. Res., 67,* 4395–4410, 1962.

Schulze, R., Automation of the sea gravimeter Gss2, *J. Geophys. Res., 67,* 3397–3401, 1962.

Talwani, M., W. P. Early, and D. E. Hayes, Continuous analog computation and recording of the cross-coupling and off-leveling errors, in preparation, 1966.

Wall, R. E., M. Talwani, and J. L. Worzel, Cross coupling and off leveling in gravity measurements at sea, *J. Geophys. Res., 71,* in press, 1966.

Worzel, J. L., Continuous gravity measurements on a surface ship with the Graf sea gravimeter, *J. Geophys. Res., 64,* 1299–1315, 1959.

The Extension of the Gravity Net to the Unsurveyed Areas of the Earth: Statistical Methods

Reporter: Richard H. Rapp[1]

Before we discuss some of the statistical methods mentioned in the title of this session of the symposium, we should define an unsurveyed area. The obvious definition, when we look at the maps showing existing gravity material, is that an unsurveyed area is an area where no gravity information is available at all, such as many oceanic areas. However, this definition depends on the detail desired; for as we look carefully at the details on such a map, we see that there are point observations at finite positions on the Earth (excluding for the moment airborne and seaborne gravity measurements). Thus, in fact, any area between our measurements is unsurveyed. An unsurveyed area can be divided into two types: (1) areas in which observations have not been made, and (2) areas in which a finite number of observations have been made. A definite border between areas may be difficult to achieve, with the effect that observed and unobserved areas become limiting cases of each other.

The problem that now presents itself is how to fill in these gaps in our data. For the first type of area, we could perhaps use extrapolation techniques; for an unsurveyed area of the second type we might use interpolation techniques. We must also ask in what form we want these anomalies. For most gravimetric computations we need the anomalies in forms of various area means, such as 5′, 10′, ⋯ 1°, 5° squares, etc. On the other hand, certain computations, such as deflections of the vertical and anomalies at higher elevations, sometimes require actual point anomaly predictions. We can thus see that the requirements for the anomalies are in area means and point values. The prediction of point anomalies and the smaller mean anomalies (say to 30′ squares) can be considered local predictions. As we proceed to 1°, 5°, and larger squares, we enter the field of general, as opposed to local, predictions.

We can see that the case of point prediction can lead directly into the determination of mean anomalies, as a mean anomaly is defined as the area mean of all point anomalies within

[1] Department of Geodetic Science, Ohio State University, Columbus.

the area under investigation. In our quest for anomalies, we would now like to know the accuracy of this estimate of the given anomaly. For this determination we compare, in effect, the given anomaly with some theoretical anomaly determined from an infinite number of points for an area mean or an actual point observation when dealing with point predictions.

One of the first, if not the first, investigations in the field of the analysis of anomalies was done by *de Graaff-Hunter* [1935]. In his work, de Graaff-Hunter defined the error of representation E_s as the root mean square value of the discrepancy between an actual anomaly and the mean of such anomalies over certain regions. He obtained actual values for E_s for squares of 2°-by-2° to 8°-by-8° in size based on a limited sample of observations in India. On the basis of his computation, de Graaff-Hunter gave an expression by which the error of representation could be evaluated analytically. This expression was a function of the square root of each side of the area. Using this equation, the error of representation for a square of the same area as the whole Earth was ±113 mgal.

More work along these lines was done in Russia in succeeding years. The phrase 'error of interpolation' as a counterpart of the error of representation was coined. The error of interpolation depends on the difference between the actual values of the anomalies and the values read from maps. This difference would depend on the observational errors at the points from which the anomaly contour map was drawn, and, on the other hand, on the errors due to an assumption of a linear gradient used in constructing the anomaly map. Various tests were made in 1937, 1951, and 1955 to compute the error of representation and error of interpolation. It was found that the error of interpolation was nearly the same as the error of representation. Tests made with the de Graaff-Hunter equations for expressing the error of representation showed that they held up well in all the areas tested. [See *Molodenskii et al.*, 1962.]

Hirvonen [1956] published results giving values for the error of representation using quite a bit more data than available to de Graaff-Hunter. At the same time he computed G_s, which is equal to the root mean square value of mean anomalies of equal squares with side s. If G_0 is the root mean square value of point anomalies, then $E_s^2 = G_0^2 - G_s^2$. Hirvonen was able to plot the variations of the function for squares from 10 km on a side, up to 30°-by-30° squares. He was then able to give an expression that would yield the mean anomaly in a square size s, given a point anomaly within the square and its expected accuracy.

At this time Hirvonen started to consider the correlation (or covariances) between anomalies in blocks of size s and various separations. One of the basic assumptions made in the computation of these covariances (and in other such computations) was that the covariances between anomalies depend only on the separation between them and not on the direction in which the covariances are computed. Given these covariances and the mean anomalies in a small square of side s, an equation that would enable a mean anomaly in some blocks whose size is some multiple of side s was given. Such an equation had no dependence on a local anomaly situation, and, once the variances and covariances for mean anomalies were established, the anomaly in any size square (as long as it was larger than the basic unit) could be established. From these covariance studies Hirvonen concluded that 30°-by-30° squares have little or no correlation.

In the following year *Kaula* [1957] published some statistical studies made in conjunction with work concerned with the accuracy of gravimetric deflections of the vertical. This paper used the correlation coefficient as the parameter of statistical interest. Data were computed for the correlation of point anomalies in the central U.S.A. Using these results, the correlation for larger size squares at various separations was computed.

In a later publication, *Kaula* [1959] reported his results from an extensive analysis of existing gravity material on a worldwide basis. In this study Markov estimation techniques were applied to establish mean anomalies in 1°-by-1° and larger size squares. Markov's estimation is usually described as a sequence of step-by-step extrapolations, which in Kaula's problem was considered with respect not only to anomaly variations but also to topographic variations, thus taking into account the correlation of free-air anomalies with elevations.

At the Twelfth General Assembly of the

IUGG in 1960, Hans Baussus [*Baussus*, 1960] presented a paper giving a unified isostatic and statistical theory of gravity anomalies. In this paper Baussus shows how a distance correlogram (or correlation coefficient function) would be constructed in a mathematical form based on various physical models of the Earth's interior. He also shows how anomaly prediction may be made using certain known anomalies and the distance correlogram.

Hirvonen [1962] and *Rapp* [1962] published some analyses of local statistical data. The statistics had been computed in Ohio and in Finland, using values of point anomalies read on various profiles. Hirvonen proposed an equation to represent the covariances of anomalies in terms of two constants and the separations of the anomalies. The equation is convenient for deriving other dependent statistical quantities. However, this equation was asymptotic toward zero, so that it would not represent the negative fluctuations of the covariance functions as found both from the local samples of Ohio and of Finland, and the much larger worldwide covariances given by Kaula. Hirvonen also obtained an integral expression to express the mean square anomaly in squares of side s in terms of a weighting function and the covariance of the anomalies.

In the Rapp report, an attempt was made to make these covariances useful in the prediction of point anomalies and, consequently, of mean anomalies in various size squares and equivalent circles. It was found that better results for predictions could be obtained if the covariance function was represented as a polynomial in anomaly separations, instead of Hirvonen's equation.

In a comprehensive report, *Moritz* [1962] presented a theory that gave an anomaly prediction and its accuracy, using a least-squares technique. In this formulation, an anomaly to be predicted is represented as a linear function of surrounding anomalies and a solution is made for the contributiion of the known anomalies from the condition that the mean square difference between the predicted and the true anomaly is at a minimum.

This theory was also extended to a prediction considering not only existing anomalies but also the elevations of these known anomalies [*Moritz*, 1963]. In this case, the predicted anomaly is a linear function of the known anomalies, the elevation of these anomalies and the elevation of the point to be predicted. In this prediction we need to know three statistical functions: the anomaly autocorrelations, the elevation autocorrelations, and the correlation of anomalies with elevation—all with respect to the separations between the variables.

If we have an anomaly that is not considered to be locally correlated with elevations, possibly a Bouguer anomaly, a prediction may be made with this anomaly using covariances of Bouguer anomalies and then reducing the predicted Bouguer anomaly to the desired free-air anomaly.

Mean anomalies and their accuracy may also be obtained by this method, using uniform point prediction throughout the area in which the mean anomaly is desired and taking the mean value.

In a report by *Rapp* [1964*a*, *b*] the least-squares prediction equations of Moritz have been applied to actual predictions in this country. To carry out these predictions, numerical values for 'local covariances' were established in 5°-by-5° blocks, using estimated 5′ mean anomalies and elevations. It was found that the best prediction of point anomalies was made by using the (approximately) ten closest known points to that point at which the prediction was to take place. No significant increase in the accuracy of the prediction was found when more known points were used. Mean anomaly predictions were also carried out in 5′ and 30′ squares. For the smaller squares, the ten closest known points to the square center were chosen, whereas in the larger squares the known point selection was made by a method that would avoid the effect of point clustering, if such existed.

The computations described above have all been carried out on the IBM 7094. We have production programs that can be used for point prediction and mean anomaly predictions with accuracy estimates in any size square, once the covariance and the known point anomalies are given. In practice, however, we have limited the mean anomaly predictions to a maximum size square of 30′, owing to the large computational effort required for larger squares.

There are other techniques available to us that enable the estimation of anomalies. Per-

haps the most widespread is the development of known anomalies into spherical harmonics. Given the anomalies, usually in area means, our basic method is to fit a surface to these data, which exist on a sphere. Then, to find the anomaly at some unknown place, the spherical harmonic expansion can be evaluated at the given latitude and longitude. All the faults usually associated with curve or surface fitting, followed by evaluation, are present in this method. Perhaps the greatest difficulty arises from the nonuniformity in the distribution of the data and the fact that the anomaly field does not follow some simple frequency functions.

On a larger scale it is possible to apply the surface-fitting concept to one-dimensional samples, such as anomaly profiles. This could be done through the use of the Fourier series, such as carried out by *Kivioja* [1962], or of some polynomial such as Legendre. These methods, however, must be carefully handled, and it should be understood that they are basically an interpolation method and that, if applied for extrapolation, they can go seriously wrong.

In the discussion we have thus far been concerned with how an anomaly will vary because of some other anomaly and, to some extent, with the effect of elevations. We are now at the stage where we must look for other features that can give us a clue to what variations can be expected in the anomalous gravity field of the Earth. The correlations that are found, such as between geologic structures, heat flow, and other mechanisms, must be interwoven in a mathematical way with the methods previously developed.

The use of statistical methods for estimating gravity anomalies is a crutch that we need because of the lack of observations. However, behind this practical function is the use of statistical methods in auxiliary computations. These methods can be used to allow analytic evaluations, or at least nonmanual evaluations, of gravimetric dependent quantities. For example, we are now investigating the use of statistical predictions for use in deflections of the vertical computation. The ultimate goal of this study, a deflection and its accuracy, will be obtained with no new manual estimation of mean and point anomalies.

The statistical method is not an end in itself. New ideas in the field of statistics must be developed, so that we may obtain the best possible predictions. But no matter what we do, it remains just that—a prediction. The ultimate test of any theory will be comparison of an observed anomaly with a predicted anomaly and its standard error.

References

Baussus, H. G., A unified isostatic and statistical theory of gravity anomalies and its significance, paper presented at 12th General Assembly IUGG, Helsinki, 1960.

de Graaff-Hunter, J., The figure of the Earth from gravity observations and the precision obtainable, *Phil. Trans. Roy. Soc. London, A., 234,* 1935.

Hirvonen, R. A., On the precision of the gravimetric determination of the geoid, *Trans. Am. Geophys. Union, 37,* 1–8, 1956.

Hirvonen, R. A., On the statistical analysis of gravity anomalies, *Publ. Isostatic Inst. IAG,* 1962.

Kaula, W. M., Accuracy of gravimetrically computed deflections of the vertical, *Trans. Am. Geophys. Union, 39,* 297–305, 1957.

Kaula, W. M., Statistical and harmonic analysis of gravity, *J. Geophys. Res., 64,* 2401–2421, 1959.

Kivioja, L., Development of gravity Bouguer anomalies of state of Ohio and the isostatic anomalies in North Atlantic in Fourier series, *Inst. Geodesy Photogrammetry Cartography Rept. 22,* Ohio State University, Columbus, 1962.

Molodenskii, M. S., V. F. Yeremeyer, and M. I. Yurkina, Methods for the study of the external gravitational field and figure of the Earth (available in translation from OTS, Washington, D. C.), 1962.

Moritz, H., Interpolation and prediction of gravity and their accuracy, *Inst. Geodesy Photogrammetry Cartography Rept. 24,* Ohio State University, Columbus, 1962.

Moritz, H., Accuracy of mean gravity anomalies obtained from point and profile measurements, *Inst. Geodesy Photogrammetry Cartography Rept. 29,* Ohio State University, Columbus, 1963.

Rapp, R. H., Correlation coefficients and their use in the prediction of mean anomalies, *Inst. Geodesy Photogrammetry Cartography Rept. 20,* Ohio State University, Columbus, 1962.

Rapp, R. H., The prediction of point and mean gravity anomalies through the use of a digital computer, *Inst. Geodesy Photogrammetry Cartography Rept. 43,* Ohio State University, Columbus, 1964*a*.

Rapp, R. H., Statistical analysis of gravity anomalies and elevations by long profiles and by areas, *Ann. Acad. Sci. Fennicae, A.*(79), 1964*b*.

On Linear Regression Prediction of Mean Gravity Anomalies

ERWIN GROTEN

Institute of Technology, Munich, West Germany

Abstract. The prediction of mean gravity anomalies for areas of 1-by-1, 5-by-5, and 10-by-10 deg² from mean anomalies of the neighboring areas is discussed. The use of regression of gravity with other geophysical information for prediction is outlined.

INTRODUCTION

Gravity anomalies are usually considered to be a random function on the Earth's surface

$$\Delta g = \Delta g(r, \alpha) \tag{1}$$

In the stationary case the translation of the origin of the coordinate system is without influence; the variance

$$C_{ii} = \text{var}\ \{\Delta g_i\ \Delta g_i\} \tag{2}$$

and the covariances, if supposed to be dependent only on the distance d between the two elements Δg_i and Δg_j, are

$$C_{ij} = \text{cov}\ \{\Delta g_i\ \Delta g_j\}$$
$$= C(d_{ij})$$

For centered anomalies, i.e.

$$\text{ave}\ \{\Delta g\} = 0$$

we obtain

$$C_{ij} = \text{ave}\ \{\Delta g_i\ \Delta g_j\} \tag{3}$$

$$C(0) = C_{ii} = \text{ave}\ \{\Delta g_i\ \Delta g_i\} \tag{4}$$

and the normalized covariance, i.e. the autocorrelation

$$A_{ij} = C_{ij}/C(0) \tag{5}$$

The corresponding functions, like

$$C(d) = \frac{1}{R}\int_{r=0}^{r=R} \Delta g(r)\ \Delta g(r + d)\ dr \tag{6}$$

with $R \rightarrow 2\pi$, are usually derived empirically from discrete values. Similarly, the covariance between two mean gravity anomalies Δg_{s_1} and Δg_{s_2}, where

$$\Delta g_{s_i} = \frac{1}{S}\int_{S_i} \Delta g\ dS \tag{7}$$

is

$$\bar{C}_{1,2} = \frac{1}{S_1 S_2}\iint_{s_1 s_2} C(d)\ dS_1\ dS_2 \tag{8}$$

and can be obtained by numerical integration.

LINEAR PREDICTION USING AUTOREGRESSION

On the Covariance $\bar{C}_{ij}$

If S_1 and S_2 in equation 8 are supposed to be trapezoids of side length s, they may be approximated by rectangles. At the geographic latitude $\varphi = 0$, we obtain approximately squares of side length 111.2 km for a trapezoid of $s = 1°$. At the latitude $\varphi = 45°$, we obtain rectangles of side lengths $a = 111.2$ km, $b = 78.8$ km for 1°-by-1° blocks. Thus, for a certain s, the numerical value of $\bar{C}_{ij}$ depends on the latitude. In Table 1 of his paper, *Moritz* [1963] has evaluated $\bar{C}_{ij}$ at the latitude $\varphi = 45°$ for mean free-air anomalies of $s = 1°$, 2°, 5°, and 10°. A matrix is given containing the values for different separations d of the centers of the rectangles $0 < d < 2\sqrt{2}s$.

On the Least-Squares Prediction of Gravity Anomalies

Moritz [1962] gives the following prediction equation for point anomalies:

$$\widetilde{\Delta g} = \mathbf{c}'\mathbf{C}^{-1}\mathbf{g} \tag{9}$$

The corresponding least rms prediction error is given by

$$m^2 = C(0) - \mathbf{c}'\mathbf{C}^{-1}\mathbf{c} \tag{10}$$

Since the autocorrelation of mean anomalies Δg_s is always larger than the autocorrelation of

point anomalies, i. e. for $d = d_i$

$$A_P(d) = \frac{C(d)}{C(0)} < A_s(d) = \frac{\bar{C}_s(d)}{\bar{C}_s(0)}$$

(where d_i is the distance between point anomalies and mean anomalies, respectively) mainly due to $C(0) > \bar{C}_s(0)$, we studied the possibility of its being useful to predict mean anomalies immediately from known mean anomalies. This question is of interest because the prediction of point anomalies is restricted to separation $d < 50$ km, owing to the limited autocorrelation of point anomalies.

It should be mentioned, however, that the estimation of mean anomalies Δg_s from point anomalies is rather difficult for large squares, owing to the usual nonuniform distribution of gravity stations; this fact involves an error{Δg_s (apparent) $-$ Δg_s (true)} of the known mean anomalies Δg_s from which prediction is made, where

$$\Delta g_s(\text{app}) = \text{ave } \{\Delta g\}$$

$$\Delta g_s(\text{true}) = \frac{1}{S_i} \int_{S_i} \Delta g \, dS$$

This error is not, however, considered here.

By introducing mean anomalies instead of point anomalies, we obtain instead of equations 9 and 10

$$\widetilde{\Delta g}_s = \mathfrak{c}' \bar{\mathbf{C}}^{-1} \bar{\mathfrak{g}} \qquad (9a)$$

$$\bar{m}_s^2 = \bar{C}(0) - \mathfrak{c}' \bar{\mathbf{C}}^{-1} \mathfrak{c} \qquad (10a)$$

$\widetilde{\Delta g}_s$ is not the 'best' estimation of the predicted mean anomaly. Since in geodesy we are not interested in gravity itself but use it only for the evaluation of other quantities, the best estimation is the one which yields the least error integral [*Moritz*, 1963] and not the least prediction error. In this paper, however, we want to compute least standard deviations for the prediction of Δg_s.

Using the average values $\bar{C}_s$ given by *Moritz* [1963], we have computed the prediction errors for some cases of interpolation, using the nearest neighbors as numbered in Figure 2. Some results are shown in Table 1 where the second column gives the number of the mean anomaly of the area S_i from which $\Delta \widetilde{g}_s$ is supposed to be predicted. The use of average values $\bar{C}_s$ is justified since we can assume that local influences, which are of great influence for the prediction of point anomalies, are smoothed out in case of $\bar{C}_s$. Hence we may not need any specific covariance function for each of the prediction areas.

TABLE 1. $\bar{m}_s$, Least Prediction Errors, mgal

No.	Predicted from No.*	1° × 1°	2° × 2°	5° × 5°	10° × 10°
1	5	±21	±18	±13	±14
2	7	±23	±19	±15	±15
3	1,5	±17	±16	±10	±12
4	3,7	±20	±17	±12	±14

* See Figure 2.

From the results in Table 1 we see that the prediction from one or two known anomalies does not yield accurate estimates $\widetilde{\Delta g}_s$.

For the compution of $\bar{m}_s$ in the prediction from *many* known anomalies Δg_s, we introduced two simplifications:

1. We neglected the fact that for rectangles S_i, e. g. $\bar{C}_{28} \neq \bar{C}_{12}$, or $\bar{C}_{28} \neq \bar{C}_{23}$, etc. (see Figure 1).

2. Introducing a second simplification, i. e. $\bar{C}_{27} = \bar{C}_{29} = \bar{C}_{24} = \bar{C}_{26} = \bar{C}(\sqrt{2}s)$, etc., which involves a very small error, we obtain for any specific s covariances $\bar{C}_{s,d}$ which depend only on the distance d between two elements.

These simplifications are admissible as we are interested only in an estimate of the prediction error from which we may decide in which case this prediction procedure is valuable.

Analytic expressions. *Hirvonen* [1956] and *Kaula* [1959] have estimated average covariances for mean isostatic anomalies of $s = 1°$, $5°$, and $10°$ and for mean free-air anomalies of $s = 1°$, $2°$,

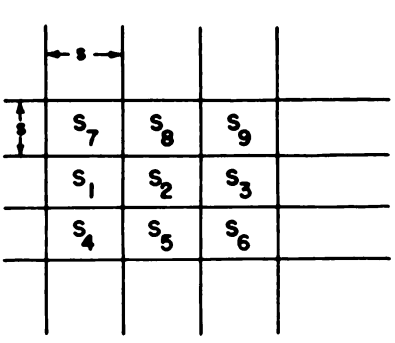

Fig. 1. Situation.

5°, and 10°, respectively. The following considerations are based on these values. As we shall see from Tables 2 and 3, the prediction errors computed from the values of Kaula show only small deviations from values given in Table 1.

To obtain analytic expressions for the evaluations of $\bar{m}$ by using many anomalies, we fitted functions of types

$$\bar{C}_s(d) = \bar{C}_s(0)(1 + c^2d^2)^{-1}$$

$$\bar{C}_s(d) = \bar{C}_s(0)(1 + cd)^{-1}$$

and tentatively

$$\bar{C}_s(d) = \bar{C}_s(0) \exp\{-c^2d^2\}$$

$$\bar{C}_s(d) = \bar{C}_s(0) \exp\{-cd\}$$

$$\bar{C}_s(d) = \bar{C}_s(0)(\tan^{-1} cd)/cd$$

within $0 \leq d \leq 30°$ to the above-mentioned values of Hirvonen and Kaula by least-squares adjustment.

Since the values $\bar{C}_{s,d}$ of Hirvonen are drawn from smaller samples than Kaula's values, a comparison between the prediction errors for free-air and isostatic anomalies of a specific s may be partly misleading.

Some results are given in Tables 2 and 3. The mean anomalies from which the predictions are made are given in the second column of each Table and are shown in Figure 2, numbered 1 to 28. For comparison also $\sqrt{\bar{C}_s(0)}$ is given in Table 2.

We may draw the following general conclusions:

1. Only the nearest anomalies are of particular interest.
2. Many known anomalies yield about the same accuracy as a few anomalies.
3. Prediction over larger distances is generally poor.
4. A maximum accuracy of about $\frac{1}{2}\sqrt{\bar{C}_s(0)}$ is obtainable.

On Linear Regression of Gravity with Other Data

Correlation of mean gravity with elevation or other anomalies, e.g. seismic travel-time fluctuations, may be mainly useful for extrapolation of Δg, if the regression coefficients are constant within the domain of interest. Correlation between gravity and other geophysical data is given by many workers, including *Durbin* [1961], *Oliver et al.* [1963], *Press and Biehler* [1964], *Woollard* [1959], and for the lower harmonics by *Lee and MacDonald* [1963], *MacDonald* [1963], *Vogel* [1963], *Wang* [1964], and others. (The worldwide nondipole profile of

TABLE 2. $\bar{m}_s$ for Interpolation Cases, mgal

No.	Predicted from No.	Free-Air				Isostatic		
		1 × 1	2 × 2	5 × 5	10 × 10	1 × 1	5 × 5	10 × 10
1	1,5	±18	±14	±10	±13	±10	±12	±11
2	2,4,6,8	±18	±12	±8	±14	±9	±10	±10
3	1,···,8	±16	±12	±8	±12	±9	±10	±10
4	1,3,5,7,9,12,15,18	±16	±12	±8	±12	±9	±10	±10
5	10,11,13,14,16,17,19,20–28	±22	±15	±17	±15	±15	±13	±14
	$\sqrt{\bar{C}_s(0)}$	±28	±23	±19	±16	±25	±19	±16

TABLE 3. $\bar{m}_s$ for Extrapolation Cases, mgal

No.	Predicted from No.	Free-Air				Isostatic		
		1 × 1	2 × 2	5 × 5	10 × 10	1 × 1	5 × 5	10 × 10
1	1	±22	±16	±14	±14	±14	±14	±13
2	5,15	±21	±16	±12	±14	±13	±14	±13
3	4,5,6	±20	±16	±14	±14	±14	±14	±13
4	13,14,16,17,24–27	±23	±18	±18	±15	±17	±16	±15

		23		24		
		11	12	13		
22	10	2	3	4	14	25
	9	1	$\tilde{\Delta}g$	5	15	
21	20	8	7	6	16	26
		19	18	17		
		28		27		

Fig. 2. Numbering sequence for squares.

Alldredge et al. [1963] and mean geoid heights [*Kaula, 1963b, c; Izsak,* 1964; and *Uotila,* 1962] seem to be negatively correlated ($-0.7 < r < -0.4$).) The use of regression with geophysical data for prediction of mean gravity anomalies for geodetic purposes (i.e. for square size of 1° by 1° to 10° by 10°) is handicapped by various factors:

1. A true geophysical reference for gravity may be needed [*Ledersteger,* 1962, 1964] instead of the level ellipsoid.

2. The dependence of gravity on the topography is only partly removed by physical standard rules as the isostatic concept [see *Jeffreys,* 1963; *Heiskanen,* 1963; *Kaula,* 1963*b*].

3. The interrelations are complex, e.g. terrestrial heat flow values are supposed to be negatively correlated with gravity in case of small-scale convection and positively in case of radiogenic heat[1] [*MacDonald,* 1963; *Knopoff,* 1964].

4. Correlation between two sets of data may exist only if the autocorrelations of the two sets are similar [*Bartels,* 1935]. Owing to the mostly strong horizontal gradients of gravity, the derivation of mean values from point anomalies is thus difficult for each comparable data set.

5. Only common disturbation sources, which are situated in the *upper* part of the mantle, can produce correlation of mean anomalies of squares of the above-mentioned sizes.

6. The generalization of the prediction equation (for correlation with elevation) of *Moritz* [1962] for several parameters, i.e. the generalization of the regression equation

$$\Delta g = a + bh + ci + dj \cdots,$$

involves the inversion of a very big matrix, even if only a few anomalies are considered.

7. The intricacy of quantitative statements on correlation of spatial functions is shown by *Wold* [1938]. Harmonic analysis methods often fail, owing to the unfavorable distribution of data.

A very tentative numerical approach has been made by comparing 5°-by-5° mean gravity anomalies (free-air as well as isostatic) with mean heat flow fluctuations using results of *Lee* [1963], *Uyeda and Horai* [1964], and *Uotila* [1962], respectively. Neglecting autocorrelation beyond a distance $d > 20°$, as well as the difference between the international ellipsoid by any corresponding true equilibrium figure, correlation coefficients have been estimated. (More independent values may be obtained after elimination of the lower harmonics in both fields.) The results from various samples are given in Table 4.

TABLE 4. Correlation Coefficients*

Region	$\bar{r}_{fa}$	$\bar{r}_{is.}$
North America and environs	+0.6	+0.7
Central Pacific	−0.2	−0.3
Outer Pacific and other areas of southern hemisphere	−0.3	−0.1
Europe and Atlantic	−0.3	−0.3

*$\bar{r}$ = mean correlation coefficient derived from different samples.
fa = free-air.
is. = isostatic.

For significance tests, randomness and normality are decisive; they are omitted. For non-normally distributed values, the coefficient r is simply a measure of linearity and not of dependence; therefore Pearson's ratio η may be preferable [*Cramér,* 1946]. Complicated non-linear relations are, however, mostly not manageable in prediction.

A similar approach, comparing mean Bouguer anomalies [*Woollard and Rose,* 1963] with seismic data [*Nuttli,* 1964] for areas of different sizes within the U.S.A., did not yield significant linear interrelations.

[1] For linear relation between temperature Δu and density anomalies $\Delta\rho$ as $\Delta\rho = \alpha\rho_0\,\Delta u$ [*Magnitskii,* 1963] geoid undulations would be simply given by $N = (f\alpha\rho_0/G)\int_\tau (\Delta u/r)d\tau$, where G = mean gravity, ρ_0 = mean density, α = expansion coefficient, and f = gravitational constant.

Acknowledgment. This study was sponsored by the USAF Research Laboratories, Office of Aerospace Research, Cambridge, Massachusetts, under contract AF 19(628)-2717, Ohio State University Research Foundation project 1613, under W. A. Heiskanen (supervisor) and B. Szabo (project engineer).

References

Alldredge, L. R., G. D. van Voorhis, and T. M. Davis, A magnetic profile around the world, *J. Geophys. Res., 68,* 3679–3692, 1963.

Bartels, J., Zur Morphologie geophysicalischer Zeitfunktionen, *Preuss. Akad. Wiss., Math.-Physik Kl., 1935*(2), 505–522, 1935.

Cramér, H., *Mathematical Methods of Statistics,* Princeton University Press, Princeton, 1946.

Durbin, P. D., Some correlations of gravity and geology, paper presented at Symposium on Geodesy in Space Age, Columbus, Ohio, 1961.

Heiskanen, W. A., Die neuesten Erkenntnisse der physikalischen Geodaesie, *Z. Vermessungsw., 88,* 283–294, 1963.

Hirvonen, R. A., On the precision of the gravimetric determination of the geoid, *Trans. Am. Geophys. Union, 37,* 1–8, 1956.

Iszak, I. G., Tesseral harmonics of the geopotential and corrections to station coordinates, *J. Geophys. Res., 69,* 2621–2630, 1964.

Jeffreys, H., On the hydrostatic theory of the figure of the Earth, *Geophys. J., 8,* 196–202, 1963.

Kaula, W. M., Statistical and harmonic analysis of gravity, *J. Geophys. Res., 64,* 2401–2421, 1959.

Kaula, W. M., Elastic models of the mantle corresponding to variations in the external field, *J. Geophys. Res., 68,* 4967–4978, 1963*b*.

Kaula, W. M., Tesseral harmonics of the gravitational field and geodetic datum shifts derived from camera observations of satellites, *J. Geophys. Res., 68,* 473–484, 1963*c*.

Knopoff, L., The convection current hypothesis, *Rev. Geophys., 2,* 89–122, 1964.

Ledersteger, K., Der physikalische Zusammenhang zwischen der statischen Abplattung und dem inneren Aufbau der Erde auf der hypothetischen Grundlage einer sechsparametrigen Gleichgerwichtsfigur, *Geofis. Pura Appl., 51,* 1–28, 1962.

Ledersteger, K., Die Neubegruendung der Theorie der sphaeroidischen Gleichgewichtsfiguren und das Normalsphaeroid der Erde, *Oesterr. Z. Vermessungsw.,* Sonderheft 24, Vienna 1964.

Lee, W. H. K., Heat flow data analysis, *Rev. Geophys., 1,* 449–479, 1963.

Lee, W. H. K., and G. J. F. MacDonald, The global variation of terrestrial heat flow, *J. Geophys. Res., 68,* 6481–6492, 1963.

MacDonald, G. J. F., The deep structure of the continents, *Rev. Geophys., 1,* 587–665, 1963.

Magnitskii, V. A., Interpretation of the mean gravity anomalies of the Earth, *Prop. Geophys. Inst. O. Yu. Schmidt, II* (178), (English transl., Jerusalem), 66–71, 1963.

Moritz, H., Interpolation and prediction of gravity and their accuracy, *Inst. Geodesy Photogrammetry Cartography Rept. 24,* Ohio State University, Columbus, 1962.

Mortiz, H., Accuracy of mean gravity anomalies obtained from point and profile measurements, paper presented at 13th General Assembly IUGG, Berkeley, California, 1963.

Nuttli, O., Seismological evidence pertaining to the structure of the Earth's upper mantle, *Rev. Geophys., 1,* 351–400, 1963.

Oliver, H. W., Anomalous gravity field in east central California, *Geol. Soc. Bull., 74,* 1293–1298, 1963.

Press, F., and S. Biehler, Inferences on crustal velocities and densities from *P*-wave delays and gravity anomalies, *J. Geophys. Res., 69,* 2979–2996, 1964.

Uotila, U. A., Harmonic analysis of world-wide gravity material, *Ann. Acad. Sci. Fennicae, Ser. A III,* 67, 1962.

Uyeda, A., and K. Horai, Terrestrial heat flow in Japan, *J. Geophys. Res., 69,* 2121–2142, 1964.

Vogel, A., *Secular Variations in the Lower Harmonics of the Earth's Gravitational Field due to Convection Currents in the Earth's Core, Medd. Geod. Inst. Uppsala Univ.,* 1963.

Wang, C. Y., On the correlation between the fluctuations of heat flow and gravitational potential of the Earth (abstract), *Trans. Am. Geophys. Union, 45,* 36, 1964.

Wold, H., *A Study in the Analysis of Stationary Time Series,* Upnsala, 1938.

Woollard, G. P., Crustal structure from gravity and seismic measurements, *J. Geophys. Res., 64,* 1521–1544, 1959.

Woollard, G. P., and J. C. Rose, *International Gravity Measurements,* G. Banta Co., Menasha, Wisconsin, 1963.

Global Harmonic and Statistical Analysis of Gravimetry[1]

W. M. KAULA

Institute of Geophysics and Planetary Physics
University of California, Los Angeles

Abstract. The most general possible linear auto-analysis (i.e., one assuming that statistical properties can be expressed by mean double products as a function of distance) of gravimetry obtains a result that agrees with the best independent test (Guier and Newton's latest satellite geoid) within 30° for the location of the eight principal extremums of the worldwide geoid. However, this geoid still gives an impression of falling short of exploiting the available data. Part of the difficulty is computational, but substantive improvement seems practicable in three directions:

1. *Linear cross analysis.* The topography has, of course, always been recognized as of primary importance, particularly in view of its influence on observation distribution. More recently, heat flow measurements and seismically deduced crustal thicknesses have become extensive enough to promise geophysically fruitful cross analyses with gravimetry.

2. *Use of a reference model derived from satellite orbits.* Satellite orbits continue to yield improved results of the low-degree tesseral harmonics. Since the long-wave variations are the part of the field for which gravimetry is statistically weakest (essentially a case of small sample size), the logical optimization would be to define the reference model for the gravity anomalies to be analyzed as a third- or fourth-degree geoid determined from satellite orbits.

3. *Nonlinear auto-analysis.* Part of the inadequacy of the linear analysis is that gravity anomalies obviously do not have the Gaussian distribution and randomness of relationship between phases which such analysis assumes; there is a definite tendency toward certain patterns such as circum-ocean arcs. Hence significant information would be obtained from mean triple products ('coskewness') and quadruple products ('co-excess'). Such higher-order spectrums would be more likely to be suggestive of geophysical laws of formation. Nonlinear analysis would, however, be a considerable computational problem.

LINEAR AUTO-ANALYSIS

Approximating the gravity anomalies over the portion of the sphere where they are known by a finite set of values f_j and over the portion where they are unknown by a finite set g_i, the linear theory states that the estimate $\hat{g}_i$ can be expressed as a linear transform of the f_j:

$$\hat{g}_i = B_{ij} f_j \tag{1}$$

where an element B_{ij} of the transform is a function only of the distance s_{ij} between the locations of g_i and f_j. (Summation is taken over the subscript j in (1) and will be understood over all repeated subscripts in products hereafter) The array B_{ij} is a function of the covariances between the g_i's and f_j's:

$$K_{ik} = B_{ij} K_{jk} \tag{2}$$

where $K_{ik}(s_{ik})$ is the covariance of g_i and f_k, and K_{jk} is the covariance of f_j and f_k [*Kaula*, 1963*a*, pp. 512–515]. The use of covariances implies stationarity, i.e. the same statistical properties in the unobserved as in the observed areas.

As previously discussed [*Kaula*, 1963*b*], the first problem is the estimation of the covariances K_{jk}, the mean product pairs as a function of distance, from the nonuniformly distributed data available. This 'broken window' problem is best formulated in terms of the spectrum, which is the Fourier transform of the covariances

$$\sigma_n^2 = \frac{2n+1}{2} \int_0^\pi P_n(\cos\psi) K(\psi) \sin\psi \, d\psi \tag{3}$$

[1] Publication 411, Institute of Geophysics and Planetary Physics, University of California, Los Angeles.

where $P_n(\cos\psi)$ is the Legendre polynomial of degree n, $K(\psi)$ is the covariance for arc distance ψ, and σ_n^2 is the degree variance of degree n. The true value of σ_n^2 would be obtained from determinations of the covariances $K(\psi)$ by mean products of the function of interest, say $f(r)$ over the entire sphere T:

$$\sigma_n^2 = \frac{2n+1}{2}\int_0^\pi P_n(\cos\psi)\,\frac{1}{4\pi}\int_T f(r)\,\frac{1}{2\pi}\cdot\int_0^{2\pi} f(s)\,d\alpha\,dr\sin\psi\,d\psi \qquad (4)$$

where r and s each denote a coordinate pair (φ, λ); dr is an element of area; and $d\alpha \sin\psi\, d\psi$ replaces ds. It is usually convenient to use the spherical harmonics normalized to have a mean square of unity. Then

$$\sigma_n^2 = \frac{(2n+1)^{1/2}}{2}\int_0^\pi \bar{P}_n(\cos\psi)\,\frac{1}{4\pi}\cdot\int_T f(r)\,\frac{1}{2\pi}\int_0^{2\pi} f(s)\,d\alpha\,dr\sin\psi\,d\psi \qquad (5)$$

Applying the addition theorem to $\bar{P}_n(\cos\psi)$ obtains

$$\sigma_n^2 = \frac{1}{(4\pi)^2}\sum_{m,i}\int_T\int_T f(r)f(s)\cdot\bar{S}_{nmi}(r)\,\bar{S}_{nmi}(s)\,dr\,ds \qquad (6)$$

where the subscript m denotes the spherical harmonic order; i denotes whether it is a sine $m\lambda$ or cosine $m\lambda$ term; and $\bar{S}_{nmi}$ is a normalized surface spherical harmonic.

In place of data over the entire sphere T, we have data only over a limited part S:

$$\hat{\sigma}_l^2 = \frac{1}{A_o^2}\sum_{m,i}\int_S\int_S f(r)f(s)\cdot\bar{S}_{lmi}(r)\,\bar{S}_{lmi}(s)\,dr\,ds \qquad (7)$$

If we define the function

$$I(\phi,\lambda) = \begin{cases} 1 \text{ in } & S \\ 0 \text{ in } & T-S \end{cases} = \sum_{n,m,i} a_{nmi}\bar{S}_{nmi} \qquad (8)$$

and let

$$f(\phi,\lambda) = \sum_{n,m,i} b_{nmi}\bar{S}_{nmi} \qquad (9)$$

then equation 7 can be changed to

$$\hat{\sigma}_l^2 = \frac{1}{A_o^2}\sum_{m,i}\int_T\int_T I(r)f(r)\cdot\bar{S}_{nmi}(r)\,I(s)f(s)\,\bar{S}_{nmi}(s)\,dr\,ds \qquad (10)$$

Replacing I and f by their expressions from equations 8 and 9 we get

$$\hat{\sigma}_l^2 = \frac{1}{(4\pi a_{000})^2}\sum_{m,i}\Big[\sum_{jkhnpq} a_{jkh}b_{npq}K_{jkhlminpq}\Big]^2 \qquad (11)$$

where

$$K_{jkhlminpq} = \int_T \bar{S}_{jkh}\bar{S}_{lmi}\bar{S}_{npq}\,d\sigma \qquad (12)$$

i.e. the integral of the triple product of the surface spherical harmonics over the sphere. Now, in equation 11, a_{jkh} is known. If we assume that each coefficient b_{npq} can be considered as random with respect to all the other b_{npq}'s and a_{jkh}'s, then we can substitute the statistical expectancy $\sigma_n^2(f)/(2n+1)$ for b_{npq}^2 and write

$$E\{(a_{jkh}b_{npq})^2\} = a_{jkh}^2\sigma_n^2/(2n+1) \qquad (13)$$

and equation 11 becomes

$$\hat{\sigma}_l^2 = \frac{1}{(4\pi a_{000})^2}\sum_n \frac{\sigma_n^2(f)}{2n+1}\cdot\sum_{m,i}\Big[\sum_{jkhpq} a_{jkh}K_{jkhlminpq}\Big]^2 \qquad (14)$$

For a set of estimates $\hat{\sigma}_l^2$, (14) can be written in matrix form:

$$\hat{\mathbf{d}} = \mathbf{N}\mathbf{d} \qquad (15)$$

where a particular element N_{ln} of $\mathbf{N}$ is

$$N_{ln} = \frac{1}{(4\pi a_{000})^2(2n+1)}\cdot\sum_{m,i}\Big[\sum_{jkhpq} a_{jkh}K_{jkhlminpq}\Big]^2 \qquad (16)$$

Equation 15 could thus be used to remove the distorting effect of the 'broken window' on the degree variances. However, since it is impracticable to take infinite dimension vectors $\hat{\mathbf{d}}$ and $\mathbf{d}$ on each side of equation 15, any actual solution will have some truncation error due to neglect of higher harmonics. Also, the computation of the N_{ln}'s by equation 16 is time consuming. Hence equation 15 has been applied only up to degree 9 of the $\hat{\sigma}_l^2$ and σ_n^2. It would be much less

TABLE 1. Estimates of Degree Variances of Gravimetry (in mgal²)

Degree, l	Before Window Correction,* δ_l^2	After Window Correction,† σ_n^2	Directly,‡ σ_n^2
0	3.83	1.64	1.92
1	2.44	−6.31	−6.47
2	20.76	−0.49	−0.03
3	96.01	77.63	76.87
4	75.56	45.86	44.13
5	42.00	13.04	9.93
6	53.76	35.96	31.96

* By equation 7.
† By equation 15.
‡ By equation 3.

time consuming if the degree variances could be corrected by applying appropriate weighting factors $W(\psi)$ to the covariances $K(\psi)$ estimated from the incomplete set over S:

$$\sigma_n^2 = \frac{2n+1}{2} \int_0^\pi P_n(\cos\psi) \cdot W(\psi)K(\psi) \sin\psi \, d\psi \qquad (17)$$

It has been shown by computer experimentation (not by derivation) that the appropriate value of $W(\psi)$ is unity; i.e., the $K(\psi)$ should be treated as if from a sample uniformly distributed over the sphere. Hence the covariances may be used directly in equation 2 to form the covariance matrices.

Table 1 gives various estimates of degree variances from the same set of mean gravity anomalies of 5°-by-5° squares.

The effect of higher harmonics on the window correction is thus quite moderate. It is interesting to note that only the δ_l^2's are all positive; the effect of the nonuniform distribution is to cause impossible negative values for the σ_n^2's. The effects of higher coefficients than those taken into account in the calculation would only cause the degree variances calculated using the window correction (by equation 15) to differ from those using the unity weighting factor $W(\psi)$ (by equation 17), if the latter was correct; the discrepancies in Table 1 appear to bear this out, since they increase with degree. The other reason would be the assumptions made between equations 11 and 14 that the coefficients b_{npq} (1) are random with respect to each other and to the a_{jkh}'s and (2) have a value squared equal to their statistical expectancy $\sigma_n^2/(2n+1)$. The effect of assumption 1 cannot be estimated without knowledge either of the coefficients themselves or of the higher moments. A measure of the effect of assumption 2 could be calculated on the assumption that the b_{npq}'s have normal distribution with 0 mean and $\sigma_n^2/(2n+1)$ variance. Such a measure would involve the variance of σ_n^2:

$$\begin{aligned} D^2(\sigma_n^2) &= (2n+1)D^2(b_{npq}^2) \\ &= (2n+1)E\{b_{npq}^4 - [E(b_{npq}^2)]^2\} \\ &= (2n+1)2[\sigma^2\{b_{npq}\}]^2 \end{aligned} \qquad (18)$$

on the assumption of normal distribution [*Cramér*, 1964, p. 208]. Then substituting $\sigma_n^2/(2n+1)$ for $\sigma^2\{b_{npq}\}$

$$\begin{aligned} D^2(\sigma_n^2) &= (2n+1)2\left[\frac{\sigma_n^2}{2n+1}\right]^2 \\ &= \frac{2(\sigma_n^2)^2}{2n+1} \end{aligned} \qquad (19)$$

Hence for low harmonic degrees we should expect a wider scatter about the true value of the degree variance σ_n^2 from different samples than for higher harmonics. Remembering the original assumption of stationarity, this result seems quite plausible, since for a low harmonic degree there is a much smaller set of 'events,' the $(2n+1)$ coefficients b_{npq}, over which statistical variations are averaged than for a high harmonic degree.

Since we were interested mainly in obtaining an expression of the gravity field to compare with satellite results, the estimation of the gravity anomalies for the empty areas by equations 1 and 2 was not performed; instead, for 30°-by-30°-square means, there was estimated the harmonic transform of $(\mathbf{f}+\mathbf{g})$, i.e. the spherical harmonic coefficients, by [*Kaula*, 1963*a*, p. 514]:

$$\hat{\mathbf{f}}_i = w_i C_{ik}[K_{jk}]^{-1} f_j \qquad (20)$$

where C_{ik} is the value of the normalized surface spherical harmonic at point k:

$$C_{ik} = \bar{P}_{nm}(\sin\phi_k) \begin{Bmatrix} \cos \\ \text{or} \\ \sin \end{Bmatrix} m\lambda_k \qquad (21)$$

$\hat{x}_i$ is the estimated value of the corresponding spherical harmonic coefficient $\bar{C}_{nm}$ or $\bar{S}_{nm}$, and w_i is its expected square value:

$$w_i = \frac{\sigma_n^2}{2n+1} \tag{22}$$

Table 2 gives the results obtained using the σ_n^2's from Table 1 in the form of normalized potential coefficients, i.e. $\bar{C}_{lm}$ and $\bar{S}_{lm}$ in

$$V = \frac{GM}{r}\left[1 + \sum_{l,m}\left(\frac{a_e}{r}\right)^l \bar{P}_{lm}(\sin\phi) \cdot \{\bar{C}_{lm}\cos m\lambda + \bar{S}_{lm}\sin m\lambda\}\right] \tag{23}$$

TABLE 2. Normalized Spherical Harmonic Coefficients

Degree	Order	Window Function		Potential From Gravimetry		Potential From Satellites	
l	m	$\bar{C}_{lm}$	$\bar{S}_{lm}$	$\bar{C}_{lm} \times 10^6$	$\bar{S}_{lm} \times 10^6$	$\bar{C}_{lm} \times 10^6$	$\bar{S}_{lm} \times 10^6$
0	0	0.213					
1	0	0.123					
1	1	0.046	−0.005				
2	0	−0.017					
2	1	0.049	−0.029				
2	2	−0.020	−0.036	0.00	0.00	2.33	−1.16
3	0	−0.043		2.93		1.01	
3	1	0.016	−0.012	0.86	−0.50	1.78	0.32
3	2	−0.041	0.043	2.25	−0.42	1.20	−0.74
3	3	0.012	0.033	0.72	2.25	0.70	0.92
4	0	−0.044		0.10		0.88	
4	1	0.007	0.027	−0.30	−0.51	−0.63	−0.37
4	2	−0.012	0.061	0.46	−0.20	0.32	0.44
4	3	0.015	0.001	1.82	−0.43	0.81	−0.03
4	4	0.002	0.022	0.51	−0.71	−0.17	0.19
5	0	−0.033		−0.43		−0.04	
5	1	0.013	0.010	−0.36	0.02	0.13	−0.03
5	2	0.019	0.041	−0.13	0.04	0.22	−0.19
5	3	0.004	0.046	0.01	0.14	0.16	−0.01
5	4	0.045	−0.014	−0.01	0.07	−0.51	−0.26
5	5	0.001	−0.012	0.02	−0.45	0.01	−0.56

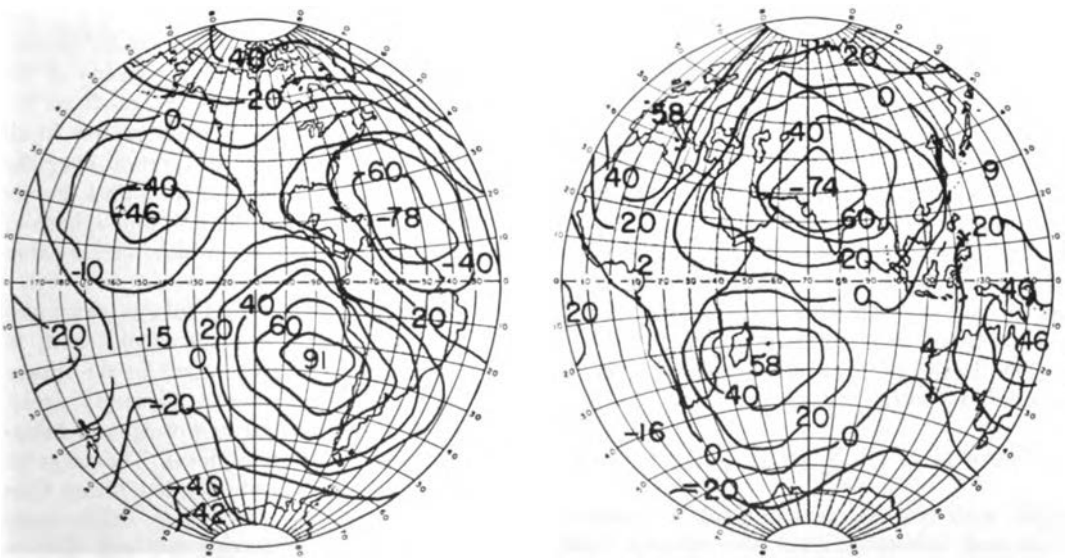

Fig. 1. Gravimetric geoid.

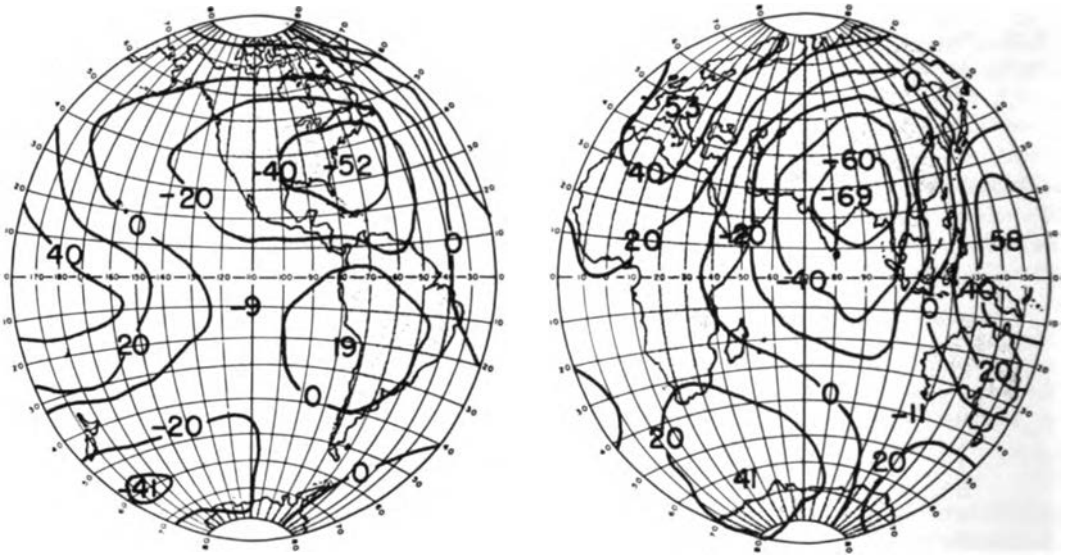

Fig. 2. Satellite geoid.

Also given in Table 2 are the normalized coefficients for the window function $I(\varphi, \lambda)$ (the a_{nmi} of equation 8) and, for comparison, one of the most recent solutions from satellite orbits by Guier and Newton (private communication, 1964).

As usual, the resemblance of two solutions for the gravity field appears much greater in the form of geoid maps than in the form of harmonic coefficients. Figure 1 is the gravimetric geoid, and Figure 2 is the satellite geoid. Of the eight principal extremums in the gravimetric geoid, seven appear in the same vicinity on the satellite geoid, as given in Figure 2. If the geoid corresponding to the complete solution of Guier and Newton up to the eighth degree is shown, the eighth feature, the north Pacific minimum, also appears on the satellite map.

The figures emphasize the dominance of the third- and fourth-degree harmonics in the geoid, since the second-degree C_{22}, S_{22} are entirely absent from the gravimetric geoid.

The degree variances σ_l^2 calculated from the gravimetric coefficients by

$$\sigma_l^2 = G^2(l-1)^2 \sum_{m=0}^{l} (\bar{C}_{lm}^2 + \bar{S}_{lm}^2) \qquad (24)$$

agree with the variances in Table 1. However, variances calculated from the satellite coefficients are in general smaller, being 6.7 mgal^2 for σ_2^2; 29.5 mgal^2 for σ_3^2; 20.1 mgal^2 for σ_4^2; and 11.8 mgal^2 for σ_5^2. These variances are somewhat closer to those obtained in older autocovariance analyses [*Kaula*, 1963*a*, p. 525], in which more elaborate sample selection was used but also in which the 5°-by-5° squares were filled out by Markov analysis, which should result in values too small in absolute magnitude. The 5°-by-5°-square means used in the present analysis were obtained by applying the autoregression analysis of equations 1 and 2 to 1°-by-1° means. The 30°-by-30°-square means were formed as the direct means of the 5°-by-5° means, and their covariances from the covariances of the 5°-by-5°-mean values. In all these operations, in which integration over the surface is implied, there were used area factors proportionate to the area on the unit sphere of the 5°-by-5° squares for which values were known.

It should be expected that taking covariance only as a function of distance should result in values too large in absolute value for the reason that the observations closest to empty areas, and hence having the greatest weight in extrapolation, tend to be nontypical. The ways to take this nontypicality into account (other than arbitrary corrections) are (1) to utilize cross correlation with the topography and (2) to determine higher-order statistics expressing

skewness and excess. The use of cross correlation with topography requires much less computer effort and therefore will be done first.

Linear Cross Analysis

There is no requirement that the measured quantities f_j in equation 1 be of the same function as the estimated quantities $\hat{g}_i$ or, for that matter, that all the quantities f_j be of the same function. If certain $\hat{g}_i$ and f_k, or certain f_j and f_k, are different functions (such as gravity and topography), for the linear estimate of equations 1 and 2 to apply it is merely necessary that the corresponding covariance K_{ik} or K_{jk} is a cross covariance, i.e. a mean product of the two different functions for the distance between them. Similarly, the entire theory of degree variances, window corrections, and spherical harmonic coefficient estimation of equations 3–17, 20, and 24 requires but slight modification to apply to cross covariances, cross degree variances, etc. The cross degree variances between two functions x and y can be expressed by equation 3, using cross covariances for $K(\psi)$, or by a modification of equation 24:

$$\sigma_l^2(x, y) = \sum_{m=0}^{l} [\bar{C}_{lm}(x)\bar{C}_{lm}(y) + \bar{S}_{lm}(x)\bar{S}_{lm}(y)] \quad (25)$$

The cross analysis has been applied thus far to obtain the cross covariances and cross degree variances of the gravity and heat flow data. The results bear out the negative correlation noted by *Lee and MacDonald* [1963]. Figure 3 is the cross covariance curve of heat flow and gravity, adjusted so that the mean produce σ_0^2 is zero. The two peaks at about 18° and 90°, and the trough at about 36°, are suggestive of two different scales of phenomena. Table 3 gives the degree variances coresponding to the covariances in Figure 3.

The ups and downs in the cross degree variances are suggestive of some physical explanation. However, more examination of the statistical problems is in order, since there are still less than one-tenth as many heat flow data (in terms of 1°-by-1° squares) as gravimetry data.

Hence, for the purpose of extrapolation of the gravity field the topography is still the most important item. It is therefore intended to perform cross covariance analyses between gravimetry and topography using the 1°-by-1°-mean values of each. It is also intended to make cross analyses of gravimetry with crustal thickness data to supplement the studies by *Woollard* [1962] and others.

Use of a Satellite Orbit Derived Reference Model

In 1964 definitive results for some tesseral harmonics of the gravitational field were finally obtained. Two satellites launched in 1963, Transit 5B and Syncom 2, provided the essential data.

Transit 5B was the final member of a set of four satellites of good perigee height at wide intervals of inclination (32°, 50°, 67°, and 90°) carrying the Doppler transmitters. Concurrent improvements were an extension of the Transit Doppler tracking network and a large-scale revision of the orbit analysis programs at Applied

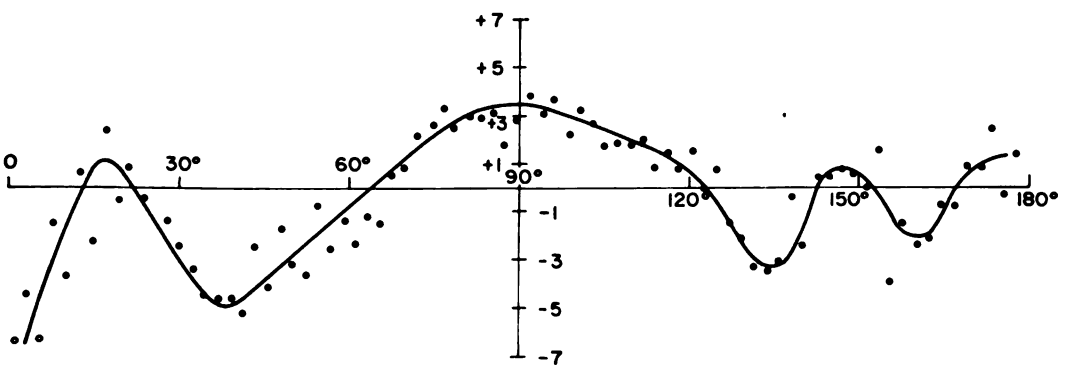

Fig. 3. Cross covariance of heat flow and free-air gravity anomalies in units of (μcal/cm^2/sec) × mgal.

TABLE 3. Cross Degree Variances of Heat Flow and Gravity Anomalies, (μcal/cm^2/sec) $\times$ mgal

Degree, n	Degree Variance, σ_n^2	Degree, n	Degree Variance, σ_n^2
1	−1.09	9	−0.10
2	−3.61	10	−0.37
3	0.33	11	−2.84
4	3.89	12	0.08
5	0.71	13	−2.68
6	−0.17	14	0.20
7	−0.07	15	1.45
8	−1.49	16	−0.51

Physics Laboratory. Hence the results obtained in 1964 by Guier and Newton (see Table 2) should be a distinct improvement over any obtained previously. A solution using largely the same data has also been made by *Anderle* [1965], whose results agree within 0.5×10^{-6} for all but one of the coefficients in Table 2; the rms discrepancy is $\pm 0.27 \times 10^{-6}$.

Syncom 2 is the first twenty-four hour 'geostationary' satellite orbit. Examination of the week-by-week semi-major axes and Earth-referred longitudes during times Syncom 2 is allowed to drift shows a smooth linear change in the axes and acceleration in the longitudes, as predicted from resonance with tesseral harmonics. This acceleration can be determined within a standard deviation which is about one-fiftieth of the expected effect of J_{22}, the equatorial ellipticity term, and thus constitutes a significant restriction of J_{21} and J_{22} as well. For the first two free-drift periods of about 81 days each, *Wagner* [1964] obtains as the following mean accelerations: observed $\ddot{\lambda}$, $-1.27 \pm 0.02 \times 10^{-6}$ and $-1.32 \pm 0.02 \times 10^{-6}$ degree/day^2. Using the Guier and Newton values for C_l^m, S_{lm}, $lm = 22$, 31, 33, 42, and 44, plus a small correction for Sun and Moon effects, we obtain a calculated $\ddot{\lambda}$ of -1.24×10^{-6} and -1.21×10^{-6} degree/day^2. There is similar agreement in the solution of *Anderle* [1965].

Such a close agreement for a radically different type of perturbation justifies considerable confidence in the Guier and Newton geoid up through the fourth degree. The agreement depends on the coefficient $\bar{S}_{22}$ being correct within about 0.1×10^{-6}, and any of the fourth-degree coefficients should be as easily or more easily determined from nearby, almost circular orbits.

It is therefore time to consider using satellite data as a means of extrapolating and interpolating the gravity field. The satellite data are, of course, strongest for the long-wave variations and are incapable of reflecting many shorter-wavelength variations of geophysical interest. A combination is therefore indicated. The appropriate gravity anomaly to which to apply our statistical analyses would be with respect to a model defined from satellite data up through, say, the fourth degree. The absence of second-, third-, and fourth-degree harmonics from the anomalies would be a condition enforced in the same way as we already enforce the absence of the first-degree and $lm = 21$ harmonics. This use of the satellite data would remove some of the statistical weakness of using the gravity anomalies to determine the long-wave properties, as discussed after equation 19.

Nonlinear Auto-Analysis

Gravity anomalies are geophysically interesting largely because they do not conform to the previously described assumptions: randomness between phases (including isotropy and normal distribution) and stationarity. Nonstationarity can only be taken into account by cross analyses. The nonrandomness of relationships between different spherical harmonics is reflected statistically in the higher moments of the field, i.e. in mean triple, quadruple, etc. products. The traditional measures are functions that are zero for a normal, or Gaussian, distribution with

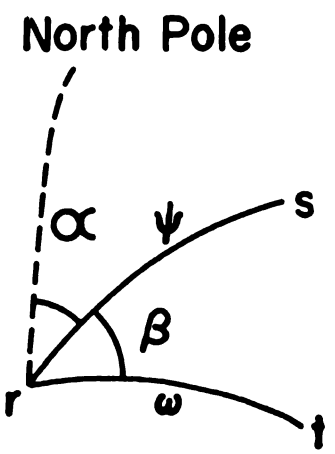

Fig. 4.

zero mean [*Cramér*, 1946, p. 184]; the coefficient of skewness

$$\gamma_1(x) = [E\{x^3\}/\sigma^3] \tag{26}$$

and the coefficient of excess

$$\gamma_2(x) = [E\{x^4\}/\sigma^4] - 3 \tag{27}$$

For example, the 7950 1°-by-1° mean anomalies in Table 2 on page 12 of *Kaula* [1959] have a skewness coefficient of −0.291. However, this same table emphasizes the effect of extreme values; eliminating the 37 values of absolute magnitude greater than 160 mgal changes the skewness to +0.114. The table also shows the effect of cross correlation with topography. If we take only the 1572 values corresponding to 0 (±500-ft) elevation, the skewness is a moderate −0.055. Thus taking the higher moments into account compounds the needs to define carefully the population being analyzed, to examine carefully the manner of formation of area mean values, and to utilize cross-correlated data wherever significant.

The fundamental statistical property used in the linear analysis was the covariance $K(\psi)$, i.e. the mean double product as a function of distance ψ, which degenerates for zero ψ to the variance σ^2, the mean square. Analogously, the leading statistical property with which we should be concerned in nonlinear analysis is the 'coskewance' $L(\psi_{12}, \psi_{23}, \psi_{31})$, i.e. the mean triple product as a function of distance.

$$L(\psi_{12}, \psi_{23}, \psi_{31}) = E\{x_1x_2x_3\} \tag{28}$$

$\psi_{ij} + \psi_{jk} \geq \psi_{ki}$ for any combination of i, j, k. For zero $\psi_{12}, \psi_{23}, \psi_{31}$, the 'coskewance' degenerates to the 'skewance' μ_3, the mean cube.

The appropriate generalization of equation 1 is

$$g_i = B_{ij}f_j + C_{ikl}f_kf_l \tag{29}$$

where B_{ij} and C_{ikl} are defined by

$$\begin{aligned} K_{im} &= B_{ij}K_{jm} + C_{ikl}L_{klm} \\ L_{imp} &= B_{ij}L_{jmp} + C_{ikl}M_{klmp} \end{aligned} \tag{30}$$

where M_{klmp} is the fourth moment, which, to the level of complication of a coskewance analysis, will be a function of the second moment.

For the 'degree skewance' the analog of equation 3 is best obtained by changing the variables in terms of which the coskewance L is defined by two distances, ψ and ω, and the intervening angle β at their common point, lettered r in Figure 4, so that the integrations can be independently made over a fixed range for each variable. The line ψ defines a coordinate axis, with respect to which the coskewance varies over the sphere with the distance ω and direction β, and hence is appropriately expressed by spherical harmonics in (ω, β). If we assume

$$L(\psi, \omega, -\beta) = L(\psi, \omega, \beta) \tag{31}$$

---

then these spherical harmonics comprise cos $m\beta$ terms only. Thence

$$\mu_{lnm}^{\ 3} = \frac{(2l+1)(l-m)!\,(2-\delta_{0m})^2(2n+1)(n-m)!}{(l+m)!\,8\pi(n+m)!} \cdot \int_0^{2\pi}\int_0^{\pi}\int_0^{\pi} P_{lm}(\cos\psi)P_{nm}(\cos\omega)\cos m\beta\, L(\psi,\omega,\beta)\sin\psi\sin\omega\, d\psi\, d\omega\, d\beta \tag{32}$$

Only the cos $m\beta$ and P_{lm} (cos ψ) terms appear in equation 32 as a consequence of

$$\begin{aligned} \frac{1}{2\pi}\int_0^{2\pi}[\cos k\alpha\cos m(\alpha+\beta) + \sin k\alpha\sin m(\alpha+\beta)]\,d\alpha &= 0, \qquad m \neq k \\ &= \cos m\beta, \quad m = k \end{aligned} \tag{33}$$

Define $L(\psi, \omega, \beta)$ as an average over the sphere T; then

$$L(\psi,\omega,\beta) = \frac{1}{4\pi}\int_T f(r)\,\frac{1}{2\pi}\int_0^{2\pi} f(\psi,\alpha)f(\omega,\alpha+\beta)\,d\alpha\,dr \tag{34}$$

and substitute in (32)

$$\mu_{lnm}{}^3 = \frac{1}{(4\pi)^3}\frac{(2l+1)(2n+1)(2-\delta_{0m})^2(n-m)!\,(l-m)!}{(n+m)!\,(l+m)!} \cdot \int_T \int_0^{2\pi} \int_0^{\pi} \int_0^{\pi} \int_0^{2\pi} P_{lm}(\cos\psi)\, P_{nm}(\cos\omega) \cdot f(r) f(\psi, \alpha) f(\omega, \alpha+\beta)\, d\alpha \sin\psi\, d\psi \sin\omega\, d\omega\, d\beta\, dr \quad (35)$$

Express $f(\psi, \alpha)f(\omega, \alpha + \beta)$ in terms of spherical harmonics referred to the point r as a pole:

$$f(\psi, \alpha)f(\omega, \alpha+\beta) = \sum_{lk}\sum_{nm} P_{lk}(\cos\psi)[a_{lk}(r)\cos k\alpha + b_{lk}(r)\sin k\alpha] \cdot P_{nm}(\cos\omega)[a_{nm}(r)\cos m(\alpha+\beta) + b_{nm}(r)\sin m(\alpha+\beta)] \quad (36)$$

Substituting equation 36 in equation 35, integrating with respect to α, ψ, ω, and β, and using orthogonality conditions obtains

$$\mu_{lnm}{}^3 = \frac{1}{(4\pi)^3}\int_T f(r)[a_{lm}(r)a_{nm}(r) + b_{lm}(r)b_{nm}(r)]\, dr \quad (37)$$

The a_{lm}, a_{nm}, b_{ln}, b_{nm} will be the spherical harmonic coefficients of the function f, referred to the polar axis and Greenwich meridian, times spherical harmonics in terms of (ϕ, λ) r, times the Herglotz factors for the rotation of the coordinate system to a pole at point r [*Erdelyi et al.*, 1953, p. 257]. Expressing $f(r)$ in spherical harmonics as well, $\mu_{lnm}{}^3$ will thus become a combination of triple products of spherical harmonic coefficients of degrees j, l, n, such that the integral of the triple product of the spherical harmonics over the sphere is nonzero:

$$\mu_{lnm}{}^3 = \sum_{jkhig} M_{jkhig}{}^{lnm}\int_T S_{jkh}S_{lmi}S_{nmg}\, d\sigma \quad (38)$$

where h, i, g denote sine or cosine terms.

The degree skewances $\mu_{lnm}{}^3$ would be appreciably nonzero if the pattern of the gravity field was a consequence of an interaction between certain harmonics S_{jkh}, S_{lmi}, since in the expression for the sum of spherical harmonics equal to a product of normalized harmonics

$$\chi = \bar{S}_{jkh}\bar{S}_{lmi} = \sum_{p=k-m}^{j+l} a_p\bar{S}_{p(k-m)g} + \sum_{p=k+m}^{j+l} b_p\bar{S}_{p(k\pm m)g} \quad (39)$$

the coefficients a_p, b_p are the average over the sphere of the triple products $(\bar{S}_{jkh}\bar{S}_{lmi}\bar{S}_{p(k\pm m)g})$. Hence the analysis of coskewance is worth pursuing as a possible indicator of the geophysical processes giving rise to the variations in the gravity field.

The analysis of coskewance has already been carried out in the study of ocean waves [*Hasselmann et al.*, 1963]. In a time series the analysis is somewhat simplified because the angle β is always zero. Hence the coskewance is a function of only two time intervals, and the degree skewance, called the bispectrum, is a function of two wave numbers. The agreement obtained between observation and theory for the bispectrums of wave cresting was so good as to be characterized as '... disappointing, for we have learned little new. ...'—a type of disappointment which we can be sure will not occur in the analysis of gravimetry. Because of the considerable computing burden involved, however, considerable more theoretical work needs to be done before applying coskewance analysis to gravimetry, topography, etc.

Acknowledgments. The covariance analyses described herein were performed in October 1963 on the computer at Goddard Space Flight Center, Greenbelt, Maryland, using gravimetric data provided by the USAF Aeronautical Chart and Information Center, St. Louis, and heat flow data provided by W. H. K. Lee of the Institute of Geophysics and Planetary Physics, University of California, Los Angeles.

References

Anderle, R. J., Observations of resonance effects on satellite orbits arising from the thirteenth- and fourteenth-order tesseral gravitational coefficients, *J. Geophys. Res.*, *70*, 2453–2458, 1965.

Cramér, H., *Mathematical Methods of Statistics*, Princeton University Press, Princeton, N. J., 1946.

Erdelyi, A., W. Magnus, F. Oberhettinger, and F. G. Tricomi, *Higher Transcendental Functions: Bateman Manuscript Project*, vol. 2, McGraw-Hill Book Company, New York, 1953.

Hasselmann, K., W. Munk, and G. J. F. MacDonald, Bispectra of ocean waves, in *Time Series Analysis*, edited by M. Rosenblatt, John Wiley & Sons, New York, 1963.

Kaula, W. M., Statistical and harmonic analysis of gravity, *Army Map Service Tech. Rept. 24*, 1959.

Kaula, W. M., Determination of the Earth's gravitational field, *Rev. Geophys., 1*, 507–551, 1963*a*.

Kaula, W. M., Application of linear regression and generalized least squares to analysis of gravimetry, paper presented at 13th General Assembly IUGG, Berkeley, California, 1963*b*.

Lee, W. H. K., and G. J. F. MacDonald, The global variation of terrestrial heat flow, *J. Geophys. Res., 68*, 6481–6492, 1963.

Wagner, C. A., Determination of the triaxiality of the Earth from observations on the orbit of the Syncom 2 satellite, *NASA—Goddard Space Flight Center Rept. X-621-64-90*, 1964.

Woollard, G. P., The relation of gravity anomalies to surface elevation, crustal structure, and geology, *Univ. Wisconsin Geophys. Polar Res. Ctr. Rept. 62-9*, 1962.

Extrapolation of Gravity Anomalies by Astrogeodetic Deflections

K. ARNOLD

Geodetic Institute, Potsdam, East Germany

Abstract. A special kind of boundary-value problem is discussed. If, in the interior of a part of the Earth's surface, gravity values are unknown and if, in the exterior area, gravity and potential values are given, it is possible to find the gravity values of the interior area. An interpolation method based on this principle is derived to find the gravity anomalies of an unsurveyed area from interior and exterior astrogeodetic deflections and exterior gravity anomalies.

An examination of gravity maps often reveals areas such as U (see Figure 1) of some hundred kilometers in diameter either without a single known gravity value or without a gravity net of adequate accuracy, whereas the surrounding area G is well covered with gravity anomalies. The circumstances producing this situation are beyond the scope of this paper. The problem under consideration here is the determination of the gravity values within the area U, if the gravity values in the exterior area G are given values.

It is not the purpose of this paper to deal with the very valuable and skillfully developed methods evolved by several authors to solve this interpolation and extrapolation problem through use of statistics. I wish to speak of a method not influenced by statistical hypothesis, which may determine fully, with no statistical averaging, the special anomalous character of the gravity field of the area U that is not gravimetrically covered. Before we go into more detail, some general considerations will be given.

The gravimetrically unsurveyed area U may may be considered a circular plane surface (Figure 2), and, in the surrounding area G, we assume the potential W and its normal derivative $\partial W/\partial n$ to be known.

The solution of the Neumann boundary-value problem for a plane surface is given by the following well-known equation:

$$W = \frac{1}{2\pi} \iint_{U+G-\sigma} \frac{\partial W}{\partial n} \frac{1}{r} \, d\sigma \qquad (1)$$

The normal derivative $\partial W/\partial n$ must be given on the whole plane surface $U + G$, to find the potential W at points in the exterior space. r is the distance between a unit particle in the exterior space and the surface element $d\sigma$ (see Figure 3). Letting this particle approach the surface σ, equation 1 yields

$$W_\sigma = \frac{1}{2\pi} \iint_{\sigma-U+G} \frac{\partial W}{\partial n} \frac{1}{r} \, d\sigma \qquad (2)$$

Dividing the area $U + G$, we find

$$W_\sigma = \frac{1}{2\pi} \iint_G \frac{\partial W}{\partial n} \frac{1}{r} \, d\sigma + \frac{1}{2\pi} \iint_U \frac{\partial W}{\partial n} \frac{1}{r} \, d\sigma \qquad (3)$$

The first integral on the right side is known, because the values of $\partial W/\partial n$ are given over the entire area G. If we consider W_σ for a point situated in the G area, W_σ is also given, according to our assumptions. The last integral is unknown, because $\partial W/\partial n$ in the U area is unknown.

By equation 3 the unique solutions for the a priori unknown values $\partial W/\partial n$ in the U area are well determined. In other words, $(\partial W/\partial n)_\sigma$ is determined from the W_σ and $(\partial W/\partial n)_\sigma$. Substitution of the plane boundary surface by a spherically shaped surface, a currently common practice in geodesy, would probably not affect the validity of this method.

A further generalization of the problem is undoubtedly possible. It can easily be proved, for example, that the boundary that separates the U area from the G area need not necessarily be a circle; any arbitrarily chosen curve will suffice. Furthermore, the gravity anomalies may be conveniently substituted for the normal derivatives $\partial W/\partial n$.

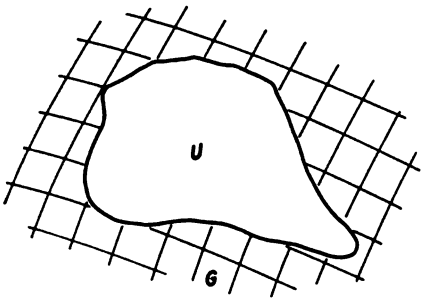

Fig. 1. Unsurveyed gravity region U.

Thus we have the following highly probable hypothesis: If a part of the Earth's surface is not covered with gravity anomalies and if for the remaining part of the Earth's surface both the gravity anomalies and the potential values are known, it is possible to arrive at a unique determination of the gravity anomalies in the unsurveyed area.

No restriction must be introduced on the geometry of the curve that separates both the areas in question. The potential values may be replaced by the disturbance potential or by the undulations.

It follows that, if the gravity anomalies and the undulations are known on the continents, it is also possible to find unique solutions for the anomalies in ocean regions. But, application of the theory of propagation of errors to the undulations indicate great uncertainties. Thus precise results may not be attainable by this method for bridging vast areas measuring thousands of kilometers, because the undulation values or the values of the geoidal heights cannot be known with sufficient precision. However, the extrapolation of the gravity anomalies over some hundred kilometers is possible and adequately precise by this method.

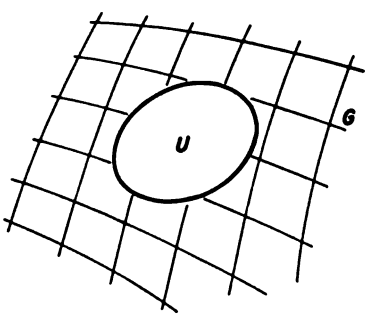

Fig. 2. Unsurveyed circular gravity region.

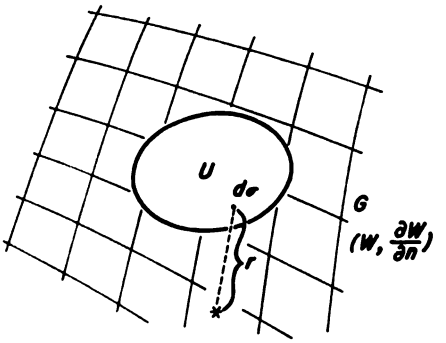

Fig. 3. Relationship of exterior point to area U.

If gravity anomalies are given in the G areas and if astrogeodetic deflections are given in the unsurveyed U area and in those parts of the G areas bordering the U area, it is possible to develop a practical method for the interpolation of gravity anomalies.

Thus, the astrogeodetic deflections Θ_s are given in some points P_i.

Now we integrate over the field of gravity anomalies of the G area according to the integral of Vening Meinesz, and we find

$$[\Theta_s]_1 = \chi \iint_G \Delta g \cdot V_M \cdot \cos\alpha \, d\sigma \qquad (4)$$

whereas the full integral of Vening Meinesz over the areas $U + G$ will yield the full deflection

$$\Theta_s = [\Theta_s]_1 + [\Theta_s]_2 = \chi \iint_{U+G} \Delta g V_M \cos\alpha \, d\sigma \qquad (5)$$

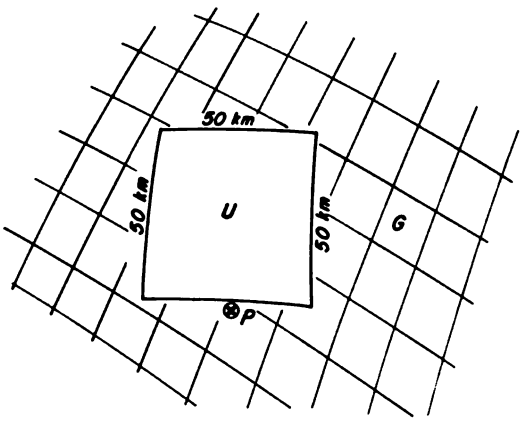

Fig. 4. Unsurveyed 'rectangular' region.

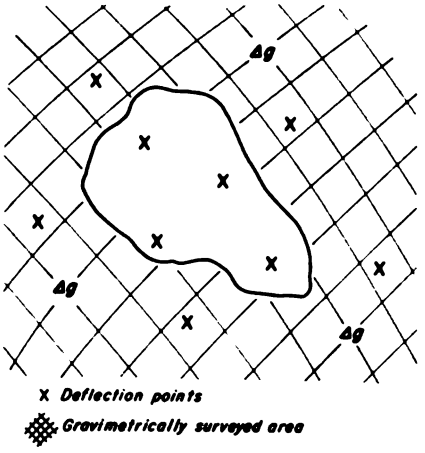

Fig. 5. Deflection points and gravimetrically surveyed area.

Here

$$[\Theta_g]_2 = \chi \iint_U \Delta g \; V_M \cos \alpha \; d\sigma \qquad (6)$$

the unknown amount of the integral over the whole area U where the Δg are unknown.

The integral (6) is substituted by a sum

$$[\Theta_g]_2 = \chi \cdot \Delta\sigma \sum_i \Delta g_i (V_M)_i \, (\cos \alpha)_i \qquad (7)$$

and the unknown Δg_i are introduced.

For small areas U

$$\Theta_a - \Theta_g = c_1 \qquad (8)$$

is a constant value.

Hence,

$$\Theta_a - [\Theta_g]_1 - \chi \, \Delta\sigma \sum_i \Delta g_i (V_M)_i \, (\cos \alpha)_i = c_1 \qquad (9)$$

This equation affords a possibility for the determination of the unknown values Δg_i and c_1.

For a numerical example, we choose a deflection point P situated near the border of a square-shaped U area that is 50-by-50 km in size (Figure 4).

If the deflection difference $\Theta_a - (\Theta_g)_1$ is known within $\pm 0.5''$, it is possible to find the mean gravity anomaly of the U area with a precision of ± 4 mgal, as can be easily shown.

Sometimes a country surrounded by well-established gravity nets has few or no existing gravity data, whereas this country and its surroundings have many astrogeodetic deflection points (Figure 5). The use of deflection values for interpolation of the gravity values in such a country seems to be a practical, convenient method, which will yield the full anomalous character of the area.

The investigation of accessible sea areas also seems to be adequate by this method.

Comment. The following remarks were contributed by William P. Durbin, Jr., after a reading of Kurt Arnold's paper:

The Aeronautical Chart and Information Center (ACIC) has just concluded a project with the University of Hawaii which is the reverse of Arnold's study. We have been able to improve upon deflection interpolation through the use of Molodenskii's expressions and the addition of a geologic correction to the mean gravity anomaly. Significantly, comparison of Arnold's work and that of ACIC shows that accuracy and distance parameters developed by both are in exceptionally close agreement. The University of Hawaii report is available at ACIC for anyone desiring a copy.

References

Arnold, K., Die Randbedingungen von Cauchy und die Hauptaufgabe der physikalischen Geodäsie mit besonderer Berücksichtigung der Eindeutigkeit der Lösung, *Gerlands Beitr. Geophys., 68,* 1–14, 1959.

Arnold, K., Exakte Extrapolation von Schwereanomalien, *Gerlands Beitr. Geophys., 72,* 139–148, 1963.

Accuracy Aspects of Gravity Prediction from Gravimetric and Astrogeodetic Data

ERWIN GROTEN

Institute of Technology, Munich, West Germany

Abstract. The prediction of gravity anomalies in unsurveyed gaps from gravity and astrogeodetic observations is discussed. This method seems to be useful for smaller gaps within well-surveyed areas of the Earth's surface.

INTRODUCTION

Arnold [1963] has shown that, given the potential T and its first normal derivative on a plane outside of an area K, both functions are unequivocally determinable within the area K. He goes on to show that this fact makes the exact prediction of gravity in K from gravimetric and astrogeodetic data, as given in area S, theoretically possible (see Figure 1).

The difficulties in the application of such a method have already been discussed in principle by *Uotila* [1960]. They arise mainly from the fact that T and its normal derivative are not known in the whole area S outside of K. Owing to the influence of the outer zones (and often not only of the outer zones), we must consider additional uncertainties.

ACCURACY CONSIDERATIONS

Arnold's [1963] definite equations read (p. 147)

$$\bar{\xi}_g - \xi_a = \sum_u x_u \, \Delta g_u + c_\xi \qquad (1)$$

$$\bar{\eta}_g - \eta_a = \sum_u y_u \, \Delta g_u + c_\eta \qquad (2)$$

ξ_a, η_a = astrogeodetic deflections of the vertical.
$\bar{\xi}_g$, $\bar{\eta}_g$ = gravimetric deflections of the vertical, which deviate from the true gravimetric deflections ξ_g and η_g, owing to the influence of the unknown gravity anomalies in the area K.
Δg_u = mean unknown gravity anomalies in the area K.
x_u, y_u = constants to be derived from the integral of Vening Meinesz.
c_ξ, c_η = correction due to the difference between the geodetic reference ellipsoid and the terrestrial ellipsoid of the world geodetic system; it is supposed to be a constant within a small area.

To simplify the following consideration we disregard, at first, any improvement due to superfluous observations by least-squares adjustment; we put $u = 1$. Further, we consider the difference between the geodetic reference and the world system to be known or to be equal to zero.

Since

$$\begin{Bmatrix} \bar{\xi}_g \\ \bar{\eta}_g \end{Bmatrix} = \frac{-1}{2\pi G} \int_{S-K} \Delta g \, \frac{\partial f(\psi)}{\partial \psi} \cdot \begin{Bmatrix} \cos\alpha \\ \sin\alpha \end{Bmatrix} \sin\psi \, d\psi \, d\alpha \qquad (3)$$

where G = mean gravity on the Earth's surface;
$2f(\psi) = S$ = Stokes' function;
ψ, α = polar coordinates.

$$\begin{Bmatrix} \bar{\xi}_g - \xi_a \\ \bar{\eta}_g - \eta_a \end{Bmatrix} = \Delta g \begin{Bmatrix} x \\ y \end{Bmatrix} = \frac{-1}{2\pi G} \int_K \Delta g \, \frac{\partial f(\psi)}{\partial \psi} \begin{Bmatrix} \cos\alpha \\ \sin\alpha \end{Bmatrix} \sin\psi \, d\psi \, d\alpha \qquad (4)$$

with Δg = mean gravity anomaly.

As the considerations are analogous for ξ and η, we consider only ξ and put $\xi = \eta = \theta$.

If K is given by the polar coordinates α_1, α_2, ψ_1, and ψ_2 and Δg = const, then

$$\vartheta_g - \vartheta_a = x \, \Delta g = -\frac{\Delta g}{2\pi G} \int_{\alpha-\alpha_1}^{\alpha-\alpha_2} \cos\alpha \, d\alpha \cdot \int_{\psi-\psi_1}^{\psi-\psi_2} \frac{\partial f(\psi)}{\partial \psi} \sin\psi \, d\psi \, d\alpha \qquad (5)$$

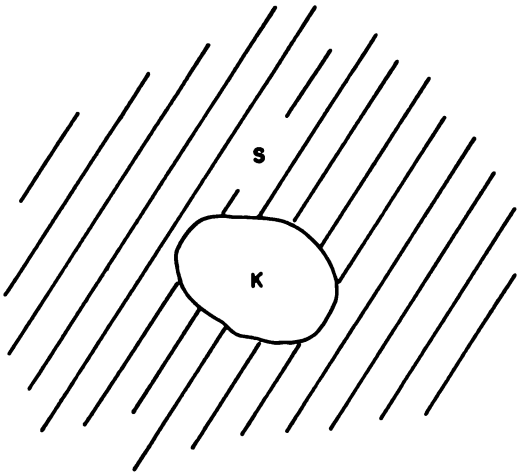

Fig. 1. Situation of K.

$$\vartheta_g - \vartheta_a = \frac{\Delta g}{2\pi G}(\sin\alpha_2 - \sin\alpha_1) \cdot T \qquad (6)$$

where

$$T = -\int_{\psi-\psi_1}^{\psi-\psi_2} \frac{\partial f(\psi)}{\partial \psi} \sin\psi \, d\psi \qquad (7)$$

T may be read from the tables of *Sollins* [1947]. For $\alpha = \alpha_2 = -\alpha_1$ we obtain

$$\Delta\vartheta = \vartheta_g - \vartheta_a = \frac{\Delta g}{\pi G} \sin\alpha \cdot T \qquad (8)$$

By partial differentiation and squaring of (8) we get the variance

$$m^2(\Delta\vartheta) = m^2(\Delta g) \sin^2\alpha \cdot T^2/\pi^2 G^2 \qquad (9)$$

Thus, the standard deviation of the predicted mean gravity anomaly reads

$$m(\Delta g) = \pm\pi G m(\Delta\vartheta)/T \cdot \sin\alpha \qquad (10)$$

From the gravity material available in 1954, *Hirvonen* [1956] estimated optimal accuracies of gravimetrically computed deflections of the vertical (dense gravity net out to $\psi = 12°$ and 14°, respectively). Some comparable results are given by *Kaula* [1957]: $m(\delta_1) = \pm 0.8''$ and $\pm 0.9''$, respectively (Hirvonen), and $m(\delta_2) = \pm 1.7''$ and $\pm 1.9''$, respectively (Kaula).

Regarding additional information since this time, we assumed a standard deviation for the difference $(\bar{\theta}_g - \theta_a)$, $m(\Delta\theta) = \pm 0.7''$, as a basis of the following computations. This value seems to be reasonable since in favorable cases the effect of the outer zones may be eliminated by least-squares adjustment, if we have several stations within any small area.

Using this value, we evaluated the standard

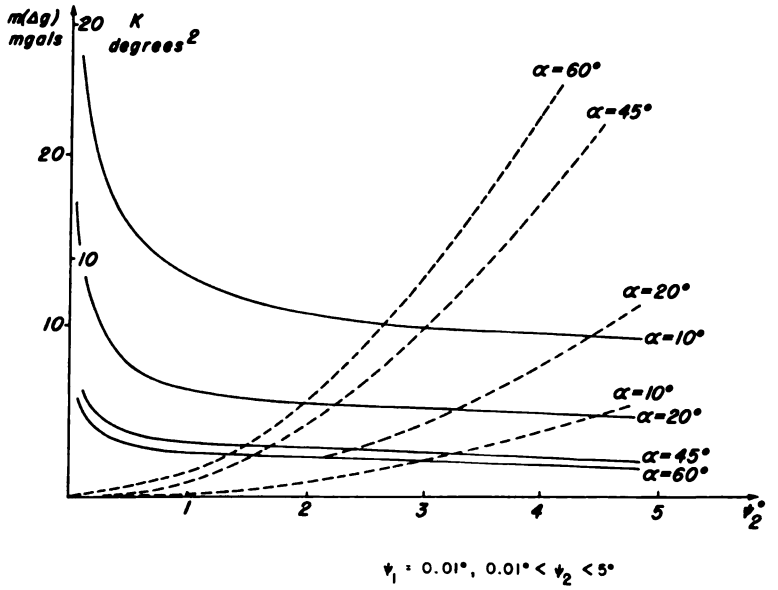

Fig. 2. Standard deviations $m(\Delta g)$ (*solid lines*); corresponding area in deg² (*broken lines*). ψ_1 is constant.

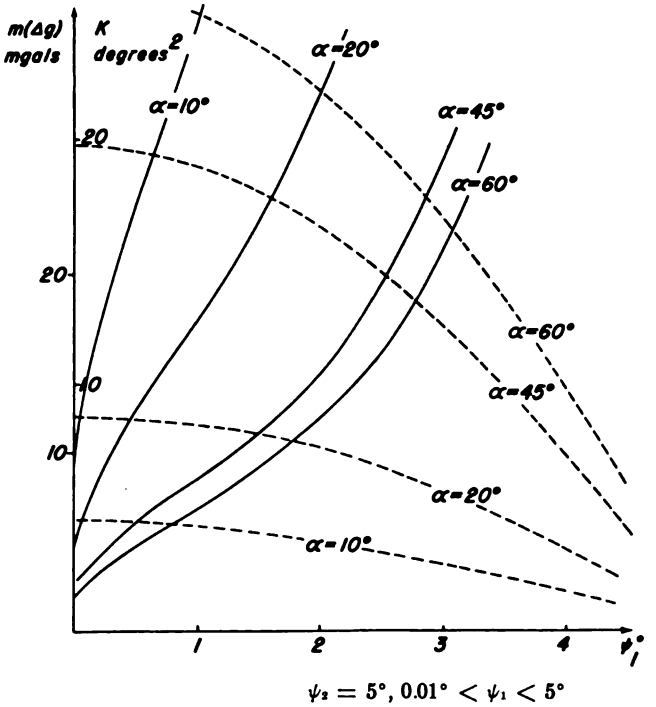

$\psi_2 = 5°, 0.01° < \psi_1 < 5°$

Fig. 3. Same as Figure 2, but with ψ_2 constant.

deviation of the predicted mean gravity anomaly in the area K for the following constant angles of $\alpha = 10°, 20°, 45°$, and $60°$.

In Figure 2 the standard deviations $m(\Delta g)$ are shown (unbroken lines). The broken lines show the corresponding area in deg². In this case ψ_1 is kept constant; i. e., $\psi_1 = 0.01°$ and ψ_2 varies between $0.01° < \psi_2 < 5°$.

Another case is shown in Figure 3, where the broken and unbroken lines have the same meanings as in Figure 2. Here, however, ψ_2 is kept constant; i. e., $\psi_2 = 5°$ and ψ_1 varies between $0.01° < \psi_1 < 5°$.

From both figures it follows that this extrapolation method is appropriate for the prediction of mean anomalies within large areas. Secondly, the area must be close to the astrogeodetic points. (The special case in which the astrogeodetic point lies in the area K is not considered.) The above-mentioned accuracy $m(\Delta\theta)$ comes into question, of course, only within the gravimetrically well-surveyed areas of the Earth's surface.

This prediction method should thus be efficient for the prediction of mean anomalies of gaps larger than 1° by 1° for areas like Europe and North America where we have many astrogeodetic stations and usually a dense gravity net.

Acknowledgment. This study was sponsored by the USAF Research Laboratories, Office of Aerospace Research, Cambridge, Massachusetts, under contract AF 19(628)-2717, Ohio State University Research Foundation project 1613, under W. A. Heiskanen (supervisor) and B. Szabo (project engineer).

References

Arnold, K., Exakte Extrapolation von Schwereanomalien, *Gerlands Beitr. Geophys., 72,* 139–148, 1963.

Hirvonen, R. A., On the precision of the gravimetric determination of the geoid, *Trans. Am. Geophys, Union, 37,* 1–8, 1956.

Kaula, W. M., Accuracy of gravimetrically computed deflections of the vertical, *Trans. Am. Geophys. Union, 38,* 297–305, 1957.

Sollins, A. D., Tables for the computation of deflections of the vertical from gravity anomalies, *Bull. Geod., 6,* 279–300, 1947.

Uotila, U. A., Investigations on the gravity field and shape of the Earth, *Ann. Acad. Sci. Fennicae, Ser. A III, 66,* 92 pp., 1960.

The Extension of the Gravity Net to the Unsurveyed Areas of the Earth: Geophysical Methods

Reporter: W. A. Heiskanen

In Session 1 we have seen that there exist on the Earth's surface large gaps in the gravity station net. Several colleagues have also shown that only the seaborne and airborne gravity measurements can fill them in a relatively short time. They have, however, also emphasized that these methods are not yet at the operational level. Other methods must therefore be found.

In Session 2 we have heard that the statistical method is very useful and important and has already been applied for many years. If the gaps of the gravity anomaly field are small, say, 1,000–1,000,000 km^2, the different modifications of the statistical method would predict sufficiently good point values and mean gravity anomaly values. The studies of Hirvonen, Moritz, Uotila, Rapp, Tengström, Tsuboi, Lambert, and Kivioja in Columbus and of several of our western and eastern colleagues indicate that fast progress in the development of this method is going on. The statistical method cannot, however, be used for the prediction of the gravity anomalies over long distances or for long areas. For instance, in the Pacific Ocean there are relatively few gravity observations, and some of them are measured at the ocean islands in which the gravity anomalies differ up to 200 mgal and more from the gravity anomalies of the surrounding ocean. Therefore, the island anomalies can *only* be used for the calibration of the gravimeters used for gravimetric survey of the open ocean.

In this respect the geophysical method is very helpful. The principle of the geophysical extrapolation method is this: If the Earth were in complete hydrostatic equilibrium, the gravity anomalies would be very small and the equipotential surfaces, including the geoid (sea level), would be a flattened mathematical ellipsoid. The deviations from the ellipsoid would very seldom exceed a couple of meters. Unfortunately, the Earth is not in hydrostatic equilibrium, as the mountains, valleys, oceans, and ocean islands which cause the irregularities of the gravity anomaly field and of the equipotential surfaces of the Earth clearly indicate.

Thus we can say that the gravity anomalies are mostly caused by the topographic mass surplus of the continent and the bathymetric mass deficiencies of the oceans and by the isostatic compensating mass deficiencies and mass surplus.

If the topography alone were dominant, the gravity anomalies would be many hundred mgal, for a 5000-meter-high plateau about 550 mgal, and the undulations of the geoid would be about 400 meters.

The Earth's crust is, fortunately, in *isostatic equilibrium,* which means that the topographic and bathymetric masses are in broad lines compensated by the compensating masses. Therefore, the gravity anomalies and the undulations of the geoid are and must be relatively small.

The studies of several geodesists have shown, in fact, that from the topographic masses of the mountains and the oceans about 90% will be compensated by the isostatic compensation, except in several local areas where isostatic compensation is not complete. Thus we can claim that the topographic and compensating masses will produce about 90% of the gravity anomalies.

Because the topographic and bathymetric masses are relatively well known and the effect of the isostatic compensating masses can also be estimated, the mean anomalies caused by the topographic and compensating masses are relatively easily obtained for the unsurveyed areas.

Now that we have high-speed computers, we can very easily compute the effect of the topography and isostasy if we have only the mean elevations of relatively small squares or blocks, say 5-by-5 km or 10-by-10 km, or 2.5′ and 5.0′. In many parts of the world the mean elevations of 5′-by-5′ already exist. At the Columbus Geodetic Center we have considered several large areas with this information, and many other geodetic institutions and countries have done the same. This effort is not yet sufficient. Therefore, we are all glad to hear that the Aeronautical Chart and Information Center is interested in estimating the mean elevations 5′-by-5′ all around the world. When this work has been done, the mean anomalies caused by topography and isostatic compensation can be obtained in a very short time.

During the last few years we in Columbus have tried to compute the gravity anomalies on the basis of the topography and isostatic compensating masses. U. A. Uotila has developed the coefficients of spherical harmonics that express the Earth's topography up to the 37th order, as Prey had done to the 17th order and Bruins to the 32nd order. Uotila has used the 5°-by-5° blocks bordered by the meridians and parallels. In the computation of the isostatic anomalies, he has used the Airy-Heiskanen $T =$ 30 km model, and values $\rho = 2.67$ and $\Delta\rho =$ 0.6.

In his computations, Uotila did not use the existing gravity anomalies in any way, so that his mean anomalies are quite independent of the observed anomalies. These values can be checked for such areas where sufficient gravity stations exist. If these values agree with the topographic isostatic anomalies, they are strong evidence for the significance of this method. *Uotila* [1964, Figure 8] gives the gravity anomalies of his model for the Earth quarter between the longitudes 0° and 90°E.

L. A. Kivioja made similar computations, although the approach was different in some respects. His starting idea is that the mean gravity anomalies of the whole Earth must be zero and that the mean gravity anomalies of the used squares 5°-by-5° must be essentially the same in unsurveyed as in surveyed areas, if the topography and other conditions are the same (oceans, coast lines, mountains, etc.). The topography and its isostatic compensation cause most parts of the anomalies. Thus the anomalies from the surveyed areas can be transferred to the unsurveyed areas if other conditions are the same.

The considerable systematic variation of the free-air and isostatic anomalies along the oceanic coasts has been included. The magnitude of the variation depends on the size, shape, elevation, and depth (the topography) and on the density of the Earth's crust. Existing 5°-by-5° mean free-air anomalies and the Airy-Heiskanen isostatic system, $T = 30$ km, were used in the computation.

The standard error of the computed anomalies is ± 12 mgal, whereas the standard error in the case that the isostatic anomaly zero had been applied would be ± 18 mgal. *Kivioja* [1963, Figure 9] shows the compensating topographic isostatic gravity anomalies of 5°-by-5° squares

in the meridian sector between the longitudes 0° and 60°E.

Uotila computed the mean elevations of 5°-by-5° squares from the development of the topography in spherical harmonics and used no observed gravity anomalies in computing the mean anomalies, whereas Kivioja estimated the mean elevations from the topographic and bathymetric maps and adjusted the obtained mean anomalies of the unsurveyed areas on the basis of the known mean anomalies. Therefore, their results cannot be the same, although the differences are, in general, rather small.

The results will certainly improve when the mean elevations of 1°-by-1° are available. When the gaps of the gravity anomaly field are filled by new and accurate observations, we can compare the predicted Δg_m values of Uotila and Kivioja with the true mean anomalies.

George Woollard and W. P. Durbin have studied the *local* structure of the Earth's crust using the geophysical method and have obtained interesting results.

References

Kivioja, Lassi, The effect of topography and its isostatic compensation on free-air gravity anomalies, *Inst. Geodesy Photogrammetry Cartography Rept. 28 (AFCRL-64-130)*, Ohio State University, Columbus, December 1963.

Uotila, U. A., *Gravity Anomalies for a Mathematical Model of the Earth, Publ. 43*, Isostatic Institute of the International Association of Geodesy, Helsinki, 1964.

The Anomalies of Potential Ng at Surface Points of Regions Gravitationally Surveyed

J. DE GRAAFF-HUNTER,[1] *Retired*

Abstract. Stokes' method for finding the potential anomalies on the geoid benefits from the use of a well-chosen reference system based on a close-fitting Earth model (stated or implied) with minimal anomalies of g. A mode of determination of *partial* potential anomalies (from which lower harmonics are absent) for the case of incomplete gravity data coverage of the globe is suggested.

To study worldwide gravity values it is necessary to compare them with the values of an artificial reference system whose characteristics are fully defined. Thus we get anomalies Δg_x for reference system (x). I shall use the Airy-Heiskanen system and the model Earth system as examples. Since the characteristics may be freely chosen, gravity γ_x, potential V_x, etc., of reference system (x) corresponding to any terrestrial point can be found without ambiguity. The simple anomaly is $g_x - \gamma_x$ for the observed point.

We note three points, not always recognized:

a. The adoption of reference system (x) in no way proves that it has any actual existence.

b. The anomaly Δg_x relates to the point where g is observed and cannot be transferred to another level.

c. Any translation of actual matter that has been imagined for the purpose of rendering anomalies more tractable requires ultimate restoration.

With reference to (b), we know the change of V_x along a vertical, but we *do not know* the corresponding change of g_x. The so-called free-air anomaly ignores the difference of these two changes. It is practically the simple anomaly Δg at the point where g is observed.

Any reference system is defined by various parameters, for which numerical values must be chosen; later, revised values may be adopted. For example, in the Airy-Heiskanen system the depth T has been variously chosen, but I understand that Heiskanen now prefers the value 30 km, having found minimal anomalies with this value.

In the model Earth system one parameter is the crustal density, for which 2.67 has usually been taken as the best average for the Earth's crust. In writing the formula for Δg_E the density of the immediate locality enters predominantly; thus, with ρ as the local density, we may write

$$\Delta g_E = \Delta g + [\mathbf{O} + 0.112(H - h)] \cdot \rho/2.67 \quad \text{mgal} \qquad (1)$$

where $\mathbf{O}$ is the terrain effect and where h and H are height and local average height in meters.

A group of values of Δg_E can be used to determine local ρ, and this method may be used to finalize the separate anomalies [see *de Graaff-Hunter*, 1964].

The two systems mentioned have one marked difference: the Airy-Heiskanen system supposed, at least originally, that the underground distribution of matter conformed to Airy's idea that the system had *actual* existence in nature. In the model Earth plan there is no such supposition; the topography is merely smoothed, and then the simple anomaly Δg is duly modified. Both are effected by a system of averaging heights.

Naturally, gravity g at the surface of the irregular Earth is not the same as corresponding γ_x of any simple reference system of Earth proportions, such as a rotating spheroid bounded by a level surface, and there is a simple anomaly

[1] Now at 7 Beaconsfield Road, Mosman, New South Wales, Australia.

$\Delta g = g - \gamma_s$, where g applies to Earth point P and γ to corresponding point of reference system with the same φ, λ, and potential V. The Δg is not accounted for by the topography alone, but the topography cannot be ignored. It is variously dealt with in various systems, leading to a generally smaller anomaly, Δg_s. On theoretical grounds it is impossible to determine the internal distribution of density from surface values of g. From the theorems of Green we know that the anomalies can be represented by an equivalent surface layer, $4\pi\Delta g_s$. This can be interpreted as inequality of loading on the bounding surface or within a thin crust.

Further, the well-known Stokes equation gives the anomaly of potential at any point of the surface in terms of Δg_s over the *entire surface*. (For the adaptation of this method to the model Earth surface and anomalies, see *de Graaff-Hunter* [1960].)

Making Stokes' equation applicable when Δg_s coverage is far from complete, as must remain the case for years to come, is still a serious problem. It is hoped that the concluding sections of this paper will contribute to its solution.

It is helpful to understand something about the Earth's structure, and *Niven's* [1931] work is valuable for this purpose. We know that there is irregular loading, and we must try to find how it is supported. Also, what could not be supported should accordingly be excluded.

By surface gravity the base of a column of granite 5 km high would crush under its own weight. Within the Earth such a column would be surrounded and there would be 'confining' pressure, analogous to hydrostatic pressure. *Niven* [1931, p. 15] mentions an instance of marble having crushing strength increased sixfold by confining pressure. Thus 30 km is perhaps the approximate depth at which crushing pressures occur. We can therefore picture the Earth with a 30-km crust surrounding a core responsive to pressure variations.

Now consider the loading $4\pi\Delta g_s = 4\pi(\Sigma \Delta g_n)_s$, in which subscript n indicates a harmonic of order n. For harmonics that change sign in a distance of the order of the crust thickness, irregularities of loading can be supported by crustal strength; with thickness of 30 km, $n = 25000/30 = 833$. In round terms we may say that, for harmonics of order above 1000, pressure irregularities will not reach the core.

For small values of n, crustal strength will avail little, and the corresponding loading anomaly will be balanced by crustal intrusion in the core or the reverse, very much as in Airy's concept. Here, indeed, there should be true isostasy, except perhaps for some very small residues due to quasi-viscosity of highly pressurized rock.

I think the situation can be expressed as follows: *Very low-order harmonics in the loading anomaly* could only exist during Earth convulsions and *must be absent in time of geological quiescence.*

Study of motion of artificial satellites has enabled *King-Hele et al.* [1963] to estimate values of the lower-order zonal harmonics of the Earth's potential but not of the tesseral harmonics. They are of order of magnitude some 10^{-6} of full potential.

In a lecture at Delft [*de Graaff-Hunter*, 1961] I proposed a method whereby the function 'f' in Stokes' integral for Ng is replaced by $f - \Delta f$, where $\Delta f = \Sigma\, c_m P_m$ and coefficients c_m are chosen to make $\Delta f = f$ at 8 values of ψ. Then Stokes' equation may be written

$$(Ng/R)_P - \frac{1}{2}\int_0^\pi (\Delta g)_\psi (f - \Delta f) \sin\psi\, d\psi$$

$$= (\tfrac{1}{4}\pi)\int_0^\pi \sum_0^7 A_m P_m\, d\omega$$

$$= \sum_0^7 c_m A_m/(2m + 1) \qquad (2)$$

where A, for values of m from 0 to 7 are related to the low-order zonals. The value of $f - \Delta f$ under the integral makes it negligible for values of ψ beyond 25°.

I was able [*de Graaff-Hunter*, 1961] to reduce the limiting value of ψ from 25° to 5°, introducing in Δf zonal harmonics up to order 10. Hence, provided the first ten harmonics of Δg_s are known or are shown to be negligible, equation 2, with 'm' extended to 10 and the upper limit of the integral changed from π to 5°, gives the value of Ng at the point P, thus requiring values of Δg_s only over the surrounding 5 degrees.

As mentioned in a previous paper [*de Graaff-Hunter*, 1961], the value of Ng can be determined throughout all regions where a full gravitational survey (including deflections) has been made and where the area is sufficiently

large to provide the requisite radial distance of 5° from a central point. For small isolated regions and regions in which there has been no gravity survey this would not be possible.

In the preceding section I gave some reasons for expecting the low-order harmonics to be absent from Δg or to be very small, but I did not indicate the possible magnitude of any residuals. This value depends on properties of the rocks at a depth such as 30 km, which are unknown, at least to me.

The method given here can no doubt be improved in detail, and the determination of low-order tesseral harmonics of potential may be increased. Efforts should be made in both areas.

References

de Graaff-Hunter, J., Earth's shape and potential, *Tydschrift voor Kadaster en Landmeetkunde,* 77(4), 193–202, 1961.

de Graaff-Hunter, J., Modification of the Stokes' geoid equation for present day use, note for I.A.G. Special Study Group 11, 1961.

de Graaff-Hunter, J., The shape of the Earth expressed in terms of gravity at ground level, *Bull. Géodésique 56,* 191–200, 1960.

de Graaff-Hunter, J., Imperfections in finding Earth shape from gravity and some suggestions for improvement, *Bull. Géodésique 75,* March 1965.

King-Hele, D. G., G. E. Cook, and Janice M. Rees, Determination of the even harmonics in the Earth's gravitational potential, *Geophys. J.,* 8(1), September 1963.

Niven, Charles Merrick, *Principles of Structural Geology,* Chapter 2, John Wiley & Sons, Inc., New York, Chapman Hall Ltd., London, 1931.

The Isostatic Reduction of Gravity Data and Its Indirect Effect

WALTER D. LAMBERT,[1] *Retired*

Formerly with U. S. Coast and Geodetic Survey
Washington, D. C.

The isostatic reduction of gravity data involves two effects, the direct and the indirect. For the direct effect we assume that all topography above the real geoid (that is, mean sea level) has throughout a conventional density, nowadays usually 2.67. We transfer these topographic masses with reversed sign down to an assumed limiting depth of isostatic compensation. The ocean waters are treated as having a negative density, because their density is less than our assumed conventional density of the land masses. These negative masses are also transferred with reversed sign down to the limiting depth of isostatic compensation. The combined effect of these transfers on gravity at a given point represents the direct effect.

This shift of matter creates a new artificial geoid. It may be called the *isostatic geoid;* it has been called the cogeoid. We must refer all our gravity data to the same geoid. Formerly, we talked of reducing land observations for the free-air reduction *down* to mean sea level, *down* to the actual geoid. We now talk of reducing such land observations *up* from the geoid to the place of observation. This approach is more logical. Observations are made where they are made, and the comparison between the ideal theoretical value and the observed value should refer to the point where the observations were actually made. Whether we reduce our observations down or up, we use the theoretical gradient of gravity simply for want of anything better. We get different reductions if reductions are referred to different geoids. The correction for the difference between the real geoid and the cogeoid, or isostatic geoid, is the indirect effect. The indirect effect is the subject of the present discussion.

In the early days of extensive isostatic calculations this indirect effect was often called the Bowie effect. Bowie was one of the pioneers in the field of isostasy. It has been suggested to me that Bowie was worried about the size of the gravity anomalies that remained even after the correction for the direct effect had been applied and that he hoped that the correction for the indirect effect would substantially reduce the outstanding anomalies. In this he was disappointed; the indirect effect is relatively small.

Long years ago, W. A. Heiskanen, with the aid of Erkki Niskanen [*Heiskanen and Niskanen*, 1941] calculated the indirect effect over much of the world for blocks bounded by meridians and parallels 5° apart. Their tables cover all longitudes and latitudes ranging from 40°S to 70°N. The largest value for the indirect effect in these tables is 10.3 mgal for a block centered at longitude 85°E and latitude 35°N. Some adjoining blocks give values as large. These values apply to northern India, Tibet, and adjacent areas. Our Rocky Mountain region gives four blocks with values each equal to +5.8 mgal. One block in the Andes region of South America gives +9.0 mgal. The largest negative value, −3.9 mgal, occurs in widely scattered ocean areas.

These values apply to the Pratt type of isostatic compensation for a depth of 113.7 km. If we had used the Airy type of compensation, approximately the same results would have been found if we had assumed a depth equal to one-half of the above, say 57 km. This value is somewhat larger than the value now generally accepted as most probable. This indirect effect is roughly proportional to the depth of compensation, as will be shown below. The general conclusion would be that the above-mentioned values for the indirect effect are probably somewhat too large for modern ideas regarding the depth of compensation.

Two articles published in 1930 [*Lambert*, 1930*a*, *b*] enable us to get an approximate idea

[1] Now at P. O. Box 1025, Canaan, Connecticut.

of the magnitude of the indirect effect. Both discuss a quantity H_R. The subscript R is meant to suggest *resultant*. Logically, the second article should precede the first. The second article shows that for more than one variant of the form of isostasy we get approximately the same value of H_R.

This approximate formula for H_R is

$$H_R = [(3/4)(\sigma/\rho)(d/a)]H \qquad (1)$$

Here ρ is the uniform conventional density of the topography, σ is the mean density of the Earth, a is the mean radius of the Earth, and d is the depth of compensation of the Pratt variety. If we are using the Airy variety of isostasy, the value of d should be doubled. The letter H suggests *height* or *elevation*, but it is not height or depth reckoned from sea level. It is reckoned from a certain lower level called *mean load level* [see *Lambert*, 1930*a*, pp. 91–92]. Now this value of H is an average value within a fairly large cap centered at the point of observation. A table on page 97 gives the values of H_R for a cap of topography 1000 meters thick and of various radii. The values are computed accurately, i.e. not by the approximate formula 1 for H_R. The purpose of the table is to show the necessity of using a fairly large cap, with the average height or depth reckoned from mean load level. An excerpt from the table on page 97 is given in Table 1 of this paper. The final lines give the value of H_R from equation 1.

We see that formula 1 gives a poor approximation for a small cap, but that we get a somewhat better approximation for the smaller depth of compensation. To get the approximate indirect effect, we simply multiply H_R by the gravity gradient 0.308 mgal per meter.

But before we compute a few values of the indirect effect for comparison with those of Heiskanen and Niskanen, we must define mean load level, the level from which H is reckoned. On page 92 we find the following formulas. For a point on land

$$H = h + \begin{cases} 5400 \\ 1650 \end{cases} \qquad (2a)$$

For a point on the ocean

$$H = + \begin{cases} 5400 \\ 1650 \end{cases} - 0.636s \qquad (2b)$$

TABLE 1. Values of H_R in Meters

Radius of Cap, km	Depth of Compensation, 100 km	Depth of Compensation, 200 km
100	4.24	6.27
200	5.05	8.47
350	5.44	9.82
500	5.59	10.42
700	5.68	10.81
1000	5.74	11.09
Formula 1	6.03	12.06

The symbol h is, of course, elevation above sea level. The formula on page 92 uses d where we now use s, since d has already been used to represent the depth of compensation. The letter s has been used here to represent the average depth of the ocean, since s might suggest 'sounding.' The upper value in each brace applies when heights and depths are in feet, the lower value when they are in meters. They were deduced from data in an encyclopedia. A footnote mentions another value, 4650 feet instead of 5400. Today we know more about ocean depths and today's figures would doubtless be different from those in the *Bulletin Géodésique* and presumably more accurate. The concept of mean load level is explained in the following quotation from the *Bulletin*, page 92.

> We reach the conception of *mean load level* by supposing any column of ocean water to be compressed *in situ* until its density becomes that of rock, that is, 2.83. This condensation leaves pratically unchanged the load per unit area of any load surface lying below the deepest portion of the ocean bottom. The new ocean surface then reproduces on a reduced scale the irregularities of the ocean bottom, and between the new surface and the original ocean surface a void is left. Suppose a spheroidal equipotential surface of reference to be drawn [about this new surface] such that the volume of rock projecting above it is equal to the volume of the void spaces below it. This spheroidal level or equipotential surface defines *mean load level*. Mean load level lies in round numbers 5400 feet or 1650 meters below mean sea level.

The coefficients of equation 1 follow from this conception and from the topographic and bathymetric data.

From an approximate comparison with the results of Heiskanen and Niskanen let us take

TABLE 2. Indirect Effect in mgal for Various Values of h and s in Meters

h*, m	H, m	Indirect Effect, mgal	s†, m	h*, m	Indirect Effect, mgal
0	1650	+3.07	0	+1650	+3.07
1000	2650	+4.93	1000	+1014	+1.89
2000	3650	+6.80	2000	+378	+0.71
3000	4650	+8.66	3000	−258	−0.47
4000	5650	+10.52	4000	−894	−1.66
			5000	−1530	−2.84
			6000	−2166	−3.02
			7000	−2802	−4.20

* Height above sea level.
† Ocean depth.

formulas 1 and 2 at their face value, together with the numerical coefficients given in connection with them. Then to get the indirect effect, we multiply H_B by the normal gradient of gravity, say 0.3086 mgal per meter. Table 2 gives the results.

Now let us consider two matters that bring in the name of our distinguished colleague, Vening Meinesz, a real authority in all matters connected with gravity. What about the matter, or the void, between the natural geoid, mean sea level, and our cogeoid (the isostatic geoid), for which we have computed the direct effect? Should there be a second isostatic computation to take account of the matter, or the void, between the two geoids? At one time I said 'yes' but Vening Meinesz said 'no' [*Vening Meinesz*, 1946]. He said that the definition involves the natural geoid only, not some computed geoid. I now agree with him. We can disregard the matter or lack of matter between the real geoid, mean sea level, and any computed geoid. The theory of isostasy applies to the natural geoid, not to any computed geoid. Even if we had taken account of the matter or lack of matter between the two geoids and made a new second-order isostatic reduction for it, the result would be near zero. The compensation would approximately cancel out the topography, and in any case the amount of matter involved would be practically negligible.

Another situation seems interesting enough to mention: the land mass of Eurasia and Africa and the large areas of ocean that lies opposite to this land mass. The effect of this placement shows up when we make a spherical harmonic analysis of the topography. We get a huge harmonic term of the first order. The pole of the first-order term representing the land mass of Eurasia and Africa lies in the western portion of the Black Sea south of Odessa. At the antipodal point is the highest negative value represented by this harmonic. Vening Meinesz and I both used the result obtained by Prey [see *Vening Meinesz*, 1949, p. 176; *Lambert*, 1930*b*, p. 169]. The coefficient of this term (its maximum value) according to Vening Meinesz is 1204 meters with density 2.67. My result is 625 meters, using the mean density of the Earth. On applying isostatic compensation we get a displacement of the Earth's center of gravity. *Vening Meinesz* [1961] considers the effect of this shift in an elaborate discussion. Using the Airy-Heiskanen definition of isostasy, a depth compensaton of 30 kilometers, and a topographic density of 2.67, he finds that this shift requires a correction in milligals of 1.9 cos θ, where θ is the angle between the point under consideration and the central point of the first-order spherical harmonic, a point in the Black Sea south of Odessa, as already mentioned. This is an indirect effect of sorts, but essentially different from the main indirect effect already discussed.

Before passing to my final recommendations, I would call attention to two sets of tables for computing this indirect effect. They are by *Lejay* [1948] and *Lambert and Darling* [1936].

It is very evident that the mathematics of this indirect effect can be very complicated. I suggest that the International Association of Geodesy appoint a special international committee to study this subject and make recommendations to the effect that all geodesists who have to do with gravity data conform to these recommendations in their publications. The committee would decide, for instance, whether to adopt the Pratt or the Airy type of isostasy. Nowadays it would probably be the Airy type. Then there is the depth of compensation and the conventional standard density of the topography. Another question involves the type of compensation, equality of mass or hydrostatic equilibrium. The committee may well find that other matters need to be considered. And it might be of interest to see how good an approximation is given by the simple formula

explained in this paper. A few well-chosen examples would be of interest, i.e. examples in which the approximation given by this simple rule is very good, fairly good, or poor.

The purpose of this suggested international committee would be merely to make it easier for geodesists of various countries to meet on common ground and to use one another's results when they are considering the various problems connected with isostasy. Of course the purpose would not be to discourage any geodesist from explaining any method that he may prefer and applying it, either because it seems closer to the facts of nature than the official one, or for any other reason whatsoever.

References

Heiskanen, W. A., and Erkki Niskanen, World maps for the indirect effect of the undulations of the geoid on gravity anomalies, *Ann. Acad. Sci. Fennicae, Ser. A LVII*(4), 1941 (also *Publ. Isostasy Inst. IAG, 7*).

Lambert, Walter D., An approximate rule for the distance between the geoid and the spheroid on the assumption of complete isostatic compensation of the topography, *Bull. Géodésique, 26,* 91–97, 1930*a*.

Lambert, Walter D., Form of the geoid on the hypothesis of complete isostatic compensation, *Bull. Géodésique, 26,* 98–106, 1930*b*.

Lambert, Walter D., The reduction of observed values of gravity to sea level, *Bull. Géodésique, 26,* 107–108, 1930c.

Lambert, Walter D., and Frederic W. Darling, Tables for determining the form of the geoid and its indirect effect on gravity, *USCGS Spec. Publ. 199,* 1936.

Lejay, R. P. Pierre, Tables pour le calcul de l'effect indirect et la déformation du géoide, *Bull. Géodésique, 8,* 1948.

Vening Meinesz, F. A., The indirect effect or Bowie reduction on the equilibrium figure of the Earth, *Bull. Géodésique, N. S. 1,* 33–107, 1946.

Vening Meinesz, F. A., The isostatic reduction and the indirect or Bowie effect, *Bull. Géodésique, 12,* 1949.

Vening Meinesz, F. A., Can we neglect the shift of the Earth's gravity center when carrying out the topographic and isostatic reduction?, appendix to 'Study of the shape of the equipotential surfaces and the gravity anomaly field in high elevations,' *Quart. Rept. Dec. 1960–Feb. 1961, OSURF Project 1114, Air Force Project DA-33-019-ORD-3356,* 1961.

Geophysical Correlations

WILLIAM P. DURBIN, JR.

Aeronautical Chart and Information Center
St. Louis, Missouri

Abstract. Where gravity data are insufficient for geodetic purposes and actual observations are not practical, nonconventional methods must be used. This paper proposes several geophysical approaches toward partial solution of the problem. The utilization of geologic, seismic, crustal, and magnetic information in a gravimetrically unsurveyed area will provide an approximate anomaly which can either stand alone or be used in conjunction with statistical methods.

Many of the ACIC (Aeronautical Chart and Information Center) geophysical and aerospace projects involve use of the methods of physical geodesy. As we have seen repeatedly at this meeting, there is a relatively large quantity of gravimetric data available for such applications, but examination of the gravity map exposes deficiencies in density and distributon.

Gravity information for the empty areas can be handled in several different ways. Admittedly, the most desirable procedure is to gain valid data by direct observation in the areas concerned. However, this method is not always practical. Until fairly recently the problem has been approached theoretically: that the algebraic sum of the Earth's anomalous gravity equals zero and that a zero free-air anomaly can be used to represent the value of gravity for such areas. The idea has been varied by computing an anomaly on the basis of a zero isostatic assumption; presuming that isostatic compensation is achieved, a zero isostatic anomaly is assigned to the area and a free-air anomaly computed, etc. Unfortunately, the computations are fairly complex, they are valid only for relatively large areas, and they suffer from the lack of observational data. Therefore, a more satisfactory method of handling the problem is necessary. The method must be quick and simple and produce values with predictable accuracies.

At the symposium 'Geodesy in the Space Age,' one solution to the problem was suggested by the possibility of correlating geology and gravity [*Durbin*, 1961*a*]. For many years exploration geophysicists have determined the dimensions of subsurface structures from gravimetric surveys, whereas others have established relationships between regional geology and gravity. The similarities between the studies indicated that if a definite correlation could be established, the reverse procedure could be employed; i.e., geologic data could be used to obtain gravity. The value of the idea was further enhanced by the fact that extensive depositories of geologic data are generally available throughout the world. Often geological surveys have been made of gravimetrically empty areas. If successful, the results of the 'reverse correlation' would have very significant application.

Our initial effort at ACIC was the correlation of gravity and surface geology. We took the reported geologic column representing an area and, by using the density and thickness of each layer, computed the mean density and total thickness of the column. By using the column thickness and the difference in density between the column and the underlying crystalline rocks, we were able to calculate equivalent mean Bouguer gravity anomaly for the column. The method was tested for accuracy in the south-central region of the United States, where the gravity field is well defined by extensive geophysical exploration. A map of simulated gravity anomalies was compiled from the dimensions of the various structures and estimated density values from published descriptions of rock types. The values were compared with mean free-air and isostatic anomalies for 1°-by-1° squares completed from direct observations. A standard deviation of ± 10 mgal compared with existing data was achieved.

Although the method was limited by a requirement for highly detailed near-surface geologic data, in theory it should have been applicable to mountainous areas. However, geologic profiles for such areas are difficult to determine. Moreover, the geological structure is usually extremely complicated. Shield areas, such as those in Canada and northern United States, present a similar problem where the low-density strata have been removed through glaciation and only poorly defined high-density crystalline and metamorphic rocks remain.

A second method for simulating gravity from geophysical data was based on an idea developed from an article published by *Woollard* [1959]. The article detailed the results of his studies regarding the approximation of crustal thickness from regional Bouguer anomalies or surface elevation. He used two curves for the approximation, one showing the relationship of crustal thickness to elevation. We discovered later that a similar relationship had also been published by *Demenitskaya* [1959] of the USSR.

By determining the equations for the curves and solving them simultaneously, an equation was derived for obtaining the Bouguer anomaly from topographic and Mohorovicic (Moho) discontinuity elevations [*Durbin*, 1961*b*]. This technique released us from sole dependence on surface structures and geologic profiles. Procedures from both Woollard's and Demenitskaya's theories were tested in the United States and Eurasia. In rugged terrain we simulated the Δg_B with approximately a 90% accuracy with the Woollard curves. Relatively large variations in the results were attributed to the fact that, since the graphics and equations expressed only elevation and anomaly, the heterogeneous nature of the crust and the local mass variations were not accounted for. To eliminate this problem, it would be necessary to incorporate factors for both near-surface and deep-seated structures into the anomaly determination.

Subsequent studies led into several areas of interest to our gravity simulation project. Studies of the relationship of free-air anomalies to relief in mountainous areas and depth of water in marine areas; the relationship of Bouguer anomalies to surface elevation with geologic corrections; relationship of the crust with its heterogeneous characteristics (thickness, composition); crust-mantle relationships and their reflections in free-air, Bouguer, and isostatic anomalies; and correlations of anomalous gravity and seismic (or both) parameters with tectonic units promise to provide part of the answers to the empty areas [*Woollard*, 1962].

At the University of Hawaii, Woollard is currently testing the prediction methods by computing mean gravity values and comparing them with observed gravity for the area west of the Mississippi. It is anticipated that this project and associated studies will develop a geophysical method for evaluating gravity that will complement existing statistical evaluation techniques. For example, what are the contributions of such various mass components as elevation, surface geology, crust, and upper mantle to a gravity anomaly?

Woollard has also determined that the correlations between near-surface geology and gravity anomalies are also extremely useful for *interpolation* rather than prediction, where the problem is one of estimating mean anomalies from sparse coverage. In a sample problem run by William Strange at University of Hawaii, twenty-eight 1°-by-1° squares in the State of Wyoming demonstrate the value of geologic knowledge where only sparse gravity data are available. One observation was assumed for the center of each square, and the mean free-air anomaly was estimated with a standard deviation of less than ± 10 mgal by using knowledge of the variation of geologic conditions (Woollard, personal communication, 1964).

ACIC has also investigated another prediction method which expresses gravity as a function of empirical observation. For example, in areas of mass excess the anomaly is usually positive, and just the opposite is true for areas of mass deficiency. There is also evidence that in areas in which there is crustal faulting, the delineation of the fault zone coincides with a zero-isostatic anomaly contour. Such knowledge should be used to plan various types of gravity surveys. Although land surveys usually run along the routes of main thoroughfares, if it were known that a maximum or minimum anomaly occurred in an area accessible by secondary routes, traverse routes could be modified to furnish a more accurate picture of the anomaly field.

There are three logical directions that we at ACIC are taking in additional studies of gravity simulation. We are continuing our examination of continental areas outside the United States to determine the extent of the worldwide application that can be made of established gravity, geology, and geophysical relationships. We are also extending our study of ocean areas (we already have a crust-gravity relationship in marine areas which is undergoing further refinement); then, based on the assumption that magnetic anomalies define the thickness of the crust in marine areas, we should be able to employ magnetic anomalies to establish simulated or predicted regional gravity anomalies. And finally, statistical procedures are being expanded to include geologic and geophysical data.

With respect to the expansion of statistical procedures, the purpose of statistics is to permit the most probable estimate of a quantity in terms of all available knowledge bearing on the estimate. The only information of this sort usually employed in statistical interpolation and extrapolation of gravity has been observed gravity anomalies and the spatial location of gravity stations. Statistical treatments should be expanded, therefore, to include geological and geophysical parameters.

In general, simple assumptions have been made regarding height correlations, and they are sufficient for obtaining the mean anomalies of 5°-by-5° squares because the local mass variations tend to be averaged out over such an area. However, to obtain reliable mean anomalies for 1°-by-1° and 2°-by-2° squares, the local mass variation and surface geology must be considered. Topographic height correlations by themselves fail to account for subsurface mass variation. For example, the central United States has few topographic extremes but many instances of intense gravity gradients: the mid-continent gravity high to mention one, the Williston Basin as another. Attempts at local Δg_m estimations by statistical procedures must take this factor into account wherever possible.

Despite all their common interests, geodesists and geophysicists rarely take advantage of the wealth of data each has to offer. Only recently have there been realistic attempts at an interdisciplinary dialogue to provide mutual assistance in solving common problems.

ACIC has performed a series of projects which has made significant strides toward developing a *practical* tie between the two disciplines.

I have described one such bridge through the gravity/geology correlation. The crust/geoid relationship is another interesting approach.

In an earlier paper at Berkeley last year [*Durbin*, 1963], I suggested correlations between the local crust and the corresponding geoid undulation. Comparisons of crustal thickness with various geoids (gravimetric, astrogeodetic, and satellite) showed a general compatibility, not only in the United States but also in various other parts of the world. The best correlation in terms of 'data scatter' is a well-defined linear relationship that has been established between values in the United States and the Columbus geoid. The simplicity is evident in the expression

$$\Delta N = 1.9H - 75$$

A subsequent check on the correlation accuracy is found in an analysis of the linear equation. If, in the correlation equation, N is set equal to zero, the crustal thickness resolves to 39.4 km. This value compares favorably with the average crustal thickness of 38 km [*Nuttli*, 1964] and the theoretically compensated crust of 38.6 km accepted for the United States, emphasizing isostatic equilibrium in the United States as stated by Heiskanen.

A possible explanation for the correlation can be found in approximating the local crust to a vertical circular cylinder of constant density, 100-km radius, and a height component equal to the seismically determined crustal thickness. At the risk of over-simplification, the disturbing potential can be expressed by a surface coating on the bottom of the cylinder, which, in turn, can be equated to the geoid through the classical expression

$$N = T\gamma$$

A similar solution was recently demonstrated by *Egyed* [1964] of Eotvos University, in which he correlated the maximum undulations of the geoid on the surface of the outer core. Approximating the core variation to spheres with seismically verified radii of 200 km, Egyed developed equivalent geoid values. (He also suggested possible correlations between magnetic variations and the character of the geoid.)

Thus we have a spectrum of the geoid correlated on a shortwave (topographic elevation) basis through the scheme of the crust to a longwave core correlation.

In related studies, the Woollard group at Hawaii has identified preliminary applications of geologic data in the interpolation of deflection values. Techniques have been tested in areas of extremely rugged topography, namely the Rocky Mountains and the Italian Alps [*Strange and Woollard*, 1964].

Three years ago the geodetic application of geophysical correlations was received with understandable skepticism. Since that time, studies both by geodesists and geophysicists in the United States and abroad have borne out our original contention. Statistical treatments are limited by the type and quality of input data and, consequently, by the scale of their product. The use of geologic, seismic, magnetic, and other geophysical data expands our horizons in physical geodesy considerably.

References

Demenitskaya, R. M., The method of research of the geological structure of the crystalline mantle of the Earth, *Sovet Geol., 1*, 1959.

Durbin, W. P., Jr., Some correlations of gravity and geology, Proceedings of Symposium on Geodesy in the Space Age, *Inst. Geodesy Photogrammetry Cartography Publ. 15*, Ohio State University, Columbus, February 1961*a*.

Durbin, W. P., Jr., Correlation of gravity and geologic data, paper presented at 10th Pacific Science Congress, Honolulu, Hawaii, August 1961*b*.

Durbin, W. P., Jr., Comparison of crustal parameters with geoid undulations, paper presented at 13th General Assembly IUGG, Berkeley, California, August 1963 (see also *Proc. VESIAC Conf. on Variations of the Earth's Crust and Upper Mantle*, University of Michigan, Institute of Science and Technology, July 1964).

Egyed, L., The satellite geoid and the structure of the Earth, *Nature, 203*, 1964.

Nuttli, Otto, Some effects of the crust and free surface on the amplitudes of *P* and *S* waves, *Proc. VESIAC Conf. on Variations of the Earth's Crust and Upper Mantle*, University of Michigan, Institute of Science and Technology, July 1964.

Strange, W. E., and G. P. Woollard, Anomaly selection for deflection interpolation, *AF23(601)-4009, Hawaii Institute of Geophysics*, July 1964.

Woollard, G. P., Crustal structure from gravity and seismic measurements, *J. Geophys. Res., 64*, 1521–1544, 1959.

Woollard, G. P., The relation of gravity anomalies to surface elevation, crustal structure, and geology, *Res. Rept. 62-9, AF23(601)-3455*, University of Wisconsin, December 1962.

Free-Air Gravity Anomalies Caused by the Gravitational Attraction of Topographic, Bathymetric Features, and Their Isostatic Compensating Masses and Corresponding Geoid Undulations

LASSI A. KIVIOJA AND ALBERT D. M. LEWIS

School of Civil Engineering
Purdue University, Lafayette, Indiana

Abstract. Mean elevations and depths of all even 5°-by-5° surface elements and their corresponding isostatic compensating masses in the Airy-Heiskanen, $T = 30$ km, isostatic system together with the published gravity information were used to compute mean free-air anomalies for all 2592 5°-by-5° surface elements covering the entire surface of the Earth. By using these free-air anomalies, geoid undulations were computed by the Stokes formula at every 5°-by-5° surface element, and the corresponding global map is given. Another similar computation by the Stokes formula was performed by using all published 5°-by-5° free-air anomalies based on actual gravity measurements and on the international gravity formula wherever available and by filling in all empty areas by the computed anomalies. The corresponding global geoidal map is given.

INTRODUCTION

Gravity anomalies are caused by irregular mass distributions in the upper layers of the Earth. The mass irregularities are either excesses or deficiencies from the average, and they belong to three main groups: (1) topographic or bathymetric masses situated a few kilometers above or under the geoid, (2) isostatic compensating masses situated between 10 and 70 kilometers under the surface, or (3) mass variations caused by irregular densities throughout the upper layers of the Earth.

The best way to get the desired gravity anomalies is by well-planned, extensive gravimetric surveying. Unfortunately, this work is presently incomplete. Because of the great importance gravity anomalies have in the Earth sciences, many methods of extrapolation from surveyed to unsurveyed areas have been under study. Which method works best in some small area, or on the worldwide scale, can be determined with finality after corresponding anomalies have been determined by gravity measurements.

BATHYMETRIC AND TOPOGRAPHIC METHOD

On worldwide scale, one good method of extrapolation is to utilize all available information on the mass distribution and to compute the effects everywhere on the Earth's surface. Only a portion of the mass distributions is known, and therefore only a part in each true gravity anomaly can be computed. However, this part is a real part in each anomaly. If the total mass distribution were known, all true gravity anomalies could be computed.

A very large group of mass irregularities is given directly by bathymetric and topographic maps. It is also known that, on the average, these formations are in isostatic equilibrium or are very close to this equilibrium. Further, the average densities of all these formations are relatively well known: the average density of the crust is not far from 2.67 g/cm^3; the average density of ocean water that covers 70% of the surface with an average thickness of 3900 meters is 1.03 g/cm^3; the density contrast at the crust-mantle boundary is taken in several isostatic models to be 0.6 g/cm^3 to combine a few smaller density contrasts into one. By estimating the volumes of various formations from bathymetric and topographic maps and by assuming an isostatic system, all these average masses become known. Their effects on gravity can be computed everywhere on the Earth's surface by Newton's law of attraction, and thus a gravity anomaly for every surface element is

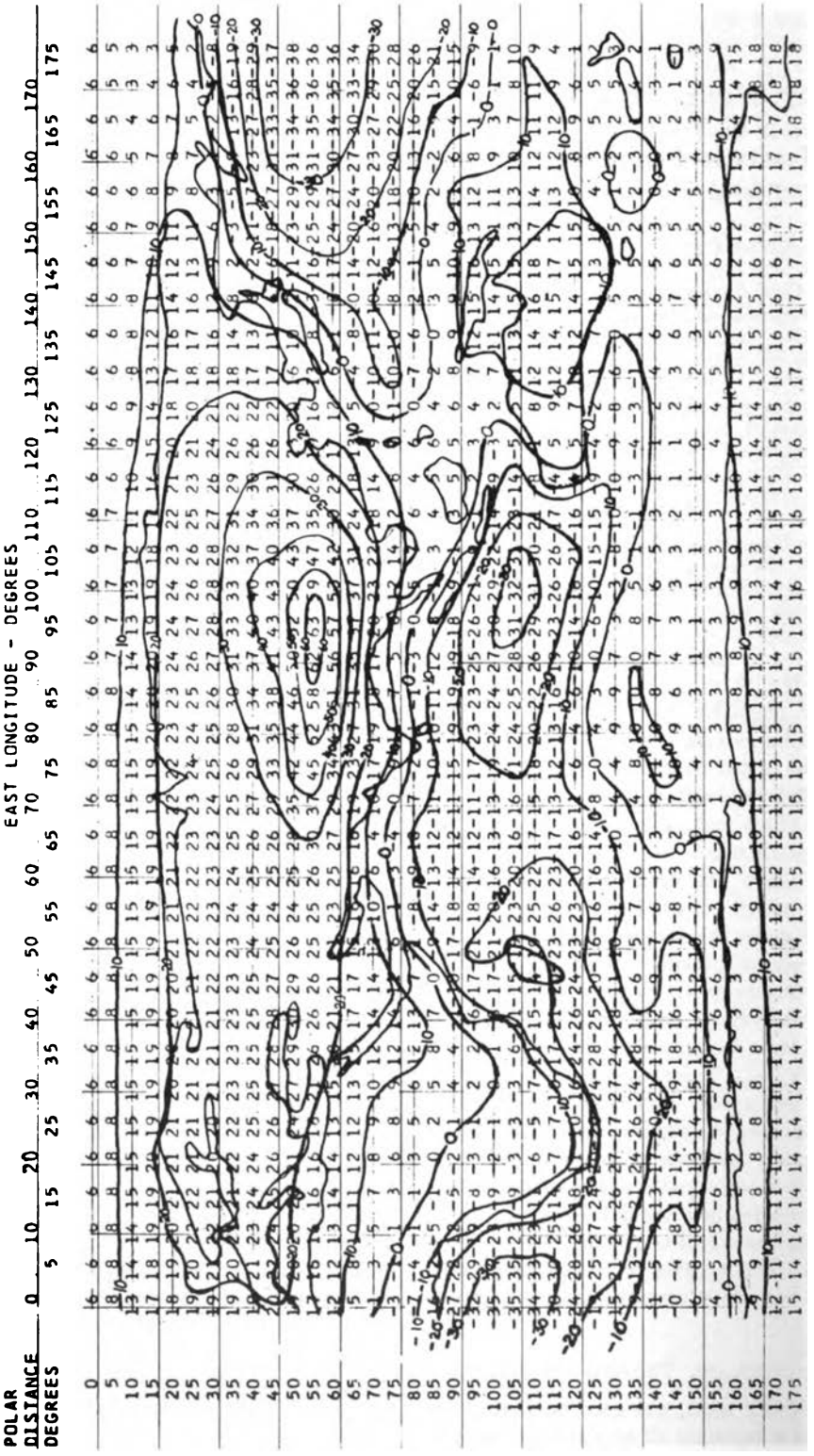

Fig. 1. Geoid undulations in meters by topography and its isostatic compensation.

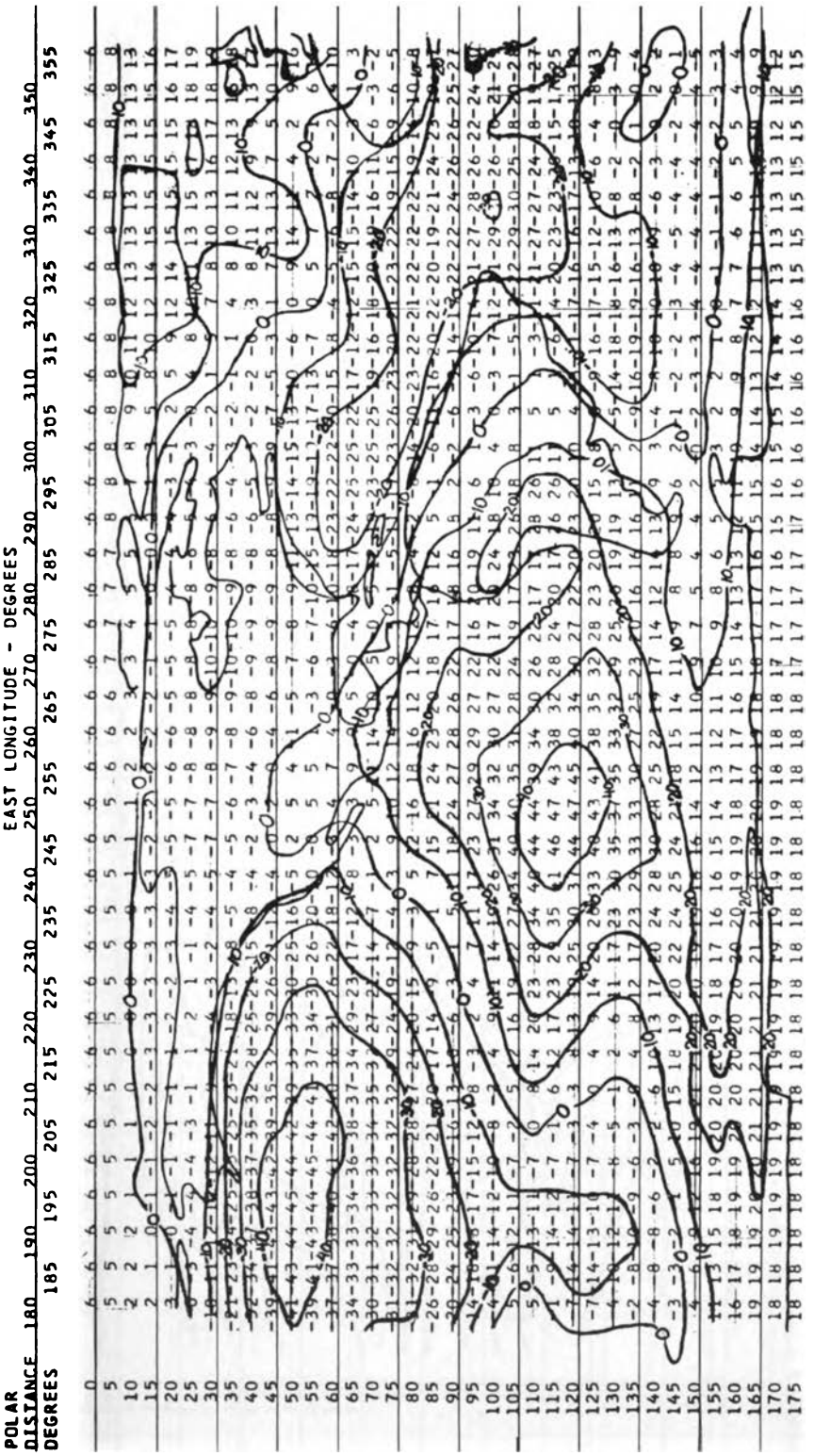

Fig. 1 (continued)

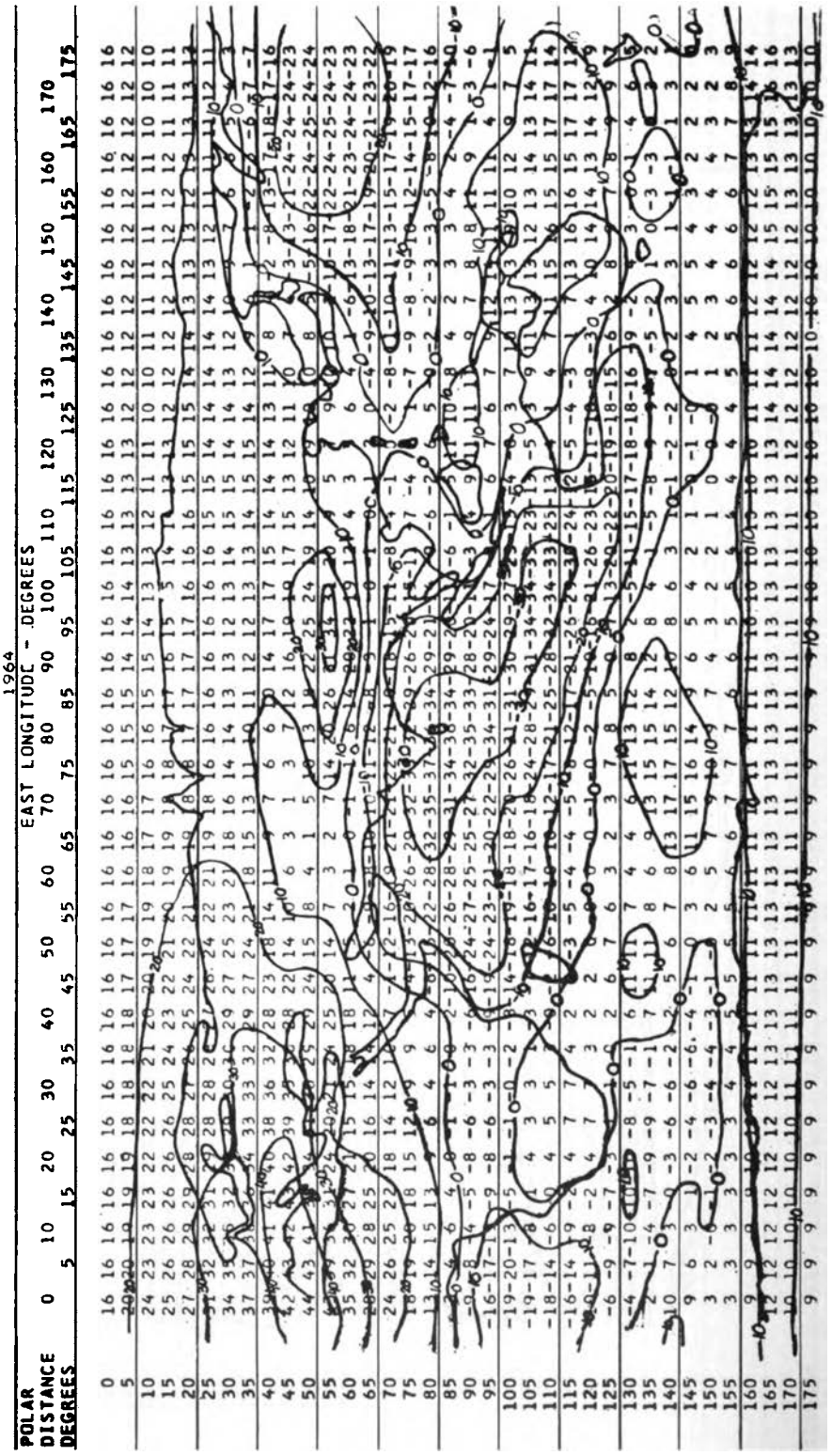

Fig. 2. Geoid undulations in meters computed from free-air gravity anomalies in 1049 5°-by-5° surface elements based on the international gravity formula published by Heiskanen and Uotila and from extrapolated free-air gravity anomalies using the gravitational effects of bathymetry, topography, and isostatic compensation in the remaining 1543 5°-by-5° surface elements.

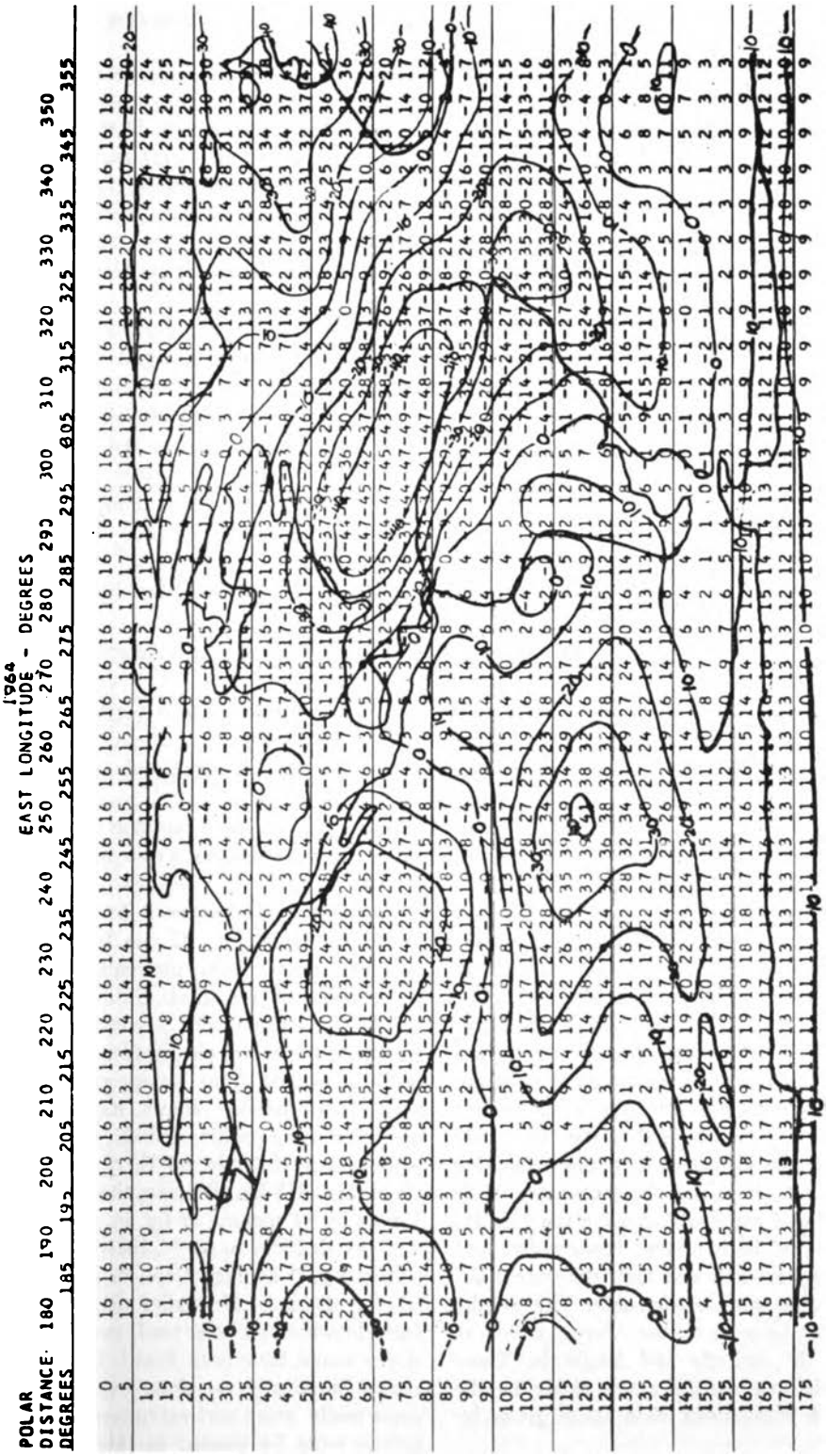

Fig. 2 (continued)

obtained. The gravity anomaly coverage is then complete; however, each anomaly is not the true complete anomaly but only a part of the true anomaly, because the known and unknown density irregularities from normal throughout the upper layers of the Earth have not been included.

The mean depths and elevations have been estimated for all even 5°-by-5° surface elements. Corresponding effects originating at each element have been computed for every 5°-by-5° surface element. The effects of isostatic compensation have been computed using the Airy-Heiskanen, $T = 30$ km, isostatic system [*Heiskanen*, 1938]. The combined effects of topographic, bathymetric, and isostatic compensating masses give a contribution to each 5°-by-5° free-air gravity anomaly. A set of such free-air gravity anomalies has been published [*Kivioja*, 1963].

Geoid Undulations by Computed Anomalies

Geoid undulations were computed using the computed free-air anomalies in the Stokes formula by the IBM 7094 computer. Stokes' coefficients were computed at all 36 even 5° latitudes for the center of gravity of each of the 2592 5°-by-5° surface elements. The results are given in Figure 1 to the nearest meter at all four corners of each 5°-by-5° surface element. These are the partial geoid undulations caused by bathymetric, topographic features and their isostatic compensating masses, assuming the previously mentioned normal average densities in all 5°-by-5° surface elements.

A similar computation was made using all available 5°-by-5° mean free-air anomalies based on actual gravity measurements referring to the international gravity formula. Heiskanen and Uotila have published these for 1049 5°-by-5° surface elements. For the remaining 1543 5°-by-5° elements, the anomalies were interpolated and extrapolated using the gravitational effects of bathymetry, topography, and isostatic compensation and their differences between adjacent surface elements. The results are given in Figure 2 to the nearest meter at every even 5° latitude and longitude. These geoid undulations naturally are closer to the actual geoid undulations than those given by Figure 1.

Comparisons with Other Geoids

It is interesting to compare the geoidal map of Figure 1 with the two superimposed geoidal maps given by *Runcorn* [1964], which were computed by *Uotila* [1962] from existing gravity data and by *Izsak* [1963] from satellite data.

These three geoids show many striking similarities:

The North Atlantic is positive by about +20 meters.

The Atlantic Ocean from the U. S. east coast toward South Africa is negative by about −25 meters.

North Africa is positive by about +15 meters.

Northwestern portion of the Indian Ocean is negative by about −20 meters.

Australia is positive by about +15 meters.

North Pacific is negative by about −30 meters.

South Pacific is positive by +10 to +40 meters.

Western part of South America is positive by +10 to +20 meters.

Eastern part of South America is negative by about −10 meters.

Areas near the north pole are positive by about +10 meters.

In addition to these common general features, these three geoidal maps also show some differences:

The greatest difference is in the area of the Himalaya Mountains. If one follows the 90°E meridian north from the equator to central Asia, one can see that Uotila's and Izsak's geoids show practically a constant undulation value, N, for this geoid profile. In contrast, the geoid computed from topography and its isostatic compensation shows its greatest slope along the same profile. At 0°N, 90°E, N is −19 meters, and at 35°N, 90°E, N is +62 meters. Over this 3875-km distance, the geoid in Figure 1 rises by 81 meters, or by an average slope of 4.3″. From 25°N to 30°N, the rise is 21 meters, giving a 7.8″ average slope in geoid over that 560-km distance. If smaller than 5°-by-5° surface elements had been used, even greater geoid slopes would have been found. If the true geoid shows practically no slope over this distance, some really great and extensive density irregularities must be present in this area, canceling

the effects of topographic and compensating masses.

When the negative areas in Figure 1 are followed, it is seen that they practically form a great circle around the world. Starting from the U. S. east coast toward South Africa, N is -20 to -30 meters. Continuing around the southern tip of Africa toward Indonesia, N is -25, -15, -30 meters. Continuing along the same great circle over Indonesia, N becomes slightly positive over a short distance from Borneo to the Philippines; N is 0, $+5$, 0 meters. Thereafter, N is -10, -20, -30, and -45 meters just south from Alaska at 45°N. Continuing over northwest Canada down to the east coast of the U. S., N is -10, -5, -8, and -20 meters again.

Other differences between the geoidal maps are mainly the relatively small shifts in the locations of the maximums and minimums and in their shapes and absolute values.

Conclusions

Examination of the geoidal maps shows that a large part of geoid undulations is due to bathymetric, topographic, and isostatic masses. Compared with the true geoid, when it is available, Figure 1 reveals areas where extensive density irregularities exist in the upper layers of the Earth. The geoid given in Figure 1 is almost uniformly as good and accurate everywhere on the Earth as it is in the best surveyed areas of North America, the North Atlantic, and Europe.

When the measured gravity anomalies are compared with gravity anomalies that have been computed from bathymetric, topographic, and isostatic masses, the differences will reveal information about the hidden density distributions inside the Earth.

Better results in several geodetic and geophysical problems can be expected by using gravity anomalies computed from bathymetric, topographic, and isostatic compensating masses in unsurveyed areas on the worldwide scale, complementing the known gravity anomalies in well-surveyed areas.

References

Heiskanen, W. A., New isostatic tables for the reduction of gravity values calculated on the basis of Airy's hypotheses, *Publ. Isostatic Inst. IAG 2*, 42 pp., 1938.

Izsak, I. G., Tesseral harmonics in the geopotential, *Nature, 199*, 137–139, 1963.

Kivioja, L. A., The effect of topography and its isostatic compensation on free-air anomalies, *Inst. Geodesy Photogrammetry Cartography Rept. 28*, 134 pp., Ohio State University, Columbus, 1963.

Runcorn, S. K., Satellite gravity measurements and a laminar viscous flow model of the Earth's mantle, *J. Geophys. Res., 69*, 4389–4394, 1964.

Uotila, U. A., Harmonic analysis of world-wide gravity material, *Ann. Acad. Sci. Fennicae, Ser. A III*(67), 18 pp., 1962.

The Prediction of Gravity

G. P. Woollard and W. E. Strange

Hawaii Institute of Geophysics
University of Hawaii, Honolulu

Introduction

The degree of success achieved in any prediction process depends on the following:

(*a*) Recognition of factors influencing the quantity to be predicted.

(*b*) Recognition of the magnitude of the effect of each individual factor on the quantity to be predicted.

(*c*) Recognition of interactions between individual factors and knowledge of the degree of interdependence between factors.

(*d*) Availability of data concerning each factor.

(*e*) One's philosophy of approach as to whether a given factor varies in a random or discrete manner.

For gravity it is known that we are dealing with a quantity that is influenced by both scalar and dynamic considerations. On the gross scale the combined gravitational effect of the Earth's mass, size, geometric shape, and rotation is expressed by a systematic change in surface gravity values with geographic latitude. The nature and magnitude of this change, which exceeds 5500 mgal, is defined theoretically by the equation of the international gravity formula that permits us to predict to a first approximation the value of sea level gravity for any location on the Earth's surface. This value ($g_\bullet$) constitutes a realistic base value to which the contribution of all other factors influencing gravity at any one point can be added. Although much has been said in recent years about the Earth's having a 'pear shape' and more recently the Earth's having a 'four-cornered shape' rather than the shape of an ellipsoid of revolution, as incorporated in the international gravity formula, the fact remains that these abnormalities in shape of the geoid have only a small gravitational effect (less than 35 mgal for the most part); furthermore the abnormalities are not fully substantiated as yet by surface gravity measurements.

We also know that gravity varies with surface elevation and that, although the vertical gradient of gravity does vary with both latitude and height, the deviation from a constant value for all ranges in latitude and surface elevation encountered on the Earth is so small that a constant can be employed to allow for the elevation effect without introducing any significant error.

Similarly it is known that there is a direct relationship between regional (2°-by-2°) variations in surface elevation and associated excess or deficiency of mass above or below the reference ellipsoid surface (sea level), and mass changes at depth associated with changes in crustal thickness and composition that accompany changes in surface elevation. The net gravitational effect of these two mass distributions is such that they tend to cancel each other. If this were not so, mean free-air gravity anomalies regardless of elevation over areas of this size where there is little topographic relief, would not approach zero so closely as they do. That a systematic deviation in mean free-air anomaly values with elevation occurs as a function of the horizontal dimensions of regional changes in topography is recognized, as well as the superimposed effect of what might be called the 'roughness coefficient' of superimposed local topography. The first effect is related to changes in mass and to the separation with change of elevation between the topographic mass above sea level and its compensating mass (crustal root) at depth. The second effect is related to the more pronounced change in the ratio between the size of the mass units and their separation. In the United States the regional changes in elevation pattern and topography are such that there is a change of +7.8 mgal per 1000-meter change in elevation from 250

to 1800 meters; above 1800 meters the change is +37.0 mgal per 1000 meters. Superimposed upon this regional effect are the effects of local changes in topography, which are even more pronounced with a change of about +99.0 mgal per 1000 meters. As surface roughness (topographic relief) generally increases with surface elevation, there is a direct correlation of free-air anomaly values with topography. This correlation indicates an apparent lack of local compensation for small topographic features, which is substantiated by the smooth change in Bouguer anomaly values. Where there are no significant associated changes in local geology, these anomalies show no correlation with local topography.

As the effect of local changes in surficial geology can be just as important as the effects associated with local changes in topography, and as regional changes in surface elevation are determined in large measure by the mean density of the crust as well as its thickness, which in turn is governed by its geological composition and by the mean density and composition of the upper mantle, geologic considerations are a factor that cannot be ignored if realistic predictions of gravity are to be undertaken.

Related factors to be considered are the effect of convection within the mantle, compositional phase transformations within the crust or upper mantle, and stress conditions that might lead to isostatic imbalance.

Although it is not practical at this time to correct for such effects quantitatively, they do represent factors that require consideration in predicting gravity. Other factors, as yet unestablished, that may be important include the actual depth of compensation. The fact that earthquakes occur down to depths of 700 km implies that a true isobaric surface may not exist above this level. We also know from the analyses of satellite orbital perturbations that areas of apparent anomalous mass exist that give regional distortions of the geoid as great as 70 meters. Large areas of anomalous magnetic field, presumably related to convection in the liquid core of the Earth, are subject to secular change in both position and field strength and may have gravitational expression. Although realistic predictions to ±5 mgal may never be possible without considering the effects of phenomena at depth in the Earth's interior, at present we know too little about these effects.

It is therefore fortunate that the Earth's near surface mass distribution is dominant in determining both local and regional changes in surface gravity field, and that nature has provided a crust whose thickness varies with elevation in such a manner that compensation is mainly accomplished at shallow depth leaving only a minor dependence on the mass distribution at greater depth above the actual isobaric surface.

Finally there is the effect of Earth curvature and the effect of distant topography and its underlying crustal structure that must be considered. As this effect changes slowly with position and elevation, it presents no problem. Therefore, except for the effect of changes in geology and the as yet undefined phenomena giving regional distortions of the geoid as revealed by satellite data, all the factors influencing gravity and their interactions can be predicted with considerable reliability from a knowledge of position and elevation.

The fact that 80% of the time isostatic anomaly residuals average close to zero (±35 mgal) for changes in observed gravity in excess of 5500 mgal on a worldwide basis indicates that we can predict gravity with at least this degree of assurance. We are concerned, therefore, with the degree to which we can significantly improve the accuracy of gravity predictions. For example, is it possible to predict values having a reliability of ±15 mgal 85% of the time in unsurveyed areas or ±5 mgal 90% of the time in restricted areas where there exists some gravity control? The writers feel that, although it may not be possible at this time to achieve such a high degree of reliability, these figures do represent realistic goals for the future, and that significant improvement can be realized through application of current geophysical and geological knowledge.

The Prediction of Gravity in Restricted Areas Having Some Gravity Control

As the prediction of gravity in an area of limited areal extent where there is some existing gravity control represents the simpler of the two prediction problems, it will be considered first. The assumptions we make in this case are:

(*a*) Any regional effect due to the crust and mantle or distant topography and its com-

pensation will be a smoothly varying function over the entire area.

(*b*) The effects of local variations in surface mass whether of topographic or geologic origin will be essentially uncompensated.

(*c*) The uncertainties in the international gravity formula and the vertical gradient of gravity are negligible.

(*d*) Changes in the curvature correction are small (usually less than 3 mgal) and can be neglected without introducing serious error.

(*e*) The Bouguer anomaly will be a smoothly varying function if there are no significant changes in geology.

To illustrate the effectiveness of this approach two examples for which the data can be checked will be used. As both the international gravity formula and the vertical gradient of gravity are to be accepted as correct under these conditions, the derivation of free-air anomaly values will be equivalent to deriving observed gravity values. In each test example where there is an intervening major topographic and geologic feature a traverse in excess of 350-km length will be used.

Rocky Mountain section. The first section selected is across the Rocky Mountain front at Pikes Peak and extends from Gunnison, Colorado, on the west to Laird, Colorado, on the east. As a preliminary test, gravity data for only the two end points, 350 km apart, will be assumed to be known but with the elevation values and locations known for four intervening points. Prediction will be based on extrapolated Bouguer anomaly values between the two end control points and on the computed mass attraction of the rock column above sea level based on the attraction of a plate corrected for the local terrain.

As the Bouguer anomaly = Free-air anomaly − (Mass correction − Terrain correction), the predicted Free-air anomaly = Extrapolated Bouguer anomaly + Mass correction − Terrain correction. In this example the density (σ) used will be 2.67 g/cm^3 in the mass correction equation ($\Delta g = 2\pi\gamma\sigma h$) for a plate. The data are given in Table 1.

It is obvious from the results shown in Table 1 that a prediction based on points that are so far apart (in this case over 450 km) does not produce reliable values. The effect of decreasing the distance between control points to about half that used above with one point (Colorado Springs) at the topographic boundary is shown in Table 2.

As seen from Table 2 the predicted free-air anomaly values do approach the actual values within 5 mgal in this case. As the Free-air anomaly = Observed gravity − (g_ϕ − Δg_h), where g_ϕ is the theoretical sea level gravity from the international gravity formula and Δg_h is the free-air elevation correction for gradient and elevation, the observed gravity value would be

TABLE 1. Prediction of Pikes Peak Free-Air-Anomaly Based on Two Remote Points

Site, Colorado	Distance between Sites, km	Elevation, m	Mass Correction σ = 2.67, mgal	Terrain Correction, mgal	Extrapolated Bouguer Anomaly, mgal	Predicted FA Anomaly, mgal	Actual FA Anomaly, mgal	Error, mgal
Gunnison		2340	262	2	−245*	+15	+15	
	170							
Pikes Peak		4293	480	57	−200	+223	+203	+20
	28							
Colorado Springs		1842	206	0	−190	+16	−17	+33
	122							
Genoa		1675	188	0	−160	+28	+21	+7
	150							
Laird		1110	124	2	−118*	+4	+4	

* Observed values.

predicted with a reliability of 5 mgal from the equation: Observed gravity = FA anomaly + $g_\phi - \Delta g_h$.

Big Horn Mountains—Black Hills section. For the second case consider an example where the topography is geologically controlled and where there are buried geologic features having no surface expression. The section selected extends from Wasta, South Dakota, east of the Black Hills, to Boulder, Montana, and crosses the Black Hills, Big Horn Mountains, the Powder River Basin, and Big Horn River Basin. Geologically the Black Hills are a domal uplift with an exposed core of crystalline rocks; the Big Horn Mountains are an uplifted fault-bounded crystalline rock mass (horst). Between these two positive topographic features lies the Powder River Basin which has an estimated depth of about 3600 meters. The Big Horn Basin lies on the west side of the Big Horn Mountains, and its western boundary is formed by the Beartooth crystalline rock uplift. The total length of the section considered is about 550 km. To obtain a larger sample of data than was considered in Table 1, a series of sites at about 12-km intervals will be considered. Control points are assumed at the geologic boundaries which are located at about 150-km intervals. To ascertain the importance of including geologic parameters the data will be considered first without regard to geology and then with regard to geology.

As seen from Table 3, the prediction procedure based on topography alone and used with apparent success in predicting gravity at Pikes Peak was not successful when applied to the Big Horn Mountains—Black Hills region. Presumably this failure resulted from the fact that the changes in geology associated with changes in topography in this area were not considered. To test this hypothesis, corrections for known changes in geology will now be incorporated in the prediction.

In allowing for changes in geology, consideration must be given to mass changes both above and below sea level. Above sea level the geologic factor can be directly incorporated by using the actual mean density of the geologic column, or incorporated as a correction to a standard density (2.67 g/cm^3). Below sea level the correction must be based on the departure of the actual density from a standard density down to such depth below sea level that it can be assumed there are no major horizontal changes in mass. As the average density of the crystalline rock complex is 2.75 g/cm^3 rather than 2.67 g/cm^3, the mass deficiency or excess effect is considered relative to this value. Table 4 shows the geologic corrections, derived on the basis of compartment determinations for zones A–O, and the revised predicted values. Although it is seen from Table 4 that the incorporation of the geologic factors did modify the mass attraction by as much as 33 mgal and that the change in sign of the modification with geologic province was such that the total geologic effect incorporated amounts to almost 50 mgal, the improvement in reliability in predicting free-air anomaly values on the average did not exceed 12 mgal. Furthermore, the residual errors after allowing for geologic changes still average about 20 mgal. It is also seen that there is an

TABLE 2. Prediction of Pikes Peak Free-Air Anomaly Based on Two Remote Points Plus One Adjacent Point

Site, Colorado	Elevation, m	Mass Correction $\sigma = 2.67$, mgal	Terrain + Curvature Correction, mgal	Extrapolated Bouguer Anomaly, mgal	Predicted FA Anomaly	Actual FA Anomaly	Error, mgal
Gunnison	2340	262	2	−245*	+15	+15	
Pikes Peak	4293	480	57	−225	+198	+203	−5
Colorado Springs	1842	206	0	−223*	−17	−17	
Genoa	1675	188	0	−170	+18	+21	−3
Laird	1110	124	2	−118*	+4	+4	

* Observed values.

apparent systematic degradation in prediction reliability in progressing from the Black Hills to the Big Horn Basin.

The poor success achieved on this test can be attributed to two factors: (*a*) the great distance between control points (150 km) and (*b*) the location of the control bases at points of geologic change. If closer spacing had been used for the control points and they had been located to include the centers of geologic features as well as the boundaries, more realistic predictions could have been achieved.

To test this conclusion consider the section from Lovell, Wyoming, to Livingstone, Montana, which takes in the Big Horn Basin and represents the area of poorest prediction reliability in both Tables 3 and 4. As shown in Table 5, use of three control points at 50-km intervals here would give good prediction reliability without regard to changes in geology.

TABLE 3. Prediction of Free-Air Anomay Vallues without Regard to Geology
Black Hills—Big Horn Mountain Area
150-km station control at topographic boundaries.

Site	Elevation, m	Topographic Mass Correction $\sigma = 2.67$, mgal	Terrain Correction, mgal	Extrapolated Bouguer Anomaly, mgal	Predicted FA Anomaly, mgal	Observed FA Anomaly, mgal	Difference, mgal
Black Hills							
Wasta, S. D.	706	78	1	−62*	+15	+15	
Boxelder, S. D.	916	102	1	−71	+30	+7	+23
Rapid City, S. D.	1035	115	1	−79	+35	+37	−2
Pactola, S. D.	1370	152	3	−87	+62	+72	−10
Tigerville, S. D.	1780	198	1	−97	+100	+112	−12
Moon, S. D.	1928	215	2	−105	+108	+123	−15
Newcastle, Wyo.	1328	148	5	−114*	+29	+29	
Osage, Wyo.	1330	148	3	−123	+22	+30	−8
Powder River Basin							
Kara, Wyo.	1317	147	1	−131	+15	+28	−13
Rozet, Wyo.	1305	146	0	−140	+6	+15	−9
Gillette, Wyo.	1361	152	0	−145	+7	+39	−32
Wildcat, Wyo.	1266	141	2	−153	−14	+17	−31
Spotted Horse, Wyo.	1218	136	2	−160	−26	+15	−41
Arvada, Wyo.	1110	124	2	−166	−44	−30	−14
Ulm, Wyo.	1358	151	2	−171*	−22	−22	
Sheridan, Wyo.	1269	142	2	−172	−32	−22	−10
Durkee, Wyo.	1214	135	1	−172	−38	−30	−8
Big Horn Mountains							
Dayton, Wyo.	1212	135	3	−173	−41	−26	−15
Burgess, Wyo.	2456	274	5	−174	+95	+158	−63
South Fork, Wyo.	2428	270	8	−175	+87	+159	−72
Five Springs, Wyo.	1242	138	2	−175	−39	−2	−37
Big Horn Basin							
Lovell, Wyo.	1195	134	0	−176*	−42	−42	
Bowler, Mont.	1448	161	1	−178	−18	+13	−31
E. Bridger, Mont.	1106	124	1	−180	−57	+10	−67
Roberts, Mont.	1392	155	0	−181	−26	+24	−50
Absarokee, Mont.	1244	139	0	−182	−43	−2	−41
McLeod, Mont.	1460	162	1	−184	−23	+9	−32
Livingston, Mont.	1366	151	1	−163	−13	−13	0
Beartooth Uplift							
Boulder, Mont.	1493	167	0	−192*	−25	−25	

* Observed values.

So we do not become overly impressed by the results shown in Table 5, a note of caution is introduced. If there is a geologic feature involving a significant change in rock density between control points, even if the points are only 50 km apart, there may be significant error. This error is shown by the data of Table 6 for the section spanning the Big Horn Mountains. The control points are only 60 km apart, but neither point lies on the central mountain block.

As seen from Table 6, the error in prediction is 41 mgal, which is about the value attributed directly to the change in surficial and below sea level geology. If there had been no significant change in density of materials, the mass effect of the exposed topographic block would have reliably defined the change in free-air anomaly values, as was true at Pikes Peak. We can, however, define more correct values in this case by making a rough calculation of the geologic effect as follows. The mountain stands approximately 1200 meters above the surrounding terrain. Its mass effect (for $\sigma = 2.75$ g/cm^3) would be approximately 132 mgal after allowing for 6-mgal terrain effect. Below ground level on the flanks this crystalline rock block is in juxtaposition with sedimentary rock whose mean density down to the basement rock surface at a depth of about 3500 meters below the

TABLE 4. Predicted Gravity Values for Big Horn Mountains-Black Hills Region with Regard to Geology
150-km station control.

	Elevation, m	Mass Effect $\sigma = 2.67$, mgal	Geological Correction S. L. (+),† mgal	Geological Correction S. L. (−),† mgal	Corrected Mass, mgal	Terrain, mgal	Extrapolated Geologic Bouguer Anomaly, mgal	Predicted FA Anomaly, mgal	Observed FA Anomaly, mgal	Error, mgal
Black Hills										
Wasta, S. D.	706	78	−7	0	71	1	−55*	+15	+15	
Boxelder, S. D.	916	102	−6	0	96	1	−66	+29	+7	+22
Rapid City, S. D.	1035	115	−3	+8	120	1	−78	+41	+37	+4
Pactola, S. D.	1370	152	−1	+11	162	3	−89	+70	+72	−2
Tigerville, S. D.	1780	198	−1	+14	211	1	−100	+110	+112	−2
Moon, S. D.	1928	215	−2	+14	227	2	−112	+113	+123	−10
Newcastle, Wyo.	1328	148	−3	+12	157	5	−123*	+29	+29	
Osage, Wyo.	1330	148	−7	+11	152	3	−125	+24	+30	−6
Powder River Basin										
Kara, Wyo.	1317	147	−11	+2	138	1	−127	+10	+28	−18
Rozet, Wyo.	1305	146	−14	−6	126	0	−129	−3	+15	−18
Gillette, Wyo.	1361	152	−14	−8	130	0	−131	−1	+39	−40
Wildcat, Wyo.	1266	141	−12	−12	117	2	−133	−18	+17	−35
Spotted Horse, Wyo.	1218	136	−10	−17	109	2	−135	−28	+15	−43
Arvada, Wyo.	1110	124	−10	−16	98	2	−137	−41	−30	−11
Ulm, Wyo.	1358	151	−13	−19	119	2	−139*	−22	−22	
Sheridan, Wyo.	1269	142	−12	−22	108	2	−144	−38	−22	−16
Durkee, Wyo.	1214	135	−10	−23	102	1	−148	−47	−30	−17
Big Horn Mountains										
Dayton, Wyo.	1212	135	−9	+7	133	3	−153	−23	−26	+3
Burgess, Wyo.	2456	274	−2	+19	291	5	−158	+128	+158	−30
South Fork, Wyo.	2428	270	−1	+18	287	8	−163	+116	+159	−43
Five Spring, Wyo.	1242	138	−7	+9	140	2	−168	−30	−2	−28
Big Horn Basin										
Lovell, Wyo.	1195	134	−12	+8	130	0	−172*	−42	−42	
Bowler, Mont.	1448	161	−9	+15	167	1	−174	−8	+13	−21
E. Bridger, Mont.	1106	124	−9	+16	131	1	−177	−47	+10	−57
Roberts, Mont.	1392	155	−8	+16	163	0	−179	−16	+24	−40
Absarokee, Mont.	1244	139	−9	+14	144	0	−182	−38	−2	−36
McLeod, Mont.	1460	162	−10	+13	165	4	−184	−23	+9	−32
Livingston, Mont.	1366	151	−11	+7	147	1	−187	−41	−13	−28
Beartooth Uplift										
Boulder, Mont.	1493	167	−1	0	166	2	−189*	−25	−25	

* Observed values.
† S. L. (+) = above sea level; S. L. (−) = below sea level.

TABLE 5. Prediction of Free-Air Anomalies with 50-km Station Control, Big Horn Basin

Site	Elevation, m	Topographic Mass Correction $\sigma = 2.67$, mgal	Terrain Correction, mgal	Extrapolated Bouguer Anomaly, mgal	Predicted FA Anomaly, mgal	Observed FA Anomaly, mgal	Difference mgal
Lovell, Wyo.	1195	134	0	−176*	−42	−42	
Bowler, Mont.	1448	161	1	−146	+14	+13	+1
E. Bridger, Mont.	1106	127	1	−116*	+10	+10	
Roberts, Mont.	1392	155	0	−128	+27	+24	+3
Absarokee, Mont.	1244	139	0	−139	0	−2	+2
McLeod, Mont.	1460	162	1	−151	0	+9	+1
Livingston, Mont.	1336	151	1	−163*	−13	−13	

* Observed values.

surface is approximately 2.52 g/cm³. This value gives an additional gravity contribution to the mountain of about 34 mgal. The sum of the two effects is +166 mgal, which is then added to the regional free-air anomaly values characterizing the adjacent area. This value is about −14 mgal. The resulting predicted free-air anomaly value for the Big Horn Mountains is +152 mgal. As seen, this is only about 6 to 7 mgal less than the actual value. We therefore can make a reasonable prediction in such cases, but only if geological factors are considered.

Conclusions regarding the prediction of gravity where there is some control. The significant conclusions brought out by the above studies are: (1) Wherever the geology, crust, and mantle vary in a smooth regular manner, it is possible to use Bouguer anomaly values with a regional (50 km) spacing of control points as a datum for the prediction of free-air anomaly values and, hence, for observed gravity values over an area with a high degree of reliability. If, however, there are abrupt changes in geologic parameters involving significant changes in density such as are associated with normal faults, and particularly horsts (uplifted fault bounded blocks) and graben (down dropped blocks), it may not be possible to predict gravity with a reliability of 30 mgal with this degree of control. (2) Inclusion of geologic considerations where there are marked changes in geology and few control points will always result in more nearly correct predicted values, but the degree of resulting reliability will in large measure be governed by whether the control points are located so that they adequately sense changes in both surface and subsurface geology. (3) In general the closer the spacing of control points

TABLE 6. Prediction of Free-Air Anomaly Values with 60-km Station Control, Big Horn Mountains

Site, Wyoming	Elevation, m	Topographic Mass Correction $\sigma = 2.67$, mgal	Terrain Correction, mgal	Extrapolated Bouguer Anomaly, mgal	Predicted FA Anomaly, mgal	Observed FA Anomaly, mgal	Difference, mgal
Durkee	1214	136	0	−166*	−30	−30	
Dayton	1212	135	3	−159	−27	−26	−1
Burgess	2456	274	5	−152	+117	+158	−41
South Fork	2428	270	8	−145	+117	+159	−42
Five Springs	1242	138	2	−138*	−2	−2	

* Observed values.

the more reliable is the resulting prediction, but, as indicated, the critical factor is not the number of control points but the nature of the geology in a given area. (4) With an adequate distribution of control points for the local geological setting it is not essential to include any corrections for geology, as the geological effect will be incorporated in the Bouguer anomaly values of the control points. Use of a standard density, such as 2.67 g/cm³, in computing the effect of the mass above sea level therefore is not only permissible but preferable with this type of control to making 'educated guesses' about subsurface geologic conditions. (5) The decision as to when a geologic correction is desirable and how best to apply it will depend on the distribution of available control data and our knowledge of the geology of the area.

Prediction of Gravity in Unsurveyed Areas

The term 'unsurveyed' as used here refers to areas in excess of 2° by 2° in which there are no data or at best one or two observations. When only one or two observations exist, we usually are not sure whether the available data are reliable or whether they are biased by unknown subsurface geologic effects or abnormalities in the crust or mantle. If the data are reliable and the geology is well known, it is much better, because the control then provides a local reference datum. If there are no data, we must either work from the nearest area of control or base all predictions on either theoretical or empirical considerations. On a theoretical basis the general equation would resemble the theoretical predicted value in the isostatic reduction.

$$g_p = g_\phi - \Delta g_h + \Delta g_m - \Delta g_t + \Delta g_g - \Delta g_{A-0} - \Delta g_{1-18} + \Delta g_c$$

where

g_ϕ is sea level gravity from the international formula.

Δg_h is free-air gravity effect for elevation above sea level.

Δg_m is effect of included mass above sea level.

Δg_t is terrain correction.

Δg_g is geologic correction.

Δg_{A-0} is local compensation effect for crustal structure.

Δg_{1-18} is effect of distant topography and compensation.

Δg_c is Earth curvature effect.

If gravity were predicted quantitatively on the above basis, it would be a laborious process. The reliability of the results can be gaged from the following. Of the various terms, Δg_h, Δg_t, Δg_c, and Δg_{1-18} can probably be determined with a high degree of reliability (± 1 mgal), if we assume elevations good to ± 10 feet and have good topographic maps. Also, the terms for g_ϕ and Δg_m can probably be determined with a reliability of ± 4 mgal, or better, 90% of the time despite uncertainties as to the actual shape of the geoid and local crustal density. The greatest uncertainty (± 10 to 50 mgal) is related to the geological correction (Δg_g) and to the local crustal compensation (Δ_{A-0}). As the magnitude of each can be as high as 40 mgal and additive, the uncertainty as regards subsurface geology and actual mean crustal density can give resultant errors in predicted values as great as 80 mgal.

The effect of using the Airy-Heiskanen or the Pratt-Hayford concept of the isostatic mechanism is not critical so long as the Pratt-Hayford depth of compensation is about twice the actual values of crustal thickness. The important factor is the degree to which the isostatic models produce an effect equaling the actual condition and not the mechanism employed to simulate crustal compensation. When we examine the data for seismic studies of the crust, it is found that in broad terms compensation is achieved through variations in crustal thickness. As the velocity structure of the indicated crust is not constant, there can be no fixed density contrast between the crust and mantle unless the mantle changes in an analogous manner. Generally this condition is not observed. So even if perfect hydrostatic equilibrium exists between the crust and mantle, there should be no regular change in crustal root compensation for changes in surface elevation. As the effects of a heterogeneous crust could be critical in determining Δg_{A-0}, the magnitude of the effect produced by probable changes in crustal density was investigated.

Effect of Changes in Crustal Density

As a first step, assume that the upper mantle is characterized by a constant density and that

the crust is in hydrostatic equilibrium with the mantle. Under these conditions, whenever the crust has a higher than normal density, it will have an abnormal thickness for a given surface elevation and hence too much root. Conversely, where the crust has a subnormal density, the value of crustal thickness will be subnormal for a given surface elevation and there will be too little root. Under either condition the gravitational effect of the mass above sea level ($\Delta g_m - \Delta g_l$) will not be exactly compensated by the sum of the terms ($\Delta g_{A-0} + \Delta g_{1-18}$) representing the gravitational effect of the local root plus the effect of distant topography and compensation. In other words, physical equilibrium conditions between the crust and mantle do not necessarily produce gravitational equilibrium. Gravitational equilibrium (zero isostatic anomaly) only obtains when the density contrast between the crust and mantle is the same as the value assumed for the reference (sea level) crustal column and when hydrostatic equilibrium actually exists.

To illustrate the magnitude of the effects involved, assume a normal density contrast between the crust and mantle of 0.39 g/cm³ and a standard sea level column whose thickness is 30.5 km. As under equilibrium conditions a hydrostatically supported body displaces its own mass, the submerged crustal root section

$$(R) = H_c \times \bar{\sigma}c/\sigma m$$

where H_c is the thickness of the crust, $\bar{\sigma}c$ is the mean density of the crust, and σm is the density of the mantle. As the displacement and hence surface elevation is dependent only on the relation $\Delta\sigma = (\sigma m - \bar{\sigma}c)$ and the crustal thickness (H), the actual distribution of mass within the crustal column plays no role in determining the surface elevation. If σm is assumed to be 3.30 g/cm³, $\bar{\sigma}c$ will be 2.91 g/cm³, and the sea level value for $R = 30.5 \times 2.91/3.30 = 26.9$ km.

For the free board $(F) = H_c - R = 30.5 - 26.9 = 3.6$ km and the ratio $R : F = 26.9/3.6 = 7.5$, a crustal column having a surface elevation (h) of 1000 meters would have a root increment $(\Delta R) = 7.5$ km and a total thickness

$$H = H_c + h + \Delta R = 30.5 + 1.0 + 7.5 = 39.0 \text{ km}$$

The gravitational effect of the mass increment above sea level with the elevation (h) = 1000 meters would therefore be

$$\Delta g_m = 2\pi\gamma\bar{\sigma}h = 41.85 \times 2.91 \times 1 = 122 \text{ mgal}$$

The effect of the compensation, if there were no Earth curvature and hence no distant topography and compensation effect, would be

$$\Delta_g = 2\pi\gamma\Delta\bar{\sigma}\,\Delta R = 41.85 \times 0.39 \times 7.5 = 122 \text{ mgal}$$

There would therefore be a zero free-air and isostatic anomaly.

Actually at 1000-meter elevation about 18 mgal of the compensation is incorporated in the Δg_{1-18} term; therefore only about 104 mgal of the compensation is achieved locally.

If we now assume the same elevation (h = 1000 meters) but assume that the crust has a density 0.1 g/cm³ greater than normal so that $\bar{\sigma}c = 3.01$ g/cm³, and if we assume that there is no change in σm with the flotation level relative to sea level remaining constant at −3.6 km, the new value of crustal thickness will be 52.2 km. This value was determined by substituting $(H - F)$ for R in the equation $R = H\bar{\sigma}c/\sigma m$ and solving for H with $F = 3.6 + h = 4.6$ km, $\bar{\sigma}c = 3.01$ g/cm³, and $\sigma m = 3.30$ g/cm³.

As the value of R under these conditions is 47.6 km, the crustal root increment is 20.7 km for a change of 1 km in surface elevation. This is 13.2 km greater than the value for a normal crustal column having the same surface elevation of 1000 meters. Although the mass attraction (Δg_m) for the column above sea level will not be greatly affected (+4 mgal), the value for the compensation will be significantly different. In this case $\Delta g_c = 41.85 \times 20.7 \times 0.29 = 250$ mgal as compared with 122 mgal for a column having a normal density. This difference of 128 mgal in negative attraction is offset, however, by the difference in mass attraction of the two crustal columns extending from the surface (+1000 meters) down to the depth at which there is a difference in crustal root (−38.0 km). This effect (a crustal geologic correction) is $\Delta_{g^*} = 41.85 \times 0.1 \times 38.0 = 159$ mgal. The change in gravitational effect for an increase in density of 0.1 g/cm³ is thus an increase in Δg_m of 4 mgal for the column above sea level, an increase of 128 mgal in Δg_{A-0} due to extra thick-

ness of the crust and a geologic effect below sea level of 159 mgal. As Δg_{1-18} remains the same, the net effect = +4 − 128 + 159 = +35 mgal.

It therefore is not surprising that we find areas, such as central Arkansas, where the crust has an abnormal thickness for the surface elevation characterized by positive free-air and isostatic anomalies. The actual free-air and isostatic anomaly values observed in Arkansas are +25 mgal, and the abnormality in crustal thickness is about +11 km.

Conversely, if we reduce the mean density of the crust by 0.1 g/cm³ and hold the same values of σm and h, it is found H would be 31.0 km for a surface elevation of 1000 meters. This value represents a decrease of 8.0 km relative to the normal values for H and ΔR. As the crustal column is now shorter than the standard sea level column, the change in compensation effect would be that of Δg_{A-0} for the normal column plus an anti-root effect for 0.5 km with $\Delta\sigma$ = 0.1 g/cm³, or 122 + 2 = +124 mgal. As (h) is still 1 km, there is no change in Δg_{1-18}, the compensation contribution from distant topography and its compensation. There is, however, a geologic effect due to the difference in crustal column attraction from the surface to −30 km. This value $(\Delta g_e) = 41.85 \times 0.1 \times 31 = 130$ mgal. A decrease in crustal density of $0.1g$ thus has a total gravitational effect of +124 − 130 = −6 mgal. The high plateau of Mexico is such an area inasmuch as the crust has a subnormal thickness of about 6 km for its surface elevation of 2200 meters and the area is characterized by negative free-air and isostatic gravity anomalies of about −15 to −20 mgal.

As shown by the above examples a fluctuation of ±0.1 g/cm³ in the density contrast between the crust and mantle can lead to anomaly changes of the order of +30 to −10 mgal and result in abnormalities in crustal thickness of +13 to −8 km for the same surface elevation. The question raised, therefore, if we are to seriously consider predicting gravity in unsurveyed areas, is how frequently are density changes of this magnitude encountered?

Relation of Crustal Thickness to Surface Elevation

In attacking this problem the depth of the mantle relative to sea level was plotted as a function of surface elevation as determined from seismic measurements of crustal thickness. Because the spread in values for any one elevation is large, and because it is desirable to incorporate the large number of measurements that have been made at sea, synthetic surface elevation values were derived from the sea measurements. This was done by condensing the water column to its rock equivalent and adding this value to the bottom elevation. Sea water has a density of 1.03 g/cm³; as it is desirable to have the resulting crustal column as compatible with continental structure as possible, the rock density used was the value for surficial crystalline rock (σ = 2.75 g/cm³). With these density values the conversion factor is 0.374.

The resulting plot shows a linear relation between surface elevation and the depth of the mantle which can be expressed as $H_m = -(33.2 + 7.5h)$ for positive values of h or $H_m = -(33.2 - 7.5h')$ for negative values of h'. H_m is the depth of the mantle below sea level in kilometers, h is the surface elevation in kilometers, and h' is the rock equivalent elevation in oceanic areas. The uncertainty in values based on the envelope, including 90% of the observations for a sample of about 350 measurements, is ±11 km. Although this relation has general application, it does not apply to the oceanic island arc trenches which show a reversed slope of about 3-km increase in crustal thickness per kilometer decrease in synthetic elevation. This suggests a tectonic control of such areas with a complete absence of compensation.

As an increase in density has a greater effect on crustal thickness than an equivalent decrease in density (as shown earlier), the 33.2-km sea level intercept value based on the best mean fit to the data must be regarded as a biased value if we are to assume random variations in mean crustal density. Actually any bias in density will be in the direction of negative values, as granitic rocks dominate in occurrence over basic rocks. Because we do not know the degree of bias present, a second plot was made in which the data were restricted to measurements in areas where gravity data exist and where the isostatic gravity values did not depart from zero by more than ±10 mgal. This plot likewise suggests a linear relationship between the depth of the mantle and surface elevation, which can be expressed as $H_m = -(31.5 + 7.5h)$. The

slope is therefore the same as before, but the intercept value defining the thickness of the sea level crustal column is somewhat less. It appears therefore that in general the density contrast between the crust and mantle is a constant and that a change of 1 km in surface elevation is accompanied by 7.5-km change in crustal 'root.'

The uncertainty in using this relation for predicting the depth of the mantle is ±8 km if we include 95% of the data sample with 50% of the points falling in the range of ±3.5 km. If the seismic data were 100% reliable, this degree of uncertainty would set a reliability limit of ±58 mgal in predicting gravity half the time under conditions for which it is felt there should be no significant variations in density for the crust and mantle.

Actually the seismic depth measurements only have a probable reliability of about ±10%. If we accept this degree of uncertainty in the seismic data, a spread in values of about 8 km is to be expected on the continents in the depth to the mantle for a given surface elevation. Therefore half the observed uncertainty in values can be automatically discounted as having physical significance. The remainder presumably does have significance but, as three parameters (crustal thickness, elevation, and isostatic gravity values) are involved and the isostatic gravity values could be biased by a surface geologic effect canceling a crustal geologic effect, it is impossible to define the actual significance of the remaining deviations from the mean relation described by the equation $H_m = -(31.5 + 7.5h)$. Because it is reasonable to assume that the other effects incorporated in the data result in random errors, the general relationship expressed by the equation should be a valid one.

Determination of Density Contrast between the Crust and Mantle

The observed change of 7.5 km in crustal thickness for a change of 1000 meters in surface elevation provides a realistic basis for determining the density contrast between the crust and mantle. As we are also fortunate in having laboratory studies of the relation between rock density values and seismic velocity values, actual values for the mean density of the crust and the mantle can be determined. A first consideration is recognition that a constant free board-to-root ratio, as 1: 7.5, does not imply a specific density contrast between the crust and mantle. This can be shown as follows. If $F/R = 1/7.5$, then $H = 1 + 7.5 = 8.5$, $F = H/8.5$, and $R = 7.5H/8.5$. Also $R = H\bar{\sigma}c/\sigma m$. If we equate these two terms for R, we find $\bar{\sigma}c = 7.5\ \sigma m/8.5$. Therefore as $\bar{\sigma}c$ only changes at a rate equal to 7.5/8.5, the rate at which σm changes, the value $(\sigma m - \bar{\sigma}c)$ will not be a constant.

Possible values of crustal and mantle density that would maintain a free-board-to-root ratio of 1:75 are as follows:

Group 1

$\bar{\sigma}c$	2.84	2.85	2.86	2.87	2.875	g/cm³
σm	3.22	3.23	3.24	3.25	3.26	g/cm³

$\Delta\sigma = (\sigma m - \bar{\sigma}c) = 0.38$ g/cm³

Group 2

$\bar{\sigma}c$	2.88	2.89	2.90	2.91	2.92	2.93	2.94	2.945	g/cm³
σm	3.27	3.28	3.29	3.30	3.31	3.32	3.33	3.34	g/cm³

$\Delta\sigma = (\sigma m - \bar{\sigma}c) = 0.39$ g/cm³

If the mantle has a density in excess of 3.35 g/cm³, the density contrast required would be 0.40 g/cm³.

The density of the mantle has been estimated on geologic considerations to have values ranging from 3.22 to 3.40 mgal. This degree of uncertainty, as regards the density of the mantle, gives an uncertainty of 6 mgal per 1000-meter change in elevation in computing the compensation. This potential degree of error in predicting gravity therefore is not one that can be dismissed as negligible.

In an effort to determine the probable correct density contrast, a study was made of laboratory-determined values of seismic compressional wave velocities for various rocks at confining pressures of 1000 bars (equivalent to the 3-km depth at which a change in seismic velocity is usually obtained) and higher pressures. These values were then related to the observed density values. Table 7 lists the average velocity and density values for the common rock types. As seen there is a significant change in velocity values in going from near surface conditions (10-bar pressure) to 1000-bar pressure. This change is due to the change in compressibility with pressure on the modulus of rigidity. At pressures greater than 1000 bars the change in velocity is relatively small and constant velocity conditions are approximated. Although the effect of increasing pressure on density is not known precisely, it must be small because holocrystalline rocks generally have a porosity of less than 2%.

If plots are made of velocity values as a function of confining pressure, it is found that only jadeite and dunite have projected velocity values in the range 8.0–8.3 km/sec at pressures corresponding to the depth of the mantle on the continent (10,000 bars) and in the oceans (4000 bars). Actually jadeite is eliminated because its projected velocity value is too high. Dunite thus appears to be the probable material comprising the upper mantle. If we assume an essentially pure olivine composition, the density of the mantle is probably about 3.31 g/cm^3 which would define the density contrast with the crust as 0.39 g/cm^3 for $F/R = 1/7.5$ and the mean density of the crust as 2.92 g/cm^3. Actually as shown earlier the density of the mantle could be as high as 3.34 g/cm^3 or as low as 3.27 g/cm^3 without requiring a change in the value of 0.39 g/cm^3 for the density contrast. The actual mantle density value assumed therefore is not critical.

Evaluation of Regional Isostatic Conditions

With the density contrast between the crust and mantle established on what appears to be a reliable basis, it is now possible to test the reality of isostatic compensation. The procedure adopted is based on the following assumptions:

1. Crustal columns 2° by 2° in cross section are in hydrostatic equilibrium with the mantle.
2. Changes in local topography and geology in an area of 2°-by-2° size are so much smaller in areal extent that on the average the gravitational effects of surficial positive and negative variations in mass effectively cancel each other.
3. As the width of crustal blocks having a given elevation decreases, the observed change in mean-free-air anomaly values with elevation for areas 2° by 2° is related for the most part to the increase in the dominance of the crustal topographic effect over the compensation effect.
4. The mean surface elevation of each 2°-by-2° block is governed by a density contrast of 0.39 g/cm^3 between the crust and mantle and the respective values of crustal and mantle density that will give a free board-to-root ratio 1:7.5.
5. Up to 1800-meter elevation free-air anom-

TABLE 7. Average Density and Seismic Velocity (Vp) Values for Holocrystalline Rocks

	Density, g/cm^3	Velocity		
		10 bars km/sec	1000 bars km/sec	4000 bars km/sec
Crustal Rocks				
Granite	2.651	5.0	6.12	6.36
Metasediments	2.747	5.15	6.06	6.27
Intermediate Rocks	2.750	5.76	6.52	6.63
Basic Rocks	2.987	6.41	6.79	6.91
Mantle Rocks				
Ultrabasics	3.241	7.14	7.73	7.85
Dunite	3.308	7.70	8.09	8.20
Eclogite	3.370	6.86	7.51	7.64

alies are the equivalent of isostatic anomalies. This last premise is based on the following considerations: (*a*) the Bouguer anomaly (BA) can be written

$$BA = FA - (\Delta g_m - \Delta g_t + \Delta g_c)$$

where FA is the free-air anomaly and the other terms are as identified earlier, and (*b*) the isostatic anomaly (IA) can be written

$$IA = BA + (\Delta g_{A-0} + \Delta g_{1-18})$$

$$BA = IA - (\Delta g_{A-0} + \Delta g_{1-18})$$

Therefore

$$FA - (\Delta g_m - \Delta g_t + \Delta g_c) = IA - (\Delta g_{A-0} + \Delta g_{1-18})$$

It follows that FA = IA where $(\Delta g_m - \Delta g_t + \Delta g_c) = (\Delta_{A-0} + \Delta g_{1-18})$.

Therefore one test of isostatic conditions is to plot observed free-air anomalies as a function of isostatic anomaly values. Such a plot was made for station data taken in the United States by the U. S. Coast and Geodetic Survey and restricted to areas of low topographic relief in order to eliminate the secondary topographic effect. Furthermore the isostatic anomaly values were selected on the basis of that depth of Pratt-Hayford compensation that yielded a minimum anomaly value in order to incorporate the effect of changes in crustal thickness with surface elevation. The resulting plot showed a 45° distribution of values whose mean value is described by the equation FA = IA + 6.

Although the source of the 6-mgal positive intercept is not definitely known, it is probably related to the size of the North American continental block. The important consideration, however, is that, on a continent-wide basis for a regional distribution of data, mean free-air anomaly values are equivalent to mean isostatic anomaly values and therefore $(\Delta g_m - \Delta g_t + \Delta g_c) = (\Delta_{A-0} + \Delta g_{1-18})$.

We can test this conclusion on a more systematic basis by dividing the country into 2°-by-2° blocks and comparing the computed gravitational effect $(\Delta g_\cdot = \Delta g_{A-0} + \Delta g_{1-18})$ for the theoretical root for the regional change in elevation, using $F/R = 1/7.5$, with the difference between observed mean Bouguer and free-air anomalies (equivalent to $\Delta g_m - \Delta g_t + \Delta g_c$) on a 2°-by-2° basis.

To obtain input values for this test, mean 2°-by-2° values of free-air anomaly and simple Bouguer anomaly values, as derived from anomaly maps, were plotted as a function of elevation. These values for increments of 500-meter change in regional elevation are listed in Table 8. As the Bouguer values had been originally computed on the basis of a density of 2.67 g/cm,[3] it was necessary to correct the anomaly values to a density of 2.92 g/cm[3] to have values compatible with the observed free board-to-root ratio of 1:7.5 and to have a crust-mantle density contrast of 0.39 g/cm.[3]

As the simple Bouguer anomaly does not include the effect of Δg_t and Δg_c in the total mass effect $(\Delta g_m - \Delta g_t + \Delta g_c)$, it is not surprising that there are 7-mgal departures in values at elevations above 2500 meters when we compare the theoretical root effect $(\Delta g_\cdot = \Delta g_{A-0} + \Delta g_{1-18})$ with observed values for BA − FA as being equal to the topographic mass effect that is actually compensated.

The data of Table 8 therefore not only demonstrate the reality of isostasy for the observed crustal structure on a 2°-by-2° basis for the United States as a whole but also suggest that we can predict gravity on the assumption of hydrostatic equilibrium with a reliability approaching 5 mgal on a regional (2°-by-2°) basis up to 3000-meter elevation if a systematic relationship can be established between mean free-air anomaly values and mean values of surface elevation. The data examined for the United States suggest that the relationship is not fixed but varies as follows:

1. The coastal (continental boundary) relation that applies from sea level to 250 meters is FA = $60h$ + 13 mgal where h is in kilometers.
2. The continental platform relation that applies from 250 meters to 1800 meters is FA = $+7.8h$ − 3 mgal.
3. The highland relation that applies from 1800 meters to 3000 meters is FA = $+38h$ − 58 mgal.

It is to be noted, however, that for any given elevation the free-air anomaly values described by the above equations only have a reliability of ±20 mgal on a 95% sample basis or ±8 mgal on a 50% basis.

If we use the above regional elevation relations as a basis for predicting local free-air

anomaly values, the effect of superimposed local changes in topography must be added to the above regional relations. It is to be noted though that the change in relations indicated at 1800 meters may be peculiar to the United States. This change is not governed by elevation but rather by the areal extent of the topographic block. The critical size appears to be 12° by 12°. Using the above equations, the effect of local changes in elevation can be added by means of the expression $\Delta FA = 99h$ mgal where h is in kilometers. This is an empirical relation, which, if we assume an average density of 2.67 g/cm³ for normal surficial material, incorporates a terrain correction of 13 mgal per 1000 meters for local relief on the assumption the compensation effect is negligible.

The Geologic Effects

If it is assumed that the two equations relating free-air anomalies to elevation apply to normal conditions, it should be possible to make suitable corrections for abnormalities in mean crustal or mantle density and to allow for surficial geologic effects. To make such corrections it is necessary to have data from seismic measurements concerning the crust and mantle and to know how regional changes in geology affect the gravity field.

As indicated earlier, regions that are characterized by a subnormal value of crustal thickness for the surface elevation are usually characterized by negative free-air and isostatic anomalies. Regions that have an abnormal value of crustal thickness for the surface elevation are characterized usually by positive free-air and isostatic anomalies. Normal values, as defined earlier from seismic data, are areas where the change in crustal root increment with elevation corresponds to a free board-to-root ratio of 1:7.5.

On the basis of the computations made earlier for the change in crustal root and gravitational effect to be expected for a change of 0.1 g/cm³ in mean crustal density, an abnormality of 1 km in crustal root has a gravity effect of +2.4 mgal when the value of ΔR is positive and −0.8 mgal when the ΔR value is negative. In an effort to check these theoretical values against observed values, normal values of mantle depth were computed using the equation $H_m = -(31.5 + 7.5h)$ and average elevation values for all areas where seismic crustal measurements had been made and where there were gravity data. The difference between the theoretical and actual depths of the mantle was then plotted with regard to sign against the isostatic anomaly value for each area. The resulting plot defined two distinct cross-cutting distributions of data. Both had a slope of 3 mgal per km of abnormal root with a negative intercept of −10 mgal for zero abnormality in the depth of the mantle.

The relation ($IA = 3\Delta R' - 10$) is to be expected for changes in crustal density under equilibrium conditions whereby any change in mean crustal density results in a similar change in crustal root increment and gravity attraction. The other relation ($IA = -3\Delta R' - 10$), which applies to a third of the data, is opposite in sign, although it has the same slope and intercept value. It is the type of relation to be expected where there is a lack of hydrostatic

TABLE 8. Comparison of Theoretical with Observed Gravity Effects for Regional Changes in Elevation

Elevation, m	ΔR (1:7.5)	Theoretical Δg^* $\Delta\sigma 0.39$	Theoretical Δg_m ($\sigma 2.92$)	Observed BA $\sigma 2.67$	Correction to $\sigma 2.92$	Corrected BA	Observed FA	BA-FA	BA-FA versus Theoretical Δg^*
0	0	0	0	+13	0	+13	+13	0	0
500	3.75	61	61	−59	−5	−64	+1	−65	+4
1000	7.5	122	122	−108	−10	−118	+5	−123	−1
1500	11.25	184	184	−158	−16	−174	+9	−183	−1
2000	15.0	244	244	−207	−21	−228	+17	−245	+1
2500	18.75	306	306	−250	−26	−276	+36	−312	+6
3000	22.5	367	367	−287	−31	−318	+56	−374	+7

equilibrium between the crust and mantle and where a change in crustal parameters produces a gravity effect of opposite sign.

When the data are examined as to what areas appear to be actually out of hydrostatic equilibrium as indicated by isostatic anomalies of over 10 mgal and having an opposite sign to that of the abnormality in crustal thickness, it is found that this condition characterizes parts of the United States west of the Rocky Mountains; the southern Appalachian Mountains; western Europe; Cook Inlet, Alaska; New Zealand; Hawaii; South Africa; Japan; and the oceanic trenches.

Areas that appear to be characterized by abnormalities in crustal density but that are presumably in hydrostatic equilibrium as indicated by isostatic anomalies having the same sign as that of the abnormality in crustal thickness are: most of the area east of the Rocky Mountains, the Colorado Plateau, the shield area of Canada, the plateau of Mexico, Alaska, and the Alps in Europe.

Although there appear to be no fixed surface criteria for recognizing areas of abnormal crustal density such as characterize most of the United States and Canada, it does appear that subsurface data and regional crustal thickness values derived from the phase velocity dispersion of earthquake surface waves can be used to define abnormalities in the depth of the mantle for regional changes in surface elevation. This information in association with knowledge of geological provinces provides a basis for deciding whether the abnormality in crustal thickness is related to a lack of true isostatic equilibrium or to an abnormality in crustal density. This decision, in itself, would eliminate a potential 60-mgal discrepancy, for example, in interpreting the gravity effect of an abnormal thickness of 10 km in the depth of the mantle. Recognition of crustal relations to geology therefore constitutes a key parameter in any prediction scheme. On the basis of available data the following relations appear to have general application.

Areas characterized by abnormalities in crustal density:

Areas of eustatic uplift (plateaus).

Ancient shield areas in general having a low surface elevation.

Folded mountain ranges.

Areas apparently out of hydrostatic equilibrium:

Intermountain basins and uplifts.

Areas of recent volcanism.

Areas of tectonic displacement (horsts and graben, island arcs, and trenches).

Inasmuch as volcanism, tectonic displacement, and eustatic uplift represent superimposed secondary events, relations in such areas are in one sense more complex and in another sense simpler than those associated with shield areas. They are simpler in that there is a direct logical relationship of gravity to causal mechanism and a resulting change in surface mass distribution. In the shields there is an inverse, and therefore illogical, relationship. Areas of uplift are marked by a deficiency in gravity, and basins filled with low density sediments, where we could expect to find a deficiency in gravity, are marked by positive gravity values. The Williston Basin in North Dakota, for example, which has a depth of about 5000 meters and which on a most conservative basis should be marked by isostatic gravity anomalies of about -30 mgal, is actually marked by positive isostatic anomalies of about $+20$ mgal. In this area not only does the crust have an abnormal root of about 14 km for the surface elevation, but there is underlying layering in the upper mantle that also contributes to the gravity field. As the empirical relationship between crustal thickness abnormality and isostatic anomalies ($IA = 3\Delta R' - 10$) in this case would suggest that the crustal density effect is canceled by the surface geologic effect, the observed anomaly presumably originates from the mantle. Similar relations are observed for the Illinois Basin, the Denver Basin, the Gulf Coast Embayment, and other basins. The interbasin divides in the shield area are either marked by near zero isostatic anomalies or negative isostatic anomalies. On a major scale, this broad inverse relationship of isostatic anomaly values to the surface elevation of the crystalline rock complex is well exemplified by the relations found between the Canadian Rocky Mountains in Alberta and the Tacconic Mountains in Maine. The crystalline rock complex (shield) is exposed at the surface from Maine to Manitoba and is buried beneath the Saskatchewan Basin from this point to the Rocky

Mountain front. On the basis of the surficial mass distribution we would expect near zero isostatic anomalies over the eastern area of exposed crystalline rocks and negative isostatic anomalies over the basin area. Actually the relations are the reverse. The shield area is characterized by isostatic anomaly values that average about −20 mgal; the basin area, by values that average about +20 mgal. Superimposed on these regional relations are local changes of ±15 to 20 mgal due to changes in basement rock type.

In areas such as the above we could be as much as 50 mgal in error in predicting regional gravity relations if cognizance is not taken of this association of basins with apparent areas of crustal sag due to regional increases in crustal density or, conversely, decreases in mantle density. As the controlling mechanism could produce simultaneously crustal uplift in one area and crustal subsidence in an adjacent area, the sign of the gravity change is both plus and minus. For example, the geologic stratigraphic evidence suggests simultaneous crustal upwarp and downwarp in the Great Lakes region where it appears that, as the Wisconsin uplift was formed over a period of about 400 m.y., the adjacent Illinois and Michigan basins were also formed. The Wisconsin uplift of exposed crystalline rocks is characterized by negative isostatic anomalies (−30 mgal) and the Illinois Basin by positive anomalies (+12 mgal). As the surficial geologic effect for the sediments in the Illinois Basin is about −20 mgal, the crustal effect is +32 mgal. The adjacent Missouri uplift is likewise characterized by −30-mgal isostatic and free-air anomalies, even though crystalline rocks are not exposed at the surface.

On the basis of the above relations we could arbitrarily assign a crustal effect of +25 mgal to all basins and −25 mgal to all uplifts in the shield area to which we could add a correction for the included sediments in the basins. Although the correction would not deviate significantly from a constant for most basins, the Gulf Coast geosyncline, which has a depth of about 12 km, would show a significant departure. Relations in this basin are controlled by the density of the mantle, as seismic measurements indicate a near normal value of crustal thickness for the surface elevation. As the observed isostatic anomaly values average about +5 mgal and a conservative estimate of the surficial geologic effect is about −80 mgal, the crustal effect must be at least +85 mgal and may well be as high as +100 mgal. It appears therefore that this major sag in the crust developed from a different mechanism than indicated elsewhere in the midcontinent area. The relations suggest attrition of the original crust by mantle assimilation. This conclusion is based on the fact that the over-all crustal column thickness is compatible with the surface elevation despite the obvious addition of about 12 km of sediments. Elsewhere, as in Cook Inlet, Alaska, such a thick sedimentary column is attended by isostatic anomalies of the order of −120 mgal with no evidence of crustal attrition.

When the data for plateaus are examined, it is found that they are characterized by negative isostatic anomaly values of about −15 to −20 mgal, which the available seismic data suggest are related to a subnormal thickness of the crust and greater than normal density contrast between the crust and mantle. However, as noted in the Basin and Range area of the United States the subnormal values of crustal thickness are in some places associated with positive anomaly values, which is indicative of a lack of isostatic equilibrium. A contributing factor here is an as yet unknown phenomenon, which could be related to Tertiary volcanism, that has resulted in the mantle having a subnormal velocity. As this implies that the mantle here has a subnormal density, a decrease in density contrast between the crust and mantle should result. Under hydrostatic equilibrium conditions a thin crust would sink to a lower than normal surface elevation. However, this condition is not observed, and we can only conclude that the crust is also influenced by whatever phenomenon is affecting the mantle and that in addition there are physical forces that are maintaining the surface at an artificial elevation. Therefore in this part of the United States (the area lying between the west flank of the Sierra Nevada in California and the Wasatch Range in Utah) values of crustal thickness and surface elevation are not true indicators of abnormality in gravity.

The gravity effect associated with intermountain basins, graben, horsts, and some uplift areas, such as the Black Hills in South Dakota and the Wichita-Arbuckle Mountains

in Oklahoma, is generally a direct expression of the surficial mass anomaly. Basins in association with ancient mountain systems, such as the Appalachian Basin, appear to have no gravity expression. In such areas the anomalous gravity field is mainly related to local variations in crustal density which for the most part can only be anticipated where the crystalline rock complex is exposed. Granite areas, for example, appear as pronounced gravity minimums, so that even a local body is indicated by a gravity deficiency of −10 to 20 mgal. Large granite masses, such as the Idaho batholith, are marked by an isostatic deficiency of −20 mgal. On a relative basis the Idaho batholith is 60 mgal lower than the adjacent areas which are characterized by +40-mgal isostatic values. Similar relations are observed in the Atlantic Piedmont province, where granites appear as pronounced minimums along the crest of a positive anomaly high of +35 mgal which extends from New England to Alabama.

From the above observed relations between gravity values and geology it is evident that the greatest potential source of error in correcting for local geologic effects lies in the reverse effect associated with basins and uplifts depending on the geologic province in which they occur. Another problem of similar nature is the changes in gravity relations associated with the same geologic feature. The Rocky Mountains and Appalachian Mountains for example change along strike as follows:

IA Values in mgal

Rocky Mountain System		Appalachian Mountain System	
Alberta, Canada	−15	Maine	+15
Idaho	−15	New Hampshire	+15
Montana	−10	New York	−10
Wyoming	+15	Pennsylvania	−10
Colorado	+10	West Virginia	−15
North New Mexico	−5	North Carolina	−20
South New Mexico	−5	Alabama	−30

Part of the above change in values can be related to the systematic change observed in free-air anomaly values with elevation. Part can be related to differences in geologic age along the strike with the older segments being more positive than the younger, presumably because of a higher degree of metamorphism developed in successive periods of orogeny. Part reflects differences in basic crustal composition and the presence of intrusions commonly associated with mountain building. In the case of the Appalachians there is an additional effect at the southern end due to the crustal subsidence associated with the Gulf Coast dragging down the enfolded crustal mountain root to create a mass deficiency that is out of isostatic equilibrium.

Conclusion Regarding the Prediction of Gravity in Unsurveyed Areas

The procedure adopted for predicting gravity in unsurveyed areas on the basis of the various factors discussed is as follows:

1. Determine elevations for 2°-by-2° squares on a 1° interval in order to obtain 1° overlap on each 2°-by-2° area.

2. Using the relation FA = $60h$ + 13 mgal for elevations below 250 meters near the coast; FA = $7.8h$ − 3 mgal for elevations above 250 meters, where the topographic black exceeds 12° by 12°; and FA = $38h$ − 58 mgal otherwise, determine regional free-air anomaly values on the assumption there are no abnormalities in crustal density.

3. Divide the area into segments representing the following types of geologic provinces having average correction factors as follows:

(*a*) folded mountain ranges	
Mezozoic age or younger	−10 mgal
Paleozoic age or older	0
(*b*) plateau areas of eustatic uplift	−15 mgal
(*c*) shield areas or covered shield areas	
superimposed uplifts	−30 mgal
superimposed basins	+20 mgal
(*d*) areas of Tertiary volcanism	−10 mgal
(*e*) major intermountain tectonic structures	
graben or other steep walled basins	−40 mgal
horsts or intermountain uplift	+30 mgal
(*f*) granitic batholiths	−50 mgal
(*g*) areas of geosynclinal sedimentation	−15 mgal
(*h*) areas of geosyncline trapped basalt	+40 mgal
(*i*) major graben not in mountains	−100 mgal

(*j*) major horsts not in mountains +40 mgal
(*k*) minor horsts and grabens, granites, etc. ±20 mgal

The above applied as smoothly varying corrections from one geologic province and feature to another should incorporate to a first approximation the effects related to subsurface geological changes in the crust and the changes associated with the near surface mass distribution. The occurrence of other changes that have no surficial expression will remain a source of potential error. If seismic, magnetic, or well data are available, of course, more exact corrections can be applied.

5. Compute local mass variations using the equation $\Delta g = 99h(\text{km})$ for changes in topography above or below the regional 2°-by-2° level. No correction for subsurface geology, however, should be included as these are incorporated in item 4.

The predicted free-air anomaly value will be the sum of the following: $\Delta F_H + \Delta F_G + \Delta F_g + \Delta F_h$, where ΔF_H is the regional elevation effect, ΔF_G is the geological province effect, ΔF_g is the effect of the local superimposed geology, and ΔF_h is the effect of the local superimposed topography. It is of course obvious that the prediction could have been based equally well on Bouguer anomaly values, as the only change involved is that for a constant times the mean elevation value. If we had adequate seismic information to evaluate ΔF_G more correctly, Bouguer anomalies would be an essential part of the correction computation.

Tests of the above procedure in predicting values of free-air anomalies for 1°-by-1° areas in the United States show the following degree of reliability.

Error, mgal	Cases + Error	− Error	Σ	%	Σ%
0 to ±1		48	48	8	8
2 to 4	68	55	123	21	29
5 to 7	70	48	118	20	49
8 to 10	43	30	73	12	61
11 to 13	44	34	78	13	74
14 to 16	30	24	54	9	83
17 to 19	27	10	37	6	89
20 to 22	12	2	14	2	91
22 to 25	12	8	20	3	94
>25	28	8	36	6	100
Σ	334	219	601	100	

As seen from the above test data, a reliability of better than ±8 mgal was obtained 50% of the time, and better than ±20 mgal 90% of the time. This indicates an average reliability of about ±10 mgal was obtained 90% of the time. This test is of course biased to some extent in that the prediction factors were derived from United States data and then used to predict values in the United States. It was to avoid a direct recycle of values that the prediction was made for 1°-by-1° areas.

The degree to which the prediction criteria will apply to detailed changes in gravity field, however, will not be any better than that indicated in the section on prediction reliability in local areas having some gravity control. As the size of area decreases to that of a point, the reliability will decrease and, without local control located so as to represent the effect of each subsurface mass contribution to the gravity field, it may not be possible to achieve better than ±20-mgal reliability as this is the average magnitude of the ΔF_g term for changes in local geology.

External Gravity Field of the Earth

Reporter: Ivan I. Mueller[1]

Introduction

One of the unsurveyed areas of the gravity field of the Earth is the space above. In the last decade the advances in rocket and artificial satellite techniques made it imperative to devise practical methods for the solution of two main problems: (1) calculation of the gravity vector at a certain elevation in space from data observed on the ground; (2) calculation of the gravity vector on the ground or on some reference surface from data observed in space.

The first problem has great significance in missile trajectory computations, in determining the gravitational perturbations of satellite orbits, in connection with inertial guidance systems, etc. The solution of the second problem is important in the utilization of airborne or satellite-borne gravity or gravity gradient observations.

The computational methods published in the past generally split the gravity potential W into the potential of the normal gravity U and the disturbing potential T in such way that at any point

$$W = U + T \tag{1}$$

Similarly, the gravity vector

$$\mathbf{g} = \text{grad } W \tag{2}$$

is also divided into two parts, the normal gravity vector

$$\boldsymbol{\gamma} = \text{grad } U \tag{3}$$

and the gravity disturbance vector

$$\boldsymbol{\delta g} = \text{grad } T = \mathbf{g} - \boldsymbol{\gamma} \tag{4}$$

The determination of the gravity vector (potential) at any point thus consists of calculating the normal gravity vector (potential) and adding the gravity disturbance vector (potential), both referred to the same point, according to equation 1 and to

$$\mathbf{g} = \boldsymbol{\gamma} + \boldsymbol{\delta g} \tag{5}$$

In certain applications gravity anomalies are used instead of gravity disturbances. The gravity anomaly Δg and the gravity disturbance are related in the principal equation of gravimetric geodesy as follows:

$$\Delta g = \delta g - (2\gamma/R)N = g - \gamma_0 \tag{6}$$

where R is the mean radius of the Earth (6371

[1] Department of Geodetic Science, Ohio State University, Columbus.

km) and

$$N = T/\gamma \qquad (7)$$

is the separation of the geop and the spherop possessing numerically the same potential constant (to which g and γ_0 refer, respectively).

In other applications the gravitation, rather than gravity, is needed. The gravitation may be easily obtained from the gravity by removing the effect of the centrifugal acceleration (the potential or its gradient).

Computation of the Normal Gravity Field

The normal gravity field of the Earth is either defined as the external gravity field of a level ellipsoid approximating the Earth or as a function consisting of the first few terms of some series development (e.g., spherical harmonics) of the spheropotential.

In the first case one approach is based on formulas derived for a homogeneous ellipsoid in equilibrium [*Pizzetti*, 1894; *Lambert*, 1961]. The equilibrium condition, however, relates the flattening of the ellipsoid, its rotational velocity, and its density in a certain condition. If in this relation the actual flattening and rotational velocity of the Earth are used, the resulting density becomes about 50% higher than the mean density of the Earth; i.e., the mass of the Earth is increased. To correct this situation a negative 'coating' is applied to reduce the mass to the desired value. The gravity field of this coated homogeneous level ellipsoid is taken as the normal gravity field of the Earth.

Another approach resulting in the same formulas is based on the theorem of Stokes, which states that a rotating body with its mass and rotational speed defines the potential outside and on the surface independently of mass distribution, provided that there are no masses outside the surface in question. If the rotating body is defined as a rotational level ellipsoid of given flattening, mass, and rotational velocity, the result is the normal gravity potential [*Hirvonen*, 1960; *Heiskanen and Moritz*, 1966].

To obtain convenient closed formulas in these calculations it is practical to use special curvilinear coordinates, whose coordinate surfaces are a family of confocal ellipsoids of revolution and a family of unparted hyperboloids of revolution having the same foci and forming an orthogonal system (ellipsoidal coordinates). The closed formulas may then be developed into a series and transformed to more convenient spherical coordinates. This approach may be found in *Cohen* [1957], *Cook* [1959], *Hirvonen* [1960], *Lambert* [1961], *Molodenskii* [1945], and *Somigliana* [1929].

The same equations may be obtained also from the second case mentioned above, i.e., from the spherical harmonic development of the spheropotential, in which there are no longitude-dependent terms and also the zonal harmonics above a certain degree (e.g., above $n = 3$) are neglected [*Heiskanen and Moritz*, 1966].

In both cases equations are provided for the spheropotential function U, and for the components of the normal gravitation or of the normal gravity in the directions of the coordinate lines specified by the curvilinear system used (ellipsoidal or spherical). To transform these into the usual system of Cartesian coordinates (axes x, y, x toward $\lambda = 0°$, $\lambda = 90°$E, and the rotation axis of ellipsoid, respectively) is a matter of a simple matrix multiplication.

Other investigations along these lines may be found in *Caputo* [1963, 1964], *Helmert* [1884], *Jung* [1956], *Lambert* [1951, 1957*a*, *b*, 1960], and *Vening Meinesz* [1959]. A numerical comparison of the different methods is given by *Daugherty and Define* [1963]. The normal gravity field of a triaxial ellipsoid is treated by *Caputo* [1965], *Wagner* [1962], and *Zagrebin* [1956].

Computation of Gravity Disturbances

Direct integration method. In this method the disturbing potential is calculated by integrating the free-air anomalies on the surface of the Earth using the generalized formula of Pizzetti:

$$T = \frac{R}{4\pi} \iint_{\sigma} S(r, \psi) \Delta g \, d\sigma \qquad (8)$$

where $S(r, \psi)$ is the generalized Stokes function; R the mean radius of the Earth; r the radius vector to the point related to the quantity T; ψ the angular distance between the points related to the quantities T and Δg, respectively; Δg the free-air anomaly, and $d\delta$ the surface element of the unit sphere.

The components of the gravitational disturbance are obtained most conveniently in the

directions of the spherical coordinates, r (radius vector), φ' (geocentric latitude), and λ (longitude), as follows:

$$\begin{aligned}
\delta g_r &= \frac{\partial T}{\partial r} \\
&= \frac{R}{4\pi} \iint_\sigma \frac{\partial S(r, \psi)}{\partial r} \Delta g_\sigma \, d\sigma \\
\delta g_{\varphi'} &= \frac{1}{r} \frac{\partial T}{\partial \varphi'} \\
&= -\frac{R}{4\pi r} \iint_\sigma \frac{\partial S(r, \psi)}{\partial \psi} \Delta g_\sigma \cos \alpha \, d\sigma \\
\delta g_\lambda &= \frac{1}{r \cos \varphi'} \frac{\partial T}{\partial \lambda} \\
&= -\frac{R}{4\pi r} \iint_\sigma \frac{\partial S(r, \psi)}{\partial \psi} \Delta g_\sigma \sin \alpha \, d\sigma
\end{aligned} \tag{9}$$

where α is the azimuth between the points to which Δg_σ and T refer.

This approach is followed by *Hirvonen* [1952, 1960] and by *Hirvonen and Moritz* [1963].

Coating method. This method is based on the fact that the disturbing masses can be replaced by a surface layer (coating) on the ellipsoid without changing the external potential. A rigorous solution may be obtained only when there are no masses outside the geoid. The method was first proposed probably by *Helmert* [1884] and applied by *Orlin* [1959], *Hirvonen* [1960], *Hirvonen and Moritz* [1963], and *Heiskanen and Moritz* [1966]. The disturbing potential is calculated from

$$T = \frac{R^2}{2\pi} \iint_\sigma \frac{\mu}{d} \, d\sigma \tag{10}$$

where

$$\begin{aligned}
d &= \sqrt{r^2 + R^2 - 2Rr \cos \psi} \\
\mu &= \Delta g_\sigma + (3\gamma/2R)N
\end{aligned} \tag{11}$$

is the density of the coating (γ is the normal gravity at sea level and N the geoid undulation computed from free-air anomalies).

The derivatives of the disturbing potential are the gravity disturbance components, which in the spherical coordinate system are

$$\begin{aligned}
\delta g_r &= -\frac{R^2}{2\pi} \iint_\sigma \mu \frac{r - R \cos \psi}{d^3} \, d\sigma \\
\delta g_{\varphi'} &= \frac{R^2}{2\pi r} \iint_\sigma \mu \frac{Rr}{d^3} \sin \psi \cos \alpha \, d\sigma \\
\delta g_\lambda &= \frac{R^2}{2\pi r} \iint_\sigma \mu \frac{Rr}{d^3} \sin \psi \sin \alpha \, d\sigma
\end{aligned} \tag{12}$$

It should be noted that this method can be applied only when the geoid undulations are known in addition to the free-air anomalies.

Continuation method. This method is based on Poisson's integral for the sphere, which applied to the harmonic disturbing potential function is

$$T = \frac{R(r^2 - R^2)}{4\pi} \iint_\sigma \frac{T_\sigma}{d^3} \, d\sigma \tag{13}$$

where the disturbing potential T_σ is on the surface and T at some fixed exterior point. T is considered as the 'continuation' of T_σ and thus is the name of the method.

The partial derivatives of T are also harmonic if they are taken in a Cartesian coordinate system; thus the same equation may also hold for the gravitational disturbance components. Using a local Cartesian coordinate system in which the axis u points to the north, v to the east, and w coincides with the vertical of the fixed point, and approximating the integration on the sphere by an integration over the tangent plane uv, the following relations are obtained:

$$\begin{aligned}
\delta g_u &= \frac{H}{2\pi} \iint_{-\infty}^{+\infty} \frac{\delta g_{u,\sigma}}{d^3} \, du \, dv \\
\delta g_v &= \frac{H}{2\pi} \iint_{-\infty}^{+\infty} \frac{\delta g_{v,\sigma}}{d^3} \, du \, dv \\
\delta g_w &= \frac{H}{2\pi} \iint_{-\infty}^{+\infty} \frac{\delta g_{w,\sigma}}{d^3} \, du \, dv
\end{aligned} \tag{14}$$

where H is the elevation of the fixed point above the sphere. The disturbance components on the surface, required in the equations above, may be calculated as follows:

$$\begin{aligned}
\delta g_{u,\sigma} &= g_\sigma \xi_\sigma \\
\delta g_{v,\sigma} &= g_\sigma \eta_\sigma \\
\delta g_{w,\sigma} &= \Delta g_\sigma + (2\gamma/R)N
\end{aligned} \tag{15}$$

where g_σ is the gravity, and ξ_σ and η_σ are the deflection of the vertical components, all on the surface. The plane approximation is sufficient

except for very high altitudes (>150 miles), in which case a spherical formula similar to (13) should be used.

It should be noted that this method, described by *Hirvonen and Moritz* [1963], can be applied only if the free-air gravity anomalies and geoid undulations (for the vertical component) and the deflections of the vertical (for the horizontal components) are available. The undulations and the deflections should be computed from free-air anomalies, using the formulas of Stokes and Vening Meinesz. In the first two equations in (15) normal gravity may be substituted for the gravity.

Other methods. The disturbing potential and its derivatives may also be calculated by means of spherical harmonic developments, whose coefficients are obtained by analysis of gravity anomalies or (and) satellite perturbations. Owing to the slow convergence of these series, this method is restricted to high altitudes (>600 miles).

Other methods of calculating the gravity above the Earth from surface data using various series expansions are also available. See, for example, *Tengström* [1959] and *Tsuboi* [1959, 1961].

Computation of Gravity Anomalies

Gravity disturbance components can be calculated only for points whose exact metric coordinates in space are known. In other circumstances, such as when the position is defined by gravimetric coordinates (astrolatitude, longitude, and (or) geopotential number), gravity anomalies have greater significance. This is true, for instance, when airborne gravity observations need to be reduced to a reference surface or compared with data obtained on the ground and extrapolated to the level of the airplane.

The computations may be performed by using an equation like (14), substituting free-air gravity anomaly for the gravity disturbance:

$$\Delta g = g - \gamma_0 = \frac{H}{2\pi} \iint_{-\infty}^{+\infty} \frac{\Delta g_e}{d^3}\, du\, dv \qquad (16)$$

where g is the gravity at a fixed point in space on a geop, γ_0 is the normal gravity on the same plumbline but at the spherop having numerically the same potential as the geop. The method is used by *Hirvonen* [1952].

Undulations and Deflections

Once the disturbing potential and the gravitational disturbances have been calculated at any point, the undulation of the geop N (the distance between a geop and the spherop having numerically the same potential) and the deflection components ξ, η may be calculated from the following simple expressions:

$$\begin{aligned} N &= T/\gamma \\ \xi &= g\delta g_u \\ \eta &= g\delta g_e \end{aligned} \qquad (17)$$

For a practical example, see *Uotila* [1960].

Practical Considerations

The integrals in formulas 8–10, 12–14, and 16 are necessarily evaluated by summation. The surface element $d\sigma$, or $du\, dv$, is replaced by a small compartment, and numerical integration is performed using the same methods employed in evaluating the Stokes or Vening Meinesz formulas [*Uotila*, 1960; *Hirvonen and Moritz*, 1963].

Comparison of the main methods described above may lead to the conclusion that, from the computational point of view, the continuation method is the simplest and that the direct integration method is the most complicated. However, although only free-air anomalies are needed for direct integration, the continuation method requires undulations and deflections in addition.

As far as the practical limit of integrations is concerned, it is generally impractical to go beyond $\psi = 20°$ (coating method), $\psi = 30°$ (direct method), unless the integration is extended for the whole Earth. In the continuation method the practical limit is 10 H. Integration beyond these limits would decrease the root mean square influence of the distant zones very slowly [*Hirvonen and Moritz*, 1963].

For the many other considerations, which space will not permit us to mention here, the reader is referred to the bibliography.

Bibliography

Arnold, K., *Schwerewerte in grossen Hoehen ueber der Erdoberflaeche*, vol. 12, pp. 51–69, Geodetic Institute Veröff., Potsdam, 1959.

Caputo, M., Gravity in space and the dimensions and mass of the Earth, *J. Geophys. Res., 68*, 15, 1963.

Caputo, M., Some space gravity formulas and the

dimensions and the mass of the Earth, *Geofis. Pura Appl., 57,* 68–82, 1964.

Caputo, M., On the shape, gravity field, and strength of the Moon, *J. Geophys. Res., 70,* 16, 1965.

Cohen, C. J., A mathematical model of the gravity field surrounding the Earth, *U. S. Navy Proving Ground Rept. 1514,* 1957.

Cook, A. H., The external gravity field of a rotating ellipsoid to the order of e^3, *Geophys. J., 2,* 3, 1959.

Daugherty, K. I., and J. D. Define, Comparison of methods for determining the Earth's external gravitational vector, paper presented at the 13th General Assembly, IUGG, Berkeley, 1963.

Groten, E., On the accuracy of the three components $\partial\Delta g/\partial xi$ at low elevation derived from gravity anomalies, *Inst. Geodesy Photogrammetry Cartography Rept. 48,* Ohio State University, Columbus, 1965.

Groten, E., Accuracy of gravity gradients at elevations, *Inst. Geodesy Photogrammetry Cartography Rept. 50,* Ohio State University, Columbus, 1965.

Heiskanen, W. A., and Helmut Moritz, *Physical Geodesy,* Freeman & Co., San Francisco, in press, 1966.

Heiskanen, W. A., and U. A. Uotila, *Study of the shape of the equipotential surface and the gravity anomaly field in high elevations, Inst. Geodesy Photogrammetry Cartography Rept. 12,* Ohio State University, Columbus, 1960.

Helmert, F. R., *Die mathematischen und physikalischen Theorieen der Hoeheren Geodaesie, II.,* Leipzig, 1884.

Hirvonen, R. A., Gravity anomalies and deflection of the vertical above sea level, *Trans. Am. Geophys. Union, 33,* 6, 1952.

Hirvonen, R. A., New theories of gravimetric geodesy, *Ann. Acad. Sci. Fennicae, A., III,* 56, 1960.

Hirvonen, R. A., and L. A. Kivioja, Interpolation of the gravitational field at high elevation, *Inst. Geodesy Photogrammetry Cartography Rept. 14,* Ohio State University, Columbus, 1960.

Hirvonen, R. A., and Helmut Moritz, Practical computations of gravity at high altitudes, *Inst. Geodesy Photogrammetry Cartography Rept. 27,* Ohio State University, Columbus, 1963.

Jung, K., Figure der Erde, *Handbuch der Physik, 1,* Springer-Verlag, Berlin, 1956.

Lambert, W. D., The problem of gravity at considerable elevations above the surface of the Earth, *Mapping Charting Lab. Tech. Paper 145,* Ohio State University, Columbus, 1951.

Lambert, W. D., Simple approximate formulas for gravity and geopotential at high elevations, *Koninkl. Ned. Geol-Mijub. Genootschap Verk. Geol. Ser,* Pt. 18, 1957*a*.

Lambert, W. D., Normal gravity at high elevations, in *Size and Shape of the Earth,* edited by W. A. Heiskanen, *Institute Geodesy Photogrammetry Cartography Publ. 7,* Ohio State University, Columbus, 1957*b*.

Lambert, W. D., Note on paper of A. H. Cook, 'The external gravity field of a rotating spheroid to the order of e^3,' *Geophys. J., 3,* 3, 1960.

Lambert, W. D., The gravity field of an ellipsoid of revolution as a level surface, *Ann. Acad. Sci. Fennicae, A, III,* 57, 1961.

Levallois, J. J., *Sur le Problème du Champ Extérieur de la Pesanteur,* Institut Géographique National, Paris, 1960.

Molodenskii, M. S., *Basic Problems of Geodetic Gravimetry* (translation 59–11257, available from OTS, CFSTI, Springfield, Va.), 1945.

Molodenskii, M. S., V. F. Eremeev, and M. I. Yurkina, *Methods for Study of the External Gravitational Field and the Figure of the Earth* (translation 61-31207, available from OTS, CFSTI, Springfield, Va.), Israel Program for Scientific Translation, Jerusalem, 1962.

Moritz, H., Studies on the accuracy of the computation of gravity in high elevations, *Ann. Acad. Sci. Fennicae, A, III,* 59, 1962.

Moritz, H., A statistical method for upward and downward continuation of gravity, *Inst. Geodesy Photogrammetry Cartography Rept. 25,* Ohio State University, Columbus, 1962.

Moritz, H., Computation of the external gravity field and the geodetic boundary value problem, *Inst. Geodesy Photogrammetry Cartography Rept. 49,* Ohio State University, Columbus, 1965.

Orlin, H., The three components of the external gravity field, *J. Geophys. Res., 64,* 12, 1959.

Pizzetti, P., Sulla espressione della gravita alla superficie del geoide, supposto ellissoidico, *Atti Reale Accad. Lincei, Rendiconti Ser. 5, 3,* 1894.

Somigliana, C., Teoria generale del campo gravitationale dell' ellissoide di rotazione, *Mem. Soc. Astron. Ital., 4.* 1929.

Tengström, E., Calculation of the external gravity anomalies and deflections of the vertical at higher elevations by means of Taylor expansions from the geoid, *Inst. Geodesy Photogrammetry Cartography Rept. 5,* Ohio State University, Columbus, 1959.

Tsuboi, C., Application of Fourier series for computing gravity anomalies and other gravimetric quantities at any elevation from surface gravity anomalies, *Inst. Geodesy Photogrammetry Cartography Rept. 1,* Ohio State University, Columbus, 1959*a*.

Tsuboi, C., Application of double Fourier series to computing gravity anomalies and other gravimetrical quantities at higher elevations from surface gravity anomalies, *Inst. Geodesy Photogrammetry Cartography Rept. 2,* 1959*b*.

Tsuboi, C., Application of sin X/x and other similar functions to computing gravity anomalies at higher elevations, starting from given surface gravity anomalies, *Inst. Geodesy Photogrammetry Cartogrophy Rept. 3,* Ohio State University, Columbus, 1959*c*.

Tsuboi, C., Weight function method for computing gravity anomalies at higher elevations, starting from given surface gravity anomalies, *Inst. Geodesy Photogrammetry Cartography*

Rept. 4, Ohio State University, Columbus, 1961.

Tsuboi, C., Upward continuation of gravity values based on the cylindrical coordinate system, *Inst. Geodesy Photogrammetry Cartography Rept. 16,* Ohio State University, Columbus, 1961.

Uotila, U. A., Investigations on the gravity field and the shape of the Earth, *Ann. Acad. Sci. Fennicae, III,* 55, 1960.

Vening Meinesz, F. A., The outside gravity field up to great distance from the Earth, *Koninkl. Ned. Akad. Wetenschap. Proc., Ser. B, 62,* 2, 1959.

Wagner, C. A., The gravitational potential of a triaxial Earth, *NASA-MAR-4: NASA TM-X-50031; NASA-X-623-62-206,* 1962.

Zagrebin, D. W., *Die Theorie das regularisierten Geoids,* Geodetic Institute, Potsdam, 1956.

Review of Formulas for the Space Normal Gravity Field of the Earth

MICHELE CAPUTO[1]

Institute of Geophysics and Planetary Physics
University of California, Los Angeles

INTRODUCTION

Among other problems that the space age has created, there are two connected with the normal gravity field of the Earth: (1) the computation of the normal gravity field in the space surrounding the Earth, and (2) the adjustment of the parameters of the Earth field and shape.

1. The theory of Pizzetti and Somigliana gave the closed expression for the formula which was later adopted by the International Association of Geodesy for the computation of the values of gravity over the rotating model then adopted for the surface of the Earth, i.e. the international ellipsoid. I am referring to the formula currently used for the computation of the gravity anomalies.

When we measure gravity at high elevations above the geoid or over the Earth's surface and want to compare the measured value with the normal field there, then the international formula needs to be extended into the space surrounding the Earth. We have therefore extended the formulas of Pizzetti's theory and thus the international formula to the space surrounding the Earth for the rotating and the nonrotating fields.

The formulas and discussion that are presented in this paper are for a field in which one of the equipotential surfaces is an ellipsoid of revolution and which can therefore be adapted to the normal field or to another field of the same type.

2. At the present time the following parameters of the Earth's shape and gravity field are observed: from artificial satellites, MG and J_2 (M, mass of the Earth; G, constant of gravitational attraction; J_2, coefficient of the second-order Legendre polynomial in expansion of the potential); from gravity measurements over the surface of the Earth, the values of gravity at the equator and north pole g_{e_1} and g_{e_2}; the rotation rate of the Earth ω. There is also a relation between a_1 and f resulting from measurement of arcs; those parameters are conditioned by three equations and must obviously be adjusted.

Approximate expressions of the formulas for this adjustment were given by *Helmert* [1884], *de Sitter and Brouwer* [1938], *Lambert* [1960], *Cook* [1959], and others; closed expressions of the same formulas were given by *Pizzetti* [1894], *Somigliana* [1929], and *Caputo* [1964].

Since some controversy could arise about the equations to be used for the adjustment, we thought it useful to call attention to the following set of formulas for the computation of the normal field in the space surrounding the Earth and the adjustment of the parameters, because the theory from which they are obtained is simple, the formulas are closed (therefore the accuracy resulting from their use is limited only by the accuracy of the observations), and because of the coordination that they achieve between gravimetric and geometric geodesy.

THE COORDINATES

One of the great achievements of geodesy was made when the international gravity formula was adopted by IAG, that is, when the international ellipsoid was adopted for both geometric and gravimetric geodesy; the results of the two could then be directly compared and integrated.

Almost all the formulas for this field were developed in closed form by Pizzetti and Somigliana for the Earth's rotating gravity field. Recently they were extended to the space surrounding the Earth. Here I will summarize

[1] Now at Department of Geophysics, University of British Columbia, Canada.

them and also give the equivalent formulas for the nonrotating gravity field of the Earth.

Symbols, coordinates, and formulas referred to here are taken from an earlier paper [*Caputo*, 1964]. We take co-ordinates l, ψ, λ related to the Cartesian x_1, x_2, x_3, and polar S, θ, μ as follows:

$$x_1 = \frac{a_1^2 + l}{d} \cos\psi \cos\lambda = S \sin\theta \cos\mu$$

$$x_2 = \frac{a_2^2 + l}{d} \cos\psi \sin\lambda = S \sin\theta \sin\mu \tag{1}$$

$$x_3 = \frac{a_3^2 + l}{d} \sin\psi = S \cos\theta$$

$$d^2 = a_1^2 \cos^2\psi \cos^2\lambda + a_2^2 \cos^2\psi \sin^2\lambda + a_3^2 \sin^2\psi + l$$

where the x_3 axis is the axis of rotation of the geoid and $a_1 = a_2 > a_3$ are the semiaxes of the ellipsoid E_0 (which approximates the geoid), whose equations are given by (1) for $l = 0$. The surfaces E_l (l = const) are ellipsoids confocal to E_0. ψ and λ are the geometric latitude and longitude on the confocal ellipsoids, namely, the angles between the normal to E_l and the plane x_1, x_2, and between the plane x_1, x_3 and the plane through P and x_3. The theory is developed by means of the Morera's functions; e.g.

$$A_{ij}(l) = \int_l^\infty \frac{ds}{(a_i^2 + s)(a_j^2 + s)R(s)} \tag{2}$$

$$R^2(s) = (a_1^2 + s)(a_2^2 + s)(a_3^2 + s)$$

The Rotating Field in Polar Coordinates

In the case $a_1 = a_2$ and by means of the functions (2), the theory of Pizzetti and Somigliana gives the following closed expression for the potential of the body of mass M that has E_0 as an outer equipotential surface:

$$W = \frac{G}{\epsilon a_3}\left[(M - \tfrac{2}{3}\nu)\tan^{-1} E + \frac{\nu}{[(1+E^2)^3 \tan^2\theta + 1]E^2} \cdot \left\{\left(\tan^{-1} E - \frac{E}{1+E^2}\right)(1+E^2)^4 \tan^2\theta + 2(E - \tan^{-1} E)\right\}\right] + \frac{\omega^2 S^2 \sin^2\theta}{2} \tag{3}$$

$$\nu = -\frac{\epsilon^3 a_3^3 \omega^2 (1+\epsilon^2)}{2[(3+\epsilon^2)\tan^{-1}\epsilon - 3\epsilon]G}$$

$$\epsilon^2 = \frac{a_1^2 - a_3^2}{a_3^2}$$

$$E^2(l) = \frac{a_1^2 - a_3^2}{a_3^2 + l} \qquad l \geq 0 \qquad \epsilon^2 = E^2(0)$$

where l is expressed as a function of polar coordinates S, θ,

$$x_1^2 + x_2^2 = r^2$$

$$r = S \sin\theta = \frac{a_1^2 + l}{d} \cos\psi \tag{4}$$

$$x_3 = S \cos\theta = \frac{a_3^2 + l}{d} \sin\psi$$

by

$$l = \frac{S^2}{2}\left\{1 - \frac{a_3^2}{S^2}(2 + \epsilon^2) + \left[1 + \frac{2a_3^2\epsilon^2}{S^2}(2\cos^2\theta - 1) + \frac{a_3^4\epsilon^4}{S^4}\right]^{1/2}\right\} \tag{5}$$

By differentiation of (3) one obtains the x_3 and r components of the gravity vector

$$g_r = \frac{GS \sin\theta}{\epsilon^3 a_3^3}\left[(M + \tfrac{4}{3}\nu)\frac{(1+E^2)^3 \tan^2\theta + 1}{(1+E^2)^2 \tan^2\theta + 1} \cdot \frac{E^3}{(1+E^2)^2} - 2\nu\left(\tan^{-1} E - \frac{E}{1+E^2}\right)\right] - \omega^2 S \sin\theta \tag{6}$$

$$g_{x_3} = \frac{GS \cos\theta}{\epsilon^3 a_3^3}\left[(M + \tfrac{4}{3}\nu)\frac{(1+E^2)^3 \tan^2\theta + 1}{(1+E^2)^2 \tan^2\theta + 1} \cdot \frac{E^3}{(1+E^2)} - 4\nu(E - \tan^{-1} E)\right] \tag{7}$$

From the formulas above, the Somigliana theorem can be proved; it is

$$\begin{vmatrix} g_1 & (1 + \epsilon^2 \cos^2 \varphi_1)^{1/2} & (1 + \epsilon^2 \cos^2 \varphi_1)^{-1/2} \\ g_2 & (1 + \epsilon^2 \cos^2 \varphi_2)^{1/2} & (1 + \epsilon^2 \cos^2 \varphi_2)^{-1/2} \\ g_3 & (1 + \epsilon^2 \cos^2 \varphi_3)^{1/2} & (1 + \epsilon^2 \cos^2 \varphi_3)^{-1/2} \end{vmatrix} = 0 \tag{8}$$

where g_i are the values of gravity at the latitudes φ_i on the ellipsoid E_0.

If we define g_{a_1} and g_{a_3}, the values of gravity at the equator and the pole, formula 8 can be written

$$g = g_{a_1} \frac{1 + (\alpha - f - f\alpha) \sin^2 \varphi}{(1 - f(2 - f) \sin^2 \varphi)^{\frac{1}{2}}}$$

$$\alpha = (g_{a_3} - g_{a_1})/g_{a_1} \tag{9}$$

$$f = (a_1 - a_3)/a_1$$

which gives the values of gravity on the ellipsoid E_0 by means of the values of gravity at the pole and the equator and by means of the flattening of E_0. The dimensions of E_0 are unspecified. By differentiation of (3) one also obtains the theorems of Clairaut and Pizzetti in the closed form

$$\frac{g_{a_3}}{(a_3^2 + l)^{1/2}} - \frac{g_{a_1}}{(a_1^2 + l)^{1/2}} = \left[3 \tan^{-1} E - \frac{3 + 2E^2}{1 + E^2} E \right] + \omega^2 \tag{10}$$

$$2\omega^2 + 2 \frac{g_{a_1}}{(a_1^2 + l)^{1/2}} + \frac{g_{a_3}}{(a_3^2 + l)^{1/2}} = \frac{GM}{R(l)} \tag{11}$$

It is clear that the six parameters g_{a_i}, a_i, MG, ω which define a gravity field of this type cannot be fixed arbitrarily; they must satisfy the two conditions (10) and (11). For the definition of the field, four parameters are therefore essential. For $l = 0$, (10) and (11) become the known expressions given by Pizzetti and Somigliana. By means of (10) α can be written

$$\alpha = -f + (2\nu G/\epsilon^3 a_1^2 g_1)[3(1 + \epsilon^2) \tan^{-1} \epsilon - 3\epsilon - 2\epsilon^3] + (\omega^2 a_3/g_1) \tag{12}$$

The series expansion of (9) in powers of $\sin \varphi$ is

$$g = g_{a_1}[1 + \alpha \sin^2 \varphi - \tfrac{1}{8} f(f + 2\alpha) \sin^2 2\varphi \cdots] \tag{13}$$

From (13) the international formula can be obtained. The closed expression for it can be readily obtained by means of (12), (9), and $f^{-1} = 297$, $g_{a_1} = 978.0490$ adopted for the international formula;

$$g = 978.0490 \frac{1 + 0.001903575 \sin^2 \varphi}{[1 - 0.006722670 \sin^2 \varphi]^{1/2}} \tag{14}$$

For the values (f^{-1} is obtained from J_2, using formula 56 of *Caputo* [1964])

$$MG = 3.98603.10^{20} \qquad a_1 = 6.378160.10^8$$

$$J_2 = 1.08270.10^{-3} \qquad (f^{-1} = 298.247)$$

adopted by the International Astronomical Union and derived from satellites observations, (9) gives

$$g = 978.032 \frac{1 + 0.0019317 \sin^2 \varphi}{[1 - 0.0066946 \sin^2 \varphi]^{1/2}} \tag{15}$$

According to (6) and (7) we have for the value of gravity in space

$$g = \frac{\sin \psi}{\sin \varphi} \frac{1 + (l/a_3^2)}{\epsilon^3 a_3^2} \frac{G(M + \frac{4}{3}\nu)(E^3/1 + E^2 \cos^2 \theta) - 4\nu G(E - \tan^{-1} E)}{\left\{ \frac{[1 + \epsilon^2 + (l/a_3^2)]^3 \tan^2 \theta + [1 + (l/a_3^2)]^3}{[1 + \epsilon^2 + (l/a_3^2)]^2 \tan^2 \theta + [1 + (l/a_3^2)]^2} \right\}^{1/2}} \tag{16}$$

where φ and ψ are given by

$$\tan \varphi = \frac{g_{z_3}}{g_r}$$

$$\tan \psi = (a_1^2 + l/a_3^2 + l) \operatorname{ctan} \theta \tag{17}$$

If we specify the parameters of (16) in order to match the international gravity formula for $l = 0$, we obtain its extension in space in closed expression:

$$g = \frac{\sin \psi}{\sin \phi}(4.041033 \cdot 10^{17} + l) \cdot \left[\frac{(4.068383 \cdot 10^{17} + l)^2 \tan^2 \theta + (4.041033 \cdot 10^{17} + l)^2}{(4.068383 \cdot 10^{17} + l)^3 \tan^2 \theta + (4.041033 \cdot 10^{17} + l)^3}\right]^{1/2} \cdot [0.01071597(E - \tan^{-1} E) - 0.0007850496(E^3/1 + E^2 \cos^2 \theta)] \tag{18}$$

This value of g can also be computed directly from g_r and g_{z_3}. The values associated with the parameters of the international ellipsoid and the international gravity formula are

$$g_r = S \sin \theta\left[-7.850555 \cdot 10^{-4} \frac{(1 + E^2)^3 \tan^2 \theta + 1}{(1 + E^2)^2 \tan^2 \theta + 1} \cdot \frac{E^3}{(1 + E^2)^2} + 5.357994 \cdot 10^{-3}\left(\tan^{-1} E - \frac{E}{1 + E^2}\right) - 5.317494 \cdot 10^{-7}\right] \tag{19}$$

$$g_{z_3} = S \cos \theta\left[-7.850555 \cdot 10^{-4} \frac{(1 + E^2)^3 \tan^2 \theta + 1}{(1 + E^2)^2 \tan^2 \theta + 1} \cdot \frac{E^3}{(1 + E^2)} + 1.071600 \cdot 10^{-2}(E - \tan^{-1} E)\right] \tag{20}$$

For the values adopted by the International Astronomical Union they are instead

$$g_r = S \sin \theta\left[-8.050380 \cdot 10^{-4} \frac{(1 + E^2)^3 \tan^2 \theta + 1}{(1 + E^2)^2 \tan^2 \theta + 1} \cdot \frac{E^3}{(1 + E^2)^2} + 5.414414 \cdot 10^{-3}\left(\tan^{-1} E - \frac{E}{1 + E^2}\right) - 5.317494 \cdot 10^{-7}\right] \tag{21}$$

$$g_{z_3} = S \cos \theta\left[-8.050380 \cdot 10^{-4} \frac{(1 + E^2)^3 \tan^2 \theta + 1}{(1 + E^2)^2 \tan^2 \theta + 1} \cdot \frac{E^3}{(1 + E^2)} + 1.082883 \cdot 10^{-2}(E - \tan^{-1} E)\right] \tag{22}$$

Obviously the values of (21) and (22) [or (19) and (20)] coincide with the values given by (15) [or (14)] which agree very well with the most recent results from ground measurements.

The Nonrotating Field

For the nonrotating field, we shall indicate with $\bar{g}$, $\bar{g}_{a_i}$, $\bar{g}_r$, $\bar{g}_{z_3}$, $\bar{W}$, and $\bar{\varphi}$ the values of gravity of the potential and the latitude. The expression of the potential $\bar{W}$ is readily obtained from (3) dropping the term $(\omega^2 S^2 \sin^2 \varphi/2)$. Similarly, one obtains $\bar{g}_r$ dropping the term $\omega^2 S \sin \varphi$ in (6), while $\bar{g}_{z_3} \equiv g_{z_3}$. The Clairaut and Pizzetti theorems are obtained by substituting $\bar{g}_{a_i}$ into g_{a_i} and dropping the terms ω^2 and $2\omega^2$ in (10) and (11), respectively. For the value of gravity we must note that

$$\tan \bar{\varphi} = \bar{g}_{z_3}/\bar{g}_r$$
$$\sin \bar{\varphi} = [(g_r^2 + g_{z_3}^2)/(\bar{g}_r^2 + g_{z_3}^2)]^{1/2} \sin \varphi \tag{23}$$

from which follows

$$\bar{g} = (\sin\varphi/\sin\bar{\varphi})g = [(\bar{g}_r^2 + g_{z_s}^2)/(g_r^2 + g_{z_s}^2)]^{1/2} g \tag{24}$$

The value of $\bar{g}$ can also be computed directly from $\bar{g}_{z_s}$ and $\bar{g}_r$. The values associated with the international gravity formula and the international ellipsoid are:

$$\bar{g}_r = S \sin\theta \left[-7.850555 \cdot 10^{-4} \frac{(1+E^2)^3 \tan^2\theta + 1}{(1+E^2)^2 \tan^2\theta + 1} \cdot \frac{E^3}{(1+E^2)^2} + 53.57994 \cdot 10^{-4} \left(\tan^{-1} E - \frac{E}{1+E^2} \right) \right] \tag{25}$$

$$\bar{g}_{z_s} = g_{z_s} \tag{26}$$

With the values recently adopted by the International Astronomical Union formulas (6) and (7) become

$$\bar{g}_r = S \sin\theta \left[-8.050380 \cdot 10^{-4} \frac{(1+E^2)^3 \tan^2\theta + 1}{(1+E^2)^2 \tan^2\theta + 1} \cdot \frac{E^3}{(1+E^2)^2} + 54.14414 \cdot 10^{-4} \left(\tan^{-1} E - \frac{E}{1+E^2} \right) \right] \tag{27}$$

$$\bar{g}_{z_s} = g_{z_s} \tag{28}$$

For use in the satellite geodesy the spherical harmonic representation of $\bar{W}$ is needed:

$$\bar{W} = \frac{MG}{S} \left[1 + \sum_1^\infty {}_nJ_{2n} (a_1/S)^{2n} P_{2n}(\cos\theta) \right] \tag{29}$$

Its spectrum is

$$J_{2n} = \frac{(-1)^n}{2n+1} \cdot \left[1 + \frac{8n}{3(2n+3)} \frac{\nu}{M} \right] f^n (2-f)^n \tag{30}$$

Table 1 gives the numerical values of J_{2n} for the normal gravity field and for the field adopted by the International Astronomical Union.

This expression of $\bar{W}$ does not allow separations of the Hamilton-Jacobi equation of motion of the satellite [see *Caputo*, 1965]. The closest expression that allows the separation is [*Vinti*, 1959; *Kislik*, 1960; *Caputo*, 1965]

$$\bar{W}^* = -\frac{E(1+E^2+\tan^2\theta)}{(1+E^2)^2 + \tan^2\theta} \cdot \frac{MG}{\epsilon a_3 \left(\frac{1}{3} + \frac{8}{45} \frac{\nu}{M} \right)^{1/2}} \tag{31}$$

TABLE 1

n	International Formula Field	Astronomical Union Field
1	−0.10920387E-02	−0.108270E-02
2	+0.24188455E-05	+0.237127E-05
3	−0.63169574E-08	−0.608519E-08
4	+0.15400898E-10	+0.142763E-10
5	−0.17580877E-13	−0.121872E-13
6	−0.18002439E-15	−0.205223E-15
7	+0.22965368E-17	+0.240742E-17
8	−0.19465272E-19	−0.198947E-19
9	+0.14553414E-21	+0.146681E-21
10	−0.10281496E-23	−0.102612E-23

$\bar{W}^*$ matches J_0 and J_2 of $\bar{W}$ exactly. The spectrum of $\bar{W}^*$ is

$$J_{2n}^* = \left[-\left(\frac{1}{3} + \frac{8}{45} \frac{\nu}{M} \right) f(2-f) \right]^n \tag{32}$$

The ratio

$$(J_{2n}^* - J_{2n})/J_{2n} \simeq -[(2n+1)/6^n] \cdot 3 - 1 \tag{33}$$

indicates that for $n = 2$ we have $J_{2n}^* - \frac{1}{2} J_{2n}$. Therefore, since the harmonics of the Earth gravity fields are $J_0 10^{-6} \simeq J_2 10^{-3} \simeq J_n$ $(n \geq 3)$,

$\bar{W}^*$ is a satisfactory expression for the use of the perturbation method in the determination of the orbit of geodetic satellites.

The Adjustment of the Parameters

The adjustment of the observed Earth parameters MG, J_2, g_{a_1}, g_{a_2}, a_1, f should therefore be performed by using equations 10, 11, and 30 for $n = 2$.

Computations made for the adjustment of the set of parameters recently adopted by the International Astronomical Union indicate that the corrections are very small. The value of $f^{-1} = 298.247$ follows from the values adopted by means of (30), and g_{a_1} can be obtained eliminating g_{a_2} in (10) by means of (11); its value $g_{a_1} = 978.0319$.

The values of g_{a_1} computed by *Uotila* [1962] in the Potsdam system are

$g_{a_1} = 978{,}0478, \qquad f^{-1} = 297.8$
from free-air anomalies

$g_{a_1} = 978.0451, \qquad f^{-1} = 298.1$
from isostatic anomalies

From the connection of the various modern absolute measurements of gravity to Potsdam we believe that the Potsdam value is in error by −13.8 mgal. Applying this correction to the values of gravity computed by Uotila, we can see that the discrepancy between the g_{a_1} computed here and the observed one is about 2 parts in a million. The same is true for g_{a_2}.

It should be noted that the mass of the Earth's atmosphere is irrelevant to the present accuracy of observation of MG and therefore to the present discussion.

References

Caputo, M., Some space gravity formulas and the dimensions and the mass of the Earth, *Pure Appl. Geophys. Basel, 57*, 68–82, 1964.

Caputo, M., On the shape, gravity field, and strength of the Moon, *J. Geophys. Res., 70*, 3993–6003, 1965.

Cook, A. H., The external gravity field of a rotating spheroid to the order of e^3, *Geophys. J., 3*, 199, 1959.

de Sitter, W., and D. Brouwer, On the system of astronomical constants, *Bull. Astron. Inst. Neth., 8*, 213, 1938.

Helmert, F. R., *Die Mathematischen and Physikalischen Theorieen der höheren Geodäsie*, vol. 2 of *Die Physikalischen Theorie*, B. G. Teubner, Leipzig, 610 pp., 1884.

Kislik, M. D., The path of an artificial satellite in the normal gravitational field of the Earth, *Iskusstv. Sputniki Zemli, 4*, 3–13, 1960.

Lambert, W. D., Note on the paper of A. H. Cook 'The external gravity field of a rotating spheroid to the order of e^3,' *Geophys. J., 3*, 360, 1960.

Pizzetti, P., Sull'espressione della gravitá alla superficie del geoide supposto ellissoidico, *Atti Accad. Naz. Lincei, Rend. Classe Sci. Fis., Mat. Nat., 5*, 166, 1894.

Somigliana, C., Teoria generale del campo gravitazionale dell'ellissoide di rotazione, *Mem. Soc. Astron. Ital., 4*, 541, 1929.

Uotila, U., Theoretical gravity formula corresponding to current gravity holdings (abstract), *J. Geophys. Res., 67*, 3605, 1962.

Vinti, J. P., New method of solution for unretarded satellite orbits, *J. Res. NBS, 63B*, 105–116, 1959.

The Computation of the External Gravity Field and the Geodetic Boundary-Value Problem

HELMUT MORITZ

Technical University of Berlin, Berlin, West Germany

Abstract. In the usual way of computing the external gravity field, the Earth is considered as a level surface, although, strictly speaking, the free-air gravity anomalies refer to the nonlevel physical surface of the Earth. The main purpose of the present paper is to give formulas and, as an appendix, some estimates for the effect of topographic height on these computations. An application of Green's identities yields direct but complicated formulas for the effect of the disturbing potential T and the gravity anomaly Δg outside the Earth. A simpler solution for T is obtained through the use of a fictitious surface layer, a coating, on the Earth's physical surface. A third method, which seems to be optimal for practical computations, is a free-air reduction to sea level. The accurate performance of this reduction is a problem of downward continuation of Δg, which may be handled by interative solution of a simple integral equation. After this reduction, however, the conventional spherical formulas can be applied. In addition, the paper presents connections between the determination of the external gravity field from surface data, which is related to the conventional boundary-value problems of potential theory, and the determination of the Earth's physical surface itself, which is a specifically geodetic boundary-value problem.

1. INTRODUCTION

The geodetic boundary-value problem may be defined as the determination of the Earth's physical surface S if the gravity vector $\mathbf{g}$ and the gravity potential W are given on it. It is none of the three well-known boundary-value problems of potential theory, where the surface S is always considered given.

Once the physical surface S has been determined, however, the computation of the gravity field outside the Earth from surface data is indeed closely related to the usual boundary-value problems of potential theory. Let, for instance, the normal component

$$g_n = -\partial W/\partial n \qquad (1)$$

of the gravity vector $\mathbf{g}$ be known at every point of S. It is the negative derivative of the gravity potential W along the surface normal n of S. If g_n is given in addition to S, then the determination of the external gravity field is identical with the *second boundary-value problem* of potential theory, or *Neumann's problem*. It is unessential in this connection that W is not harmonic, owing to the effect of centrifugal force.

According to the theory of Neumann's problem, the solution is formally given by

$$W_P = \iint_S g_n(Q)G(P, Q)\, dS \qquad (2)$$

The integration is extended over the physical surface S. Q denotes the variable point on S where the surface element dS is situated; P is the fixed point outside S at which W is to be determined. $G(P, Q)$ is Green's function for our problem. For simplicity we have assumed W to be harmonic in (2); in reality this formula should also take the centrifugal force into account.

Green's function $G(P, Q)$ depends on the surface S. Since the Earth's physical surface is extremely irregular and difficult to handle mathematically, it is impossible to determine the function $G(P, Q)$ for it at the present time. Hence a slightly modified approach is taken, which to a certain extent abandons the rigid formulation in terms of a second boundary-value problem.

First, the gravity potential W on S is used as additional information. Secondly, a normal potential U is introduced, and the disturbing potential $T = W - U$ and the gravity anomaly Δg are used instead of the potential W and the gravity g.

Let this additional information be that S is an equipotential surface $W = W_0 = \text{const}$. Then our problem can be solved. We have the well-known formulas

$$T_P = \frac{R}{4\pi} \iint_\sigma S(r_P, \psi)\, \Delta g\, d\sigma \qquad (3)$$

$$\Delta g_P = \frac{r_P^2 - R^2}{4\pi r_P} \iint_\sigma \frac{\Delta g}{D^3}\, d\sigma \qquad (4)$$

Figure 1 illustrates the notations used. R is the mean radius of the reference ellipsoid $U = W_0$, which for the present purpose may be considered as a sphere of radius R. Let H be the elevation of the exterior point P above sea level; then

$$r_P = R + H \qquad (5)$$

D is the spatial distance of P from the variable point Q on the sphere representing the reference ellipsoid:

$$D = (r_P^2 + R^2 - 2r_P R \cos\psi)^{1/2} \qquad (6)$$

ψ is the angular distance of Q from P; $d\sigma$ is the element of solid angle situated at Q. Finally, the function

$$S(r_P, \psi) = \frac{2R}{D} + \frac{R}{r_P} - 3\frac{RD}{r_P^2} - \frac{R^2}{r_P^2}\cos\psi \cdot\left(5 + 3\ln\frac{r_P - R\cos\psi + D}{2r_P}\right) \qquad (7)$$

is the generalized Stokes function.

Since the gravity disturbance vector δ is the gradient of T, that is

$$\delta = \text{grad}\, T = (\partial T/\partial x, \partial T/\partial y, \partial T/\partial z) \qquad (8)$$

we find its components by forming the partial derivatives of (3).

An alternative way of computing T_P is using a surface layer, a coating, on the reference ellipsoid. Then

$$T_P = \frac{R^2}{2\pi} \iint_\sigma \frac{\mu}{D}\, d\sigma \qquad (9)$$

where the density μ of the coating is given by

$$\mu = \Delta g + 3T/2R \qquad (10)$$

Δg and T being taken at sea level (see, e.g., *Hirvonen and Moritz* [1963]).

The preceding formulas are not rigorously valid for the physical surface S, because S is not equipotential. Compared with the Earth's radius R, the elevation h of S above sea level, i.e., above an equipotential surface, is rather small. Thus a development in a power series with respect to h is feasible. The approximation of zero order, neglecting h completely, is then given by equations 3 through 10. The purpose of the present paper is to find first-order approximations that are linear in h.

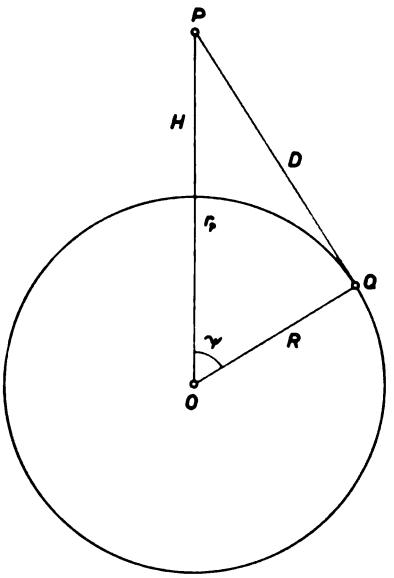

Fig. 1. Sphere representing the reference ellipsoid.

2. A Solution for T

The point of departure is Green's identity

$$4\pi T_P = \iint_S \left\{T\frac{\partial}{\partial n}\left(\frac{1}{l}\right) - \frac{1}{l}\frac{\partial T}{\partial n}\right\} dS \qquad (11)$$

extended over the physical surface S. Figure 2 shows the notations used.

From *Moritz* [1964, p. 21] we take the formula

$$\partial T/\partial n = ((1/\gamma)\,(\partial\gamma/\partial h)T - \Delta g'')\cos\beta \qquad (12)$$

where

$$\Delta g'' = \Delta g + g_1 \qquad (13)$$

and

$$g_1 = -\gamma(\xi\tan\beta_1 + \eta\tan\beta_2) \qquad (14)$$

γ is normal gravity, ξ and η are the components of the deflection of the vertical, β is the angle of (maximum) inclination of the terrain, and β_1 and β_2 are the angles of inclination of the north-south and the east-west terrain profile, respectively. To a sufficient approximation

$$(1/\gamma)(\partial\gamma/\partial h) \doteq -(2/R) \tag{15}$$

and

$$\cos\beta \doteq 1 \tag{16}$$

so that (12) becomes

$$-(\partial T/\partial n) = (2T/R) + \Delta g'' \tag{17}$$

This is introduced in (11), giving

$$4\pi T_P = \iint_S \left\{\frac{\partial}{\partial n}\left(\frac{1}{l}\right) + \frac{2}{Rl}\right\} T\, dS + \iint_S \frac{\Delta g''}{l}\, dS \tag{18}$$

We have

$$(\partial/\partial n)(1/l) = -(1/2l^3)(\partial l^2/\partial n) \tag{19}$$

and

$$\partial l^2/\partial n = \mathbf{n} \cdot \operatorname{grad} l^2 \tag{20}$$

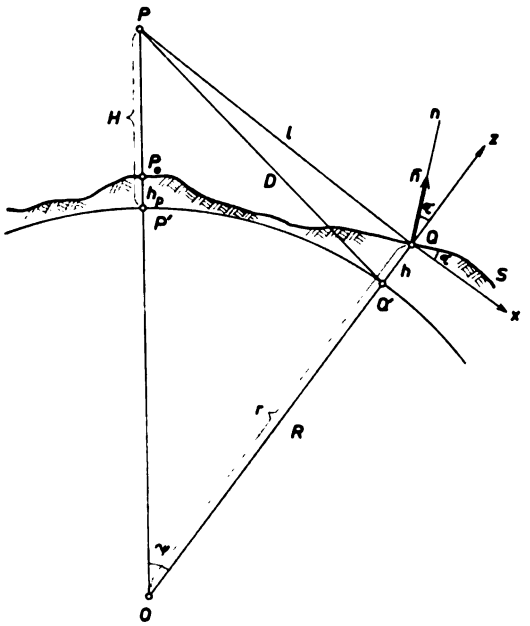

Fig. 2. Topography.

according to a basic formula of vector analysis. $\mathbf{n}$ is the unit vector along the normal. From *Moritz* [1964, p. 20] we take the formula

$$\mathbf{n} = \cos\beta\left(-\frac{\partial h}{\partial x}, -\frac{\partial h}{\partial y}, 1\right) \tag{21}$$

so that

$$\frac{\partial l^2}{\partial n} = \cos\beta\left(-\frac{\partial l^2}{\partial x}\frac{\partial h}{\partial x} - \frac{\partial l^2}{\partial y}\frac{\partial h}{\partial y} + \frac{\partial l^2}{\partial z}\right) \tag{22}$$

Let the z axis be the line OQ, and let the x axis lie in the plane containing the points O, P, and Q, which is the plane of drawing of Figure 2. Then

$$\frac{\partial l^2}{\partial x} = \frac{\partial l^2}{r\, d\psi} \qquad \frac{\partial l^2}{\partial y} = 0 \qquad \frac{\partial l^2}{\partial z} = \frac{\partial l^2}{\partial r} \tag{23}$$

where

$$r = R + h \tag{24}$$

Figure 2 shows that

$$\partial h/\partial x = \tan\tau \tag{25}$$

and

$$l^2 = r_P^2 + r^2 - 2r_P r\cos\psi \tag{26}$$

Differentiating (26) with respect to r and ψ, inserting in (23), and taking (25) into account, we find that (22) becomes

$$\frac{\partial l^2}{\partial n} = 2\cos\beta(A + h - r_P\sin\psi\tan\tau) \tag{27}$$

where

$$A = R - r_P\cos\psi \tag{28}$$

Thus we find from (19)

$$\frac{\partial}{\partial n}\left(\frac{1}{l}\right) = -\frac{\cos\beta}{l^3}(A + h - r_P\sin\psi\tan\tau) \tag{29}$$

This formula is rigorous. We now wish to develop the quantities involved in (18) as power series with respect to h, retaining only terms linear in the elevation h and the inclination β. Then (26) becomes

$$l^2 = r_P^2 + R^2 - 2r_P R\cos\psi + 2(R - r_P\cos\psi)h$$

or, by (6) and (28)

$$l^2 = D^2 + 2Ah = D^2\left(1 + \frac{2A}{D^2}h\right)$$

so that

$$\frac{1}{l} = \frac{1}{D}\left(1 - \frac{A}{D^2}h\right) = \frac{1}{D} - \frac{A}{D^3}h \qquad (30)$$

$$\frac{1}{l^3} = \frac{1}{D^3}\left(1 - \frac{3A}{D^2}h\right) = \frac{1}{D^3} - \frac{3A}{D^5}h \qquad (31)$$

Equation 29 assumes the form

$$\frac{\partial}{\partial n}\left(\frac{1}{l}\right) = -\frac{1}{D^3}$$
$$\cdot\left\{A + \left(1 - \frac{3A^2}{D^2}\right)h - r_P \sin\psi \tan\tau\right\} \qquad (32)$$

Setting $\cos\beta \doteq 1$, as we have done, is in agreement with our linear development since

$$\cos\beta = 1 - \tfrac{1}{2}\beta^2 + \cdots \qquad (33)$$

differs from 1 only by quadratic terms.

The disturbing potential T is split up into a part T_0 independent of h and a part T_1 depending linearly on h:

$$T = T_0 + T_1 \qquad (34)$$

Higher-order terms T_2, T_3, etc., are neglected. In the same way Δg is split up according to (13), since g_1 depends linearly on the inclination β.

The expressions (32), (30), (34), and (13) are inserted in (18), only linear terms are retained, and zero-order and first-order terms are separated. Furthermore we may put

$$dS \doteq R^2\left(1 + \frac{2h}{R}\right)d\sigma \doteq R^2\, d\sigma \qquad (35)$$

neglecting h/R in agreement with Molodenskii [*Molodenskii et al.*, 1962, p. 122]. Thus (18) becomes

$$4\pi T_{0,P} + 4\pi T_{1,P}$$
$$= R^2 \iint_\sigma \left(-\frac{A}{D^3} + \frac{2}{RD}\right)T_0\, d\sigma$$
$$+ R^2 \iint_\sigma \frac{\Delta g}{D}\, d\sigma$$
$$+ R^2 \iint_\sigma \left(-\frac{A}{D^3} + \frac{2}{RD}\right)T_1\, d\sigma$$
$$+ R^2 \iint_\sigma \frac{g_1}{D}\, d\sigma$$
$$+ R^2 \iint_\sigma \left(-\frac{1}{D^3} + \frac{3A^2}{D^5} - \frac{2A}{RD^3}\right)T_0 h\, d\sigma$$
$$+ R^2 \iint_\sigma \frac{r_P \sin\psi}{D^3} T_0 \tan\tau\, d\sigma$$
$$- R^2 \iint_\sigma \frac{A}{D^3}\Delta g h\, d\sigma \qquad (36)$$

Since the zero-order terms are independent of h, the sum of the zero-order terms on the left side of this equation must be equal to the sum of the zero-order terms on the right side. The same holds for the first-order terms.

The zero-order terms are of no further interest. The quantity T_0, corresponding to $h = 0$, is naturally obtained from Δg by means of the spherical formula (3):

$$T_{0,P} = \frac{R}{4\pi}\iint_\sigma S(r_P, \psi)\Delta g\, d\sigma \qquad (37)$$

For T_1 we find from (36)

$$T_{1,P} = \frac{R^2}{4\pi}\iint_\sigma \left(-\frac{A}{D^3} + \frac{2}{RD}\right)T_1\, d\sigma$$
$$+ \frac{R^2}{4\pi}\iint_\sigma \frac{g_1}{D}\, d\sigma$$
$$+ \frac{R^2}{4\pi}\iint_\sigma \left(-\frac{1}{D^3} + \frac{3A^2}{D^5} - \frac{2A}{RD^3}\right)T_0 h\, d\sigma$$
$$+ \frac{R^2}{4\pi}\iint_\sigma \frac{r_P \sin\psi}{D^3} T_0 \tan\tau\, d\sigma$$
$$- \frac{R^2}{4\pi}\iint_\sigma \frac{A}{D^3}\Delta g h\, d\sigma \qquad (38)$$

This equation clearly shows that $T_{1,P}$ depends on the products $T_0 h$, $T_0 \tan\tau$, and $\Delta g\, h$, and on the first-order terms g_1 and T_1.

The term T_0 on S is given by Stokes' formula

$$T_0 = \frac{R}{4\pi}\iint_\sigma \Delta g\, S(\psi)\, d\sigma \qquad (39)$$

The quantity g_1 depends on the deflections of the vertical according to (14). The term T_1 on S may be obtained, for instance, by Molodenskii's formula [*Molodenskii et al.*, 1962, pp. 122–123]

$$T_1 = \frac{R}{4\pi}\iint_\sigma G_1 S(\psi)\, d\sigma \qquad (40)$$

where $S(\psi)$ is Stokes' function and G_1 is given by

$$G_1 = \frac{1}{16\pi R} \iint_\sigma \frac{h - h_P}{\sin^3 \psi/2} \mu \, d\sigma \qquad (41)$$

μ being defined by (10).

3. A Connection with Molodenskii's Problem

Note that (38) gives T_1 at a point outside S, whereas (40) gives it at a point on S. Equation 40 thus constitutes a solution of the boundary-value problem for the Earth's physical surface S. For, if we know the disturbing potential T along S, then we can find the height anomaly ζ by

$$\zeta = T/\gamma \qquad (42)$$

and so determine S itself [*Molodenskii et al.*, 1962; *Moritz*, 1964].

Now it is interesting that a solution for T, equivalent to (40), can be found from (38) itself. For this purpose we have to make the transition $P \to P_0$ to a point on the surface S. We know that Green's identity (11) changes discontinuously during this transition, 4π being replaced by 2π, if P lies on S.

It is convenient first to shift the level from which h is reckoned, so that it contains the point P_0 at the foot of the plumb line through P (Figure 2). We thus have to replace h in (38) by $h - h_P$ and to reckon H from P_0. Then the transition $P \to P_0$ is effected; it means putting $H = 0$. We then have

$$D = 2R \sin \psi/2 = l_0 \qquad (43)$$

$$A = R - R \cos \psi = 2R \sin^2 \frac{\psi}{2} = \frac{l_0^2}{2R} \qquad (44)$$

Inserting this in (38), replacing h by $h - h_P$ and 4π by 2π, we obtain after a transformation that requires some care

$$T_1 - \frac{3R}{4\pi} \iint_\sigma \frac{T_1}{l_0} \, d\sigma = \frac{R^2}{2\pi} \iint_\sigma \frac{g_1}{l_0} \, d\sigma + \kappa \qquad (45)$$

where

$$\kappa = \frac{R^3}{2\pi} \iint_\sigma \frac{-\delta \cos \psi + \tau \sin \psi}{l_0^3} T_0 \, d\sigma \qquad (46)$$

Here we have replaced tan τ by τ and introduced the quantity

$$\delta = (h - h_P)/R \qquad (47)$$

Equation 45 is the approximation linear in h of an equation originally given by Molodenskii [*Molodenskii et al.*, 1962, p. 90; *Moritz*, 1964, p. 21]. Molodenskii calls this an integro-differential equation, because he considers ξ and η, which are the horizontal derivatives of T, as unknown. We shall assume ξ and η to be given, however; approximate values are sufficient. Then (45) is a linear integral equation for T_1.

Its solution can be found to be

$$T_1 = \frac{R}{4\pi} \iint_\sigma g_1 S(\psi) \, d\sigma + \kappa + \frac{3}{8\pi} \iint_\sigma \kappa S(\psi) \, d\sigma \qquad (48)$$

This equation serves the same purpose as Molodenskii's solution 40.

The integral equation 45 was also obtained by *de Graaff-Hunter* [1960], but his way of solving it is not entirely satisfactory.

4. A Solution for Δg

The first-order term grad T_1 of the gravity disturbance vector

$$\boldsymbol{\delta} = \text{grad } T = \text{grad } T_0 + \text{grad } T_1 \qquad (49)$$

may be found by forming the partial derivatives of (38).

An expression for the corresponding first-order term of the gravity anomaly Δg outside the Earth was derived by *Moritz* [1962*a*]. In the following, an improved derivation based on this paper will be given. The notation will be slightly changed. The quantities R, α, r, tg α cos $(\phi - \psi)$, Q of the 1962 paper are now denoted by l, β, s, $-\tan \tau$, P, respectively, in order to conform with the notation used in the present paper.

As we did in the previous paper, we shall replace the sphere by its tangential plane; this corresponds to letting $R \to \infty$. This is possible here because only a limited area surrounding P_0 is relevant for the computation of Δg_P. As a plane approximation we obtain from (17) by setting $R \to \infty$

$$-\partial T/\partial n = \Delta g'' = \Delta g + g_1 \qquad (50)$$

$$-\partial T/\partial H = \Delta g_P \qquad (51)$$

Inserting this in equation 97 of *Moritz* [1962a] we find

$$\Delta g_P = -\frac{1}{4\pi}\iint\left(\frac{1}{D^3}-\frac{3H^2}{D^5}\right)T\,dx\,dy + \frac{H}{4\pi}\iint\frac{\Delta g+g_1}{D^3}\,dx\,dy - \frac{3H}{4\pi}\iint\left(\frac{3}{D^5}-\frac{5H^2}{D^7}\right)Th\,dx\,dy + \frac{3H}{4\pi}\iint\frac{s}{D^5}\,T\tan\tau\,dx\,dy - \frac{1}{4\pi}\iint\left(\frac{1}{D^3}-\frac{3H^2}{D^5}\right)\Delta g\,h\,dx\,dy$$

Now we set again

$$T = T_0 + T_1$$
$$\Delta g_P = \Delta g_{0,P} + \Delta g_{1,P}$$

This is inserted in the preceding equation, and the zero- and first-order terms are separated.

The zero-order terms, corresponding to $h = 0$, yield

$$\Delta g_{0,P} = -\frac{1}{4\pi}\iint\left(\frac{1}{D^3}-\frac{3H^2}{D^5}\right)T_0\,dx\,dy + \frac{H}{4\pi}\iint\frac{\Delta g}{D^3}\,dx\,dy$$

The solution of this equation is given by

$$\Delta g_{0,P} = \frac{H}{2\pi}\iint\frac{\Delta g}{D^3}\,dx\,dy \qquad (52)$$

because this is the well-known plane approximation of (4). The first-order terms give

$$\Delta g_{1,P} = -\frac{1}{4\pi}\iint\left(\frac{1}{D^3}-\frac{3H^2}{D^5}\right)T_1\,dx\,dy + \frac{H}{4\pi}\iint\frac{g_1}{D^3}\,dx\,dy - \frac{3H}{4\pi}\iint\left(\frac{3}{D^5}-\frac{5H^2}{D^7}\right)T_0h\,dx\,dy + \frac{3H}{4\pi}\iint\frac{s}{D^5}\,T_0\tan\tau\,dx\,dy - \frac{1}{4\pi}\iint\left(\frac{1}{D^3}-\frac{3H^2}{D^5}\right)\Delta g\,h\,dx\,dy \qquad (53)$$

This is the desired solution. It differs from equation 100 of *Moritz* [1962a] by the terms containing T_1 and g_1, which were omitted there by mistake.

5. Solution by Means of a Surface Layer

The coating method for an equipotential surface, equations 9 and 10, can be generalized for the physical surface S of the Earth. We represent the disturbing potential T outside S as the potential of a surface layer on S of density χ:

$$T_P = \iint_S \frac{\chi}{l}\,dS \qquad (54)$$

We again apply our usual approximation, linear in h. By (30) and (35) we have

$$T_P = R^2\iint_\sigma\left(\frac{1}{D}-\frac{A}{D^3}\,h\right)\chi\,d\sigma \qquad (55)$$

The surface layer χ is split up into a part χ_0 independent of h and a part χ_1 proportional to h:

$$\chi = \chi_0 + \chi_1 \qquad (56)$$

This corresponds to (34). Then (55) becomes

$$T_P = T_{0,P} + T_{1,P} = R^2\iint_\sigma\frac{\chi_0}{D}\,d\sigma + R^2\iint_\sigma\frac{\chi_1}{D}\,d\sigma - R^2\iint_\sigma\frac{A}{D^3}\,\chi_0 h\,d\sigma \qquad (57)$$

that is

$$T_{0,P} = R^2\iint_\sigma\frac{\chi_0}{D}\,d\sigma \qquad (58)$$

$$T_{1,P} = R^2\iint_\sigma\frac{\chi_1}{D}\,d\sigma - R^2\iint_\sigma\frac{A}{D^3}\,\chi_0 h\,d\sigma \qquad (59)$$

The quantities χ_0 and χ_1 on S can be determined by making the transition $P \to P_0$ to a point on the surface S itself. This is quite analogous to the transformation of (38) described in section 3, by which a solvable linear integral equation for T_1 was found. In our present case a linear integral equation for χ is obtained, which was found and solved by Molodenskii. According to *Molodenskii et al.* [1962, p. 122] we have

$$2\pi\chi_0 = \Delta g + \frac{3}{8\pi}\iint_\sigma \Delta g\, S(\psi)\, d\sigma$$

$$= \Delta g + \frac{3T_0}{2R} = \mu \qquad (60)$$

$$2\pi\chi_1 = G_1 + \frac{3}{8\pi}\iint_\sigma G_1 S(\psi)\, d\sigma$$

$$= G_1 + \frac{3T_1}{2R} \qquad (61)$$

where G_1 is given by (41). Equation 60 also follows directly by comparing (55), for $h = 0$, and (9).

If we compare (59) with (38), we see that the coating method yields a considerably simpler formula for computing T_1. It will be remembered that T_1 is the effect of the topographical height h, T_0 corresponding to a level Earth, $h = 0$.

The gravity disturbance vector δ may be found in a relatively simple way as the gradient of (57). The coating method is, however, less suited for computing external gravity anomalies Δg_P.

6. Solution by Reduction to Sea Level

It can be shown (Moritz, forthcoming paper) that Molodenskii's solution, equations 39 through 41, may be transformed in a purely formal manner into

$$T = \frac{R}{4\pi}\iint_\sigma \left(\Delta g - \frac{\partial \Delta g}{\partial h}\, h\right) S(R + h_P, \psi)\, d\sigma \qquad (62)$$

The geometrical interpretation of this new equation is obvious. The gravity anomalies Δg at the physical surface of the Earth are reduced 'in free air' to sea level by adding the term $-h\ \partial\Delta g/\partial h$. Then T at the point P_0 of the physical surface, which has the elevation h_P above sea level, is computed by using (3), which is Stokes' formula generalized for points above sea level.

This is the 'free-air reduction to sea level' described by *Moritz* [1964, section 6.4]. The indicated formal derivation of (62) shows that the difficulties of analytical continuation have no effect on an approximation linear in h. These difficulties, inherent in free-air reduction to sea level, were the reason why Molodenskii, who used this method in 1949 for solving his integral equation, gave it up later. He then developed another solution, which is based on a coating on the physical surface and corresponds to equations 39 through 41.

Free-air reduction to sea level has, however, enormous practical advantages, as emphasized by *Bjerhammar* [1963]. It reduces the problem to the simple case of a bounding level surface, to which spherical formulas such as equations 3 through 10 may be applied. The computation of the external gravity field, of spherical harmonics, etc., can thus be handled rigorously by means of the conventional formulas.

All we have to do is to reduce Δg to sea level, obtaining

$$\widetilde{\Delta g} = \Delta g - \frac{\partial \Delta g}{\partial h}\, h \qquad (63)$$

as an approximation linear in h, and use $\widetilde{\Delta g}$ instead of Δg in the spherical formulas (3) through (10). The effect of topographical elevation h, which otherwise involves complicated formulas, is thus automatically taken into account.

The vertical gradient of the gravity anomalies may be computed by well-known formulas such as the integral expression

$$\left.\frac{\partial \Delta g}{\partial h}\right|_P = -\frac{2}{R}\,\Delta g_P + \frac{R^2}{2\pi}\iint_\sigma \frac{\Delta g - \Delta g_P}{l_0^3}\, d\sigma \qquad (64)$$

where again

$$l_0 = 2R \sin \psi/2$$

As we have seen, free-air reduction to sea level is valid at least to an approximation linear in h. It may be expected, however, to be accurate to a considerably higher approximation. For this reason, Bjerhammar has suggested to compute the reduced anomalies $\widetilde{\Delta g}$ by solving the equation

$$\widetilde{\Delta g}_P = \frac{r_P^2 - R^2}{4\pi r_P}\iint_\sigma \frac{\widetilde{\Delta g}}{D^3}\, d\sigma \qquad (65)$$

for $\widetilde{\Delta g}$. It is (4) applied to a point P at the physical surface of the Earth which has the elevation h_P above sea level; there is

$$r_P = R + h_P \qquad (66)$$

Formula 65 may be considered as a linear integral equation for $\widetilde{\Delta g}$, if the surface anomalies Δg are given.

Bjerhammar [1963] has also described how (65) may be solved. A different way of solving the integral equation (65) is an iterative method that is well suited for practical computation.

For this purpose we must transform (65). Consider a fictitious anomalous point mass at the center of the spherical Earth. Its attraction is proportional to $1/r^2$, so that the gravity anomaly caused by this point mass may be written, omitting a constant factor

$$\Delta g = (R/r)^2$$

At sea level, $r = R$, we have $\widetilde{\Delta g} = 1$. Now apply equation 65 to this special function, finding

$$\left(\frac{R}{r_P}\right)^2 = \frac{r_P^2 - R^2}{4\pi r_P} \iint_\sigma \frac{d\sigma}{D^3} \qquad (67)$$

Let $\widetilde{\Delta g}_P$ denote the value of $\widetilde{\Delta g}$ corresponding to Δg_P, i. e., lying on the same radius vector OP. Multiply (67) by $\widetilde{\Delta g}_P$, which is a constant with respect to the integration, and subtract from (65). This gives

$$\Delta g_P - \left(\frac{R}{r_P}\right)^2 \widetilde{\Delta g}_P = \frac{r_P^2 - R^2}{4\pi r_P} \iint_\sigma \frac{\widetilde{\Delta g} - \widetilde{\Delta g}_P}{D^3}\, d\sigma$$

The factor $(R/r_P)^2$ of $\widetilde{\Delta g}_P$ can be set equal to 1 without loss of accuracy. Thus we obtain, as an alternative to (65), the integral equation

$$\widetilde{\Delta g}_P = \Delta g_P - \frac{r_P^2 - R^2}{4\pi r_P} \iint_\sigma \frac{\widetilde{\Delta g} - \widetilde{\Delta g}_P}{D^3}\, d\sigma \qquad (68)$$

which recommends itself for iterative solution by means of an automatic computer.

As a first approximation set

$$\widetilde{\Delta g}^{(1)} = \Delta g$$

then compute a second approximation

$$\widetilde{\Delta g}_P^{(2)} = \Delta g_P - \frac{r_P^2 - R^2}{4\pi r_P} \cdot \iint_\sigma \frac{\widetilde{\Delta g}^{(1)} - \widetilde{\Delta g}_P^{(1)}}{D^3}\, d\sigma$$

a third approximation

$$\widetilde{\Delta g}_P^{(3)} = \Delta g_P - \frac{r_P^2 - R^2}{4\pi r_P} \cdot \iint_\sigma \frac{\widetilde{\Delta g}^{(2)} - \widetilde{\Delta g}_P^{(2)}}{D^3}\, d\sigma$$

and so forth. The convergence of this process should be very rapid.

In this way the 'downward continuation' of the gravity anomalies from the physical surface (Δg) to sea level ($\widetilde{\Delta g}$) may be effected. It is characteristic for all problems of downward continuation that they cannot be solved directly but only by iterative inversion of the formula for upward continuation. The iterative process just explained may also be performed as a plane approximation, by replacing the sphere by its tangential plane. This is described by *Moritz* [1962*b*].

7. Conclusion

In the present paper we have described and compared three methods for computing the gravity field outside the Earth, taking account of the fact that the free-air anomalies are given on the physical surface of the Earth, which is not a level surface. The direct formulas (38) for T and (53) for Δg are very complicated. The solution (59) for T according to the coating method is simpler, but this method does not provide a suitable solution for Δg. Practically the best method is the free-air reduction to sea level.

According to this method, the solution is effected in two steps:

1. Downward continuation of Δg from the physical surface to sea level, using (63) or an iterative solution of (68).

2. Computation of the external gravity field using the simple spherical formulas (3) through (10). This is a process of upward continuation. In this way the irregularities of the Earth's physical surface are fully taken into account.

Appendix

Estimates for the Effect of Topographic Elevation on the External Gravity Anomalies

We shall now give some estimates for the magnitude of $\Delta g_{1,P}$ according to (53). First we neglect the terms containing T_1 and g_1, which are usually unknown. The geoidal undulation N, and hence $T_0 = \gamma N$, may often be considered constant over limited areas. Then the sum of

the third and fourth term of (53) becomes, omitting the constant factor $(3H/4\pi)T_0$

$$
\begin{aligned}
&-\iint \left(\frac{3}{D^5}-\frac{5H^2}{D^7}\right)h\,dx\,dy \\
&\quad+\iint \frac{s}{D^5}\tan\tau\,dx\,dy \\
&\quad=\int_{\alpha=0}^{2\pi}\int_{s=0}^{\infty}\left\{\frac{\partial}{\partial s}\left(\frac{s^2}{D^5}\right)h+\frac{s^2}{D^5}\frac{\partial h}{\partial s}\right\}ds\,d\alpha \\
&\quad=\int_{\alpha=0}^{2\pi}\int_{s=0}^{\infty}\frac{\partial}{\partial s}\left(\frac{s^2}{D^5}h\right)ds\,d\alpha \\
&\quad=\int_{\alpha=0}^{2\pi}\left\{\frac{s^2}{(s^2+H^2)^{5/2}}h\right\}_{s=0}^{s=\infty}d\alpha=0
\end{aligned}
$$

Here we have transformed to polar coordinates s, α by

$$x = s\cos\alpha \qquad y = s\sin\alpha \qquad dx\,dy = s\,ds\,d\alpha \tag{69}$$

and used the fact that

$$\tan\tau=\frac{\partial h}{\partial s} \qquad \left(-\frac{3}{D^5}+\frac{5H^2}{D^7}\right)s=\frac{\partial}{\partial s}\frac{s^2}{D^5}$$

Thus we have found the important result that the third and the fourth term of (53) cancel if T_0 can be considered constant over the area of integration. Then there remains only the last term of (53)

$$\delta=-\frac{1}{4\pi}\iint\left(\frac{1}{D^3}-\frac{3H^2}{D^5}\right)\Delta g\,h\,dx\,dy \tag{70}$$

According to the mean value theorem of integral calculus, this is equal to

$$\delta=\frac{\overline{\Delta g}}{4\pi}\iint\left(-\frac{1}{D^3}+\frac{3H^2}{D^5}\right)h\,dx\,dy=\overline{\Delta g}\cdot J \tag{71}$$

where $\widetilde{\Delta g}$ is a certain mean value of Δg taken over the area of integration.

We shall now compute the factor

$$J=\frac{1}{4\pi}\iint\left(-\frac{1}{D^3}+\frac{3H^2}{D^5}\right)h\,dx\,dy \tag{72}$$

for two different models.

First, let the terrain consist of a conical mountain of height h_1 and slope β, superposed on a plane (Figure 3). The point P is situated on the axis of the cone, H being its elevation above the plane. Then

$$h=\begin{cases}(a-s)\tan\beta & \text{if } s<a\\ 0 & \text{otherwise}\end{cases} \tag{73}$$

Thus we find on transforming to polar coordinates according to (69)

$$J=J_1=\frac{1}{4\pi}\int_{\alpha=0}^{2\pi}\int_{s=0}^{a}\left(-\frac{1}{D^3}+\frac{3H^2}{D^5}\right)\cdot(a-s)\tan\beta\,s\,ds\,d\alpha \tag{74}$$

Since a and β are constants, and

$$D=\sqrt{s^2+H^2} \tag{75}$$

this integral can be evaluated in closed form by the usual methods, giving

$$J_1=\tfrac{1}{2}\tan\beta\left(\ln\frac{a+d}{H}-\frac{a}{d}\right) \tag{76}$$

On introducing the angle ω according to Figure 3, this may be written

$$J_1=\tfrac{1}{2}\tan\beta\left(\ln\cot\frac{\omega}{2}-\cos\omega\right) \tag{77}$$

A second model will now be considered. It represents a so-called 'two-dimensional' body, extending from infinity to infinity in one horizontal direction, the cross section normal to this direction being the same everywhere. This direction is taken normal to the plane of Figure 3, so that this figure now represents a cross section of the new model. The same notations will be used as in the first model. Figure 4 shows the difference between model 1 and model 2.

For the second model, assume the coordinate

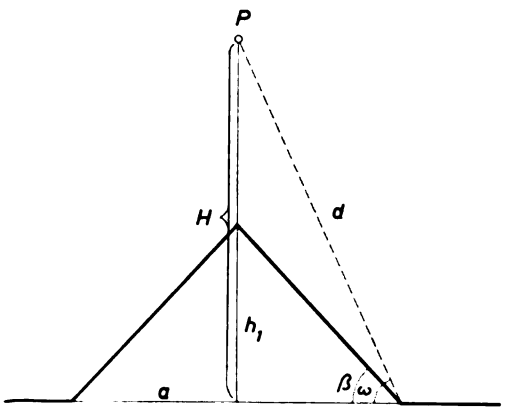

Fig. 3. Cross section of the model.

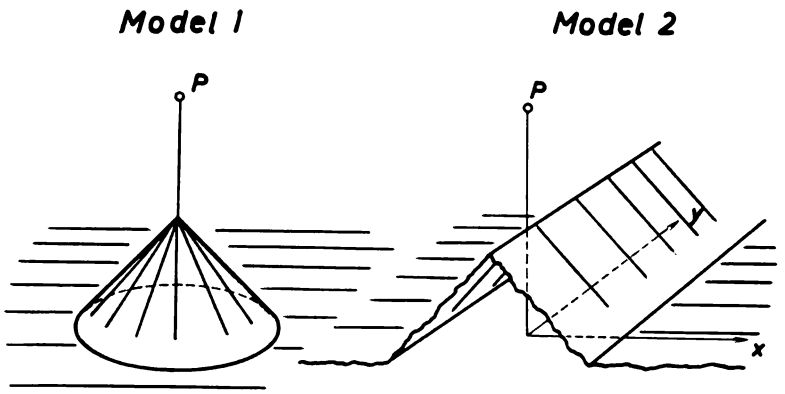

Fig. 4. Two models.

axes as shown in Figure 4. Then we have, corresponding to (73)

$$h = \begin{cases} (a - x) \tan \beta & \text{if } x < a \\ 0 & \text{otherwise} \end{cases} \tag{78}$$

so that, corresponding to (74)

$$I = J_2 = \frac{1}{4\pi} \int_{x=-a}^{a} \int_{y=-\infty}^{\infty} \left(- \frac{1}{D^3} + \frac{3H^2}{D^5} \right) \cdot (a - x) \tan \beta \, dx \, dy \tag{79}$$

Since

$$D = \sqrt{x^2 + y^2 + H^2}$$

this integral can again be evaluated in closed form. After somewhat laborious calculations we obtain

$$J_2 = -(2/\pi) \tan \beta \ln \sin \omega$$

The effect may be expected to be largest if P lies close to the top of the mountain, that is, if

$$H \doteq h_1 \qquad \omega \doteq \beta$$

Table 1 gives values of J_1 and J_2 for this limiting case, for several inclinations $\beta = \omega$. Multiplying J_1 or J_2 by $\overline{\Delta g}$ gives the effect δ of topographic elevation on the computed Δg at P. It is seen to be much larger for the second model, which represents a large-scale deviation from the plane,

TABLE 1. Effect of Topography

$\beta = \omega$	J_1	J_2
2°	0.053	0.074
10°	0.128	0.196
20°	0.145	0.249
40°	0.102	0.236
60°	0.043	0.159

whereas the first model represents a local irregularity only. Both effects are seen to be largest for inclinations of about 20°.

As a matter of fact, these values imply quite extreme conditions. In practice, the correction δ should hardly exceed 10% of $\overline{\Delta g}$ even for low altitudes H in rugged areas.

Acknowledgment. The research on this paper has been sponsored by the Air Force Cambridge Research Laboratories, Office of Aerospace Research, U. S. Air Force, under contract AF 19 (628)-2771, Ohio State University Research Foundation Project 1613, Supervisor W. A. Heiskanen, Project Engineer Bela Szabo.

References

Bjerhammar, A., A new theory of gravimetric geodesy, *Roy. Inst. Technol. Stockholm, Div.: Geodesy*, 1963.

de Graaff-Hunter, J., The shape of the Earth's surface expressed in terms of gravity at ground level, *Bull. Géodésique, 56*, 191–200, 1960.

Hirvonen, R. A., and H. Moritz, Practical computation of gravity at high altitudes, *Inst. Geodesy Photogrammetry Cartography Rept. 27*, Ohio State University, Columbus, 1963.

Molodenskii, M. S., V. F. Eremeev, and M. I. Yurkina, Methods for study of the external gravitational field and figure of the Earth (translated from Russian, 1960), 1962.

Moritz, H., Studies on the accuracy of the computation of gravity in high elevations, *Publ. 38*, Isostatic Institute of International Association of Geodesy, 1962*a*.

Moritz, H., A statistical method for upward and downward continuation of gravity, *Inst. Geodesy Photogrammetry Cartography Rept. 25*, pp. 1–16, Ohio State University, Columbus, 1962*b*.

Moritz, H., The boundary-value problem of physical geodesy, *Inst. Geodesy Photogrammetry Cartography Rept. 46*, Ohio State University, Columbus, 1964.

On the Influence of Gravity Anomalies on Satellite Orbits

K. ARNOLD

Geodetic Institute, Potsdam, East Germany

Abstract. By examination of the perturbations in the orbital elements of near-Earth satellites, gravity anomalies are determined for large unsurveyed areas of the Earth's surface. These interpolated anomalies in conjunction with average anomalies over surveyed areas may be used to determine the potential field of the Earth.

It is well known that satellite orbits are influenced by the gravitational field of the Earth. To describe the gravitational field, it is usual to to introduce spherical harmonics, but in physical geodesy there is also good precedent for describing the gravitational field by means of the gravity anomalies of the Earth's surface. The methods of physical geodesy thus make it possible to express the potential at the Earth's surface and in the Earth's external field by these gravity anomalies on the Earth's surface. The mathematical method employed is the boundary-value problem of physical geodesy, which establishes a solution for the external field of the Earth, if gravity values are given on the Earth's surface.

Our gravity measurements on the Earth's surface, which are executed by pendulums and gravimeters and which are interpolated and extrapolated by one of the several statistical or geophysical methods, are of great value for satellite geodesy.

To find the potential at the Earth's surface, we must introduce the free-air anomalies into Stokes' formula. Since our aim is not, however, to have potential values at the Earth's surface but to find potential values in space, we have to introduce the generalized Stokes formula.

We have the following formula for the disturbance potential at the satellite point S:

$$T(S) = \frac{r}{4\pi} \iint_q \Delta g_P \cdot \Phi_1(S, Q)\, dq \qquad (1)$$

where

T, the disturbance potential, is the difference between the gravitational potential and the normal potential from the theory of Somigliana;

r is the geocentric distance to the satellite;

q is the Earth's surface;

Q is a point on the Earth's surface;

Φ_1 (S, Q) is the generalized function of Stokes;

and where

$$\Phi_1(S, Q) = \tau^2\left[\frac{2}{D} + 1 - 3D - \tau\cos\psi \cdot\left(5 + 3\ln\frac{1 + D - \tau\cos\psi}{2}\right)\right]$$

$$\tau = R/r \qquad (2)$$

$$D^2 = 1 - 2\tau\cos\psi + \tau^2 \qquad (3)$$

$$\cos\psi = \sin\varphi_S \sin\varphi_Q + \cos\varphi_S \cos\varphi_Q \cos(\lambda_Q - \lambda_S) \qquad (4)$$

or, as a series development

$$\Phi_1(S, Q) = \sum_{n=2}^{\infty} \frac{2n + 1}{n - 1}\, \tau^{n+2} P_n(\cos\psi) \qquad (5)$$

According to the so-called 'new theory' of physical geodesy, we must now add the correction term due to the variations in the topography.

$$-h\frac{1}{2\pi}\int_0^{2\pi} d\vartheta \int_{r=0} \frac{\Delta g_P - \Delta g_{P-0}}{\rho^2}\, d\vartheta \qquad (6)$$

where h is the height difference between the variable point Q at the Earth's surface and the subsatellite point at the Earth's surface. This correction term has values up to 10 and 30 mgal even in the Mittelgebirge (rolling country); in

extreme cases it may reach 50 mgal and more. The effect on the satellite of this correction is similar to the effects caused by spherical harmonics of a very high order.

Vening Meinesz has considered the influence of such a spherical harmonic at points of great height. He found that at the height of 60 kilometers the influence has diminished to less than 1% of its Earth surface value. We see that for most satellite orbits the sophistications resulting from the 'new theory' are negligible for the purposes of satellite geodesy.

We can now determine the disturbance potential T in the exterior space and can see what effect a 5-mgal gravity anomaly in a 10°-by-10° square has on the position of a satellite.

The rectangular coordinates of a satellite are given as functions of the orbit elements by the following formula:

$$\begin{bmatrix} x_s \\ y_s \\ z_s \end{bmatrix} = \frac{a(1-e^2)}{1+e\cos v} \cdot \begin{bmatrix} \cos(v+\omega)\cos\Omega - \sin(v+\omega)\sin\Omega\cos i \\ \cos(v+\omega)\sin\Omega + \sin(v+\omega)\cos\Omega\cos i \\ \sin(v+\omega)\sin i \end{bmatrix} \tag{7}$$

The variations in these satellite coordinates, as they are caused by mean gravity values of 10°-by-10° squares, yield from the Lagrange perturbation equations

$$\begin{bmatrix} \frac{da}{dt} = a' \\ \frac{de}{dt} = e' \\ \frac{d\omega}{dt} = \omega' \\ \frac{di}{dt} = i' \\ \frac{d\Omega}{dt} = \Omega' \\ \frac{dM}{dt} = M' \end{bmatrix} = A \cdot \begin{bmatrix} K_1 \\ K_2 \\ K_3 \end{bmatrix} \tag{8}$$

where A is the coefficient matrix, and K_1, K_2, K_3 are the components of the gradient of the disturbance potential.

$$\text{grad } T = \begin{bmatrix} K_1 \\ K_2 \\ K_3 \end{bmatrix} \tag{9}$$

K_1 is the disturbance component perpendicular to the orbit plane and positive in the direction to the north pole. The K_2 component is situated in the orbit plane perpendicular to the radius vector and heading in the direction of the velocity vector. The K_3 component has the direction of the radius vector and is positive to the exterior.

We reach K_1, K_2, K_3 by the following method: if B is the deflection in the meridian and L the deflection in the prime vertical at the height of the satellite

$$B = \frac{1}{r}\frac{\partial T}{\partial \varphi}; \qquad L = \frac{1}{r\cos\varphi}\cdot\frac{\partial T}{\partial \lambda} \tag{10}$$

and if

$$\operatorname{cotg}\chi = \cos(\omega+v)\,tg\,i \tag{11}$$

then we have

$$\begin{aligned} K_2 &= B\cos\chi + L\sin\chi \\ K_1 &= B\sin\chi - L\cos\chi \end{aligned} \tag{12}$$

$$K_3 = -\frac{1}{4\pi}\iint_q \Delta g_F[2\Phi_1(S,Q) + \Phi_4(S,Q)]\,dq \tag{13}$$

$$\begin{aligned} B &= -\frac{1}{4\pi}\iint_q \Delta g_F\,\Phi_2(S,Q)\,dq \\ L &= -\frac{1}{4\pi}\iint_q \Delta g_F\,\Phi_3(S,Q)\,dq \end{aligned} \tag{14}$$

$$\begin{Bmatrix} \Phi_2 \\ \Phi_3 \end{Bmatrix} = \tau^3 \begin{Bmatrix} \psi_2 \\ \psi_3 \end{Bmatrix} \left[\frac{2}{D^3} + \frac{6}{D} + 3\frac{D-1+\tau\cos\psi}{D\sin^2\varphi} - 8 - 3\ln\frac{D+1-\tau\cos\psi}{2}\right] \tag{15}$$

$$\Phi_4 = \tau^2\left[\frac{1-\tau^2}{D^3} - 1 - 3\tau\cos\psi\right] \tag{16}$$

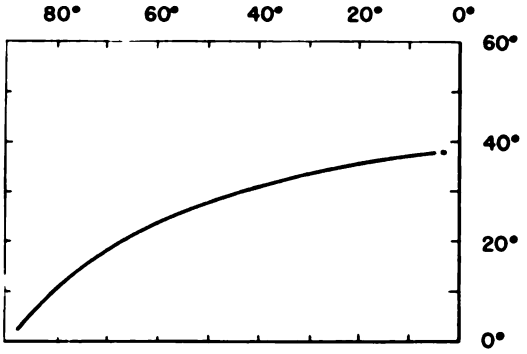

Fig. 1. Orbit arc of Explorer 9.

$$\Psi_2 = \sin\psi\cos\alpha = \sin\varphi_Q\cos\varphi_S - \cos\varphi_Q\sin\varphi_S\cos(\lambda_Q - \lambda_S) \quad (17)$$

$$\Psi_3 = \sin\psi\sin\alpha = \cos\varphi_Q\sin(\lambda_Q - \lambda_S)$$

For the evaluation of these integrals we approximate the process of integration by a summation formula. The surface elements dq are replaced by the 10°-by-10° squares Δq. Thus we have, for instance

$$K_3 \cong -\frac{1}{4\pi}\sum \Delta g_F[2\Phi_1 + \Phi_4]\,\Delta q \quad (18)$$

For a numerical example we have investigated the influence of all 10°-by-10°-square mean gravity anomalies on an orbit arc of the satellite Explorer 9.

The orbit arc (Figure 1) under investigation begins over the equator at longitude 80°W and ends over the Greenwich meridian at approximately latitude 39°N. Thus we have one-quarter of one revolution of the satellite.

The orbit elements are approximately

$a = 7.968 \cdot 10^6$ meter
$e = 0.1062$
$i = 38.8°$
$\omega = 265.8°$
$\Omega = 203.7°$
$M = 110°$
$(M = 190°)$

The Earth's surface has been divided in 10°-by-10° squares. By our summation process, we have determined the influence of 5-mgal mean gravity anomalies in these 10°-by-10° squares along the 90° length of the orbit arc.

Figure 2 shows the height of the satellite during this orbit arc. Near the end of this arc the satellite comes down to 750 km, reaching the point of its perigee. The height at perigee is very important, because the influence of these gravity anomalies on the satellite orbit is

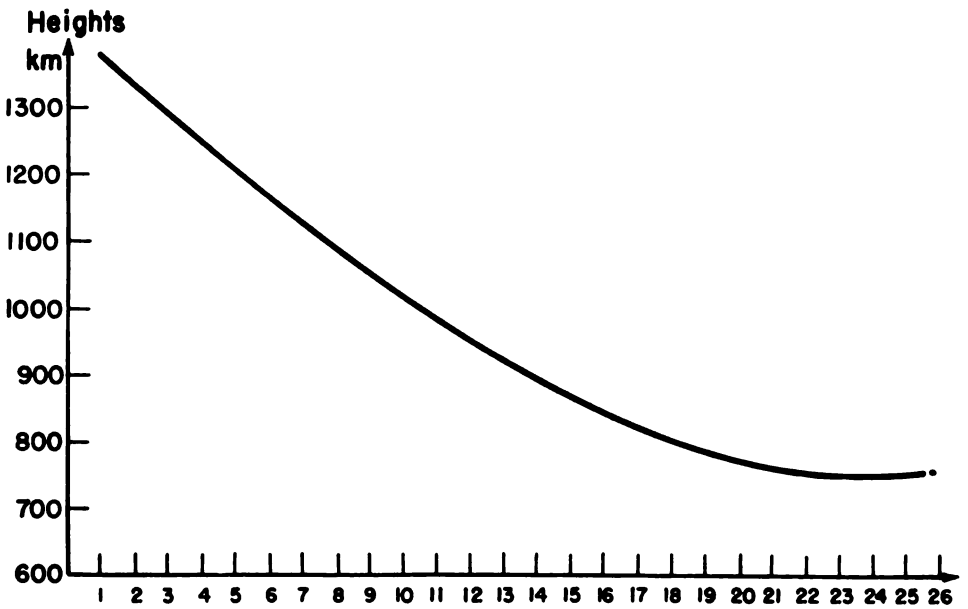

Fig. 2. Heights for Explorer 9.

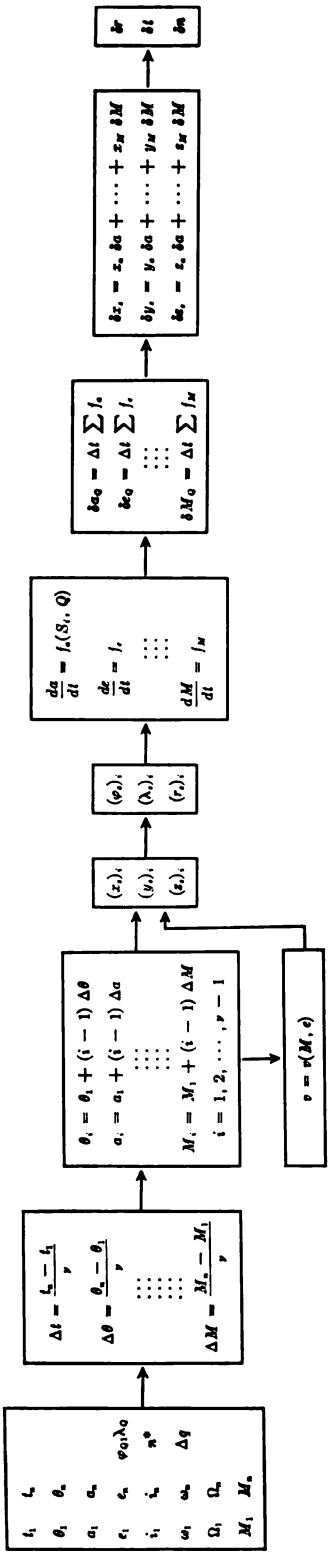

Fig. 3. Disturbances in the rectangular coordinates.

enhanced enormously if the satellite moves deeper into the Earth's atmosphere. Thus the influence of the mean gravity anomalies will enlarge rapidly as the distance of the satellite from Earth diminishes.

If D is diminished to half its value, the values for Φ_2, Φ_3, Φ_4 are increased eightfold, as can be seen in our formulas.

Finally, we must integrate over the 90° orbit arc to determine the influence on the orbit elements. The changes in the orbital elements are represented by

$$\begin{aligned} \delta a &= \Delta t \sum \frac{da}{dt} \\ \delta e &= \Delta t \sum \frac{de}{dt} \\ \delta \omega &= \Delta t \sum \frac{d\omega}{dt} \\ &\cdots \\ \delta M &= \Delta t \sum \frac{dM}{dt} \end{aligned} \tag{19}$$

where δa is the change during time Δt and Δt is the time difference between the integration points along the satellite orbit. We have chosen Δt equal to both 60 and 30 sec to give evidence of the influence of the differing values. Both of

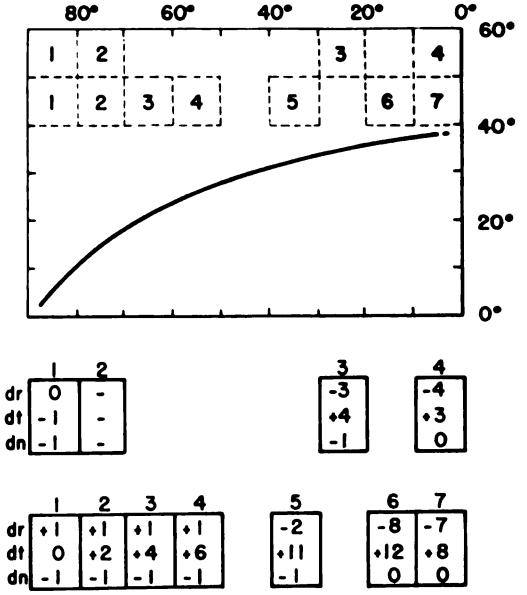

Fig. 4. Coordinate variation.

these integrations, which were executed by an electronic computer, agreed within 10–15%. From these disturbances in the orbit elements

$$\delta a,\ \delta e,\ \delta \omega,\ \cdots,\ \delta M \qquad (20)$$

we determined the disturbances in the rectangular coordinates of the satellite position at the end point of the 90° orbit arc (Figure 3).

The rectangular coordinates, which are based on the equator as the reference plane and for which the rotation axis is a coordinate axis, seemed unsuitable for consideration here. We have therefore determined the disturbances of the coordinates of a system that is connected in a more natural way to the orbit plane of the satellite; i.e., we have determined the disturbance component in the radial, tangential, and normal directions of the satellite orbit

$$\begin{bmatrix} dr \\ dt \\ dn \end{bmatrix} \qquad (21)$$

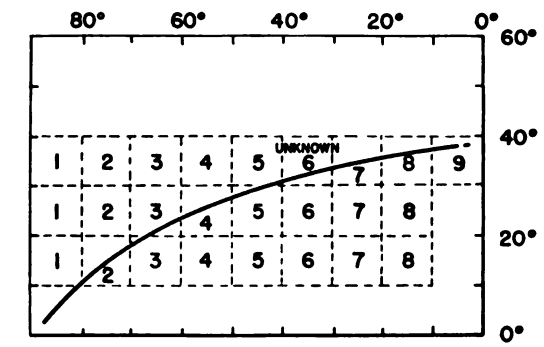

	1	2	3	4	5	6	7	8	9
dr	+2	+3	+3	+3	+3	0	-4	-9	-7
dt	+1	+3	+8	+13	+20	+23	+21	+17	+10
dn	-1	-1	-1	-1	-1	0	0	0	0

	1	2	3	4	5	6	7	8
dr	+4	+6	+7	+6	+2	0	-3	-5
dt	+1	+6	+12	+16	+14	+11	+8	+6
dn	-1	-2	-1	+1	+1	+1	+1	0

	1	2	3	4	5	6	7	8
dr	+7	+8	+6	+3	+1	-1	-2	-3
dt	+1	+7	+9	+7	+6	+4	+3	+2
dn	-1	0	+1	+2	+1	+1	+1	0

Fig. 5. Coordinate variation.

taken for the endpoint of our 90° orbit arc (Figures 4 and 5), and we have reached the values given in Figure 4.

The shifts of the satellite positions as given in the first line of Figure 5 are of special interest.

For the areas 1.5, 1.6, 1.7, 1.8, and 1.9 the tangential shifts dominate. They reach +20, +23, +21, +17, and +10 meters for a mean anomaly of 5 mgal.

From this fact we can derive that, on the strength of a 5-mgal mean gravity anomaly, the linear tangential velocity of the satellite is disturbed and enhanced, so that the satellite will have passed the endpoint of the arc by the amount of about 20 meters as opposed to the case of a mean gravity anomaly of 0 mgal.

We can therefore develop a method for the interpolation of gravity anomalies by satellite methods.

For instance, if for the 10°-by-10° area the 1.6 mean gravity anomaly is unknown, it is possible to find this value by satellite observations under the presupposition that the mean anomalies for the surrounding squares are given.

We must observe the satellite at a distance of about 2000 km before it enters the 10°-by-10° square 1.6; i.e., we must observe its position and the corresponding time date. We must also observe the satellite a second time about 10 minutes later, i.e. at a distance of about 2000 km from its point of exit from square 1.6.

From the mean orbit elements we reach the mean velocity of the satellite, and from the mean gravity anomalies in the surrounding squares we will find the velocity disturbance caused by them. The residual disturbance of the satellite velocity comes from the unknown mean gravity anomaly of area 1.6.

We may roughly approximate that a 20-meter tangential satellite shift is equivalent to 5 mgal and that a 100-meter shift is equivalent to 25 mgal.

Returning to equation 1 we have determined the disturbance potential T due to some common gravity anomalies; the free-air anomalies published by Uotila which refer to a certain level ellipsoid of given axis, for a given equator gravity value and for a given flattening. However, in satellite geodesy we deal with the real potential, taking into account all the terms contained in the potential function. Instead of

a mathematically idealized normal potential we have used the real potential.

For the real potential we introduce the following expression:

$$V = \frac{k\mu}{r} - \frac{k\mu}{r} J_2 \left[\frac{R}{r}\right]^2 P_{20}(\sin\varphi) + T_r \quad (23)$$

The disturbance potential T_r thus defined must be determined from the disturbance potential T, as given by the free-air anomalies derived from the international gravity formula.

The real values for the real potential are given by satellite observations

$$\begin{aligned} J_2 &= 0.001,082,7 \pm 1 \cdot 10^{-7} \\ k\mu &= 398,603 \cdot 10^9 \ \mathrm{m^3\,sec^{-2}} \\ R &= 6,378,160 \pm .15 \ \mathrm{m} \end{aligned} \quad (24)$$

which are sufficiently precise for our purposes.

The disturbance potential, as derived from the free-air anomalies, and the real potential are related in the following way:

$$V = U^* + T$$

U^* is here the normal potential.

$$U^* = \frac{k\mu^0}{r}\left[1 - J_2^0\left[\frac{R^0}{r}\right]^2 P_2(\sin\varphi) - J_4^0\left[\frac{R^0}{r}\right]^4 P_4(\sin\varphi) + O(f)^3\right] \quad (25)$$

and

$$J_2^0, \quad J_4^0, \quad k_\mu^0$$

are from the theory of Somigliana and are based on the following data:

$$\begin{aligned} f &= 1/297 \\ m &= 0.003,467,827 \\ \gamma_e &= 978,049 \ \mathrm{mgal} \\ R^0 &= 6,378,388 \ \mathrm{m} \end{aligned} \quad (26)$$

Taking all these relations into account, we find the disturbance potential T_r, which gives the real potential by adding the zonal harmonic of the second order.

To reach the anomalies that yield T_r according to the generalized Stokes function, we must add the following term to the free-air anomalies:

$$\Delta g = \Delta g_F - 9P_2(\sin\varphi) + 7P_4(\sin\varphi) \ \mathrm{mgal} \quad (27)$$

φ, deg.	$\Delta g - \Delta g_F$
0	+7
10	+6
20	+3
30	−1
40	−4
50	−6
60	−6
70	−4
80	−3
90	−2

and finally

$$T_r = \frac{r}{4\pi} \iint_q \Delta g \, \Phi_1(S, Q) \, dq \quad (28)$$